Geophysical Exploration for Archaeology:

An Introduction to Geophysical Exploration

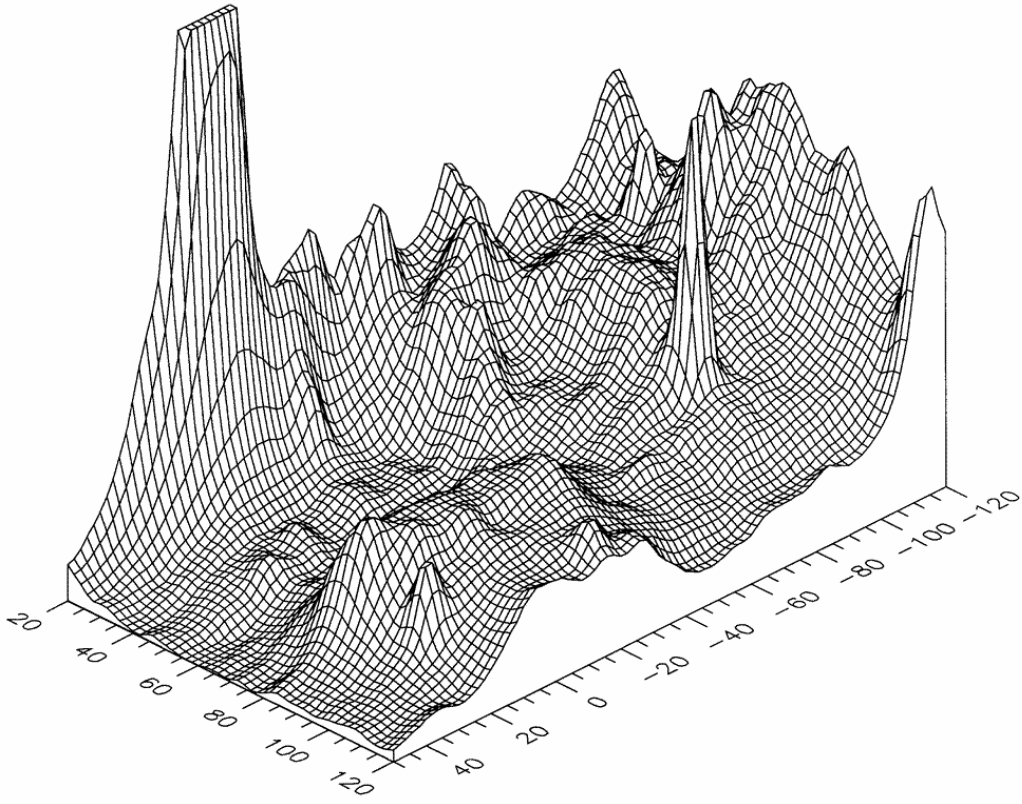

Midwest Archeological Center
Special Report No. 1

1998

Geophysical Exploration for Archaeology:

An Introduction to Geophysical Exploration

By

Bruce W. Bevan
Geosight

Midwest Archeological Center
Special Report No. 1

United States Department of the Interior
National Park Service
Midwest Archeological Center
Lincoln, Nebraska
1998

Geophysical Exploration for Archaeology:
An Introduction to Geophysical Exploration

page

Preface ii
Introduction ---------- 1
Sources of equipment 1
Survey preliminaries ---------- 2
Setting up a grid 3
General survey procedures ---------- 6
Resistivity Surveys 7
Instruments ---------- 8
Mapping 12
Sounding ---------- 17
Magnetic Surveys 18
Instruments ---------- 19
Before the survey 20
Simple procedures ---------- 21
Magnetic interpretation 24
Conductivity Surveys ---------- 29
Instruments 30
Interpretation procedures ---------- 31
Mapping 33
Detailed procedures ---------- 39
Radar Surveys 43
Equipment ---------- 44
Survey procedures 47
Interpretation ---------- 50
Self-Potential Surveys 57
Equipment ---------- 57
Procedures 59
Survey details ---------- 61
Special Topics 62
Soil chemistry ---------- 62
Multiple instruments 63
Maintenance, reliability, safety ---------- 64
Special survey conditions 66
Notes on the Figures ---------- 68
References 88

Preface

The cost and effort of the printing and distribution of this report have been provided by the Midwest Archeological Center of the National Park Service.

This volume was written in order to assist individuals who do their own geophysical surveys at archaeological sites. This is one volume (volume B) of a three-volume report. This volume is moderately self-contained, and it is not necessary to read the other two volumes in order to understand most of the information here.

The three combined volumes of this report are available only as a microfiche (sheets of microfilm that can be read with a magnifying lens or with a special microfiche viewer). You may obtain a copy of this microfiche at no charge by writing the author at:

Bruce Bevan
Geosight
356 Waddy Drive
Weems, VA 22576
USA

Volume A of the report has a general description of the Petersburg Battlefield where this survey was done, and it summarizes the history of the site; this volume also has guidance about how a geophysical survey might be specified and how an excavation might follow a geophysical survey. Volume A includes the publication references and notes about the figures in all three volumes. While volume A is not technical, volume C is very technical. Volume C describes how geophysical measurements change with time and weather; it also shows how detailed methods of geophysical interpretation can add information to a survey. Volume C also discusses the elaborate procedures of resistivity pseudosections and seismic surveys.

This is the third edition of the report. The first and limited edition was photocopied for a National Park Service course which was held at the Colonial National Historical Park; that edition is dated 24 April 1995. The second edition, dated 26 January 1996, corrected typographical errors in the first edition; the second edition is available only as the microfiche mentioned above. Further errors have been corrected in this third edition.

Note that the National Park Service does not endorse specific models of the geophysical instruments which were applied to these geophysical surveys. There are many different instruments made by many different manufacturers which are also excellent for geophysical surveys of archaeological sites.

Additional Note. This is the third edition of a report originally published as Geosight Technical Report Number 4, Volume B, which was last revised March 6, 1998. The original title page bears the notice “This report may be freely copied and distributed.” The main text pages of the present volume match the pagination of the original, except that the designation “B- ” has been omitted from the page numbering scheme in this most recent printing. For example, the text on p. B-23 in the original document corresponds exactly to the text as it appears on p. 23 in this version. All figures and figure notes are numbered as in the original, but the pagination is unique to this reprinting for the References and Figure Notes sections, which originally appeared in Volume A.

Introduction

This volume is written for all archaeologists who would like to learn how to do geophysical surveys. While this volume is more detailed than volume A, I have kept the technical complexity to a minimum. Even if you are not interested in doing your own geophysical surveys, you may wish to look quickly at this volume in order to learn more about the practices of geophysical exploration. This might help you to specify how a geophysical survey should be done by someone else.

There are many advantages if you do your own geophysical survey. You will be able to do it just as you wish and when you wish. Since you will probably be excavating the site after your survey, you will easily be able to compare the excavation finds to your geophysical results. You may even wish to start an additional survey after your excavations have begun in order to understand the character of a feature which extends outside your excavation.

You may also do geophysical surveys in the bottom or along the sides of your excavations. These may reveal invisible features just behind the excavated surface. A geophysical survey on a vertical excavation surface can provide an objective map of the character of the soil through a shallow depth into the unexcavated soil. Any of the different types of survey can be done within excavations; the major difference is that the measurements are made very close together.

I believe that any archaeologist could do good geophysical surveys; the mental and physical requirements of archaeology and geophysics are very similar. There are some differences too. While geophysics is easier on the knees, it also requires precision while doing repetitive work. You definitely do not need to have a technical background to do geophysical surveys, but you will save time if you can make simple electrical repairs; cables and connectors frequently break. Geophysical surveys can be done (and often are done) in weather which would halt most excavations. If you do not mind doing a walking reconnaissance as a search for archaeological sites, you do not mind collecting spider webs on your ears as you pass between the trees; geophysics is the same. If you wish to do good work, you will have to do at least one or two geophysical surveys a year; if you do fewer, you will forget the procedures.

In this volume, I will be emphasizing topics which have not been described very completely in other publications. I will not duplicate the clear introductions which others have given to resistivity and magnetic surveys. However, I will describe how to do resistivity soundings, and I will also describe simple procedures for magnetic mapping and interpretation. My discussions of conductivity and radar surveys will be more complete than usual, because rather little has been written about practical procedures for these surveys before.

Sources of equipment

Geophysical equipment is expensive. You should not plan on buying equipment for the first few surveys that you do; you should rent or borrow the instruments. Most of the companies which manufacture geophysical instruments will rent, and sometimes loan, their instruments so that prospective buyers can become familiar with them before they consider a purchase. There are also many companies which rent a wide selection of geophysical instruments. The ones which I have heard of are listed below:

Addison and Baxter Ltd.
12 Howard Way
Cromwell Business Park
Newport Pagnell, Buckinghamshire
UK MK16 9QR

Bison Instruments, Inc.
5610 Rowland Road
Minneapolis, Minnesota 55343
USA
phone 612-931-0051

and

J.D.Fett Instrument Rentals
Building 2
4807 Spicewood Springs Road
Austin, Texas 78759 USA
phone 512-346-4042

Geophysical/Geological Instrument and Supply Co.
900 Broadway
Denver, Colorado 80203 USA
phone 303-863-8881

and

Mitcham Industries, Inc.
Post Office Box 1175
Huntsville, Texas 77342 USA
phone 409-291-2277

Terraplus USA Inc.
625 Valley Road
Littleton, Colorado 80124 USA
phone 303-799-4140

There are also two directories which list the manufacturers of geophysical instruments; both of these are published once a year. One of these is called The Geophysical Directory, and the address is in Volume A. The other is the yearbook of the Society of Exploration Geophysicists; this is published in every May issue of their magazine called The Leading Edge.

If you are familiar with electronics, you may construct some instruments yourself, such as a proton magnetometer (Harknett 1969; Steponaitis and Brain 1976) or a resistivity meter (Williams 1984).

In the following sections, I will give additional information about specific types of instruments.

Survey preliminaries

If you are doing a survey at a site which is new to you, you should learn enough about it so that you can decide which instruments might be suitable. Ground-based or aerial photographs will give a good idea of topography and trees, and perhaps also the brush at the site. If the site is very remote, you may find that only satellite photographs are available. Be sure to check if any other geophysical surveys have been done in the general area of the site. Check for surveys at nearby archaeological sites; if you can, also check for geophysical surveys which have been done for other applications in the area. These publications may reveal difficulties with the local type of soil and rock which will affect your survey. Try to get copies of historical maps and photographs of the site. Convert all of these maps to the scale of your site map so that they can be compared.

If you cannot find a detailed geological map of the area, a world map may have enough information to help (Choubert and Faure-Muret 1976). The voltage and frequency of the local power lines should be checked (U.S. Department of Commerce 1975). The anticipated temperature and rainfall during the survey period should also be estimated (Rudloff 1981).

You should check for all of the sources of difficulty and interference which are listed in Fig. A94 and Fig. A95. If there are buried pipes or wires at the site, try to get maps of them. If there is a likelihood of many unknown utility lines, you may need to try to locate them before you start the survey. You could use a line-tracing instrument to map conductive pipes and wires. There are two separate components to these instruments; one component induces an alternating current with an audio frequency onto the conductor and the other component allows you to follow the signal and delineate the conductor.

It may also be valuable to make a preliminary test of the site

with the geophysical instrument which you intend to use; this is particularly important for magnetic and conductivity surveys. A series of fast, unrecorded measurements will indicate the range of values to be expected. This test may also locate some large geophysical anomalies which should be included or excluded from the area of the survey.

If the survey will be done in an area where grass is mown, it will help if the mowers can be notified so that there is not a conflict between their work and yours.

Setting up a grid

The normal procedures of archaeological mapping are almost always suitable for setting up the grid for a geophysical survey. The analysis of magnetic maps is somewhat simpler if their grids are aligned close to magnetic north. When errors are made in a geophysical survey, they can create false anomalies which are extended along the direction in which the measurements are made. For this reason, it may help if the grid is not aligned with the suspected direction of buried structures.

Sometimes, a geophysical survey is done to map a feature whose approximate location is known. Even if the area is known exactly, the area of survey should go well outside the feature. This will allow the geophysical character of the feature to be compared to the surrounding earth where there are no features. The total area of survey is likely to be 3 - 5 times the area of the feature.

If a geophysical survey is to be done on the side of a moderately steep slope, it may be necessary for coordinates to be determined by distances on the sloping surface, rather than horizontal distances. If it is not possible to correct the measurement locations to a horizontal surface, this should be mentioned in your report.

Your usual methods of coordinate nomenclature will be suitable for the geophysical survey. If the grid is aligned closely with north, these coordinates can be called East and North, resulting in a point being described as E141.5 N52.0, for example. At some archaeological sites, a coordinate label specifies an area, such as a 10 m square area for excavation; since these types of coordinates do not specify points, they are difficult to use for a geophysical survey. It is easier if the coordinates are small numbers. If the state plane coordinates of the USA or the coordinates of the Universal Transverse Mercator system are used, these numbers can be truncated for simplicity of recording. In most geophysical recording systems, positive coordinates are North and East, while South and West are given negative values; a designation of South 23 is the same as a North value of -23. In this report, the borders of all of the contour maps have negative values for south and west coordinates; grid north is always toward the top of each figure. In some coordinate systems, the labels X and Y will substitute for approximate East and North directions.

A geophysical grid is defined by a reference point and a direction, or by two reference points. If there is an historical building at the site, it may be practical to align the geophysical grid with the direction of that building, and make a corner of that building the reference point for the grid. This is what I did at Petersburg; see Fig. A77.

If the area of survey is larger than 200 m long, it may be necessary to use a good transit, theodolite, or EDM (Electronic Distance Measurement) instrument to locate the stakes. Since the area of my staking at Petersburg covered a distance of about 700 m, I used

a theodolite to determine the stake locations.

Small dots in Fig. A68 locate the wooden stakes which I set; these are spaced to form 100 ft (30 m) squares. I drove wooden stakes which were about 2 cm square into the ground so that they extended above the ground by only about 1 cm. This prevented any problem from lawn mowing and people walking in the area. I also sprayed blue paint on the ground and grass in the vicinity to help locate the stakes. I worked at Petersburg at intervals separated by a month or so. When I arrived for a period of field work, I had to relocate the stakes. If the blue paint from the prior survey was still readily visible (as it was in the winter), the stakes were easy to find. If the paint was lost, I had to relocate the stakes with a tape measure. Then, I placed flags on tall plastic rods to mark each stake location for the week of my survey; I removed these at the end of the week. I left the flags in the wooded area between surveys, but these were gradually lost during the two years of survey. On average, it took me 1.8 hours to relocate and mark these stakes every time I returned to Petersburg.

Most surveys are done in smaller areas, and simple equipment is adequate for setting up the grid. One of the most valuable items is an optical right angle sight. These small instruments use glass pentaprisms to allow quite accurate 90 degree angles to be determined. They cost about US $100 and can be bought from companies which sell equipment to surveyors. A tape measure can be used to make a 90 degree angle with the aid of a triangle whose sides are a multiple of 3, 4, and 5 m (Gardner 1964), but the optical sight is much easier and more accurate.

It is much better to have geographic north (also called true north) on the site map rather than magnetic north; this is because the direction of magnetic north changes from year to year (Layne 1995). In the USA, magnetic north has changed direction by 5 - 10 degrees during the last century. At London, where records have been kept longer, magnetic north has changed by over 30 degrees in the last 400 years. For all practical purposes, true north is a constant direction. While magnetic north can be estimated to an error of less than about 3 degrees with a compass, different procedures are needed to find geographic north. While these procedures are somewhat more difficult, they are also more accurate than a compass measurement. Five different methods are outlined below.

Get an accurate map of the area (such as a U.S. Geological Survey topographic map if the area is in the USA) which has a true north arrow or a latitude / longitude grid. See if there is a long linear feature near your area of interest; this feature might be a straight section of road or railroad track. Measure the true angle of this feature on the map with a good protractor to an accuracy of about a degree. With a transit, theodolite, or EDM, transfer this angle from the feature to your site. As an alternative, measure the azimuth of the linear feature with a magnetic compass (if there is iron at the feature, put a pair of stakes offset from the feature by at least 10 m and measure their angle); subtract the measured true angle and the result is the magnetic azimuth of true north.

At Petersburg, the straight section of the park road, shown in Fig. A68, may be adequate, but it is rather short. I measured this angle, but it gave me an error of about 2 degrees.

If you know the magnetic declination at the location, this will allow you to convert magnetic north to true north. First, calibrate your compass (without this, you should expect an error of as much as about 5 degrees); a precise needle compass, such as a surveyor's compass or a trough compass on a theodolite is needed. The accuracy

of the measurement is also limited by the fact that the direction of magnetic north changes by about 0.2 degree during the average day. Then, determine the magnetic declination at your site on the date of your measurements. There are several ways of doing this.

A recent, good navigational or topographic map of the area will show the magnetic declination at a particular date and may also give an estimate of the annual change in declination. Without a correction for the annual change, maps older than 10 years may have an error of over one degree. A local surveyor may know the current value of declination. In the USA, the current magnetic declination for any location can be determined by contacting the National Geophysical Data Center (NOAA, Code E/GC4, 325 Broadway, Boulder, Colorado 80303). Fig. C17 is a plot of the change in magnetic declination at Petersburg which I have determined from the computer program USHD which is available from the NGDC above. Outside the USA, the current magnetic declination can be estimated from a global approximation of the magnetic field of the Earth; this procedure is described in Volume C.

At Petersburg, my measurements with a magnetic compass indicate that magnetic north is about 7 degrees west of the grid north which I used; I estimate that the error of this magnetic north direction could be about 2 degrees. As seen in Fig. C17, true north during the time of this survey was about 9 degrees east of magnetic north, so true north should be about 2 degrees to the east of grid north.

The procedures above are adequate if you wish to determine the direction of true north to an accuracy of about 1 degree; if you need an angular accuracy of one minute or better you could measure the direction of the Sun, or a planet or star. For this astronomical method, you will need to know the precise time, and the location of the measurement to a moderate accuracy. The direction to the Sun can be calculated for any time and location, just as was done for the photographic analysis of Fig. A85. True north is determined by measuring the actual direction to the Sun and comparing it to the calculated direction (Davis and others 1986 p. 430).

Accurate time is best gotten from short wave radio stations, such as WWV from the USA (5, 10, 15 MHz), CHU from Canada (7335, 14670 kHz), or the BBC (the start of the 6th pip marks the hour). An accuracy to within about a half second is needed. The location of your test can be determined with adequate accuracy using a good map.

The angle or the azimuth of the Sun can be measured with a transit, theodolite, or compass, depending on the accuracy needed. An Electronic Distance Measuring instrument probably is not suitable for observation of the Sun, for the Sun's brightness can damage the sensors of the EDM.

The true angle of the Sun can be calculated by one of several approaches. If you will do only infrequent measurements of true north, it may be easiest to get an almanac (Elgin, Knowles, and Senne 1994). The angle of the Sun may also be determined by trigonometric calculations with a simple hand calculator (Duffett-Smith 1988).

My solar measurements at Petersburg indicate that true north is an angle of 2 degrees 2 minutes east of the grid north which I used. I measured this direction twice (in 1991 and 1993) and found a difference between the two measurements of less than 2 minutes.

The geographic coordinates of two staked locations can be determined with a GPS receiver; differential measurements will usually be necessary for sufficient accuracy. These coordinates can be converted to a geographic direction relative to true north. A gyroscopic compass may be suitable if the site is underground or if clouds prevent a solar observation (Davis and others 1981 p. 486).

General survey procedures

The general procedures which I use are described here. While others have different procedures, I find the methods here to be very efficient and fast.

Geophysical surveys are commonly done within rectangular areas, but other measurement procedures are best for some applications. The boundary of the site may be defined by trees or bushes and therefore it could be a complex shape; the geophysical survey can be extended to fill the irregular area, although this will take more survey time than that needed for a simple rectangular area. Geophysical measurements are often made in a checkerboard pattern. The grid of points is a square pattern and the spacing between the measurements is the same in the two perpendicular directions. Widely-spaced lines of measurement may be suitable for locating large features or for defining the boundary of a site. These may be single, isolated lines; however, sometimes a group of two or three closely-spaced parallel lines can give more reliable data. These groups of lines may be widely separated. The lines of measurement may also radiate from a point; this may be suitable only for the survey of a mound.

During the geophysical survey of a rectangular grid, points are most readily located with the aid of a guide rope which crosses the grid. Tape measures may be placed along the two opposite sides of the grid and the guide rope may be stretched between the corresponding points on the two tape measures. Instead of tape measures, which will blow aside, it may be better to place temporary markers at the points where the guide rope will be set; small stakes, stones, or spray paint marks can be used for this.

While fiberglass or cloth tape measures are accurate, they are difficult to use if the site is windy. Calibrated ropes, called rope chains or surveyor's ropes, are much easier to work with. These are essentially non-elastic ropes which have permanent markers along their length at 0.5 m intervals. These can be pulled quite tight and there is no problem with them turning the wrong side upwards. These rope chains can be bought from several manufacturers of survey equipment.

A normal rope which has been calibrated is also excellent for the guide rope which defines each line of measurement. If it is non-elastic, it will be more accurate. However, if there are trees in the way, or if the surface is steep, a non-elastic rope will be too short at its ends and points will be in error. For these situations, an elastic rope will be better. A normal cotton or nylon rope can be stretched by about 1 m in a 100 m length. This rope can be prepared with markers along it which indicate each measurement point. These markers may be painted bands; distinctive marks should indicate 10 m multiples.

After each line of measurement is finished, the guide rope can be moved parallel and a new line begun. For conductivity and magnetic surveys, you will be able to estimate short distances visually from the rope to the measurement points, and it may not be necessary to move the rope for every line of measurement. Depending on the accuracy needed, it may be possible to estimate the correct distance from the rope for one or two lines of measurement on either side of the rope. This will save time. For most types of survey, it is good to try for a maximum error in the location of measurements which is about a quarter of the distance between measurements.

Unless there is a good reason for another orientation, the guide rope should always be extended the long direction of the survey rectangle. This will reduce the number of times that the rope needs

to be moved, and it will speed the survey. For the same reason, the lines of measurement should be as long as possible.

There are several different types of measurement traverse which are suitable for geophysical surveys. For some surveys, a zig-zag or boustrophedon survey will be fastest; after you finish a line, you turn around and measure in the other direction. For some surveys, measurements may be more accurate if they are recorded while traversing in only one direction. For other surveys, a serpentine sequence may be easiest and fastest. A few measurements are made along a line moving away from the guide rope; then you move forward one measurement interval and make measurements moving toward the rope and then across it to the other side.

During my survey of the Taylor House grid at Petersburg, my preferred direction for the guide rope was east-west, and the traverses were 170 ft (52 m) long. For the Fort Morton survey, my magnetic and conductivity measurements were made along continuous north-south lines which were 600 ft (183 m) long. During the Fort Morton surveys, I moved the rope after every 3 or 5 measurement traverses. I placed a line of flagged poles to mark the next line of the rope; because of the hill there and the woods, it was not possible to see from one end of the survey line to the other. In the wooded area, the rope could not be moved sideways, but had to be pulled in and reset on the next line; each shift took me about 22 minutes.

Many geophysical instruments are computerized now, and there is no need to write down any measurements. However, it is still important to write down many notes about the survey. These notes will indicate the spacing between measurements, the direction of the traverses, the direction in which parallel lines progress, and the settings of the geophysical instrument. The notes will also indicate the date of the survey and the start and stop times. The weather can be noted, for it may affect the measurements.

If the measurements are recorded with pencil and paper, these should be written as a matrix of numbers on a page; a notebook with lines ruled in perpendicular directions will simplify this, and I have found it best to write the numbers at the intersections of lines. The numbers should not be written as isolated lists of numbers, for this makes it difficult to compare one measurement traverse to the next. As you do the survey, you will want to compare your current measurements to those you found on the adjacent line which you just finished. If you find that they are consistently higher or lower than those numbers, it will alert you to a possible error. Also, you may be able to see the pattern of measurements, and this may suggest that you should extend your area of survey in order to explore the geophysical anomaly further.

If your measurements are stored in the internal memory of your geophysical instruments, you may have little idea of what your survey has found until you make a map of your measurements later. Do not wait until the end of your survey to do this, unless you are willing to gamble that you made no error which will cause you to have to redo all of your measurements.

Resistivity Surveys

If you have never done a geophysical survey before, a resistivity survey should be the first one you do. Resistivity surveys are simpler than all of the other surveys, and there are fewer things to go wrong. While the measurements can be rather slow, resistivity surveys give good results at more sites than will any other type of survey. Good introductions to resistivity surveying have been given

by several authors (Clark 1990; Weymouth and Huggins 1985; Aitken 1974; Tite 1972; Clark 1969). Because of these other good sources, this section will rather short, and I will emphasize procedures which are not described in these other introductions.

With a resistivity survey, the electrical resistivity of the soil is measured. The unit of resistivity is the ohm-meter, abbreviated ohm-m, where a Greek capital omega can replace the word ohm. This unit indicates the difficulty of sending an electrical current through the soil. A high value of resistivity means that the soil does not readily conduct an electrical current. Sand, gravel, stone, and very dry soil have a high electrical resistivity. Soil which has a large fraction of clay, or which is wet or saline, has a low electrical resistivity. Metals have the lowest resistivity. A short list of approximate resistivities is given below:

Soil	Resistivity, ohm-m	Conductivity, mS/m
Sand, gravel	1000 - 10,000	0.1 - 1
Silty sand	200 - 1000	1 - 5
Loam	80 - 200	5 - 12.5
Silt	40 - 80	12.5 - 25
Clay	10 - 40	25 - 100
Saline soil	5 - 10	100 - 200

The values for electrical conductivity are also listed; as you can see, these increase as the resistivity decreases. Conductivity is measured with a quite different type of instrument; it will be described later.

Instruments

Resistivity meters are the least expensive of all of the geophysical instruments. This is partly because they are rather simple in their electronic circuitry; it is also due to the fact that they are widely used for many applications. While geophysical exploration is a common application, resistivity meters are also used to determine the quality of a grounding rod of an electrical power station or a transmitting antenna. A few years ago, I wrote a summary of the resistivity meters which I could locate and which were available for sale (Bevan 1993); this list may still provide some help to your selection of a meter. If you are familiar with electronics, you may be able to build your own resistivity meter (Williams 1984).

The basic parts of a resistivity meter are very simple. Fig. B1 shows that you can construct one with a very few components. This simple meter will be excellent for your initial tests and will show you the general principle of a resistivity meter; it may also be helpful as an emergency meter. This resistivity meter will be slower to operate than a more expensive meter, but its accuracy may be almost as good.

The major expense for this meter will be the purchase of a good digital multimeter for measuring voltage and current. The only other parts for this meter are: a 6 - 12 volt battery, metal rods for electrodes, and wire.

You will be able to buy the equipment for this resistivity meter at many electrical stores. Digital multimeters are small hand-held instruments for measuring voltage, current, and resistance. These instruments are powered by a battery, perhaps a 9 V battery or several small 1.5 V cells of the AA size. The measurements are shown on a liquid crystal display (LCD); there will be 3 - 4 digits of precision shown on the display.

Probably any digital multimeter (DMM) would be adequate for this resistivity meter. You will be measuring a direct current (DC) voltage of about 5 to 500 mV (millivolts; 5 mV = 0.005 V) to a precision of about 1 mV. You will also be measuring a current of about 1 - 10 mA (milliamperes; 1 mA = 0.001 ampere) to a precision of about 0.1 mA.

It is likely that the older type of analog meter, which has a pointer moving over a dial, would not be adequate for this work; however, if you have nothing else, you should try this type of meter. This type of meter is called a volt-ohm-milliameter or VOM. The principal disadvantage of a VOM is that difficult to read the dial with sufficient precision. Digital multimeters also have a higher input impedance (generally over 10 megohm) than a VOM; this means that the meter itself does not change the measurements by drawing too much power from the circuit being measured.

Your next purchase will be a battery for sending an electrical current through the earth. A voltage in the range of 6 to 12 V will probably be fine. You could use a common lantern battery (6 V) or a lightweight and rechargeable motorcycle battery (12 V). As indicated in Fig. B1, you may also make a 9 V battery, with 6 medium-sized C cells (each with a voltage of 1.5 V) wired in series. The C cells were held in a plastic battery compartment. Since the current output from this battery is very small, this battery would last for over a year's worth of measurements.

The voltage of the battery is not very important. If you wish to measure the earth to a depth greater than 10 m, or if the soil is quite dry, you may need a higher battery voltage in order to get enough current to flow in the soil; a lower precision DMM or VOM may also require a higher voltage for the battery. Commercial resistivity meters can apply voltages of 40 - 1000 volts to the earth. At these higher voltages, painful or dangerous shocks are possible if one is not careful; since you know that you can grab both terminals of a 12 V battery without harm, this lower voltage is quite safe.

You will also need four metal electrodes; these will be driven into the soil to a depth of about 2 - 10 cm. The electrodes can be made of iron, aluminum, brass, or any other metal. Nails or screwdrivers will work fine. Meat skewers made for barbecues are ideal; these are iron rods which are 25 cm long and which are plated to minimize rusting. They are pointed on one end and have a loop at the other; this allows them to be easily pushed into the soil. Surveyor's pins cannot be used because of the paint which insulates them.

The final major item which you will need is wire, perhaps a length of about 5 - 10 m. This wire will connect the battery and DMM to the electrodes. This wire should have a plastic insulation, which must not be cracked or damaged so that bare metal is visible. Stranded copper wire would be fine; solid copper wire breaks more readily than stranded wire. The diameter of the copper in the wire can be in the range of 18 to 22 gauge (a diameter of 0.6 - 1.0 mm).

You can probably use as many as eight connectors for making contact from the ends of the wires to the battery and the electrodes. Alligator clips are excellent, and the name is a good description of the jaws; these clips can have screw terminals. You will need a knife and a screwdriver to prepare these wires with the clips at the ends. If the spacing between your electrodes will be 1 m, then it will probably be easiest to make four wires, each about 2.5 m long and each with alligator clips at each end of the wires. There would be an advantage to having two red wires and two black wires; this would

help you from confusing the different wires on the ground. It might also help if the clips had insulating plastic boots over them.

Fig. B1 illustrates the procedures for operating this simple meter. In Step 1, a tape measure is stretched along the line of measurement and the electrodes are stuck into the soil; the spacing between each adjacent electrode is the same. This distance is called s and it is 1 m for this example. When the electrodes are equally-spaced along a line, the arrangement is called the Wenner configuration. There are many other arrangements of the four electrodes which could be used, and these configurations have different names. The Wenner configuration is excellent for most applications.

If a resistivity profile or map is desired, the spacing between the electrodes remains constant for all of the measurements. If features are thought to be underground at a particular depth, the spacing between the electrodes can be about the same as that depth. With this spacing of 1 m, features between a depth of about 0.5 and 1.0 meter will be accentuated; however, deeper and shallower features will also be detected.

The depth of the electrodes is not very important. An insertion depth of between 2 cm and 10 cm will probably be suitable. It is best that their depth not be more than about five percent of the spacing between the electrodes, otherwise the depth may slightly affect the measurement. It is also best that the electrodes should go deep enough to reach moist soil. If the soil is very dry, the measurement accuracy may be improved by pouring water around each electrode. If you find it necessary to change the location or depth of electrodes during a measurement, you may have to start the measurement over again.

For Step 2, connect the digital multimeter to the middle pair of electrodes. If the leads from the DMM are too short or do not have clips on them, you could use extra wire and alligator clips to span the distance. Remember that no bare conductor or clip should touch the soil or vegetation on it; if this happened, there would be a different path for current flow and an incorrect reading. You can prevent this by placing bare connectors on small plastic sheets.

Set the DMM to read a DC voltage of about 200 mV (if the scale is adjustable) and turn on the meter to measure the voltage between the inner pair of electrodes. Since the battery is not yet connected to the earth, you might expect that the voltage would be zero. While the voltage you measure will be small, it will not be zero. This is because the chemical reaction of corrosion is generating a voltage at the electrodes; because of small differences in soil moisture and chemistry at the two electrodes, there is a net voltage measured at the DMM. This example shows a measured voltage of 19 mV. Commercial soil resistivity meters use alternating current rather than direct current for their measurements; there is no residual voltage like this 19 mV with those meters.

At first, you should watch the voltage at the inner electrodes for a minute or two to see if it remains rather constant. If it changes by a significant amount (perhaps 20 percent), you may not be able to use this simple meter at the site. Before giving up, you should test different electrodes to see if they show less change; you might even consider stainless steel or lead electrodes. You might also try measuring the voltage at a constant delay time after you set each group of electrodes.

The voltage connections of the digital multimeter are labeled as plus and minus (and the standard leads from the meter are colored red

and black). For this example, the red (positive) lead from the meter is connected to the electrode on the right. The voltage shown in the example of Fig. B1 is negative (V0 = -19 mV). If the leads from the meter would be switched, the voltage would be positive.

Next is Step 3: Leave the voltmeter on and connect the battery to the outer pair of electrodes. Since the positive terminal from the DMM is connected to the right hand side of the four electrodes, it is best if the positive wire from the battery also is connected to the right hand side of the electrode array. Fig. B1 shows these polarities.

A different voltage will now be measured. This will probably have a magnitude which is much larger than the voltage measured in step 1. For the example of Fig. B1, the measurement is a positive voltage of V1 = 93 mV. Note that this is much smaller than the 9 V of the battery; most of the battery's voltage is "lost" very close to the two outer electrodes.

If the measured voltage was -10 mV rather than +93 mV, it would mean that the battery did not change the voltage very much at the middle pair of electrodes. It would also mean than it would not be possible to get a very accurate measurement of resistivity. It might help to try watering each electrode or driving them deeper into the soil; you might also use a higher battery voltage.

The final measurement is Step 4. The current going through the earth from the battery is measured. The DMM is switched to measure current; on some meters, it is also necessary to change the location of one of the wires going into the meter. The connections to the inner pair of electrodes are removed and the DMM is put in the path of the battery. Fig. B1 shows the polarity requirements: the positive terminal from the DMM can be connected to the positive wire from the battery.

The meter would not be damaged by having its connections reversed; the only change would be that the current would have a negative value. The example in Fig. B1 has a current of I = 2.2 mA coming from the battery.

If this current was less than 0.5 mA, it could have indicated trouble with the measurement. A low current is an indication that the resistivity measurement is going to be less accurate. The procedures mentioned in step 3 could be used to try to increase this current.

Since the battery voltage was 9 V, Ohm's law allows a calculation of the electrical resistance between the outer pair of electrodes. This resistance is the ratio of 9 V divided by 2.2 mA, or a value of 4100 ohms. This is a low resistance and means that there is no difficulty with the measurement. A resistance of 50,000 ohms would indicate that the soil was quite dry and sandy; the resistivity measurement would then be less accurate.

With Step 5, the earth resistance can be calculated by the simple equation of Fig. B1. Be careful with the signs of numbers. The current, I, should always be a positive value. Voltage V1 will usually be positive also; however, V0 may be either positive or negative. The difference of the voltages must also be positive.

The calculation of this example gives a resistance of 51 ohms. If you are doing a resistance profile or map, you can plot this value of resistance; by convention, it is plotted at a point which is at the midpoint of the four electrodes.

You may ask why four electrodes are used for this measurement of resistance, for you may have noticed that the DMM has the capability for measuring resistance directly. Also, in step 4, the resistance between the outer pair of electrodes was calculated; this value was

4100 ohms, quite different from the 51 ohms which we calculated here.

The answer is this: We must use four electrodes rather than two because this allows the measurement to be little affected by how deeply the electrodes are inserted into the soil. If you switch the DMM to measure resistance and then connect the two leads from the DMM to a pair of electrodes in the soil, you will find that the resistance will change by a large amount if the depth of the electrodes is changed only a little; therefore, this measurement is telling us almost nothing about the soil itself. With four electrodes, this effect of electrode depth is almost eliminated.

The resistance value of this calculation would be very different if we used a different electrode spacing or if we otherwise changed the arrangement of the four electrodes. It can be convenient if we convert the resistance values to the more universal values of resistivity. This is Step 6.

The conversion of resistance to resistivity is done with the simple equation shown at the bottom of Fig. B1. The resistance value is multiplied by the electrode spacing and then by a constant value of 6.28; for this test, the calculation yields a resistivity value of 320 ohm-meters.

Unlike a value of resistance, a resistivity value can be looked up in a handbook and it can be readily compared to other sites and surveys. This value of 320 ohm-m indicates that the soil at this location must be quite sandy or rocky. It says that there definitely must not be a large fraction of silt or clay in the soil.

Stores which sell equipment for gardeners have a soil moisture meter which will indicate if the soil needs watering. These meters have a single metal rod with an insulated electrode at its tip. The meter measures the electrical resistance between the two metal parts of the rod; some meters will have the rod made of two dissimilar metals so that it acts like a battery also (Logan 1945 p. 198). In principle, these gardening meters can be used to measure the resistivity of the soil. Their principal disadvantage is that they are very sensitive to changes just at the junction between the two parts of the electrode; if the insulating gap was larger, these meters would measure a larger volume of the soil. The rods have to be inserted to the depth at which measurements are wished.

Mapping

If you have many measurements to make, your survey will go much faster if you have a good resistivity meter. A good resistivity meter sends an alternating current into the soil, and this eliminates the constant voltages which would otherwise be measured at the electrodes. While the home-built meter described above may require more than a minute to make each measurement, a standard resistivity meter may only require about 10 s to make each measurement.

Resistivity surveys are commonly done by making measurements along a straight line. If the four earth-contacting electrodes are equally spaced, the survey is said to be done with the Wenner configuration of electrodes. A sketch of this is shown at the bottom of Fig. A89.

When the Wenner configuration has the four electrodes close together, the measurement emphasizes soil contrasts which are close to the surface. If the spacing between the electrodes is larger, the measurement is affected by strata which are deeper in the soil. If you are searching for a moderately compact object (ideally, a sphere) in the soil, the distance between the adjacent resistivity electrodes should be roughly the estimated depth to the middle of that object

(Van Nostrand and Cook 1966 p. 263). If you wish to locate the edge of a buried soil stratum, the electrode spacing should be about twice the estimated depth of the layer (Barker 1989). Since a resistivity measurement will readily detect features both shallower and deeper than its optimum depth, there is no need to try to be very precise in selecting a spacing for the electrodes. It is generally more important to select a spacing which makes it easy to do the field measurements.

After a measurement is completed, there are two ways of moving the electrodes down the line of the survey. If you have a number of people to help, four people can each move one of the electrodes. With this approach, you can move each electrode any distance you wish, but it is generally adequate to move them a distance which is equal to the spacing between the electrodes. Instead of having four people move the electrodes, you could construct a rigid bar to hold the four electrodes at the proper spacing (Ehrenhard, Athens, and Johnson 1984); then, one person can move all four electrodes at a time.

As another approach, you could leapfrog the electrodes, one at a time. Just have someone move an end electrode and its wire to the opposite end of the array. The person carrying the resistivity meter will move the wires and connections on the meter at the same time. There are ingenious switching systems which will eliminate the need for the meter operator having to move the connectors (John Weymouth 1982 personal communication).

Each measurement is plotted in your notebook at the midpoint between the four electrodes. You should also record the direction of the line of electrodes which you used; the measurements would be somewhat different if the line of the four electrodes was rotated by 90 degrees.

Resistivity surveys are most easily done at a site which has moist soil; if the soil is very dry, it may be difficult to drive the electrodes into the soil and poor contact with the soil will cause errors in the measurements. You can check for these errors by moving each of the four electrodes by a small amount; an error is detected if there is a large change in the resistivity then. If the soil is dry, a better electrical contact to the electrodes is possible if a small amount of water is poured around each electrode. While this will affect the reading, the error will be smaller than if the electrodes were not watered. Resistivity measurements can be made on hard or concrete pavements if absolutely necessary. Moisten a thin sponge with saltwater and put a metal plate on top of it; with four of these, an adequate contact to the pavement may be possible. Electrodes may be driven into the mortar of a wall, but the spacing between the electrodes may not be uniform, and you may have to adjust your measurements for this (Tagg 1964 p. 17). If a rock or tree root prevents you from inserting an electrode at the correct point, shift the electrode a short distance perpendicular to the line of the four electrodes.

For normal soil, any type of metal rod can be a good electrode; screwdrivers or meat skewers are suitable, but they are short. You may add extensions to these so that you do not have to bend over to place an electrode. Since normal iron electrodes will rust, you may use stainless steel to minimize any cleaning that you have to do.

For your first surveys, the Wenner configuration is the simplest and easiest to begin with. Since I do geophysical surveys by myself, the Wenner array is not practical for me. I apply a method called a pole-pole configuration (Sumner 1976 p. 23); for this configuration, two electrodes, rather than four, are moved during the survey. The

other two electrodes remain at a fixed location for the entire survey. A sketch of this arrangement is given in the middle of Fig. A89.

The two fixed, or reference, electrodes should be quite distant from the area of survey, and also distant from each other. For my surveys, I typically take the current reference electrode to a distance of about 200 m from the area where I will do the survey. I then take the voltage reference electrode about 100 m along a line toward the current electrode and then carry it about 100 m to the left or right. This pole-pole arrangement cannot be used at all sites, for the long wires going to the reference electrodes may cause difficulty if there are people walking in the area; you can use a shorter distances to the reference electrodes if a slightly larger error in the measurements is acceptable (this error is a broad gradient in the measurements, and it is generally correctable).

During my surveys at Petersburg, the reference electrodes were located in different areas for the surveys which I did on the two sides of the park road which separates the Taylor House grid and the Fort Morton grid. The electrode locations are plotted in Fig. C157.

It takes additional time to place the distant reference electrodes for the pole-pole array. However, the resistivity maps generated with the pole-pole array can be simpler than those made with the Wenner array. This is because Wenner resistivity maps can have auxiliary or spurious patterns adjacent to small features. Instead of finding just high resistivity measurements over a high resistivity feature, there might also be abnormally low values of resistivity before and after the feature along the line of measurement (Weymouth and Huggins 1985 p. 224). This problem is reduced with the pole-pole array.

The pole-pole array is not the same as what has been called the twin-electrode, two-electrode, or two-probe array (Clark 1986; Aspinall and Lynam 1970; Kelly, Dale, and Haigh 1984). For those other arrays, the two reference electrodes are placed close to each other; this makes it easier to set the two reference electrodes. However, the resistance values measured with the twin-electrode array cannot be converted to resistivity. This means that the type of soil cannot be determined, and it also means that a resurvey of a site cannot be compared to an earlier survey. While the pole-pole array takes more time to set up, the benefits which it offers can be worth the time.

For the Petersburg surveys, the spacing between the two moving electrodes of the pole-pole array was fixed at 5 ft (1.5 m). This array detects features to the same depth as does the Wenner array (Roy and Apparao 1971), so my survey accentuated features in the depth range of 0.7 to 1.5 m. For these resistivity surveys, I placed two calibrated ropes along parallel lines, spaced by 5 ft (1.5 m). I made measurements with the electrodes along one line, and also with the electrodes perpendicular between the two lines. The measurement sequence is illustrated in Fig. C80. The measurements were plotted at the midpoint between the two electrodes. The conversion from resistance to resistivity is the same for the pole-pole array as it is for the Wenner array; see Fig. C87.

The locations of my resistivity measurements in the Taylor House grid are shown in Fig. B2. The resistivity map of the area is plotted as Fig. B3. It took me 5.5 hours to make the 1414 measurements of this map; this does not count the time required to place or retrieve the reference electrodes.

The negative numbers at the bottom border of the contour map indicate that those coordinates are to the west. Numbers on some of

the contour lines indicate the electrical resistivity along that line; the resistivity of unlabeled lines can be determined from the adjacent labeled lines. Small tick marks or hachures along a line indicate that the contour encircles low values.

If the soil below this area was uniform, the resistivity would have been constant everywhere and there would be no contour lines in this map. Irregularities in the soil cause small and large areas to have different resistivity, and the contour lines reveal the patterns of these changes; these patterns are called geophysical anomalies.

Note that most small-area anomalies have a high resistivity; these anomalies may be due to a poor contact at an electrode. There is very little correlation between the small-area anomalies found by this survey and the anomalies detected by the radar, magnetic, and conductivity surveys.

This map has a small-area irregularity, noisiness, or graininess; this makes it difficult to see some of its patterns. The larger patterns can be clarified by smoothing the measurements of the map. This has been done for Fig. B4. The smoothing is a simple operation. Each original measurement has been replaced by the average of the sum of that measurement and the eight surrounding measurements. This simplifies the map of Fig. B4 and shows the general pattern of the resistivity. However, this smoothing also removes small-area anomalies, and it also increases the area of each anomaly. These changes must be kept in mind during the interpretation.

The resistivity is highest on the east side of the survey area; the soil there must be sandier than the soil to the west. The high values throughout the map indicate that the upper layers of soil must be quite sandy. There is a U-shaped pattern near E20 N90. This is centered on the eastern side of the Taylor House cellar (compare the map to Fig. A3). The low resistivity may be caused by the brick wall of the cellar, but the anomaly does not correlate with the location where the cellar wall is closest to the surface. Perhaps the anomaly could be partly caused by a trench which was dug to remove some of the brick from the wall during the Civil War.

There is not much to be done for the interpretation of this resistivity map. The areas of high and low resistivity are simply distinguished; this has been done in Fig. A21.

It can be valuable to check on the reliability of the resistivity measurements, and a good way of doing this is just to repeat the measurements on one line more than once. This is what I did at the end of my measurements for the Taylor House. Three repeated lines are plotted in Fig. B5; these show an acceptably small difference between them. This was not a complete test however, for I did not move the guide rope between the repeated surveys.

A resistivity measurement will change if the array of electrodes is rotated to a different direction. Features within the soil can cause these differences, and the soil itself may have a resistivity which is dependent on the direction in which the electrical current flows. It is possible that plowing the soil will create this directionality, for it shears the soil. The archaeological excavations in the Taylor House area found that the soil had been disturbed by plowing to a depth of about 0.3 m (Brooke Blades 1992 personal communication).

Natural changes in the formation of the soil or during the deposition of the deeper sands could also influence the directionality of resistivity measurements. I tested for this directional effect at the Taylor House with a measurement of azimuthal resistivity (Taylor and Fleming 1988). The location of the test is shown in Fig. B2, and

the results are plotted in Fig. B6. The resistivity is clearly higher when the line of the electrodes was in a north-south direction. While I do not know if this might be indicating something about the plowing of the soil here, the test might be a reference for comparisons at other sites.

The area of the Fort Morton grid was too large for me to do a complete resistivity survey there; however, I made resistivity maps of the three small detailed areas shown by rectangles in Fig. B7.

The resistivity map of the Bombproof detail located one of the bombproof trenches very clearly and it also shows parts of two other trenches. The original measurements are plotted in Fig. B8 and the smoothed version is given in Fig. B9.

By comparison with Fig. A36, it is seen that the trench #2 was detected most distinctly by the resistivity survey. All of the trenches are detected as higher than normal resistivity; this suggests that high resistivity sandy soil from near the surface may have replaced the silty soil at the bottoms of the trenches when they were filled in at the end of the war.

The resistivity map also suggests why the other trenches were not as readily detected. There is an area of low resistivity in the middle of the Bombproof detail. This covers part of the bombproof trenches; it also degraded the radar profiles in this area. It is possible that this low resistivity soil was from the mounds of soil over the two powder magazines which were just to the west. The excavations for these two powder magazines were probably deeper than any of the other fortifications here; at that greater depth, they would have encountered a lower resistivity soil which would have been brought to the surface and mounded over the top of the magazines. When these mounds were leveled, the soil might have been shifted to the east and this lower resistivity soil might now cover the bombproof trenches and thereby mask them.

Fig. B10 is a surface or "fishnet" plot of the data of Fig. B9. The low values in the foreground are near the northern magazine; the southern magazine does not have this anomaly. These types of plots allow the relative amplitudes of the patterns on geophysical maps to be easily seen.

The resistivity measurements over the Trench detail are plotted in Fig. B11. The line of the main fortification trench is marked by high resistivity along line E480. Therefore, this is the same polarity as the anomaly of the trench found in the Bombproof detail. The smoothed map of Fig. B12 does not add much, for the original data had a simple pattern already. The resistivity is rather high in the northern part of the area; there must be a greater thickness of sandy soil there.

Metal objects are only rarely detected by resistivity surveys; this is generally good. A large metal object should be detectable as a very low resistivity, and this is just what was found with the resistivity survey over the Iron detail; see Fig. B13. This area had the lowest resistivity of any place tested in the Fort Morton grid; however, the west side of the Taylor House survey area had even lower readings of resistivity.

The other geophysical surveys delineated a buried iron pipe in the northwest corner of the Fort Morton grid. Resistivity profiles were made across this pipe; the line of the profiles is shown at the top of Fig. B7 and two sets of measurements are plotted in Fig. B14. Both measurements indicate a drop of about 30 ohm-m, independent of the orientation of the two electrodes of the pole-pole array. While I do not know if this low resistivity is caused by the pipe itself, the

anomaly is clearly located at the pipe.

Sounding

Resistivity profiles and maps show how the soil changes in the horizontal or lateral direction; these types of surveys reveal the location and shape of buried features, but they do not indicate very much about the depth of the features. A simple variation of this survey will allow the depth of broad features to be estimated. This procedure is called a resistivity sounding.

A resistivity sounding furnishes estimates of the thickness and resistivity of soil layers in an area. This information can be very valuable for a prediction of the depth and type of soil which will be encountered by an excavation. The depth of bedrock might also be determined by a resistivity sounding.

With a resistivity profile, the separation between the resistivity electrodes remains at a fixed value, and the electrodes are shifted about the area to be surveyed. With a resistivity sounding, the center of the array of electrodes remains at a fixed location, and the spacing between the electrodes is changed. When the electrodes are more widely separated, the measurement of resistivity averages through a greater depth. An analysis of the measurements of a resistivity sounding will then estimate the depths of soil layers.

The Wenner array is excellent for resistivity soundings. A basic electrical schematic of a resistivity meter is shown in Fig. B15, and the separation between adjacent electrodes is the quantity S. This figure shows the first resistivity sounding which I made at the Taylor House. For that sounding, the center point between the four electrodes was at E66 on line N85; this is east of the Taylor House cellar. The 12 measurements which I made are indicated by circles in the graph; I changed the spacing between the electrodes in steps from 0.1 to 3 m. Note that both of the axes of this plot are logarithmic; this is the typical way of plotting soundings and it is the best way.

The graph of Fig. B15 reveals some interesting facts. The values of resistivity are higher than would be found at an average site; the soil must have a large fraction of sand or gravel within it. Had the soil underground been quite uniform and unchanging with depth, the sounding would have plotted as a horizontal line. It is not, and so the soil is stratified. The resistivity is lower when the electrode spacing is larger; therefore, the resistivity decreases with increasing depth underground. Finally, the sounding curve is rather flat for small and large electrode spacings; the readings gradually decrease from high to low and do not show more complicated changes. This suggests that the soil stratification is rather simple; there are only two distinct layers which were detected.

A simple analysis can furnish an estimate of the thickness of the upper soil layer, and it can also give good estimates of the actual resistivity of the soil in the two layers. The analysis is done by the procedure called curve matching (Keller and Frischknecht 1966 p. 135). The measurements are plotted in the standard form shown in Fig. B16, and then these measurements are compared to the calculated curves which are in Fig. B17.

The curve of Fig. B16 is just slid over the surface of Fig. B17 (without rotation) until the measurements most closely match one of the calculated curves in Fig. B17; this match can be seen by holding the two sheets in front of a light. A reference point in Fig. B17 is then transferred to Fig. B16; this point is where the horizontal line marking a resistivity = 100 intersects the vertical line indicating that the spacing = 1; these are both solid lines in Fig. B17. This

reference point is marked with a square in Fig. B16. The vertical coordinate of this point is the interpreted resistivity of the upper layer (1400 ohm-m); the horizontal coordinate is the thickness of the upper layer (0.6 m). Comparison of the measurements to the model curves also shows that the measurements fall midway between the curve labeled 0.2 and that labeled 0.1; therefore, the ratio of the resistivity of the lower layer to that of the upper layer is 0.15 and the resistivity of the lower layer is 0.15 x 1400 = 210 ohm-m.

You will see that two of the points on the measured curve are rather different from the smooth curves in Fig. B17. The low resistivity measured with S = 0.8 m could be an error. The low value with S = 0.1 m could also be an error, but it is also possible that there is a thin layer with lower resistivity right at the surface of the soil. This analysis has assumed that there are only two layers; if there are actually three or more different layers, the resistivity sounding curve might show smooth oscillations between three or more high and low values of resistivity. While a qualitative analysis may be enough for you, if you wish to analyze the depths of the different layers, a more complicated curve matching is needed (Orellana and Mooney 1972; van Dam and Meulenkamp 1975).

The analysis of this resistivity sounding assumed that the soil had a very simple stratification, and that the resistivity of the soil did not change in a lateral direction; this means that a resistivity map of the area would show no features. If this assumption is not correct, the resistivity sounding curve may be affected by these lateral changes. Fig. B19 illustrates a resistivity sounding which I did over the cellar of the Taylor House. The measurements, indicated with circles, show the same type of resistivity decrease which was found to the east; that resistivity sounding is shown in Fig. B15. However, there is an additional dip in the measurements when the electrodes were separated by a distance of about 4 and 5 m. It is impossible for horizontally stratified soil to cause this abrupt a change in the sounding curve; therefore, the cause of the dip must be a lateral change in resistivity, rather than a vertical change. The outline of the buried cellar is estimated in the figure; notice that the outer electrodes cross from inside to outside the cellar at a spacing of about 5 m. This lateral contrast is the cause of the unusual values of the sounding.

Volume C describes methods for the measurement and analysis of resistivity soundings which are more complicated and precise.

Magnetic Surveys

After resistivity surveys, magnetic surveys should be the next procedure you should consider doing as you begin to learn about geophysical exploration. With a magnetic survey, there are more detailed procedures to learn than are needed for a resistivity survey.

After you have made a magnetic map, you will be able to estimate the depth and mass of the buried iron-containing objects. This will give you valuable information, but it will require additional time for learning the method. The basic procedures for doing magnetic surveys, and interpreting the measurements, have been clearly described by several writers (Breiner 1973; Weymouth and Huggins 1985; Weymouth 1986; Clark 1990; Logachev and Zajarov 1978).

A magnetic survey is typically done with two people, and this may be fewer than the number needed for a resistivity survey. A magnetic survey is much faster than a resistivity survey, and it can readily be done in wooded areas. The cost of a magnetometer will be more than the cost of a resistivity meter.

Magnetic Surveys

Instruments

There are many different types of magnetometers, but all of them measure the same thing: The strength or amplitude of the Earth's magnetic field. Iron-containing objects are good "conductors" of this magnetic field, and the field will tend to concentrate in those objects; because of this concentration in the object, the field nearby will be reduced. With a magnetic survey, one measures the warping or distortion of the Earth's field caused by iron objects.

The unit of magnetic field is the nanotesla, abbreviated nT; this unit name is called the gamma in older writings (1 gamma = 1 nT). The average strength of the Earth's magnetic field is about 50,000 nT. The amplitude of the magnetic anomaly from typical archaeological artifacts may be in the range of 1 - 100 nT, which means that the changes in the measurements during a survey are very small. With a resistivity survey, the ratio of the highest to the lowest measurement may be about 10; with a magnetic survey, this ratio may be much smaller, perhaps about 1.01. However, magnetometers are very accurate, and most will measure to a precision of 0.1 nT.

The names for the different types of magnetometers describe some fundamental aspect of their physical principle of operation. The most common instruments are called proton (or proton precession), cesium (or alkali vapor), Overhauser, or fluxgate magnetometers (Dobrin and Savit 1988 p. 660). All of these different types of magnetometers are suitable for archaeological surveys, and the differences in their capabilities are not always important.

Any of these different types of magnetometers can be configured in two different modes; they can have a single sensor and measure the total magnetic field of the Earth, or they can have two sensors and measure the difference in the field at the two sensors. This latter type of instrument is called a magnetic gradiometer. While fluxgate magnetometers are almost always configurated only as magnetic gradiometers, the other instruments can be changed from one mode to the other. Fig. A87 has a sketch of a magnetometer in two different modes of its operation.

There are advantages and disadvantages to the two modes of operation. A magnetic gradiometer allows an automatic correction for changes in the strength of the Earth's magnetic field during a survey; a total field instrument requires a more difficult correction. A magnetic gradiometer is not affected by moderately distant iron objects; these may be cars passing on a nearby road. Also, a magnetic gradiometer can distinguish features which are closer together than can a total field magnetometer. However, it is necessary to make measurements at a closer spacing with a gradiometer than with a total field instrument (Reid 1980). A magnetic gradiometer will be more difficult to carry, since it has two sensors rather than one. A gradiometer will indicate the wrong measurement if it is tilted; a total field magnetometer does not have this problem. Since a magnetic gradiometer measures the difference between two nearby sensors, the anomalies which it measures will be smaller than those measured with a total field magnetometer.

Some modern magnetometers allow a great flexibility in their operation; this will allow them to be applied to a wide variety of sites and circumstances. In addition to being able to be operated as both total field instruments and as gradiometers, the spacing between the sensors can be changed in the gradiometer mode and the sensor height can be set at any value. These options allow the resolution of the measurements to be changed. These modern magnetometers will allow

a difference mode between two widely-spaced sensors: One sensor may be stationary and provide a correction for the temporal change in the Earth's field. Alternatively, both sensors may be separately carried in order to double the search rate for isolated features.

Almost all magnetometers now being manufactured have their measurements stored within the internal memory of the instrument. No manual recording is needed and the measurements can be automatically transferred to a computer. Most magnetometers allow the operator to make a trade-off between the speed at which measurements are made and the accuracy of those measurements. You will need to consider all of these factors when you decide on which instrument you will rent or buy for your survey. An earlier review of many instruments is getting moderately old now (Bevan 1991), but it might give you some information to help your decision.

Magnetometers measure the total field or the strength of the Earth's magnetic field; they do not measure the direction of the Earth's field. A magnetic compass measures only the direction of the field, and not the strength (although the oscillation period of the compass needle is related to the strength of the field). Electronic magnetometers were first developed in the middle of this century; before that, magnetometers were entirely mechanical and were not dissimilar to magnetic compasses or dip needles (Swanson 1936; Wilson 1931; Howell 1959 p. 361; Haanel 1904). This type of mechanical magnetometer was used for an early archaeological survey (Gramly 1970); however, the speed and accuracy of these instruments is low. If you are seeking a massive iron object, a compass may be all you need to locate it. This is was done in 1956 for a successful search for a boat which was sunk on the Mississippi River during the Civil War (National Park Service 1971). The massive iron object near Fort Morton at Petersburg is quite detectable with a magnetic compass. The circles and squares in Fig. B20 show that the apparent direction of magnetic north changed by about 2 degrees near the iron-filled well. The deflection of the compass needle is indicated in Fig. B21, although it is exaggerated by a factor of 20 there for clarity.

Before the survey

For your first surveys, you should try to select sites which will have magnetic anomalies which have a rather large amplitude, for these will be easier to survey; historic sites usually have much larger anomalies than prehistoric sites.

Before you begin a magnetic survey, it is good to check if there is very much modern iron trash in the area of the survey. This may be on the surface of the ground and quite visible. If the magnetic sensor for your survey will be at an elevation of about 1 m, iron objects the size of a metal can lid or larger are best removed from the survey area. If the magnetic sensor will be lower than 1 m, you might also remove every iron object larger than a small nail. If you do not have enough time to clear a site of this magnetic trash, you will need to analyze the magnetic measurements and indicate where trash is likely to remain. There may also be additional iron at a shallow depth in the soil. You can search for this with either a metal detector or with an audio-indicating fluxgate magnetometer; if it is necessary to do a careful search for buried iron trash, this site cleaning may take longer than the magnetic mapping of the area.

It might be valuable to do a quick and unrecorded exploration of the site before you begin your mapping. This will tell you the range of measurements to be expected. It might also indicate that only a small part of the site should be mapped; the other areas may have no

anomalies or they may have too much interference from unmovable iron objects.

You should also check for iron on the person who will carry the magnetic sensor. You have to be most careful with any iron which is closest to the sensor. You can distinguish iron objects from other metals readily with a small magnet; just see if it sticks to the metal. While the metal in keys and eyeglasses can be non-magnetic, zippers and belt buckles can be quite magnetic; some shoes have a steel bar in them and these can cause serious errors to a magnetic survey. You can check all of the clothing of the sensor carrier with the magnetometer which you will be using. Just tie the magnetic sensor to a tree at the same height that the sensor will be carried. Make a few magnetic measurements with no one near the sensor. Then have the sensor carrier stand closer to the sensor than normal, and make a few measurements as that person rotates at 90 degree angles around a circle. Finally, make a few more measurements with the carrier away from the sensor, in order to make sure that these measurements are about the same as they were at first. If the maximum change with the carrier close to the sensor is only about 1 - 2 nT or less, then that person will probably have no noticeable affect on the measurements of the magnetic map.

You should decide what the height of the magnetic sensor should be. For almost all surveys, this will be in the range of 0.3 - 1.5 m. If you seek to locate small and shallow objects, you will need a low sensor; for larger and deeper features, a higher sensor elevation can be suitable. Perhaps a good guide would be to have the sensor at an elevation which is roughly the depth of the features underground. If there is modern iron trash in the soil, or if the stones in the soil are magnetic, you will need a sensor height which is greater than normal. Otherwise, you will generally wish to have a sensor height which is as low as possible (Smekalova, Myts, and Melnikov 1993). This will increase the amplitudes of the magnetic anomalies, but it will also require that the measurements be more closely spaced. If the features are quite broad, you may use a higher sensor and more widely-spaced measurements.

It is generally best that the spacing between your measurements be about the same as or smaller than the height of the sensor above the ground or above the features. Most archaeological surveys are done with a measurement spacing which is between 0.5 and 2 m. The magnetic maps which I measured for the survey at the Taylor House will show you the effect of changes in the measurement spacing. Remember that measurements with a magnetic gradiometer will require a smaller measurement spacing than measurements with a total field magnetometer.

Simple procedures

Expensive and complex magnetometers are neither necessary nor sufficient for high-quality magnetic surveys. You will be able to do excellent work with a simple magnetometer and you will not need a computer. In this section, I will describe the simple procedures which were used to make a magnetic map at the archaeological site of Fort Laramie, Wyoming, during a National Park Service course.

The part of the survey illustrated here was a 5 x 7 m rectangle. The survey was done with a single proton magnetometer. While the magnetometer could have stored its measurements in its internal memory, they were written on paper instead; see Fig. B22. The height of the magnetic sensor was fixed at an elevation of 0.7 m, although anywhere in the range of 0.4 - 1 m would have been good. The spacing between the measurements was set at 0.5 m, slightly less than the

sensor height.

When a magnetic survey is done with a total field magnetometer which has a single sensor, it is necessary to monitor the temporal change in the Earth's magnetic field. During each day, the field rises and falls by a large enough amount that it may have a large effect on the magnetic measurements for the map. Fig. B27 shows that the Earth's field might change by about 30 - 60 nT during a day's survey. If the changes are not too abrupt, it is easy to correct for them. Just measure the magnetic field at one point several times during the survey; this check point is called the base station location.

For the magnetic survey at Fort Laramie, these temporal checks were made at a point near E0 N0 in Fig. B22. A few preliminary magnetic measurements near that point showed that there was no large magnetic anomaly there; had there been one, the temporal checks might have been in error if the exact point was not relocated for each measurement. Before the start of each line of survey, the magnetic field at the base station location was measured; these values were written at the bottom of the page of measurements, just below the broken line in Fig. B22.

The magnetic survey was done with three people. One recorded the measurements, one carried the magnetic readout, and one carried the sensor. The equipment was similar to that at the bottom of Fig. A87, except that there was only one sensor on the vertical staff rather than two. The sensor carrier stopped near each measurement point and set the sensor so that it was directly over the point. The person with the readout was at a distance of about 2 m so that the somewhat magnetic readout console had little effect on the measurements. Measurement traverses were also made in only one direction to further reduce the effect of iron in the readout. The readout operator called out the measurement to the person who recorded the measurements as a matrix in a notebook.

The numbers recorded in Fig. B22 are abbreviations of the total values. The actual field at this site was around 55,700 nT and only changes from this value are recorded. For example, a value of 29 in the map means a field of 55,729 nT and a value of 697 in the map means a field of 55,697 nT. This simplifies the recording of the measurements. Additional information is recorded at the side of the map in Fig. B22; this should be on each page of field data. The direction of north and a scale are essential, along with the date of the survey. The sensor height and the traverse direction should also be noted.

The base station measurements, written below the broken line in Fig. B22, indicate that the change in the Earth's magnetic field was larger than normal. This survey was done on two days, and the break between days was between lines E2 and E2.5. The Earth's magnetic field was definitely stormy on the second day; this was the cause of the abrupt change in the base station value for the last line. While an adequate correction for this change was possible, if you notice large changes during your survey, you might just wait for the next day to do the survey, just as you might wait for a thunderstorm.

The correction of the shift in the magnetic field can be simple to do. Just adjust each column of measurements so that the apparent value of the Earth's field at the base stations remains at a constant value; this is done by adding numbers to each column. Find the greatest reading at the base station; this is 53. Then determine what number should be added to every other base station reading so that the sum is 53; this will cause the Earth's field to be effectively

constant at 55,753 nT. These additions are listed at the bottom of the figure.

The results of these column additions are shown in Fig. B23. Notice that the change in the values from column to column is much smaller now.

The next step is one of making a contour map of the measurements. While a computer can do this readily, it is valuable to be able to draw contour maps by hand. It is convenient to start this map by drawing a contour line at a simple number; for this map, a value of 50 would be good. At first, it may be easiest to do a preliminary step before starting to draw. Examine each adjacent pair of numbers, and check to see if one is greater than 50 and the other is less than 50. If so, place a dot on the page at about where the contour line will go between the numbers; for a good map, you may do an approximate linear interpolation between the numbers. The figure shows how I have placed these points for the 50 contour line.

This first contour line is drawn in Fig. B24. The contour line simply connects the dots. At the right hand side of the map, notice the contours indicated with broken lines. The four numbers in the square there form what is called a "saddle surface", and there are dots on all four sides of the square. There are two alternative ways of contouring this square; either one could be used, and the broken line contour would be just as accurate as the solid line contour which I drew. Choose one or the other, whichever makes the map simpler or easier to visualize.

After the first line is finished, select other contour line values in multiples of perhaps 10 or 100 and draw these lines. Then, continue to draw contours with lines spaced between these first lines until the map is generally filled with contour lines. As you draw each contour line, you will see that high numbers will be on one side of your advancing line, while low numbers will be on the other side. It is best to draw smooth contour lines, for this clarifies the map.

The resulting contour map is shown in Fig. B25. This map makes the pattern of the numbers easy to see; the pattern of the measurements is very difficult to visualize in Fig. B23. When you draw a contour map, lines should not obscure the measurements by being drawn through them, unless you are working with a copy of your original measurements.

The numbers show those areas of the map which have high values and which have low; however, it can be helpful to finish the map by distinguishing these polarities. Just get a red and blue pencil and shade in the anomalies; it is conventional to use a red color for high values and a blue color for low values. You may also put short perpendicular tick marks (hachures) on the contour lines which are low values; most of the other maps in this report have this convention. You can draw the contour lines of anomalies with high values using solid lines, while the contours of low readings are given broken or dashed lines. Another possibility is that of placing random dots in the areas with either high or low values.

An adequate interpretation of a magnetic map is simple to do, and it adds much information which the map itself does not reveal. This procedure is summarized in Fig. B26. The first step is one of locating the magnetic anomalies. These are just the areas on the map where the measurements are abnormally high or low. For a magnetic map, the highs are generally the most important; there are three distinctive areas with high measurements on this map. Find the peak value at each high anomaly. Then, estimate the magnetic field nearby but away from the anomaly; this value is called the background. This

estimation is more difficult than finding the high value. This is because other nearby anomalies confuse the map, and the measurements approach the background value gradually. The background value may be a single value for the entire map, but generally it should be chosen for each anomaly, for there may be wide-area changes in the magnetic field.

For the next step, draw a contour line around the anomaly at a value which is halfway between the peak and the background value. Approximate the average diameter of this contour line, which perhaps will be oval or irregular. The depth of the object below the sensor is approximately equal to this diameter. To get the depth underground, just subtract the sensor height. Next, the mass of buried iron is estimated. The equation at the bottom of Fig. B26 shows the calculation; the equation gives an estimate of the maximum iron mass, in kg.

For the final step, the iron is located on the map. There is often a small amplitude magnetic low to the north of each magnetic high. This low is also caused by the magnetic object. It is usually possible to tell that a magnetic low is associated with a magnetic high by noting the close spacing of the contour lines between them. Even if the associated low is not in a northerly direction, the object is probably along a line from the peak high a short distance toward that low. Sometimes there is no clear low associated with a magnetic high. The magnetic high at E4 N6 is an example; there are lows to the northeast and southwest, but there is no concentration of contour lines from the high to either low. For this anomaly, the source can be estimated to be at the anomaly peak.

It is more likely that these estimates of depth and mass are too large than too small. This is because the analysis has assumed that the objects are compact or spherical. If the object is actually spread out along a line or in a lens shape, the estimates of both depth and mass will be too large. The mass estimate has also assumed that the object is iron; in fact, it may be fired earth or a volcanic stone. A magnetic survey cannot usually distinguish these different magnetic features. If the feature is actually fired earth, such as a kiln, fireplace, or furnace, the mass of fired earth could be roughly 100 times the weight of iron which was estimated from this analysis. If the feature is a concentration of bricks in a wall or foundation, the mass of brick could be about 1000 times the iron estimate. Igneous rock can be similar to brick in its magnetic properties.

One must always be cautious about geophysical anomalies which extend in the direction of the measurement traverses; these could be caused by errors. The left side of the figure shows an elongated anomaly which is probably caused by a short, abrupt change in the Earth's magnetic field during the measurement of that line. The base station readings were not frequent enough to correct for this change.

Magnetic interpretation

This section will explain some of the basics of magnetic interpretation in greater detail than was done in the prior section. Even more detailed procedures are described in Volume C.

There is a tendency for beginners who do magnetic surveys to filter, "enhance", and otherwise display or modify their measurements, but not to interpret them. With interpretation, one tries to describe the buried feature itself (its material, shape, depth, size, and orientation) rather than just describing the geophysical measurements. It is indeed more difficult to interpret a magnetic survey than to only present the magnetic map of a survey. However, the basic

procedures for interpretation are not very difficult, and you will add much information about what is underground if you do a simple interpretation of your measurements.

The magnetic anomalies of many objects detected by geophysical surveys will be rather circular. These circular patterns are just caused by the fact that the objects are rather small, and the magnetic survey did not reveal anything about their shape. The depth of these objects can be estimated by a procedure called the half-width rule (Breiner 1973 p. 31; Telford, Geldart, and Sheriff 1990 p. 87; Hinze 1990), and this rule was applied to the analysis of the simple survey above.

A justification for this approximation is given in Fig. B28. A mass of 1 kg of iron is assumed to be buried underground at a depth of 0.5 m, while the magnetic measurements are made at an elevation of 0.85 m above the ground. This figure shows the calculated magnetic map which would result if this iron object was at Petersburg. The circular contours reveal the high magnetic values. The magnetic low, which is north of the high, is indicated with a hachured contour line.

The peak of the anomaly is 21.3 nT, and the solid line contour is half this value. The average diameter of this half-width contour is 1.38 m; this is almost the same as the depth of the iron below the sensor, which is 1.35 m. This is the half-width rule: The depth of the object below the sensor can be estimated from the diameter of the anomaly at half its peak amplitude.

The calculations of Fig. B28 have been made assuming that the survey was done at Petersburg, and also that the measurements were made with a total field magnetometer. However, the half-width rule is a good approximation for any location and with any type of magnetometer. This is revealed by the nine calculated maps of Fig. B29. The three rows of maps show the calculations at the magnetic poles (the dip of the Earth's field is 90 degrees), in areas where the Earth's field dips by 45 degrees (in countries such as Guatemala, Tanzania, and Jordan), and in areas where the Earth's magnetic field is horizontal (countries such as Brazil, Nigeria, and the Philippines). The three columns have the calculated anomalies for three different types of magnetometers. The column on the right is for a total field magnetometer, such as a proton magnetometer. The middle column assumes that the total field magnetometer has two sensors, one above the other, and the gradient is calculated from the difference in the field at the two sensors. The left column is for a magnetic gradiometer which measures only the vertical component of the magnetic field; fluxgate magnetometers are this type.

For these calculations, a steel mass of 1 kg is assumed to be 1 m below the elevation of the magnetic sensor; this is the lower sensor of the gradiometers. The broken line contours are at intervals of either 10 nT or 10 nT/m. The solid line contour is drawn at a level which is half the peak anomaly. For each of the maps, the average diameter of this contour line is about 1 m.

The maps reveal two other interesting things. First, the pattern of the anomaly is very similar for the three magnetometers at each value of magnetic dip, except for the different map calculated with the vertical component gradiometer at the magnetic equator. Second, the iron object is assumed to have only a permanent magnetization; the magnetic anomaly at the equator is half of what it is at the poles, and it is also a negative value at the equator, a magnetic low.

If the magnetic object is not small, the magnetic anomaly may indicate something of the shape of the object. Buried iron pipes are usually very apparent because of the linear pattern of their

anomalies. Fig. B30 illustrates two calculated patterns which can be found over pipes. Model #1 at the top of the page has a pattern which is similar to that measured over a drainage pipe in the southeast corner of the Fort Morton grid; see the lower right corner of Fig. B43. This pipe is possibly made of a single iron sheet which forms a pipe having a diameter which is probably about 0.5 m. Model #2 at the bottom of Fig. B30 is more typical of pipes; this model assumes that pipe segments have a strong permanent magnetization and each segment was rotated at a random angle when the pipe was set in the ground. This chain-like pattern is exactly what was measured over pipes in the northwest corner of the Fort Morton grid; see Fig. B41.

As features become larger or longer, a magnetic map will begin to reveal their shape. However, the shape will still be blurred and it will only approximate the actual shape of the feature. A large, square magnetic feature will result in a magnetic map like that illustrated at the top of Fig. B31. The interpretation of a magnetic map would be simplified if a uniform pattern of high magnetic readings was found over a magnetic object; this does not happen. Instead, this figure shows that there are low readings at one end of the object and high values at the other end. The map also shows an interesting fact. If there is a hole in a magnetic object, it is detected predominantly as a magnetic low; the small square in the middle of the figure locates this hole.

The map at the bottom of Fig. B31 shows another type of feature which can be encountered by an archaeological survey. Normally, the magnetic anomaly of objects measured in the northern hemisphere will have its magnetic low on the north side of the high. However, if the object is above the sensor, the magnetic high will be north of the low. Elevated magnetic objects are commonly found as electrical transformers on utility poles and as roofs which have iron sheets or ceramic tiles.

Several different magnetic surveys were done at the Taylor House. These were done to illustrate the effect of different spacing between the magnetic measurements. Fig. B32 shows a low resolution survey; Fig. B33 shows a medium resolution survey; and Fig. B34 shows a high resolution survey.

The magnetic map of Fig. B32 was made with measurements spaced by 5 ft (1.5 m). While this survey was fast, it detected most of the features in the area of survey. Solid line contours are at intervals of 10 nT; a few broken line contours interpolate to a level of 5 nT. Note that the magnetic field is not indicated on the contours. This is because the actual value at each contour line is not very important; it is the relative amplitude and the lateral gradients of the anomalies which are important. This magnetic map was interpreted using the half-width rule, and the magnetic objects were assumed to be located at the peak of the magnetic highs. This interpretation is given in Fig. A15. A broken line in that figure marks the linear magnetic pattern which is caused by the southern brick wall of the cellar. The width of the anomaly along a north-south line has been assumed to be suitable for the half-width rule, even though this is an elongated magnetic anomaly; there is a fairly good agreement between the depth determined by this approximation and the depths determined by more detailed procedures for the interpretation.

If the spacing between the measurements is halved, four times as many measurements are needed for a survey. The magnetic map of Fig. B33 has a measurement spacing of 2.5 ft (0.8 m), half that of the map in Fig. B32. Note that the area of the anomalies is typically smaller in this map; this is the result of the higher resolution. As seen in

the interpretation of Fig. A14, more objects were located by this survey. For this interpretation, the half-width rule was also used; by comparison with the magnetic calculation of Fig. B28, the magnetic object was assumed to be 0.3 m from the peak of each magnetic high towards the low. The magnetic anomaly of the brick foundation was analyzed by a more complex procedure which is described in Volume C.

Magnetic measurements were spaced by 1 ft (0.3 m) for the magnetic map of Fig. B34. This close spacing is seldom economical, for the survey takes a long time. This survey was done during 3 days of field work, and there are 17,271 measurements in the map. By way of comparison, there are only 714 measurements in the magnetic map of Fig. B32, and that map required only about 1.5 hours of field time.

There are three different contour levels in this map. There are a few broken line contours; these are at intervals of 5 nT. The solid line contours indicate 10 nT intervals, while the broad line contours are at 100 nT; the switch between these two levels is generally apparent by a gap in the contour line spacing. Because of the small details in Fig. B34, the magnetic map is enlarged in three sections as Fig. B35, Fig. B36, and Fig. B37.

A very detailed magnetic interpretation was made of the map of Fig. B34, and the results are shown in Fig. A13. For this analysis, mathematical models were made of each of the most important magnetic anomalies. This procedure is described in Volume C.

The area of the Taylor House magnetic survey is far enough from the park road that passing cars caused little difficulty for the survey, however, it was necessary to stop the survey whenever trains were moving on the track to the west. The magnetic anomaly of these distant iron objects can be greatly reduced with a magnetic gradiometer. The improvement is shown in Fig. B38. These curves show how the magnetic anomaly from an object like a car decreases with increasing distance. At a distance of 10 m from a car, the magnetic anomaly detected by a gradiometer will be about 10% of the anomaly which would be detected by a total field magnetometer; at 30 m, the anomaly with the gradiometer is reduced to only about 1% of that of a total field magnetometer.

The Taylor House grid was mapped with a magnetic gradiometer also. The map of Fig. B39 was surveyed with a measurement spacing of 2.5 ft (0.8 m), the same as with the total field map of Fig. B33. The two maps show similar detail. The magnetic sensor for the gradiometer measurements was somewhat higher above the ground, and this reduced the amplitudes of its anomalies.

The magnetic map of Fort Morton shows hundreds of large and small objects. The map, in Fig. B40, is drawn with three different contour intervals: 2.5, 10, and 100 nT. While the same type of line is drawn for each interval, it is generally possible to see where the contour interval changes, for these shifts are near the edge of "terraces" where the spacing between lines abruptly changes. Magnetic maps often have a very wide range in the amplitude of their anomalies, and it can be necessary to draw them with several contour line intervals. The magnetic map is enlarged in the two sections of Fig. B41 and Fig. B43.

The relative amplitudes of the high readings on the magnetic map are indicated with the surface plot of Fig. B45. An iron pipe under the former park road is on the right side, while the pipes near the former farm house cause the group of highs on the left side. The small cluster of highs in the near corner of the map is located at a Civil War battery. The highest peak in the map is caused by the iron-filled well.

This survey required five days of field work and a total of

46,827 measurements were made at intervals of 2.5 ft (0.8 m). As with all of the other magnetic surveys here, a separate base station magnetometer was used to monitor the temporal change in the Earth's magnetic field. This magnetometer was programmed to make measurements at intervals of about 1 minute and to store them in its memory. The spatial magnetic measurements of the map were corrected for the temporal change by a subtraction of the base station magnetometer reading at the time when the spatial reading of the map was made. In order to simplify the correction from one day to the next, the sensor of the base station magnetometer was set at the same place for each day's survey. If you change the location of your base station, you can just remeasure the last line you surveyed the prior day and this will allow you to determine the difference between the two base stations.

The interpretation of the magnetic survey of the Fort Morton grid was done using the approximation of the half-width rule. The estimated values of the mass and depth of iron are marked in Fig. B42 and Fig. B44. As with the interpretation map of Fig. A30, different symbols indicate the approximate mass at each anomaly. The upper number of each pair shows the mass, while the lower number indicates the depth. The distribution of these depths is shown in Fig. B46. Almost no objects were detected below a depth of 2 m. As seen in Fig. B47, small objects were generally shallow, while massive objects were deep.

Fig. B40 shows one anomaly which covers an unusually large area; this anomaly is centered at about E550 S150. The interpretation of this magnetic anomaly is that it is caused by iron objects which are in a well. The pattern of the magnetic anomaly appears to be similar to that of the calculated map shown in Fig. B28. There is a large high, and north of it, there is a wide area with low magnetic field; the contour lines with tick marks show this low. However, the large depth extent of the iron in this well causes its anomaly to be different from that of a small object. Because of its unusual character, the anomaly is given a detailed analysis in Volume C.

A detailed magnetic map was made of the 100 ft (30 m) square at the bombproof trenches of Fort Morton. This map is plotted in Fig. B48. While many magnetic objects were detected, there is no indication of the trenches which were detected by the radar and resistivity surveys. The interpretation of the magnetic map is shown in Fig. A39.

Note that there is a tendency for some of the contour lines to be extended in a north-south direction. These reveal an error in the measurements and these effects are called striations; they appear along north-south lines because that was the direction of my measurement traverses. The map shows that these striations have an amplitude of about 0.5 nT. I made my measurement traverses in only one direction in an attempt to minimize these striations; however, iron which I was carrying contributed to the striations. The Earth's magnetic field changed rather fast on the day of this survey, and it is possible that the base station magnetic measurements were not sufficiently frequent for the temporal correction; the interval of these measurements was 30 s. While some of the measurements appeared to be affected by lightning noise also, this noise is apparent as errors in scattered measurements, and it is unlikely that the striations were caused by the lightning.

I am disappointed that I did not notice that the hat which I wore for some of my magnetic surveys at Petersburg was magnetic. There was an iron wire around the brim of the hat. When I finally discovered

and removed the wire, I found its mass to be 6 g. My measurements and calculations indicate that this wire would have caused a maximum magnetic anomaly of 0.4 nT. I did not record when I wore this hat, but probably I did wear it for those magnetic surveys which I did in the summer, including this survey of the bombproof.

While the striations are too apparent on the magnetic map, they do not appear to cause a serious problem for the interpretation of the map. The striations are completely removed by the smoothing shown in Fig. B49. However, this map cannot be used for the interpretation of small-area anomalies, since the anomalies have been blurred. Their peaks have reduced and their areas are increased; an interpretation of this smoothed map would indicate depths which are too large.

The magnetic anomalies of the Trench detail are found primarily in only part of the survey area. In Fig. B50, the main fortification trench is along line E480 and the magnetic survey detected nothing of the trench itself. However, strong magnetic anomalies are found just to the east of the trench, and it appears that some of the iron objects may be within shelter pits dug by the soldiers during the siege. The interpretation of this map is given as Fig. A47.

Several magnetic maps were made of the intense anomaly of the Iron detail. These are plotted in Fig. B51. The map at the lower right was measured with a magnetic gradiometer. This gradient map reveals a magnetic anomaly at E513 S137 which is lost in the large magnitude of the three total field maps which are also on the page.

The spacing of the contour lines shows how the amplitude of the anomaly decreases as the height of the sensor increases from 0.59 to 0.8 to 1.16 m.

Striations are evident on each of the maps; these are caused by positional errors of about 10 - 20 cm during the survey. While a smoothing filter could improve the appearance of these maps, the maps have not been modified. Striations are always most evident where magnetic measurements are made with a spacing which are closer than they need to be; since this anomaly has a smooth circular pattern, the locational errors are particularly evident.

Conductivity Surveys

Conductivity surveys are much faster than resistivity surveys, although conductivity surveys are more complicated to do. Because of their speed, I do many more conductivity surveys than resistivity surveys. This section will be somewhat more detailed that the prior sections. This is because relatively little has been written about doing conductivity surveys; I will describe the practical procedures which I have found to be helpful in doing the field work and also in interpreting the results of a conductivity survey. These conductivity instruments can also be used to measure the magnetic susceptibility of the soil; since this is the most complex application of the instruments, the discussion of this is left for Volume C.

The unit of electrical conductivity is the siemens per meter, abbreviated as S/m. Conductivity is simply the reciprocal of resistivity. For example a resistivity of 100 ohm-m is the same as a conductivity of 0.01 S/m. Because most conductivity values will be much less than one, the most common unit for conductivity is the mS/m (millisiemens per meter), and the resistivity of 100 ohm-m is the same as 10 mS/m. In the earlier section on resistivity in this volume, there is a short table which lists the approximate conductivity of different types of soil.

Conductivity Surveys

Instruments

The general and correct name for a conductivity instrument is an electromagnetic (EM) induction meter. Common metal detectors are special types of electromagnetic induction meters. Conductivity meters are most similar to the transmitter-receiver type of metal detector; these metal detectors have coils of wire in two boxes which are separated by a staff, this separation allows the detector to search to a good depth underground.

Conductivity meters also have a pair of coils. The two circular coils are obvious with the EM34 instrument sketched in Fig. A88. The coils are hidden within the ends of the other two instruments in the figure. All of these instruments are manufactured by Geonics Limited, and the model numbers are listed in the figure. Other manufacturers have different types of electromagnetic induction meters for sale. These instruments from Geonics are the only ones commonly applied to archaeology. This is partly because two of these instruments have a depth range which is excellent for archaeological features. These instruments have also been designed to display the actual conductivity of the ground, rather than a more technical parameter. The interest of the company in archaeology is illustrated by the fact that it has prepared a collection of reprints titled: "Selected papers on the application of geophysical instruments for archaeology".

The EM34 is designed for detecting features at depths ranging from 10 to 50 m. This is suitable for only a small fraction of archaeological sites. However, if large mounds are to be explored, or the course of an ancient river is to be traced, this instrument may be excellent. The depth of exploration is determined by the spacing between the two circular coils of the instrument; this can be set at 10, 20 or 40 m. Because of this large separation, it is best that two people operate the instrument, one carrying the small transmitter coil and its electronic box, and the other carrying the larger receiver coil and the display console. The coils are typically set on the ground, either flat as shown in Fig. A88, or vertical.

The principle of the measurement is as follows: An alternating current is sent through the transmitter coil; the frequency of this current is in the audio range. This current generates a magnetic field about the coil and this magnetic field readily goes into the earth. When this magnetic field passes though conductors in the soil, an electrical current is generated in them; these conductors may be just strata of the weakly conductive soil; metals are not necessary. These electrical currents in the soil generate a second magnetic field, which is detected by the receiver coil of the EM instrument. This indirect coupling from the transmitter coil, through the soil, and to the receiver coil, allows the measurement of the electrical conductivity of the earth. While these instruments do detect metal, they are not made for this application; they are designed to detect the much weaker conductivity contrasts found in different soils.

The other two conductivity meters, the EM31 and the EM38, also have a pair of coils; their coils are hidden within the ends of the instruments. These two instruments detect shallow features most strongly; the maximum effective depth at which the two conductivity meters will detect features is dependent on the spacing between the coils. With the EM31, this maximum depth is about 6 m; for the EM38, the maximum depth is about 1.5 m. If features are within the depth range of the EM38, it can be best to use this instrument, for it will allow a higher resolution with its geophysical maps; the EM38 will detect smaller features than those which can be detected with the

EM31.

The EM38 is more sensitive to electromagnetic noise from power lines and lightning than is the EM31. For this reason, it is sometimes necessary to select the EM31. The EM31 is carried at an elevation of about 1 m above the ground; a shoulder strap, not drawn in Fig. A88, supports the weight of the instrument. Because of this elevation, surveys are easy to do if the brush at a site is lower than this. The EM38 is usually carried quite close to the ground, and brush is more of a problem with it. Because it is shorter, the EM38 is easier to use in wooded areas; where trees are dense, the EM31 is more difficult to carry through the woods, and it may be almost impossible to rotate the 4 m long boom of the instrument in a horizontal direction if trees are close together.

Interpretation procedures

These conductivity meters are excellent for locating many types of soil contrasts. If there is a broad pit which has been dug into sandy soil and then it has been refilled with organic matter, it might be detectable as a high conductivity anomaly. A lens of stone rubble from a building, now buried in silty soil, may be revealed as a low conductivity area. Had the pit been dug in silty soil, and if the building rubble was in gravelly soil, both features might be invisible to a conductivity survey, for the archaeological features would then be too similar to the surrounding soil.

Conductivity surveys will define the location and approximate shape of some features, but quite different features can cause similar conductivity anomalies. Fig. B52 shows the cross-sections of three features which are detectable as high conductivity. In the figure, the dotted soil strata have low conductivity, while the hachured areas are higher in conductivity. Each of these three types of features can cause similar conductivity highs.

While these conductivity meters are not designed for locating metal, they do it, and sometimes too well. If there are buried pipes and wires in the area, the conductivity anomalies which they cause can hide other features in their vicinity.

Fig. B53 illustrates how readily the EM31 will detect a buried pipe; the middle profile line is mapped at the top of Fig. B7. All three parallel lines reveal the same pattern. This pipe was mapped by the magnetic, radar, and conductivity surveys of Fort Morton. The radar indicates that this pipe is about 0.6 m underground, or 1.6 m below the EM31. The distance between the anomaly maxima is 19 ft (5.8 m); the interpretation manual from Geonics suggests that this distance should be about the depth of the pipe below the EM31. In this case, this interpretation must be wrong, and the depth determination from the radar is more reasonable.

For the profiles shown in Fig. B53, the long bar of the EM31 was oriented perpendicular to the pipe. If the bar is aligned parallel to the pipe, the conductivity profiles are different; see Fig. B54. The anomaly is entirely positive in this case, and its high is about double that of Fig. B53. There is a sharp drop right over the pipe, but this does not go to a negative value of conductivity. Fig. B54 and Fig. B53 show that both conductivity anomalies are the same for distances from the pipe greater than 10 ft (3 m). The pipe is detectable for a lateral distance of more than 30 ft (9 m). If there are several pipes at a site, the conductivity map of the area may show little more than just the pipes.

The EM38 is affected by pipes over a narrower span. This is illustrated with a comparison of Fig. B55 to Fig. B53. The detection

distance of this pipe with the EM38 is about half that with the EM31. Fig. B55 and Fig. B53 also show that the amplitudes of the anomaly highs are about the same for the two instruments; however, the EM38 detects a weaker negative anomaly over the pipe.

The response of the conductivity meters to metal objects is easy to test. The EM38 and EM31 can be hung by ropes from a tree branch, and metal objects can be slid under the instruments. Since the objects are not buried in soil, this procedure eliminates the effects of lateral changes in the soil.

Fig. B56 illustrates the anomalies which I measured over three metal objects; each was square and 0.55 m on a side. The metal mesh gives the strongest anomaly. The EM31 was hung from a tree at an elevation of 1.5 m. These objects were slid on the ground below the EM31 and along the length of the instrument. The vertical dashed line marks where the objects were directly under one of the coils of the instrument; this is called a magnetic dipole of the instrument. With two of the objects, the maximum anomaly was detected at that point.

With these same three metal objects, the EM38 detects the very different patterns shown in Fig. B57. The anomalies have only high conductivity and the peaks of the highs are at the middle of the instrument, rather than at the dipoles or coils. The metal mesh or screen still gives the strongest anomaly, and the metal loop still gives the smallest anomaly.

A closed loop of wire causes almost the same anomaly as a metal plate of the same size. If, however, the wire is made into a loop, but the two ends are not connected together, then the wire has little effect on the conductivity meters.

Both the EM31 and EM38 will detect large metal objects. While the EM38 will detect small metal objects, the EM31 will not. Fig. B58 illustrates the conductivity lows which were measured over metal objects which were 14 cm on a side. Note that these profiles are rather similar to what the EM31 measured over metal objects 1.5 m on a side; there are conductivity lows close to where one of the coils of the EM38 is centered over the objects. I do not know why the foil gave a larger anomaly than the thick plate.

It is likely that many of the metal objects which are in the area of my survey at Petersburg are projectiles from the battle during the Civil War; while many projectiles were salvaged during and after the battle, there must still be many in the soil. I borrowed four shells or shell fragments from the park's collection and tested them; the projectiles are sketched in Fig. C41. The conductivity anomalies of these iron artifacts are plotted in Fig. B59. While the whole mortar shell gave a strong negative reading, the other shell fragments just gave weak lows. Lead bullets must be very common in the soil; the EM38 will only detect them if they are very close to one of the coils of the instrument. For my conductivity mapping at Petersburg, I deliberately raised the EM38 above the ground so that these hundreds or thousands of small objects would not be detected.

For the illustrations above, I moved a metal object on the ground along a line below the stationary conductivity instrument. This same procedure will furnish a map, and an example is illustrated in Fig. B60. The square at the middle of the map shows the size of the metal foil; the long rectangle shows the size of the EM38. The sides of the map indicate dimensions, in meters. I subtracted the approximate conductivity of the soil from the measurements in this map.

There is a conductivity high in the middle of this anomaly; it has a peak value of about 3 mS/m. A contour line at half of this peak value, or 1.5 mS/m, has a diameter of about 0.5 m. This is the height

of the EM38 above the metal object. My tests have indicated that this half-width rule may be suitable for estimating the depths of metal objects; the rule is only valid if the object is detected as a conductivity high.

I measured a pattern of low-high-low readings like that in Fig. B60 during my survey at the Taylor House. The points marked with triangles in Fig. B61 show my conductivity measurements when the EM38 was moved along the surface of the soil; in this case, the lows were very strong, but the conductivity high was weak. Each of the lows is found where one of the two dipoles of the EM38 passes over the metal object; the spacing between the two lows is just the 1 m spacing between the coils.

When the instrument is raised in the air, the anomaly changes to a positive value. The amplitude of this anomaly decreases as the EM38 is lifted higher in the air. The width of the anomalies at half their peak value appears to be equal to the depth of the metal below the EM38. Both of these positive anomalies indicate that the depth of the object could be about 0.45 m. This object was also detected by the magnetic and radar surveys; an analysis of the data from both of those surveys confirms that the depth of the object is 0.45 m.

With this confirmation of the suitability of this half-width rule for the EM instruments, I applied it to the interpretation of the conductivity highs which were detected by the surveys at the Petersburg battlefield.

For large features, the conductivity instruments indicate the true conductivity contrast of the feature. If there is a lens of conductive or clayey soil which is 5 m wide within sandy soil (which has a low conductivity), the EM31 and EM38 will indicate this feature with measurements which actually show high conductivity over the conductive feature. Unfortunately, if the feature is rather small, the conductivity contrast indicated by the EM31 or EM38 can have the opposite polarity of the actual feature. If the conductive feature above was a clay-filled pit in sandy soil, and the diameter of the pit was only about 1 m, then the EM31 would indicate this feature as a low conductivity anomaly, and not its true high conductivity. For the EM38, it is possible that this switch in anomaly polarity may occur for features smaller than about 0.5 m in size.

Mapping

If you are doing a conductivity survey with the EM38, you will have to check for metal in your clothing which may affect the measurements. If the EM38 is carried close to the ground, you should be particularly careful with your shoes. Just set the EM38 on the ground and watch the measurement as you move your foot close to one of the end coils of the instrument. If you see any change in the reading, you will have to keep your shoes well away from the conductivity meter. If the EM38 is carried low on the ground, metal at waist height or higher will have rather little effect, but you should remove metal objects larger than about 15 cm in size. If you are carrying the EM38 above the ground, you will have to be even more careful with metal which you are carrying. Most of the normal metal objects which you could carry have no effect on the EM31.

The measurements of these conductivity meters are displayed on a meter dial; the meter's needle points to the value along a linear scale. These readings can be read from the dial and written down in a notebook. For sites with rather silty or clayey soil, the readings of conductivity, and the conductivity anomalies, are typically rather high and this method works well. If the soil is rather sandy,

the conductivity readings can be very small; it is difficult to read the meter accurately, and low amplitude anomalies may be undetected.

For these sites, the analog reading of the meter dial is best converted to a digital value to allow a greater precision in the measurements. Some of the current versions of these conductivity meters have these digital meters on them. If yours does not, you can always connect a digital voltmeter in place of the analog meter in the instrument.

For my surveys at Petersburg, I operated the EM31 and EM38 conductivity meters with a digital data logger. This extra electronic instrument converts the analog or voltage signal from the conductivity meter to a digital value and records it in the memory of the logger. These readings can later be sent to a computer. The data logging allows more precision in the measurements, and it also allows a much greater speed of measurement. However, it also adds another complexity to the survey, and something more to go wrong. Still, it is usually the best way to operate the conductivity meters.

An example of the speed of a conductivity survey using a data logger is illustrated in Fig. B62. The 735 measurements of this Taylor House map were made in only 1.5 hours. It was adequate for locating the high conductivity area on the west side of the Taylor House cellar, at W10 N100.

I resurveyed the area a few months later; this time I took slightly longer (1.8 hours this time) and was more careful with my measurements. The EM31 has a short delay time before its measurement settles down to the correct value; for this resurvey, I waited at each point about 2 s before recording the measurements so that their accuracy would be better. However, there is little difference between the maps of Fig. B62 and Fig. B63, even with the two month delay in measuring the second map.

There is not much which can be done for the interpretation of these conductivity maps. As shown in Fig. A17, I just marked the areas of high and low conductivity. The small-area low conductivity anomalies could be caused by shallow metal objects, and I marked these differently. The long conductivity anomaly at the south side of the grid is almost surely caused by a pipe going east-west just outside the area of the grid; this pipe was detected by the magnetic and radar surveys also.

The measurements of the conductivity meters will be different if the instruments are rotated about a vertical axis. This difference is sometimes valuable for indicating buried metal and other abrupt changes in conductivity. However, this procedure will increase the time needed for the survey, although it may not double. The measurements of a conductivity meter should not change if the front and back of the instrument are interchanged; this is because of the principle of reciprocity (the measurement should be the same if the location of the transmitter coil is switched with the receiving coil).

I resurveyed the Taylor House grid, making measurements with a spacing of 2 ft (0.6 m), rather than 5 ft (1.5 m). The map in Fig. B64 shows the conductivity patterns when the long bar of the EM31 was oriented east-west. It would have been possible to make a pair of measurements at each point, swinging the bar of the EM31 by 90 degrees between them. If the measurements are close together, as these are, it is easier to do a separate survey with the bar of the EM31 going north-south. This map is plotted in Fig. B65.

The two conductivity maps are rather similar. The accuracy of the conductivity data can be improved by averaging the two maps. This has been done in Fig. B66. This map is just the average of Fig. B64

and Fig. B65. The contours lines are less irregular; except for the averaging, no smoothing has been done to the data. Because of the better quality of this averaged data, it has been possible to draw good contour lines at a closer interval. A surface map of this conductivity data is plotted in Fig. B68; this shows the high conductivity near the Taylor House cellar as a rise in the foreground.

The interpretation of this averaged conductivity map is plotted in Fig. A16. The difference between this interpretation, and the interpretation of the survey which had a measurement spacing of 5 ft (1.5 m, shown in Fig. A17) is small; however, this higher resolution survey would be more trustworthy in its location of both small and large features.

Fig. B67 is a plot of the difference between the maps made with the two orientations of the EM31 (Fig. B64 - Fig. B65). These differences will be largest where there are metal objects in the ground, and the several large anomalies are indeed likely to be caused by metal. There is an interesting high in the middle of the cellar, at W10 N85; this is not apparent on either conductivity map by itself.

This difference map accentuates errors in my measurements of the two original surveys; for this reason, the map of Fig. B67 has been smoothed. With earlier maps in this volume, I have shown that a good transformation for smoothing replaces each measurement with the average of the nine measurements centered on that point. There is a small variation on this which is more suitable when the measurements show a striated pattern. The same nine measurements are averaged, but the weighting of the three rows is different. Along the direction of the striations, the six measurements of the outer two rows are added together. The three measurements in the central row are added together and the sum is multiplied by two. The two sums are then added. Since the sum of these weights is now 12 (1x3 + 2x3 + 1x3) rather than 9, the overall sum is divided by 12; this average replaces the measurement at the central point. This transformation can be called striation smoothing, and this has been applied to the original data of Fig. B67.

Just as with the EM31 surveys, I also did a fast EM38 survey of the Taylor House grid. The measurement spacing was 5 ft (1.5 m) and the data plotted in Fig. B69 required 2.5 hours to survey. The EM38 emphasizes features which are at a shallower depth than those which predominate on the EM31 maps. The Taylor House cellar is now visible as an elongated high conductivity anomaly. Notice also that small-area peaks, probably caused by metal, are now detected as highs, rather than as lows with the EM31. This has allowed the depth of some of the objects to be estimated, and the interpretation is given in Fig. A19.

I resurveyed the Taylor House grid with the EM38, making measurements spaced by 2 ft (0.6 m). Just as with the EM31 survey, I separately mapped the conductivity with the bar of the EM38 oriented east-west and also north-south. These two maps are plotted as Fig. B70 and Fig. B71. The average is given in Fig. B72. The irregularity of the contour lines is primarily caused by small features which were detected, but measurement noise also contributes to it. The smoothed map of Fig. B73 clarifies the large-area anomalies. However, the interpretation of this survey was done with the unsmoothed map of Fig. B72. This interpretation is plotted in Fig. A18. Notice than many more objects were located by this high resolution survey than were detected by the lower resolution survey, interpreted in Fig. A19.

Both surveys mapped an oblique line of anomalous conductivity which starts at W70 N0; this is a refilled trench that was dug during

the Civil War. There appears to be a concentration of metal objects deep within it. The EM38 conductivity survey shows this trench to have high conductivity, while the EM31 indicates a low conductivity. The EM38 is probably correct. Because the width of the trench is about the same size as or smaller than the intercoil spacing of the EM31, its anomalies can be reversed. Note that these conductivity surveys suggest that this trench has a low resistivity; this differs from the high resistivity of the trenches detected by the resistivity surveys of the Fort Morton area. In the Fort Morton area, the resistivity surveys detected the refilled trenches, but the conductivity surveys did not; in the Taylor House area, the conductivity survey detected a trench, but the resistivity survey (Fig. B3) did not.

The surface map of EM38 conductivity, in Fig. B74, shows the high values at the cellar in the foreground; the conductivity of the pipe in the background is so high that the values have been truncated in the figure. Note that this EM38 conductivity survey shows many metal objects as conductivity highs, while the EM31 survey showed them to be apparent lows. This difference is caused by the fact that the metal is "close" to the EM31 but "far" from the EM38. These conductivity instruments have a nonlinearity for very conductive features. As the conductivity detected by the instruments goes to an extremely high value, the reading on the meter can actually decrease; when the instruments are very close to metal (relative to the coil spacing of the instruments), the reading will be negative.

Before I began the survey at Petersburg, I thought that the EM31 conductivity meter would readily detect the refilled trenches in the Fort Morton grid. I made a few long conductivity profiles across the grid; these lines were spaced by 50 ft (15 m). They did not reveal a nice fort-like pattern, so I filled in the conductivity measurements with lines at a 25 ft (7.6 m) spacing, and I thought that this would help. The resulting map is plotted in Fig. B75. While a buried wire and a pipe are very apparent in the map, there is still no trace of the fort.

Since the quick survey did not work, I did a slow and detailed survey of the entire grid, making measurements at intervals of 5 ft (1.5 m). The 11,811 measurements mapped in Fig. B76 took me six days of field time, but they still do not reveal the fort.

Buried pipes and a wire are very apparent. The linear patterns at the top of the page are caused by remnants of pipes from a farmhouse which was there early in this century. The long line going to the south end of the map is a buried electrical wire which provides power to a tape recorder that has an announcement which describes the history of the area for visitors. A metal pipe is also near the southeast corner; this is an iron culvert under the former park road. The current park road is at the northwest corner, and that area was not surveyed.

While the contour interval in the map of Fig. B76 is 0.25 mS/m, the lines are not labeled, for they are too irregular and complex. The complexity of these contour lines is caused by electrical noise and by irregularity of the soil. While it is not apparent in the map, the highest soil conductivity is found in the northwest corner, near the former farm house.

The great irregularity of the contour lines in the original data, mapped in Fig. B76, makes the patterns very difficult to see. The smoothed data plotted in Fig. B77 reduces most of that irregularity. However, it also broadens and blurs the anomalies. This is most apparent for anomalies which are small in area and high in amplitude.

Notice the rather square pattern at E595 S250; this is caused by a strong conductivity low, possibly a metal object, which is there. For this 3x3 matrix smoothing, the measurement at each point is replaced by the average of the 9 measurements which surround that point.

In Fig. B77, contour lines are drawn in the range of 5 - 13 mS/m; white areas inside dense contours have values above or below that range. The pipes and the wire have low values along their length, but there are high values of conductivity at a greater distance from the center of the utility lines. This is just what is shown in Fig. B53.

Many metallic objects were detected by the EM31, and Fig. B76 shows these as conductivity lows. The locations where there is metal can be accentuated by subtracting the smoothed map of Fig. B77 from Fig. B76. This has been done in Fig. B78. Most of the small patterns there are caused by buried metal objects. The pipes and the wire are very clear in this map; notice that the pipe which follows a line like a backwards L at the top of the map ends with a T-pattern on the west.

The map of Fig. B78 provides the start of the interpretation of the conductivity measurements of Fort Morton. High conductivity anomalies which are isolated and small in area could be caused by metal objects which are rather deep underground; they are marked with circles in the interpretation map of Fig. A32. If there is low conductivity in the middle of the anomaly, the metal is probably shallow, and an X in Fig. A32 locates these points. The approximate extent of broad-area conductivity anomalies was also delineated in the interpretation. The linear patterns on the east side of Fig. B76 are along a side of the former road; perhaps there was a shallow ditch there at one time, and it has been filled with soil which is different from what was originally there.

Because of the low conductivity of the soil in the Fort Morton grid, I had difficulties with the EM38 conductivity survey. I found ways of reducing my difficulties, but only after I finished this survey. While the map shown in Fig. B79 does not have high quality data, it is adequate to reveal many things. The many small circular black patterns there are mostly caused by shallow metal objects; these objects are larger than nails, and are probably at least 10 - 20 cm in size. Pipes and a wire cause the linear patterns; notice that these patterns are not as broad as those found with the EM31.

The large patterns in the EM38 conductivity map were made apparent by smoothing the measurements; see Fig. B80. Before this striation smoothing was done, it was first necessary to remove most of the effect of metal objects from the map. This smoothed map reveals the large-area conductivity features which are plotted in the interpretation map of Fig. A33. The small features were located with the aid of the difference map of Fig. B81. The diameter of the oval patterns in this map increases where the anomalies have a greater area or amplitude; the diameter is therefore an indicator of the clarity of detection of the objects. The EM38 conductivity survey did not locate the linear patterns along the edge of the former park road; these were quite clear with the EM31. I would expect that these features should be shallow, and therefore likely to be readily detected with the EM38. The failure of their detection may be due to the different depth weighting of the EM38 and EM31; perhaps high and low conductivity strata cancel each other out with the EM38.

I resurveyed three small parts of the Fort Morton grid with both the EM31 and EM38. Since these measurements were spaced by 1 ft (0.3 m) rather than 5 ft (1.5 m), it was possible to detect small features much better. The EM31 conductivity map of the Bombproof detail is shown in Fig. B82. The two powder magazines at the fort were detected

as high conductivity anomalies; these are located along line E335, at about S195 and S250.

This survey was done in the summer, and lightning noise caused difficulties with the data; the map here has been smoothed with the striation filter described above. The interpretation is plotted in Fig. A40. Except for a lateral gradient in the conductivity, and a few possible metal objects which are indicated with low values, rather little was detected by this survey.

As is usual, the EM38 survey detected many more metal objects. The map of Fig. B83 locates them as oval patterns; the long axis of the ovals is in the direction of the EM38, north-south. Since the full range of the measurements has not been contoured, the middle of these anomalies can be white; this helps to show the hachures on the contour lines and therefore it reveals that most of the small anomalies are lows. When this map is smoothed, the conductivity pattern is simplified (see Fig. B84). The difference of the original and the smoothed maps, in Fig. B85, reveals only low conductivity anomalies. These are probably shallow metal objects and they are marked with + signs in the interpretation of Fig. A41.

There are so many metal objects in the Bombproof detail that they interfered with the visibility of the larger patterns in the data. For Fig. B86, each of the small-area, high amplitude anomalies were removed from the data. This finally reveals more of the anomalies. Two high conductivity anomalies near the bottom of the survey area could be caused by deeper metal objects, and these have been indicated in Fig. A41. A few other anomalies are apparent as a central low value which is surrounded by high conductivity; these could indicate metallic objects at an intermediate depth. A different symbol (a plus in a circle) locates these in Fig. A41.

None of the EM38 and EM31 conductivity maps of this area revealed anything of the bombproof trenches. While the resistivity map of Fig. B9 shows one of these trenches clearly, neither the EM31 nor the EM38 conductivity map give any hint of this trench. This lack of detection by the EM instruments does not indicate any fundamental failure of the instruments. The difficulty is probably just caused by the stratification of the soil here. While resistivity and conductivity are just reciprocals of each other, there is no way that the maps measured with a resistivity survey can be simply converted to maps which are identical to those measured with the EM38 or EM31 instruments. This is because the three instruments measure depth-weighted averages of the soil's resistivity or conductivity. Since this weighting is different for the different instruments, the readings cannot be directly compared. This different weighting can cause one instrument to detect a feature clearly and another to miss it completely.

The conductivity surveys of the Trench detail are plotted in Fig. B87, Fig. B88, and Fig. B89. The total range in the conductivity measured with the EM31 in this entire area was only about 1 mS/m. If the analog meter of the instrument was read, the anomalies here would be impossible to record, for the deflection of the needle would be too small. The digital recording of the data logger has allowed the very faint changes to be mapped.

The EM38 conductivity is mapped as Fig. B88. Low readings are marked by hachured contours; these may be caused by metal objects. Note that two objects (along line E502 at S28 and S45) are lows which are surrounded by a ring of high values. With the smoothed map of Fig. B89, two local regions with only high conductivity are apparent: at E465 S52 and E485 S18. These two anomalies are probably caused by

metal objects which are moderately deep underground. They are interpreted in Fig. A49. Two of the low conductivity anomalies detected by the EM31, and mapped in Fig. A48 with broken lines, were detected by the EM38 as deep metal objects; these two metal objects may be particularly large.

As with the other conductivity surveys at this site, the conductivity measured by the EM38 is usually somewhat lower than that measured with the EM31. Since the EM31 measures to a greater depth, this just indicates that the deeper soil is more conductive than the shallow soil.

The EM31 conductivity map of the well in the Iron detail shows a very simple pattern; it is at the upper left corner of Fig. B90. The predominantly low values just mean that metal is rather shallow in comparison to the 3.66 m coil spacing of the EM31. The anomaly is a circular low, which is surrounded by a very weak ring of high values. This map is the average of the readings which were made with the bar of the EM31 going north-south and east-west. The difference of these two readings is mapped in the upper right part of the figure. In both maps, the contour interval is 0.25 mS/m.

While the EM31 shows the anomaly of the well to be a low, the EM38 shows it as a high; this map is at the lower left of Fig. B90. Because of the high conductivity which the EM38 detected at the well, the depth can be estimated. This is indicated as 2.4 m in Fig. A53. The EM38 also located several other metal objects in the vicinity and these are also mapped in the interpretation figure.

Detailed procedures

The procedures described below can make it more difficult to do conductivity surveys, but these procedures may result in more accurate and reliable conductivity anomalies, particularly at sites where the conductivity of the soil is not high.

All of the conductivity meters are rather sensitive to electrical interference. At Petersburg, the greatest difficulty came from the sferic noise of lightning; this is the same noise which can be heard on radios as static crashes. The effect of lightning noise is obvious in Fig. B91. The same line was measured when there was a thunderstorm nearby, and when none was near. While the EM31 is less sensitive than the EM38 to the static of lightning, the interference can still be severe. All of the measurements which were made when this thunderstorm was near had to be discarded, and the area was later re-surveyed. Because of the low amplitude of the conductivity anomalies at Petersburg, the conductivity instruments were particularly sensitive to noise. If the amplitude of the anomalies had been about 5 mS/m or more, as it can be at some sites, the lightning would have caused little difficulty.

At other sites, I have detected the most severe noise from nearby electric lines. The source of this interference is probably not the 50 or 60 Hz frequency of the electrical current. It is more likely caused by abrupt changes in the electrical current flowing on the line, which is caused by heavy machinery starting or stopping; even light dimmers in houses can create electrical noise on nearby wires (Skomal 1978). If you plan to do conductivity surveys in cities or near high voltage power lines, it is important to first test the noise at the site.

At Petersburg, there was little noise from industries or high voltage wires. However, I monitored the noise during my conductivity surveys, often making one or more tests each day. I did these tests by just keeping the conductivity meter stationary and making a series

of measurements. Fig. B92 shows examples of my tests at Petersburg. The noisy measurements, on 9 August, were made when there was a thunderstorm nearby, and the data shown with asterisks have a greater variability. I have quantified this variability by calculating the standard deviation (s.d.) of the measurements; these values are listed on the graph.

At other sites, I have found that most of the noise detected by the conductivity meters appears to come from power lines. I have made over 16 measurements of EM noise at over 10 different archaeological sites. The table below summarizes my findings of the power line noise which I have measured with the EM38; the noise detected by the EM31 is half these values.

	Noise standard deviation, mS/m
City	0.2 - 0.6
Village	0.1 - 0.3
Rural	0.05 - 0.1

The EM38 is more sensitive to interference than the EM31. While the measurements of Fig. B93 were made on a rather quiet day, late summer at Petersburg is the most common time for thunderstorms. The magnetic coils in the EM38 are located at the ends of the instrument. In the normal mode of operation of the EM38, measurements are made with the thin edge of the instrument vertical; the control knobs for the meter are then on top of the instrument. In this mode, the magnetic field from the coils is directed in a vertical direction, and this the called the vertical dipole mode. If the instrument is set with its large surface on the ground, this is called the horizontal dipole mode. While there is not much difference between the north-south and the east-west orientations in horizontal dipole mode, the lightning noise in horizontal dipole mode is much worse than the noise measured with a normal, or vertical, orientation of the dipoles.

Measurements with the EM38 resting on its side examine the soil to a shallower depth, and this can be valuable for some sites; these measurements with horizontal dipoles, combined with measurements with vertical dipoles, allow one to estimate how the conductivity of the soil changes with increasing depth. There is some tendency for the horizontal dipole mode to be most sensitive to lightning noise, while vertical dipole mode is most sensitive to power line noise.

Another example of severe interference is illustrated in Fig. B94. This graph shows that it can be impossible to get good measurements when lightning is nearby. Three different conditions are tested in this figure. The short broken lines indicate the noisiness which I measured with simple measurements. Note that the major effect of the noise is usually a decrease in the value of apparent conductivity. If maps are made when this noise is severe, a series of low values are seen along measurement traverses in the map.

The noise from lightning and power lines can be reduced by averaging a series of readings with the conductivity meter stationed at one point. In Fig. B94, the solid line shows the great reduction which is possible with this averaging. I programmed the data logger to sample the measurements from the EM38 at intervals of 0.5 s; I also set the logger to average these samples for about 5 s, which is about 9 samples. On ten different occasions, I compared the noise of the EM38 with and without this averaging; I calculated the ratio of the standard deviation of the unaveraged readings to those measurements where about 9 samples were averaged. The average of this ratio was 3.2, which is approximately equal to the square root of 9. If the noise had a normal statistical distribution and each sample was

independent, one would expect the noise to be reduced by a factor of three. This reduction in the noise can be very helpful in making a good conductivity map.

I also calculated this ratio of noise without and with averaging for the Geonics EM31; for the 13 times at Petersburg when I tried this, the average ratio was 1.6, rather lower than the ratio for the EM38. This lesser improvement with the EM31 is due to the fact that its raw or displayed measurements are already averaged; there is about a 1 s integration time within the instrument. This averaging is visible as a slightly sluggish movement of the meter needle as the instrument is moved along a line of measurement.

Seasonal changes in the noise measurements with the EM38 are plotted in Fig. B95. Lightning is most frequent in summer, and also in late afternoon; so is the noise. The EM31 tests indicated the same peaks; however, Fig. B95 shows that the EM31 noise is less. Lightning noise can be a great problem in tropical areas; when noise is most severe, it can be best to survey at first light in the morning.

The electronic circuitry within the EM31 has a built-in averaging which helps to reduce the noise of its measurements. The effect of this averaging is seen in Fig. B97. The horizontal axis of the graph shows the time of survey, and the asterisks mark the measurements which were made at about 1 s intervals at each 5 ft point along line N80. Note that the EM31 tends to overshoot its measurements. That is, if the measurements at the prior point were low, the first readings of the EM31 at the new point will also be low. There appears to be an inertia to the measurements. Because of the 1 s integration time of the EM31, it can be necessary to wait for a second or two at a point before reading the measurement. The EM38 does not have this built in averaging; while this makes it more susceptible to noise interference, it also makes it respond faster to changing conductivity along a measurement traverse.

Conductivity surveys with the EM38 are typically done with the instrument setting on the surface of the ground. This maximizes the conductivity anomalies of buried features, since the instrument is then closest to the features. However, when the instrument is set directly on the ground, it is very sensitive to features very near the surface of the soil; these may be small bits of metal trash. If your site is rather trashy, it may be necessary to elevate the EM38 above the surface.

The effect of elevation is illustrated in Fig. B98. Note that the apparent conductivity decreases as the instrument is lifted; this is because the reading with the elevated instrument averages the conductivity of a layer of air, which is zero. Note also that when the EM38 is directly on the ground's surface, the readings are very irregular. This is almost surely due to the density of small metal objects at this site. When one of the two end coils of the EM38 is very close to one of these small objects, it causes a very low reading, or sometimes a high. Because of the irregularity of the readings which are measured when the EM38 on the ground, a different procedure is needed; if there is metal trash at the site, it will be necessary to raise the instrument, even though this reduces the anomalies of interesting and deeper features.

Since there were so many shallow metal objects in the soil at Petersburg, all of my EM38 measurements there were made with the instrument elevated above the ground surface. This height ranged from 0.3 m in the Fort Morton grid to almost 0.7 m in the Taylor House grid. The upper illustration in Fig. A88 shows the EM38 being carried in a sling; this can be used to lift it above the ground. In order to

keep the elevation of the instrument constant, I instead tied the EM38 to a triangular frame made of plastic pipes. The EM38 was high enough that there was no difficulty caused by the downed trees and the brush in the wooded part of Fort Morton. My detailed conductivity surveys in the Fort Morton grid were made on grassy areas, and the measurement spacing was 1 ft (0.3 m). For these surveys, I tied the EM38 between two wooden boards and pulled it along the lines of measurement; this travois is sketched in Fig. A88. With all of these procedures, it is important to keep all metal quite distant from the EM38. I made sure that there was little or no metal in the carrying frames, and the metal of the data logger was also carried well away from the EM38. The EM31 is much less sensitive to moderate sized metal objects which are nearby.

The measurements of apparent conductivity are decreased when the EM38 is lifted in the air. It is not necessary to correct for this decrease, but I did it so that the surveys in the different areas could be more readily compared. I determined the correction factor from tests like that shown in Fig. B98. I multiplied the readings with the elevated instrument by factors which ranged from 1.16 to 1.54; these factors would be different for a site with different soil stratification.

The measurements of the conductivity meters will change with changes in temperature. This effect is most noticeable with the EM38, and at sites with low conductivity, such as Petersburg. During part of my EM38 conductivity survey of the Fort Morton grid, my lines of traverse moved between wooded and open areas. The difference between the sunny and shaded areas caused the instrument to warm and cool. As an example of this, I once set the EM38 on the ground in a sunny area while I moved the 600 ft (182 m) long rope which guided my lines of measurement. During the 22 minutes that the instrument rested in the sun, the apparent conductivity indicated by the meter rose by about 6 mS/m; it took about 23 minutes with the instrument in the shade for the instrument to cool down and return to the conductivity of the former value. This drift of the EM38 was quite large relative to the low conductivity of the soil here, and the later correction for this drift complicated the analysis of the survey.

While other tests have not shown as severe a thermal drift as I found during the Fort Morton survey, temperature changes are always a cause of difficulty for EM38 surveys. This difficulty can be greatly reduced by encasing the EM38 in insulation. After this Fort Morton survey, I made a shell of expanded plastic (Styrofoam) which fits outside the EM38; this insulation is about 0.9 cm thick. I added a thin layer of laminated wood over this plastic to protect it from abrasion. My measurements suggest that this insulation reduces the thermal drift rate of the EM38 by a factor of about 10.

The manual for the EM38 gives a good description of the procedures for calibrating the instrument. Fig. B99 may help you to understand the operation of the two controls which control the calibration. Notice that if the QP (quadrature phase) zero knob is incorrectly set, all readings shift up or down by a constant. If the IP (in phase) setting knob is incorrect, the amplitude range of the measurements is accentuated or muted. That is, the QP zero setting determines a constant which is added to the measurements, while the IP zero setting determines a multiplying factor for the measurements.

I analyzed this effect by measuring a line of conductivity at the Taylor House three times. For the first survey, I set the EM38 correctly. For the other two surveys, I incorrectly set one and then the other of the two calibration controls. Fig. B99 just shows the

correlation between the measurements with correct and incorrect settings. If there was no error, the repeated measurements should have fallen along the diagonal dashed line.

The EM38 is calibrated from measurements with the instrument held high in the air. While the EM31 seldom needs calibration, it can be done with the same procedures if it can be held at a height of 6 m or so in an area where the soil has a low conductivity. I have found one way of doing this is to lift the EM31 up into a tree and calibrate it there.

Radar Surveys

Petersburg is an unusually difficult site for conductivity surveys; it is also unusually good for ground-penetrating radar surveys. You may wish to think that the success of the radar at Petersburg will be duplicated if you try radar at your site; it probably will not. At many sites where I do geophysical surveys, I never even consider a radar survey; this is because it is obvious that the radar is unsuitable. If I were to rank those sites where I have done radar surveys in order of the success of the survey, this site at Petersburg would be in the upper 5 per cent.

If you are beginning to do your own geophysical surveys, you should not begin with radar. When the factors of equipment cost, ease of survey and interpretation, and suitability for general sites are considered, ground-penetrating radar is ranked lower than resistivity, magnetic, and conductivity surveys. That is why this section is placed in this part of the report.

At their best, however, radar surveys reveal a greater richness of detail of underground features than that furnished by any other type of geophysical survey. Radar surveys also detect a wider variety of features than other surveys do. Because the radar detects so many features, it may be less able to furnish an identification of them; different features may look rather similar. However, the capability of radar for identification is improved by of the good depth information which it provides. When radar profiles are made along parallel lines, a rough approximation of the three-dimensional form of a buried feature can be determined from the profiles. This form or shape information is usually the best guide to the identification of the features which are detected by the radar.

Radar is an interface detector. This is quite different from resistivity, magnetic, and conductivity instruments. They generally detect the volume, area, or mass of features; their anomalies increase as these parameters increase. Radar is best for detecting rather abrupt changes in the soil; if the soil contrasts are diffuse or graded, the radar may not be able to detect them. For example, in sandy or gravelly soil, the water table is a rather sharp interface, and the radar can map it clearly. If the soil is silty, there is a very broad region where the moisture of the soil changes from dry to water-saturated; the radar will probably be unsuccessful at locating this interface. The burrows of animals and insects in the soil can also blur the boundaries between soil strata.

Radar will generally detect features of a given size at a greater depth than will other geophysical instruments. However, the radar is not suitable for detecting thin soil strata. A floor pavement below a prehistoric house will probably not be found with the radar, unless there is a good contrast in the soil above and below the pavement.

Radar is generally excellent for mapping soil stratification. If there is a modern fill soil layer over an important cultural layer, a radar survey is suitable for searching for this deeper layer,

providing that the fill soil does not contain a lot of building rubble or metallic trash. Radar is best for profiling soil strata which are moderately flat and which do not have an angle of dip which is greater than about 20 degrees. If strata dip at a sharp angle, the radar profiles do not reveal the shape of their interfaces. A broad and shallow lens of cultural debris may be buried at a site; the radar can be excellent for mapping the thickness and depth of this feature; in fact, a good topographic map can be made to show the three-dimensional shape of the feature. If, instead, there is a steep-sided pit which has been refilled with debris, the radar will never be able to detect the sides of the pit; it may readily detect the debris in the pit, but the radar image will not reveal that there is a pit there. The radar image of this pit would probably be the same as that of a boulder which was underground there.

The soil at a site has a major effect on the suitability of a radar survey. If the soil is stratified, this stratification should contrast with the features you seek. Most archaeological features are rather small; if there are small features naturally in the soil, the difference between the cultural and natural features may be impossible to determine. Stones in soil are a particular source of confusion; if bedrock is shallow, the soil will probably be stony. Soils in or near glaciated areas can also show complex patterns.

If you are trying to locate flat surfaces, such as the floors of structures, with the radar, your success will be better if there are no natural and rather flat interfaces in the soil. However, if there is planar stratification visible on the radar profiles, features dug into and through these strata may be more apparent. In general, the radar gives the greatest success where there is little stratification visible on the radar profiles; Petersburg is such a site.

The type of soil and its conductivity have a major influence on the depth to which the radar can profile. In clayey, saline, or silty soil, the profiling depth may be so shallow that the radar is worthless. If you know the type of soil at a site, you can make a good prediction of the suitability of a radar survey (Doolittle and Collins 1995). Measurements of the electrical conductivity or resistivity of the soil also provide a good prediction.

If it is not possible for you to get a resistivity meter to the site for tests of the soil resistivity, you might have a sample of soil sent to you for tests; a volume of about a half liter will be adequate. You can put this soil in a small plastic bowl and saturate the soil with distilled water. Then, you can measure the resistivity of the soil using small pins rather than large electrodes. These pins can be stuck into a small wooden or plastic stick so that they are spaced by about 1 cm. These pins can then be touched to the surface of the soil and a measurement of resistivity made with the Wenner configuration using your normal resistivity meter. If the spacing between the pins is much smaller than the distance from the pins to the container, you will get an adequately good reading. Since the soil will be wet, you may underestimate the actual resistivity of the soil at the site, but this is better that an overestimate.

Equipment

For many years, there were only one or two manufacturers of ground-penetrating radars. Now, there are at least five different suppliers of these instruments. There is a good range in the price and in the capabilities of the radars. There are light-weight and portable radar systems that are readily carried to a distant site and which operate from simple batteries. There are also complex radars

which have excellent control of the profile images which are created. These more complex radars may adjustable to be best at many different site conditions; they may be very fast and they may have a higher resolution in their profile images.

There are different procedures for sending the radar signals into the earth. Most radars send the short pulse of a radio wave into the soil; these are called pulsed or impulse radars. However, other radar systems send a much longer duration radio wave into the earth; the frequency of this wave changes during the transmission. This type of radar is called a chirped, a swept frequency, or a frequency modulated (FM) radar. Both types of radar are equally suitable for surveys at archaeological sites.

Fig. A86 has a sketch of the ground-penetrating radar which I used at Petersburg. This is a pulsed radar. It is bulkier than most modern radars; it is my opinion that it gives higher quality profiles than many other radars provide. A gasoline-powered electric generator provides the 200 W of electrical power required by the equipment. Most of this power is used by the recording equipment.

The radar images are displayed on the graphic recorder as black and white shades on a paper scroll. The recorder shown in Fig. A86 has electro-sensitive paper. A small spark burns off a white coating on the paper and exposes a black layer below. This paper slowly feeds as a profile is being generated, allowing an immediate indication of the findings of a radar traverse. The control unit sets the maximum depth range of the radar, and also other technical parameters. The complete data of the radar profiles is stored with a tape recorder. This provides a backup copy of the paper image. The data can also be used to make additional, and possibly larger-scale, copies of the radar profiles. Further processing of the radar data is also possible from this tape copy.

The central part of the radar is within the boxy antenna sleds. With my radar, a long electrical cable connects the recording equipment to the antennas. Other radars use a fiber optic cable for this connection. With some systems, the recording equipment is combined with the antenna, and no cable is needed. The connecting cable for my radar is long enough that I can readily make profiles as long as 100 m; this is a convenient length for profiles.

The radar antennas shown in Fig. A86 also contain the electronics for the transmitter and receiver. The particular antenna sleds which are sketched there have separate antennas for the transmitter and the receiver, but this is not necessary since the same antenna can be used for both the transmitter and receiver. The antennas are mounted on the bottom surface of the boxes. Much of the radar pulse goes into the soil below the antenna, however, part is radiated into the air. The power of this radiated signal is quite low, less than the power radiated from hand-held transceivers used for communications. Should you wish to limit your exposure to these radar signals, you should investigate the frequency and power from a particular radar in more detail.

The two antennas which I found most suitable for the survey at Petersburg are sketched in Fig. A86. As this figure suggests, lower frequency antennas have a larger size. I have described these antennas by the predominant frequency which is apparent on a radar profile made with the antenna resting on rather typical soil. A manufacturer may describe an antenna by the frequency of the signal when the antenna is elevated in the air; these frequencies will be higher that the frequencies of my description. For example, the 180 MHz antenna has a frequency in air of about 300 MHz, while the 315 MHz

antenna has an air frequency of about 500 MHz.

By the way, these frequencies are about in the band where television signals are transmitted. There are also many other signals in these bands. While there will be a small amount of radio interference to a radio or television which is very near the radar, most of the interference will go the other way. Since the radar has such a sensitive receiver, it detects radio signals from other transmitters in the vicinity as interference. Mobile transmitters in cars or trucks are particularly a problem in cities; small hand-held transceivers cause interference if they are close also. Look for nearby transmitter antennas near a site before considering a radar survey.

You will select a radar antenna on the basis of what you know about the soil and also the size and depth of the archaeological features at a site. If the features are larger than 2 m in size, most of the common radar antennas will be suitable. The 180 MHz antenna of this survey can detect some features as small as about 0.2 m in size, while the 315 MHz may be able to detect features as small as 0.1 m in size. These small features may have to have a depth which is less than 0.5 m to be detected. Remember that there are many natural features in the soil which are small in size. If you are trying to locate post holes, there are also many stones, rodent tunnels, and tree roots which are about the same size and which will be detected at least as readily. If you need to search the upper 0.5 m of the soil, you will need a fairly high resolution antenna, probably the 315 MHz antenna or one with even higher frequency.

There is a good correlation between the depth at which a radar antenna will profile and the electrical resistivity of the soil. Fig. B100 shows some of my measurements. Depths and resistivities are plotted there for 79 different sites where I have measured both. If the resistivity is greater than 1000 ohm-m, the 315 MHz antenna has generally been the best; if the resistivity is less than 100 ohm-m, the 180 MHz antenna is generally best. While the maximum depth at which features are detected is dependent on the contrast of the underground features, the depths here have been estimated from the maximum depth at which distinct echoes were detected at each site.

A specific radar antenna will be optimum for exploration though a particular range of depths. You will be able to select an antenna which is most suitable for your site. The antennas are distinguished by the frequency of the radio wave which they transmit. High frequency antennas allow the detection of small features at a shallow depth; lower frequency antennas will detect features which are deeper, but the features must be larger and they must not be too shallow. Radar antennas are primarily limited by the maximum depth at which they can profile, but they are also limited by the minimum depth at which features can be detected. As the frequency of the antenna is reduced, both the maximum and minimum depth of exploration increase.

I tested four different radar antennas during my survey at Petersburg. Radar profiles made over the cellar of the Taylor House and also the bombproof trenches of Fort Morton illustrate the tradeoff between resolution and profiling depth. These antennas are described by either their resolution or their characteristic frequency; the adjectives "low", "medium", "high", and "very high" distinguish both the resolution and the frequency of the four antennas and their profiles.

A low resolution radar profile across the cellar is illustrated in Fig. B101. This antenna is not sketched in Fig. A86; it is larger than the two antennas there and it is about 1 m square. The

horizontal span of the radar profile is 50 ft (15 m); tick marks at the top of the profile show 5 ft (1.5 m) intervals. The black bands at a depth of about 1.5 m are echoes of the radar signal from the floor of the cellar. This is the antenna which I used for the first radar survey at Petersburg (in 1979) and it readily detected the cellar then.

The same line is profiled with a medium resolution antenna in Fig. B102. Note that shallower features are detected with this higher frequency antenna. The darker echo bands with this profile are just caused by the fact that the settings of the radar were different for this profile and that of Fig. B101.

There is a very pronounced difference with the next higher frequency antenna, whose profile is illustrated in Fig. B103. The very thin echo bands indicate its higher frequency and its capability for detecting thinner strata. The flat echo bands which are very apparent below a depth of 1.5 m are just caused by a defect in the radar.

The highest frequency antenna gives the rather faint, but fine-detailed echoes plotted in Fig. B104. This antenna is not illustrated in Fig. A86; it is only about 0.25 m long. Notice the echo on the profile at N70; this is from an object which is about 0.25 m underground. It is detected weakly with the 315 MHz antenna, but not detected at all with the two lower frequency antennas. However, the detection of the cellar is so weak with this antenna that this antenna is much less suitable than the other antennas for features at a depth of greater than 1 m. However, this antenna can detect features as shallow as about 10 cm.

Four radar profiles from Fort Morton also illustrate the effects of resolution and depth. With a low frequency antenna, the echoes from four trenches of the bombproof are difficult to isolate on the profile of Fig. B105. During my 1979 search for Fort Morton with this antenna, I could not identify the fort on the profiles which I made with this antenna; see Fig. C150. The trenches of the fort are more distinct in the higher resolution profiles of Fig. B106 and Fig. B107. With the highest resolution profile, shown in Fig. B108, only one of the trenches is detected with a strong echo.

If a radar survey is to be done in a city, it may be most important to select an antenna which will detect less interference from the many other radio transmissions. I have always found that the 315 MHz antenna detects much less noise in cities than the 180 MHz antenna. Even though the 180 MHz antenna should be able to profile to a greater depth, I have found that noise can limit its profiling depth to be less than that of the 315 MHz during surveys in cities.

Survey procedures

Radar profiles are easiest to interpret if they cover rather long spans. If the profiles do not extend to a good distance outside a feature, the feature might not be recognized as anything unusual. As with my other surveys, I find it best to make the radar profiles go the long length of a site rather than the short width.

A site will usually be surveyed with the radar by making a set of parallel profiles across it. The spacing between these profiles is determined by the time allowable, and also the size of features to be mapped. For some applications, widely spaced profiles can be very suitable. For most of my surveys at many sites, I have started with a line spacing of 1 - 2 m. If interesting features are found, I can go back and make profiles midway between the original profiles in order to resolve the shape of the features better.

Radar Surveys

If long or linear features need to be mapped, but their direction is not known, it can be important to make radar profiles going in two perpendicular directions. If the direction of the features are known and constant, just profile across the width of the features. It is necessary to make difficult choices about strategy. After an area has been surveyed with lines spaced by 1 m, should the next group of profiles be midway between those first profiles, or should they be at the same spacing, but in a perpendicular direction? The information from the initial survey may answer this question, but it is almost always good to make at least some profiles in a perpendicular direction.

The lines of profile can be marked with a rope which has calibrated marks along its length at fixed intervals. I find it best to set this rope slightly off the line of the profile, so that the antenna goes just next to it during the traverse. The recorded traverses with the antenna should be made in only one direction, and not in a zig-zag fashion. If alternate profiles are in opposite directions, they are difficult to interpret; however, it may be possible to make an electronic correction of the profile direction. If there are trees in the area of survey, it will usually be necessary to profile in only one direction in order to keep the cable from the antenna to the recording equipment from getting wrapped around trees.

I can operate my radar by myself, since I can turn the recorders on and off from where I am at the radar antenna. Some radar systems will require two people for their operation. The recording equipment for my radar is usually in the back of my car. After I have finished a line of traverse, I sometimes walk back to the recorders to note the location of the traverse on the profile and to take a look at what the profile revealed. Otherwise, I have no immediate indication of the findings of the survey.

It is possible that the long electrical cable connecting the radar antenna to the recording equipment will become twisted (actually, rotated) during a survey; this will make it more likely that the cable will become caught in weeds or brush. This twisting can be prevented by pulling the antenna so that it effectively makes S-patterns on the ground; you can make these S-patterns if you never pull the antenna over its cable (while you can actually cross the cable, you should quickly cross over it to the original side). A cable twist is generated each time the antenna is pulled around in a circular loop. The cable will be easiest to pick up and store if it is not twisted. I find that a light wooden spool is best for holding the antenna cable; an axle allows the cable to be quickly unspooled.

Whenever I can, I follow a convention that the right side of a profile should be on the north or east side of the line of survey; this convention is also common for drawing archaeological sections. However, some site conditions will make it easier to traverse in a different direction. Sometimes it is easier to pull an antenna uphill or downhill, depending on the slope. I usually walk backwards when pulling a radar antenna; in severe weather, it is more pleasant to have a strong wind on one's back. During the radar survey at Fort Morton, I made radar profiles to the south, rather than to the conventional north direction. This was because of the woods which were on the south side of the grid. If the antenna is pulled into the wooded area, the cable will not get caught on a branch or stump. If the bend of the antenna cable, between its stationary and moving sections, is in a wooded area, it is likely to get caught on a small projection such as a short stump of a bush or root; this will halt the traverse until the cable snag is cleared.

I like to keep the horizontal scale of my radar profiles as constant as possible; this simplifies their interpretation and it also improves the accuracy of locations. If one pulls the radar along a line at an irregular rate, the scale of the profiles is also irregular. I use a small metronome to help me keep my speed constant; this is constructed from a standard type 3909 integrated circuit. It is connected to a small electronic buzzer and set to give beeps at intervals of about 1 s. I pull the radar antenna at a speed such that there is a constant time period between intervals along the guide rope. With my radar, a good speed may be in the vicinity of 1 meter per 5 seconds. If markers on the guide rope are at 1 m intervals, I just spend my day counting up to five.

Each radar can be adjusted to set how rapidly echo scans are built up on the radar profiles. With my radar, these echo scans are vertical lines on the profiles; they are usually so close together than the separate lines cannot be distinguished. The frequency of these echo scans, the traverse speed of the antenna, and the depth setting of the radar determine the aspect ratio of the radar profiles. Fig. B109 illustrates two ratios.

The aspect ratio is the compression of the horizontal scale relative to the vertical scale. For typical radar profiles, this compression is usually quite large. At the left side of the two profiles in Fig. B109, the rectangular shapes indicate a length of 1 m on their horizontal and vertical sides. A large horizontal compression allows slightly different depths to be readily determined. While you could make the horizontal and vertical scales of a radar profile to be the same, this would require a very long and narrow paper profile. Remember that a high compression causes the apparent slopes of dipping interfaces to be exaggerated. An aspect ratio of about 15 is generally good and this is about what I normally use.

Radar antennas should not normally be set directly on the surface of the ground. If they are, small and shallow contrasts in the soil have a marked effect on the antenna; this is generally undesirable. If the antenna is lifted slightly, these effects are greatly reduced. This difference is shown in Fig. B110. On the right side of the figure, the sharp vertical lines in the profile make the features more difficult to locate. The antenna can be lifted slightly with runners or wheels. I find that flat-bottomed antennas can be lifted by putting foam plastic on their bottom side; a heavy duty abrasion resistant plastic sheet can cover this foam (high density polyethylene is excellent). The foam plastic below an antenna must not be electrically-conductive; thick, conductive foams are relatively rare, and a resistance meter quickly checks for them.

The slightly elevated antenna has two disadvantages. It somewhat reduces the strength of the echoes from underground features, and it increases the echoes from overhead features, such as electric wires or tree limbs. In some circumstances, it can be better to have the antenna directly on the ground. However, if it is directly on the ground surface, a small pile of grass can cause a significant and confusing radar echo. These are most apparent with the higher frequency radar antennas.

A rainstorm can cause a noticeable change in the appearance of radar profiles. It is not always clear whether radar profiles are better if the soil is dry or wet, but they are distinctly poorer just after rain has started to seep into the soil. I tested the effect of rain several times during my survey at Petersburg. Fig. B111 shows one comparison. There was a total rainfall of 7.4 cm in the period between these two profiles. Note that the profile is simpler before

the rain, and that the echo amplitudes are larger after the rain. At this site, radar profiles made a day after a rainstorm are excellent and show a higher contrast in the features than before the rain. However, radar profiles made only a few hours after a rain are inferior. There is an example at the top of Fig. B112. A day after the end of the rain, the moisture has had a chance to spread into the soil, and this reduces the contrast of this unwanted soil moisture interface. The radar profiles of Fig. B111 and Fig. B112 are partly along the line of one of the bombproof trenches at Fort Morton.

I have seen similar effects at sites with different soil. Radar surveys, like resistivity surveys, appear to give the best results when the soil is neither too wet nor too dry. I have not done enough radar surveys on frozen ground to have seen any noticeable effects, however the interface between frozen and unfrozen soil should cause an echo on a radar profile. Frozen soil has a higher electrical resistivity, and this may improve the profiling depth at some sites.

Interpretation

The first step in the interpretation of a radar survey is a determination of the speed of the radar pulse in the soil. With this information, you will be able to estimate the depth of the features which are detected.

I find that the best method for this speed determination is a simple calculation based on the shapes of radar echoes which are encountered on the profiles of a survey. The two profiles in Fig. B113 show arc-shaped radar echoes; the width or roundness of these arcs is proportional to the velocity of the radar wave in the soil.

Select echoes which show clear and smooth arcs. Pipes and wires are usually excellent for this measurement. Since a trench might have been dug for the pipe or wire, the soil directly over the pipe may not be the same as the surrounding undisturbed soil. However, for most of the echo arc, the radar signal will have traveled through the unexcavated soil. If you suspect that the echo might be from a broad feature, such as an underground tank, it should not be used.

These radar echo arcs are mathematical hyperbolas. They are simply the result of the changing distance from the radar antenna to the reflector. The radar antennas send a broad beam of radiation into the soil; therefore, the antenna detects a feature before it has reached it along the line of the traverse. As the antenna passes over the top of the feature, the distance to the object decreases, and then it increases again as the antenna goes away from the object.

The geometry of this is drawn at the top of Fig. B114. The letter "r" indicates the changing distance or range to the object, while "d" is the depth or minimum distance to it. The velocity of the radar pulse is "v" and the time required for the pulse to go from the antenna to the object, or back again, is "t1", meaning the one-way echo delay time.

The simple equations at the top of the figure are solved for the velocity; this result is at the bottom of the figure. The velocity calculation is based on three measurements which you will make on each echo arc. These distances are marked with broken lines at the bottom of Fig. B114.

For the first step in the analysis of an echo, draw a horizontal line across the arc near the lowest point where the arc is clear. Measure the distance across this arc on the paper copy of the profile. Then convert this paper distance to the actual ground width of the arc. This conversion can be done from the distance between tick marks at the top of the profile.

Next, measure the echo delay time to the horizontal line you have drawn. The illustrations with this report show where I find the zero point of the depth or delay time on the radar profiles to be. Different radar systems may have a different zero point. Your setting of the radar will determine the proportionality between the distance on the paper copy of the radar profile and the echo time.

Finally, measure the echo delay time to the top of the echo arc. For my radar antennas, there are typically about three nested echo arcs. This triplication is just caused by the fact that there are three pulses of the radio wave sent into the soil (actually these are just three half-cyles of a very short radio wave). I measure a distance to the white line between the first and second echo arcs.

With these two times and the one distance, the velocity can be determined with a simple calculator. Measure a few of these arcs to see if they give a consistent value for the velocity. There is a more detailed discussion of my measurements of radar pulse velocity in Volume C. I found that a good estimate of the velocity in the Taylor House grid was 0.090 m/ns; the velocity for the Fort Morton grid was 0.094 m/ns. These velocities have calibrated the depth scales of the radar profiles and maps in this report.

Fig. B115 is a plot of the velocities of the radar signals which I have measured at 79 sites; these are the same sites which are included in Fig. B100. The average pulse velocity which I have measured is about 0.1 meter per nanosecond (m/ns). This speed is about a third of the speed of light (or the radar pulse) in air. The speed of the pulse is somewhat higher in high resistivity soils, such as sand, but the resistivity does not have a strong effect on the velocity. In principle, there should be a difference in the velocities determined from radar antennas with different frequencies. However, I have never seen a noticeable difference.

After you have estimated the velocity of the radar signal in the soil, you can prepare a paper scale which shows the echo depths. This scale can be set next to a radar profile and the depths can be easily read from it.

You can then begin to map the plan position of the different types of radar echoes. Cluster the echoes by their appearance and plot the location of the echoes with symbols on a map. It is good to use a symbol which gives a hint as to the character of the echo. Small and compact symbols can mark small and compact echoes. Linear symbols indicate the location of a long echo pattern found along a traverse. Use different symbols to distinguish the clarity of the echoes also. Fig. B116 has a key to the symbols which I find useful for my radar maps. The profiles which are illustrated here show my definition of these different types of echoes.

There is typically no clear boundary between these different classes. Also, I find that my definition of different types of radar echoes can change somewhat as I do an interpretation; this does not cause much difficulty. My major goal is to make sure that the important lateral contrasts in the echoes have been marked. This is why I sometimes put a short vertical line on the interpretation map to mark where there was a change that I could not readily categorize.

Here are approximate definitions of the different symbols in Fig. B116. Irregular strata appear to be the result of contrasts in the earth, such as lenses of differing types of soil. Chaotic echoes and fine-scale complexity appear to be due to many small objects in the soil; chaotic echoes appear most likely to be due to metal objects or to air pockets, typical of rubble or trash underground. The echo pattern for irregular strata is smoother than the pattern mapped as

having chaotic echoes or a fine-scale complexity. Whenever possible, individual reflecting objects are mapped with circular symbols. Where there are too many objects to map separately, because of limits on interpretation time or the density of the echoes, then the echoes are just grouped with a linear symbol such as the chaotic echo symbol. Weak echoes are faint, obscured, or otherwise unreliable. Distinct echoes appear to be reliable indicators of buried objects. The most distinct, smooth, and large amplitude echoes are marked with a dot within a circle. Reverberations are caused by multiple echoes from an object or soil interface. Normally there are about three echo bands caused by each interface; with reverberations, there are many more vertically-aligned echoes from each interface. Typically, these reverberations are found where the radar signal reflects several times between metallic objects and the surface of the soil. In some cases, they will be caused by echoes between two or more objects which are underground, or between the upper and lower surfaces of a sharp contrast in the soil.

All radar echoes cannot definitely be categorized into separate types; examples can always be found which are in between any two classes of echoes which have been defined. Radar interpretation does not have to be perfect, but a good interpretation should try to extract as much information from the radar records as can be justified by time and cost. You may wish to have a procedure which will be completely automatic, so that you do not have to make any judgments about the radar information and so that an interpretation can be done by any unskilled person. This cannot be done yet. Indeed there are computerized processes which will alter a radar image (some people might call this an enhancement), but most of these processes give little benefit. However, some procedures for extracting and mapping radar echoes from selected depths can provide an objective display of their spatial patterns; these procedures can be done with a computer (Battelle 1981; Goodman and others 1994; Grumman and Daniels 1995) or with paper copies of profiles. Computers are very valuable for eliminating much of the detail of preparing radar echo maps and illustrations. The figures with this report illustrate drawings which have been drafted semi-automatically, even though the interpretation itself was not done with a computer.

It is easiest to see changes in the character of an echo along a profile; it is more difficult to spot the changes from one parallel profile to another. A few profiles, made perpendicular to the major direction, can help this.

On my first interpretation of a set of radar profiles, I try to evaluate each profile separately, without reference to the other profiles. This gives me my most unbiased map of the locations where features are distinct. After I have mapped these echoes, I re-interpret the profiles, taking a closer look near those areas where I have already mapped an echo. I try to see if there are faint traces of the same type of echo which I did not see on the first examination.

The radar surveys at the Taylor House will illustrate the interpretation of radar profiles. The first survey which I did in the area was in 1979; my interpretation of those radar profiles is given in Fig. B117. That survey was done with a low frequency and low resolution antenna; while it was adequate for locating the cellar, the higher resolution antennas of my 1992 survey have been much more suitable for this site.

The echo maps from these higher resolution radar surveys are plotted in Fig. B119 and Fig. B122. In order to generate these figures, a total length of 27,740 ft (8.5 km) was profiled with the

two antennas. The lines of profile are plotted in Fig. B118. These profile lines are much closer together than is typical; the time required for this detailed a survey usually cannot be justified. However, this survey has shown how even rather small and faint features can sometimes be reliably mapped.

A total of 1878 echoes are mapped in Fig. B119 and Fig. B122. There is not enough room in the figures to show the depths of the different echoes. For the 180 MHz antenna, these depths are indicated separately in Fig. B120 and Fig. B121; see Fig. B123 and Fig. B124 for the 315 MHz antenna. Depths are in decimeters (dm), multiply these numbers by 0.3 to convert them to depths in feet. These map pairs, which separate the echoes by the direction of traverse, help the interpretation, for they can show linear patterns more clearly than a map which combines echoes from both directions of traverse.

When radar profiles have been made along perpendicular lines, it is possible to locate features more accurately, although this may not always be needed. Fig. B125 shows the procedure. Points are plotted on the radar echo maps (like those of Fig. B120) to indicate where the object was closest to the radar antenna along the line of traverse. The object may not be directly under the line of the traverse; instead, it may be off to the side of the path of the radar. This is because the signal beamed from the radar antenna spreads out to the left and right of the antenna. The radar interpretation maps in this report, such as those in Fig. A11, have this refined location of features, which is derived from the detailed echo maps.

A selection of the most interesting radar profiles is included with this volume; additional radar profiles are in Volume C of the report. An index of the radar profiles in this report, made in the Taylor House grid, is plotted in Fig. B126.

The cellar floor of the Taylor House is clearly indicated at a depth of about 1.5 in Fig. B127; a perpendicular profile is illustrated in Fig. B128. Tick marks at the tops of these profiles indicate 5 ft (1.5 m) intervals along the profile. I put these markers on the radar profiles when I did the field traverse. There is a button on the handle of the radar antenna; I pushed this whenever the middle of the antenna passed 5 ft points along the guide rope. At 50 ft (15 m) intervals, I put two markers on the profile; this allows points to be quickly and reliably located.

Black bands on the profile indicate radar echoes. Darker bands indicate stronger echoes. The radar signal alternates from positive to negative to positive in its polarity. All of these alternations are identically printed in this profile as black bands. Sometimes it can be valuable to distinguish the positive and negative polarities, but I have not done that for the profiles here. The white areas on the radar profile locate regions where the amplitude of the radar echo was low. The amplitude is low as the polarity of the echo changes, so there are white lines between the dark echo bands.

The upper black bands are rather horizontal and unchanging. These bands are primarily a result of the transmitted signal going directly to the receiver; echoes from the surface of the earth can also appear there. These bands can sometimes hide the echoes from features which are at a shallow depth in the soil. The echo bands which are below these horizontal bands reveal information about underground features.

Echo bands are typically triplicated, although sometimes there will be two, four, or five echo bands caused by one feature or interface. This triplication is just caused by the three half cycles of the transmitted signal, a sinusoidal wave going from positive to

negative to positive. The depth of a reflector is determined by the distance on the profile from the surface to the first thin white band which is below the first distinct dark band. If there are three dark bands numbered from 1 to 3 counting from the surface, measure to the line between bands 1 and 2. If there are more than three black bands, it is more difficult to determine the depth. It is not uncommon for there to be uncertainty in the depth of objects by an amount equal to the width of an echo band. Also, interference between radar echoes can obscure and distort the echo arcs. The numbers at the bottoms of the profiles which illustrate this report show my estimation of the depth of the objects; these depths are in meters.

The radar profiles of the Taylor House cellar show a relatively flat lower surface and also a moderately complex group of echoes above that. These shallower echoes might be caused by the rubble which fills part of the cellar. The profiles of Fig. B127 and Fig. B128 also show echo peaks or arcs at a depth of roughly 0.5 m at the ends of the cellar. It is possible that these are caused by the intact brick foundation. I mapped these apparent wall depths in Fig. A9; they are in fair agreement with the findings of the most detailed magnetic survey.

After the radar echo maps are prepared, clustering of echoes will be apparent and the boundaries of these clusters can be estimated. For the Taylor House, these interpreted boundaries are drawn in Fig. A11 and Fig. A12. Broken lines in those figures indicate boundaries which are not as distinct. For some radar surveys, I find that it can be valuable to distinguish the different types of clusters of echoes on the interpreted map; for this survey, those distinctions have not been strong and so I have only indicated the clarity of the clusters.

The conductivity and resistivity maps of this grid (Fig. B4, Fig. B66, and Fig. B73) all show high resistivity on the eastern side of the area. One possible interpretation of this is that rather sandy soil has been spread on the surface in this area; perhaps this was done when the fortifications were leveled. The radar profiles do not reveal this soil interface, but the depths of the features do suggest the possibility of fill soil. The statistics of the echoes from the high resolution antenna are plotted in Fig. B129; these suggest that the radar echoes are slightly deeper on the east side of the survey area. Perhaps a layer of soil has been spread on the surface there.

Many features are immediately apparent on the radar profiles even as the field work is being done; the cellar of the Taylor House is obvious by a quick look at a profile just after the traverse is finished. Some features only become apparent after a detailed examination and mapping of the radar echoes. The radar echo map of Fig. B122 shows a line of echoes which goes from the southwest corner of the Taylor House cellar to near W80 N20; this is almost surely caused by a trench which was at this location during the Civil War (see Fig. A6). This feature is so indistinct on the radar profiles that I never noticed it until I had completed this combined echo map.

Fig. B130 illustrates one difficulty in determining the depth of a feature. At the point labeled Gt6 there are echo arcs which indicate that there is an object at a depth of 1.4 m. I suspect that this object is actually at a depth of about 0.6 m, where there is a very faint echo. The arcs at 1.4 m are probably a second echo, or reverberation, from the object; the radar signal made two round trips between the surface and the object. The arcs at the very bottom of the profile probably indicate the third echo from the object. This type of echo is relatively rare; it can usually be identified by the fact that there are vertically-aligned echoes which have roughly an

equal spacing between them.

The very high frequency radar antenna is not very suitable for this site because the radar echoes from a depth of over 0.5 m are quite faint. However, I did some profiles with it over the cellar of the Taylor House. The echo map of Fig. B131 is a plot of the findings. While relatively little was located, two refilled archaeological excavations appear to cause the echoes at the northeast and southwest corners of the area.

The radar profiles of the Fort Morton grid were widely spaced; Fig. B132 locates them. The total profile length for the mapping of Fort Morton was 55,355 ft (16.9 km). The three areas of the detailed resurveys are readily apparent in the figure.

The combined echo map of the main area of survey is plotted as Fig. B133. The backwards-D shape of the fort can be seen; bottoms of refilled fortification ditches were mapped by the radar. The radar maps are split by the direction of traverse in Fig. B134 and Fig. B135. The buried power line is apparent near the left side of Fig. B134; notice that this wire was not detected very well on the north-south profiles, as revealed by the map of Fig. B135. This is because the traverse then crossed the wire at a much smaller angle. Fig. B136 locates the radar profiles from the Fort Morton area which are illustrated in this report.

The radar profile of Fig. B137 goes lengthwise down one of the bombproof trenches of the fort; the radar indicates that the bottom of the trench is about 0.9 m underground. Several small objects were detected by the radar as small arcs, but these are not marked at the bottom the profile. The unchanging gray bands at a depth of about 1 m near E475 are caused by an electronic ringing within the radar system, and not by any soil stratification. Another view of a bombproof trench is given on the left side of Fig. B138. This profile shows a rather flat lower surface there; the profile also shows a complex pattern above that surface which could be caused by debris in the soil which fills the trench, or by the mixture of fill soil itself. The radar echo from the main fortification trench is not very clear, but two crossings of the covered way or zig-zag trench are very distinct.

Fig. B139 is a profile which crosses the front of Fort Morton. The radar detected no trace of the earth ridge or parapet there, for this was scraped back into the excavated area when the fort was leveled. The excavation shown in the figure was made by the soldiers as a source of the soil which built up the parapet; they used the soil behind the parapet so that they could make their excavations while they were protected by the parapet. The cross-section of the fort, at the top of Fig. A73, shows this excavation below the broken line. The buried wire going to the tape recorder causes the echo on the left side of the profile, at E259.

On the right hand side of Fig. B140, there is a very clear group of echo arcs which is caused by an underground pipe. The pipe causes three very strong arcs with additional, but faint, echoes above and below those three. There was formerly a farm in the northwest corner of the Fort Morton grid, and most of the echoes here are caused by underground remnants of the demolished structures.

The two profiles in Fig. B141 appear to locate a wire. When the radar antenna crossed over this wire at a shallow oblique angle (the left profile), it revealed a pattern which is similar to that of a broad soil interface. Perpendicular radar profiles reveal very narrow echo arcs along this line; the feature cannot be caused by a soil contrast. Because of the 10 ft spacing between the profiles, the interpretation of the radar in this part of the survey area is less

certain. The magnetic and EM surveys do not appear to have detected this feature. This means that it is not an iron pipe; if it is a wire, the failure of the EM survey to detect it is puzzling.

The extended echo, or reverberation, shown in Fig. B141 is a clue that the object is metallic. Another clear reverberation is illustrated with Fig. B142; I use an asterisk to mark reverberating echoes. This object must be at least about 10 cm long. Segments of metal wires are a common cause of these patterns. While this echo appears to start at a depth of about 0.3 m, the object may actually be at a shallower depth.

The geophysical summary of Fig. A22 identifies an area of debris near the northeast corner of the Fort Morton area; the profile of Fig. B143 illustrates this. The undulating symbol marks a span where the soil strata are irregular. While the area of this irregularity is well-defined, it does not correlate with the locations of any Civil War fortifications. This echo pattern may be caused by large-area excavations which were made during the siege, but the proximity to the park road suggests that this could be an area which has a layer of recent debris. The basin-shaped echoes on the right side of the profile are caused by the fill of the former park road. While the surface is now grass-covered, there is probably a layer of gravel in the ground below.

A dense mesh of radar profiles resulted in a very thorough survey of the Bombproof detail; it is illustrated in Fig. B144. While some of the trenches in this grid were easy to detect with the radar, others were detected only faintly. However, the closely spaced lines allowed these faint echoes to be delineated with a good reliability. Fig. B145 is the combined echo map. The directional radar maps of Fig. B146, Fig. B147, and Fig. B148 show the depths of the echoes. The southern powder magazine, at E340 S250, and the north-south trench, at E360, were not at all clear on the radar profiles; they could be mapped and identified because of the close spacing of the radar profiles. Even with this close spacing, the radar did not give clear information on the area near E380 S245. The resistivity survey (Fig. B9) and EM38 conductivity survey (Fig. B86) both hint at the possibility that rather silty soil may have been spread in this area, and this has attenuated the radar signals here. It is possible that this soil was spread during the leveling of Fort Morton after the war.

In Fig. B149, a drawing of the cross-section of the bombproof is compared to a radar profile of the existing trenches. Note that the right-most radar echo band, which appears to be caused by a fourth bombproof trench, is not shown in the cross-section or the map of the fort. It is possible that this trench was dug after the map of the fort was prepared.

The lines of radar profile which were made at the Trench detail are mapped in Fig. B150 and the combined echo map is shown in Fig. B151. If the purpose of this survey was the location of the main line of the Civil War fortification, the lines were much closer together than they needed to be. However, some smaller features on the right side of the area would only be clear with rather closely-spaced lines. The findings of the separate surveys are plotted as Fig. B152, Fig. B153, and Fig. B154.

The two radar profiles in Fig. B155 reveal the main fortification trench. The main trench is on the left side of the profiles; there are extensions of the trench, like bays, going to the right. These appear to be dugouts or similar excavations which are along the back wall of the main trench. In addition, there are isolated pits behind the main line of the fortification. The profile of Fig. B156 may be

crossing several of these. The historical photographs of this general area suggest that many huts were built behind the main line of the fortification.

The radar detected a complex cluster of echoes in the Iron detail at the well; Fig. B157 has the information. While the magnetic survey of this area was spectacular, and the conductivity and resistivity surveys gave interesting results also, the radar profiles were not particularly impressive. However, this survey did indicate that there are a number of separate objects in this area, and many of them appear to be metallic. The radar profiles of Fig. B158 show the echoes which were detected by the two different radar antennas.

Self-Potential Surveys

Self-potential, or SP, surveys measure voltages at the surface of the earth. The equipment needed for this survey is both simple and inexpensive; however, the survey speed is quite slow. These surveys have not been used very much for archaeology, and so relatively little is known about the benefits and best applications of SP surveys. This is an excellent technique for experimentation.

It is difficult to find practical information about doing the field work and interpretation for most types of geophysical survey. SP surveys are different; several authors have written excellent descriptions of the procedures (Corwin 1990; Wynn and Sherwood 1984; Corry, DeMoully, and Gerety 1983; Burr 1982; Corwin and Hoover 1979).

Self-potential surveys are used extensively for engineering applications, measuring the corrosion rate of metallic pipes which are underground (Lattin 1979). I have seen very interesting articles about the procedures of these engineering applications, but I have never found a good and complete summary. As near as I can tell, there is very little communication between those in this engineering discipline and those who apply SP for exploration geophysics, often as a search for minerals.

Water which contains a small amount of salt becomes ionized; when this water moves through the soil, the moving charged particles are an electrical current. These currents create voltages which can be measured at the surface; even the very slow movement of water seeping in the soil can generate detectable voltages. Since archaeological features can cut into natural soil strata, they can alter the rate at which rainwater will seep through the soil; these earthen types of features might be detectable with an SP survey.

There is an interesting converse to the fact that moving groundwater will generate electrical currents. Just as the converse of an electrical generator is a motor, if voltages are applied to the earth's surface, groundwater can be pumped. This is called electro-osmosis (Probstein and Hicks 1993; Gray 1969), and it has been applied to the preservation of building foundations and mud brick walls by preventing moisture from rising within them.

Another interesting aspect of self-potential is the fact that burrowing animals, like moles, can detect electrical voltages in the soil (Conniff 1994); I do not know if they may be affected by the small voltages which are measured by an SP survey. There appear to be many mole tunnels in the Fort Morton grid, but I never checked to see if there was a change in the density of their excavations near the Iron detail, where the SP voltage is rather large.

Equipment

The very simple items which you need for a self-potential survey are illustrated in Fig. A90. Probably any digital voltmeter

(sometimes called a digital multimeter, DMM) will be excellent for these surveys. You will be measuring voltages in the vicinity of 0.010 volts (0.01 V = 10 mV) and you will need to be able to read the value to a precision of 0.001 V (1 mV, one millivolt). Most of these digital voltmeters will have a high input impedance; this just means that very little current flows into the voltmeter when it is making a measurement. This input impedance should be greater than one megohm, and probably all digital voltmeters exceed this. Analog voltmeters have a moving needle which points to the value on a dial. While not as good as a digital meter, many of these meters may be suitable for SP surveys also; you should use an analog meter if you cannot get a digital voltmeter. If you have one of these analog meters which does not have a sufficiently precise voltage scale, you might try to measure with the meter's most precise current scale; this may sometimes allow good measurements.

It would be nice if the leads from the voltmeter could be just touched to the soil surface to measure the voltage there. This does not usually work, however, because chemical reactions between the metal of the electrodes and the soil changes the small voltages which you wish to measure. Instead, it is necessary to use special electrodes to contact the soil; these are called non-polarizing electrodes.

The essential aspect of a non-polarizing electrode is that the electrical current flows from a metal (such as copper) to a solution of a salt of that metal (such as copper sulfate in water) and then into the soil. For the simple electrodes shown in Fig. A90, the wire from the voltmeter connects to a copper wire which goes into the water solution. The ceramic of the flower pot just allows the solution to very slowly seep through it and moisten the bottom of the pot. This pot is just set on the soil to make the voltage measurement.

This type of non-polarizing electrode is called a copper-copper sulfate (Cu-CuSO4) electrode. It is the type which is most commonly applied to self-potential surveys. Another type of electrode uses a different metal, this is the silver-silver chloride (Ag-AgCl) electrode. These Ag-AgCl electrodes are most commonly found in chemistry laboratories, where they are used to measure the acidity of solutions; they are called reference junction half-cells in that field. These Ag-AgCl electrodes are less sensitive to changes in temperature than are Cu-CuSO4 electrodes; however, they are also more expensive. Cu-CuSO4 electrodes can be purchased from geophysical supply companies or companies which sell equipment for corrosion testing; you can also make your own Cu-CuSO4 electrodes if you wish to. I tested several types of non-polarizing electrodes during my survey at Petersburg, and I got the best results with the electrodes which I made myself.

The basic ingredient is a flower pot. Any ceramic, non-glazed pot will do. If there is a hole at its bottom, this can be plugged with a cork or with epoxy putty. It is possible that there are salts within the ceramic which might affect the measurement, so I have washed my pots out with fresh water. I just filled the pots with water and let them set for a week in the air; water will slowly seep through the pot and I rinsed this off every day.

To complete this pot as a copper-copper sulfate electrode, just bend a short copper wire so that it goes from the edge of the pot down to the bottom. Then, add a quantity of distilled water to the pot to a depth of about a centimeter. Finally, put in copper sulfate crystals, and add more later as these dissolve; make sure that these blue crystals are always visible at the bottom of the pot. If these

crystals are always visible, the solution is saturated with copper sulfate, and this is necessary. If the flower pots are dry before the start of the survey; it may take about 15 minutes for the solution to seep through the ceramic.

Copper sulfate is available from chemical supply companies and perhaps also from stores which sell hardware. A quantity of 500 g will be sufficient for many thousand measurements. There are different grades of purity of copper sulfate available, and I believe that the common chemical grade is adequate for these electrodes. If you can find only lower purity (industrial grade) copper sulfate, try it.

You will need at least two of these copper-copper sulfate electrodes, but a few more may speed the survey. Copper sulfate is not particularly dangerous. I recall reading somewhere that it damages leather, but I have not tested this. Copper sulfate is commonly used to kill algae in ponds. If too much is used, fish will be killed also (Environmental Protection Agency 1973 p. 89). While only small amounts of this chemical seep through the SP electrodes, you may reduce this by making the solution into a jelly (Burr 1982). Perhaps the copper sulfate which seeps into the soil will remain there a long time and cause difficulty for a future geophysical survey which is capable of locating the element copper.

You will also need some small electrical clips to connect the voltmeter to the copper wires at the pot. Finally, you will need an insulated wire which is probably as long as the largest area which you wish to survey, but a maximum length of about 40 m would be fine. A tape measure or calibrated rope can be used to define the line of each measurement traverse.

Procedures

I made self-potential measurements in three areas of Fort Morton; these are located in Fig. B159. The surveys gave the best results in the Iron detail, where the other geophysical instruments indicated that there was a large mass of iron underground. My measurements of the earth voltage, or potential, are plotted in Fig. B160. The voltage is distinctly low at E526, over the iron mass.

I used two of the flower pot electrodes for this survey. I kept one stationary at E509 S145, the end of the line. This was the reference electrode and I measured voltages relative to it. It is a convention for SP surveys that the negative lead of the voltmeter is connected to this reference electrode. I scraped away the grass below this reference electrode so that it's bottom would touch bare soil. Measurements of voltage were made at intervals of 1 ft (0.3 m) along a line by placing the moving electrode at those points; the grass was scraped from these points also.

Fig. B160 shows that the voltages are very small, but they show a clear pattern. There are two possible causes for this anomaly. The feature there is almost surely a well which is filled with iron artifacts. Water from the surrounding soil could be seeping into the well shaft, creating this voltage anomaly. As a second possibility, the iron and other metal in the well could be rusting. The chemical reaction of rusting metal creates currents and voltages in the soil; this action is rather similar to the operation of a battery.

The measurements in Fig. B160 required 15 minutes. The soil was slightly moist, and the electrodes made good contact with it. If the soil had been quite dry, I could have dug a shallow hole to where slightly moist soil is found. If the soil is very dry, water should not be put on soil to artificially moisten it for this will cause the

readings to be in error; the movement of the water in the soil will create unnatural voltages.

It is important that the electrodes touch the bare soil. Fig. B161 shows that I got very erratic readings when I tried to just press the electrodes on the surface of the grass; the anomaly is completely lost. I made these measurements with commercial Cu-CuSO4 electrodes. The broken line of the graph indicates that these electrodes gave fairly good measurements when the grass was scraped from below the electrodes, however, the measurements were somewhat more irregular than my measurements with the flower pot electrodes.

The value of non-polarizing electrodes is illustrated by Fig. B162. The voltages are large, but erratic, when stainless steel electrodes are driven into the soil. While the voltage is low in the middle of the line, the anomaly is small relative to the variability of the measurements.

You may notice that the voltage which you measure between a pair of non-polarizing electrodes slowly changes. If you see the voltage drifting, just wait about 15 seconds or so for it to stabilize. If you find that you need to wait for each electrode to stabilize in the soil, your survey will be faster if you have several electrodes moving along the line. While measurements are made at one electrode, the rest can be sitting in the soil, so that little or no wait will be necessary when the voltage is to be measured.

If you use several electrodes, you will have the additional complexity of correcting for the different inherent voltages between the electrodes. You should number each electrode, and perhaps use electrode number 1 for the reference. Before you start your survey, put all the electrodes close together in a container which contains a shallow layer of copper sulfate solution. Now, measure the voltage to each pot relative to the reference electrode; these can be called calibration voltages. When you make your measurements along the ground, subtract the appropriate calibration voltage from each measurement. If your calibration test of pot number 3 indicated a voltage of 3.1 mV relative to the reference pot, just subtract 3.1 mV from every voltage reading with pot number 3.

For most of my measurements at Petersburg, I used Ag-AgCl electrodes. These electrodes are about 15 cm long and about 1 cm in diameter. In order to support the electrodes, and for better contact to moist soil, I cored 2.5 cm diameter holes into the soil at the points of measurement; these holes went to a depth of about 13 cm. I set the electrodes in the bottom of these holes. When I moved the electrodes across the bottom of the holes, the voltage I measured would change by 3 - 10 mV. While I do not know the reason for this, I believe that it might be due to the sensitivity of the small electrodes to slight changes in the type of soil which they are contacting. The electrodes which had a large contact surface did not have this problem, perhaps because they average the effect of small soil particles. In this case, lower resolution helps.

Fig. B163 illustrates repeated measurements with these Ag-AgCl electrodes. While both surveys found the same low voltage anomaly, the irregularity between the surveys is about 5 - 10 mV and this would make it difficult to detect weaker SP anomalies.

This is exactly what I found with my continuing self-potential surveys at Petersburg. Three lines of measurement are plotted in Fig. B164, Fig. B165, and Fig. B166. The line segments at the bottoms of those graphs locate features which were along the measurement traverses; none of these features was detected by the voltage measurements. While there were lateral gradients in the voltages,

there were no anomalies associated with the archaeological features.

The measurements in Fig. B161 were also smoothed with the filter suggested by Wynn and Sherwood (1984). The measurements are so irregular that this filter does not help much.

While these tests were made along single lines, I also measured the two-dimensional pattern of voltages within the Iron detail; these measurements, made at 2 ft (0.6 m) intervals, are plotted at the upper left corner of Fig. B167. That contour map is so complex that it is almost impossible to see any patterns in it. However, a simple 3x3 matrix smoothing of the measurements yields the very clear pattern shown at the upper right in the figure.

These measurements were made with the Ag-AgCl electrodes. I had assumed that these electrodes would give me the most reliable readings; I tested the simple flower pot electrodes against these "good" electrodes only after my surveys were almost finished at Petersburg. Perhaps some time I will be able to use the flower pot electrodes to remeasure all of the lines where the Ag-AgCl electrodes found so much irregularity. It is possible that an even larger electrode surface area would help; possibly the surface of the electrodes could be as large as 0.2 m in diameter for even less noisy data.

I have not done enough SP surveys to have determined how much trees will affect the measurements. I suspect that there will be a significant effect; you should note the location of nearby trees. Buried pipes may also affect these surveys.

Survey details

Some details of SP surveys and their interpretation are here. You will probably not have to concern yourself with these details during your first few self-potential surveys.

If the soil below the SP electrodes is very dry, the voltage measurements will probably be erratic. It is possible to determine if the soil is so dry that a poor contact is made with an electrode. Just measure the electrical resistance between a pair of electrodes while they are setting on the soil. During my surveys at Petersburg, I measured the resistance between the two flower pot electrodes to be about 9000 ohm. Because of their smaller surface area, the Ag-AgCl electrodes had the much higher resistance of 110,000 ohm.

While this test will show you if there is a problem with an electrode, or its wiring, it does have a disadvantage. The resistance measurement polarizes the electrodes; this is because the measurement sends a current through the electrodes. The voltages return to the normal value in an exponential fashion, as seen in Fig. B168, and it may be 5 - 10 minutes before the electrodes are close enough to their normal conditions. This polarization is dependent on the current which was applied during the resistance measurement, and also on the duration of the resistance measurement.

There is a large difference in the voltage of one self-potential electrode as compared to another; this effect must be adjusted after you have made your measurements. It is a good idea to keep records on these changing voltages, for it may alert you to difficulties with an electrode. The measurements of my Ag-AgCl electrodes are listed in Fig. B169. The voltages there are in millivolts (mV). While there are large differences from one electrode to another, the differences are fairly constant with time.

My measurements with two different Cu-CuSO4 electrodes are listed in Fig. B170. The drift in the voltages of these electrodes is larger than the drift of the Ag-AgCl electrodes. With my field measurements,

the voltage changed by 11 mV in only two hours. It is possible that a temporal correction will be necessary if small amplitude anomalies are being sought.

The same solar effects that cause the Earth's magnetic field to change during a day can also cause SP voltages to change. I tested this at Petersburg. The plots in Fig. B171 show that the changes were so small that no correction was needed for the spatial measurements. Because of the short distances between the electrodes, it is likely that these effects will not be a problem for archaeological surveys.

Another effect is seen if you move the wires to the electrodes while you measure the voltages. When the wires move in the magnetic field of the Earth, you are making an electrical generator and you will see the voltage change. If there is a long span of moving wire, or if you have a coil of wire which moves, the voltage from the Earth generator will be very apparent.

The references listed at the start of this section describe some of the procedures for the interpretation of SP anomalies. I measured only one interesting pattern with this survey at Petersburg, but its interpretation gave an interesting result.

I found that the measurements mapped in Fig. B167 could be closely modeled by a small concentration of electrical charge; this is called an electric monopole. With a computer program, I used a semi-automatic procedure to find the amplitude and location for this monopole charge which best fit the measurements. This best fit was found with a monopole having a charge of -0.25 nC (nanocoulombs) at a depth of 3.5 m and located at E525.8 S144.8; this assumes that the relative permittivity (dielectric constant) of the soil is 10. This charge is about that caused by an excess of roughly one thousand million electrons.

Fig. B172 shows that the measurements are quite erratic, but this model does match their general trend; the two-dimensional map at the lower right corner of Fig. B167 also shows that the model approximately matches the measurements.

The current which could be flowing away from the monopole source can be estimated if the soil is assumed to have a resistivity of 200 ohm-m. This current is: charge / (permittivity * resistivity) and the calculated value is 14 mA. This current could be due to several different effects, including the seepage of water, but a likely cause is the corrosion of metal, most likely iron. From the measurements of Evans (1926 p. 45), the current above could be caused by the corrosion of iron at the rate of 0.35 g/day (by way of comparison, a dime in the USA has a mass of 2.5 g). If this corrosion had been steady since 1865, a total mass of 17 kg of iron would have rusted.

Special Topics

Soil chemistry

Geochemical exploration can be suitable for locating distant or buried ores (Siegel 1974; Hawkes 1957). The concentrations of some chemicals in the soil have also been found to be good indicators of the former use of the land by humans (Eidt 1985; Carr 1982).

As part of the archaeological investigation (Blades 1993) of the Taylor House area, soil samples were removed from the plow zone at 10 ft (3 m) intervals and the concentrations of magnesium (Fig. B175), calcium (Fig. B173), phosphorus (Fig. B174), and potassium (Fig. B176) were determined, along with the pH of the soil (Fig. B177).

These measurements were interpreted by Brooke Blades (Blades 1993 p. 49) and he notes that some concentrations of phosphate were correlated with the locations of former structures in the area. All

of the chemical concentrations are highest on the western part of the Taylor House grid; this geophysical survey also found the greatest density of debris and metallic artifacts in that area.

There is an interesting change in the concentration of calcium (Fig. B173) and phosphorus (Fig. B174) at about W30; both chemical maps show very much lower quantities in the eastern half of the area. The resistivity map of Fig. B4 shows the highest resistivity in that area, except for the Taylor House cellar. The interpretation of the geophysical data indicated the possibility that rather clean sand might have been spread on the surface in the eastern part of the survey area. This finding may agree with the low concentration of calcium and phosphorus in that area.

Multiple instruments

If one geophysical survey is good, are two better? Sometimes. One instrument may be ideal for a site, and nothing else is needed. Additional surveys increase the time and cost of the work. It is a little bit like photography. If you take a black and white photograph, this will have most of the information you need to record. If you also take a color photograph, perhaps you add 50% additional information, but you about double the cost. If you further take an infrared photograph, you might increase the information by an additional 25%, but the increase in cost is more than that.

Of all of the surveys at archaeological sites which I have done, exactly half have made significant applications of more than one type of geophysical instrument. However, I have never applied more geophysical instruments to one site than I have for this survey at Petersburg.

If you wish a greater reliability to the findings of your survey, you may choose instruments which will generally detect the same or similar features; these might be conductivity and resistivity meters, or perhaps magnetometers and magnetic susceptibility meters. If you wish to detect the greatest variety of features, you will make a selection of instruments such that each of them will detect generally different features from the others. David Orr, who has specified many geophysical surveys for the National Park Service, has found that there will be generally little correlation between the findings of a radar and a magnetic survey at many of his sites, and he finds this combination of surveys to be particularly efficient at locating a wide variety of features.

It is usually possible to make fair predictions of the suitability of different geophysical instruments for a site before the survey begins. If these estimates are wrong, it may be valuable to have several different geophysical instruments at a site so that preliminary tests with them will suggest which is best.

The information from each type of geophysical survey can be first interpreted independently from the findings of the other surveys. Then, correlations between the measurements and findings can be evaluated in case these combinations suggests any additional information. Some of these tests with the data from this survey are included in Volume C.

The different geophysical surveys may be done sequentially, one after the other. In some circumstances, several different types of survey can be done together. If there is an on-going excavation at a site, there may be extra people at some times, and additional geophysical surveys can put them to work. When I have done projects like this, I have never found it practical to have more than three geophysical surveys going on at once. Parallel surveys may be needed

if the area of survey is large, or if the survey needs to be quickly completed.

If you are going to have topographic and geophysical surveys done at the same time that you are excavating, you will have a busy site. It can definitely be done, for the different crews will be tolerant of each other. A medium sized site can get rather dense with tape measures and guide ropes. Since I find it most efficient to do geophysical surveys along long lines, it is best that these surveys all be done with traverses going along parallel lines, otherwise the guide lines will weave into a fabric.

With parallel or concurrent geophysical surveys, it will be necessary to carefully test for interaction between the instruments. Generally, identical types of geophysical instruments will affect each other's readings if they are near each other. Resistivity and conductivity instruments will interact at the greatest distance. Magnetometers will interact at a shorter distance. Ground-penetrating radars will also interfere with each other, but the problem is not as bad as I would have thought.

If the same types of geophysical instruments are operated at a site, it will generally be necessary to measure their relative calibration. This will be most reliably done by measuring a single line of survey with each of the instruments. Then the correlation between pairs of instruments can be determined with a best-fitting straight line. If the measurements of the two instruments are Z1 and Z2, this correlation will reveal the constants a and b in the linear equation: Z1 = a * Z2 + b and this will allow the measurements of one instrument to be converted to equivalent measurements with another instrument. While the measurements of both instruments could also be compared at a single point, this may only reveal the quantity b in the equation above.

Dissimilar geophysical instruments will sometimes also interfere with each other. The magnetic field generated by a magnetometer may affect a conductivity meter. The wires of a resistivity meter will affect a conductivity meter. The iron mass of a radar may affect a magnetic survey. Everybody who is walking around will affect a seismic survey. The geophones of a seismic survey are magnetic.

If you are going to have several instruments operating at once, you will have to make careful tests of their interaction if the instruments will be within about 30 m of each other. Probably the best method is to have the first instrument make a series of measurements while it is stationary. The second instrument is brought closer and closer to the first instrument. This second instrument is either turned on and off, or is set to take a series of measurements; the measurements should be taken at the same time as the first instrument and also deliberately at slightly different times. The first instrument should be closely watched for any unusual change in its measurements. The second instrument should be kept farther away than the distance of this first noticeable interaction.

This was a test of the one-way effect of the second instrument on the first. A second test should be made of the effect of the first instrument on the second.

You must also check for any interference between the geophysical instruments and the field computers at the site. If walkie-talkies are being used nearby, they are another source of interference.

Maintenance, reliability, safety

If you can do simple electrical repairs, you should keep some simple spare parts for your equipment. Connectors and wires are

always the first components to fail; switches are second. While most geophysical instruments are waterproof, they may be temporarily damaged by falling into water. However, when they are dry again, they will probably work fine. If they fall into saltwater, they should be rinsed thoroughly with fresh water before drying (Kerr 1990).

If a geophysical instrument operates with internal, primary cells, rather than a rechargeable battery, the internal cells should generally be removed when the instrument will not be used for a few weeks. This will minimize the possibility of chemical leaks from the cells causing corrosion within the instrument. Some computerized instruments have a lithium cell inside which will power the internal clock and data memory for the periods when the primary cells are out of the instrument. It is possible that these lithium cells will have a shorter life when the primary power is removed from the instrument. If a geophysical instrument operates on rechargeable batteries, it is important to have a spare battery pack which can be substituted during the day, when the internal battery dies; this may be an identical rechargeable battery or possibly an external primary battery.

Some simple tests may help to reveal if a geophysical instrument is operating correctly or not. With a resistivity meter, it is only necessary to connect the meter as a two-electrode resistance meter (connect the instruments wires V+ and I+ together, and also V- and I- together); then, just measure the value of a resistor (about 10 - 1000 ohm) which you keep for this test. You may check the relative calibration of several resistivity meters this way also. With a ground-penetrating radar, it is easy to check if the transmitter is working by holding a portable radio near the antenna. You should be able to hear the pulsing of the radar over a wide frequency range. You can test if a conductivity meter is transmitting a magnetic field. All you need is a small coil of wire and an audio amplifier; the frequency of most of these instruments is in the audio frequency range and you will be able to hear the hum. That same equipment can also test a magnetometer; the energizing signal going to the sensor of a proton magnetometer will cause a click. The signals to the sensors of other types of magnetometers may also be audible.

I generally keep each of my geophysical instruments wrapped in a sheet of clear plastic. While this does not make the measurements any better, and probably does not make the instruments last much longer, it does keep them from getting scratched in brush and other accidents. If they do not look like they have been carelessly handled, other people who use them take better care of them.

If you are making a large number of measurements, a computer will be very valuable for recording the data. With a paper copy of your measurements, the condition of your recording is immediately visible. Since this is not true for a digital copy on a disk, you will have to make extra care that your data are not lost or otherwise unusable. The best protection is one of making several copies of the data on separate floppy disks. In high risk situations, you may need to keep these disks in separate locations. The data should be recorded in the standard format of ASCII (American Standard Code for Information Interchange); this will allow the data to be recovered even if the disk directory is damaged. With computerized instruments, it is important to be able to transfer the measurements to a computer in the field; this will allow a partial days's data to be saved and the memory of the geophysical instrument to be cleared. Small and portable computers are common now, but you should try to make sure that the one you choose will operate on several sources of power; these may include the internal battery, a car battery, and also

another separate and external battery.

The hazards from your geophysical instruments are minor. If you are concerned about the radio waves emitted by a radar, you should evaluate the power and frequency from them. Most resistivity meters have a rather low voltage and current; they can give a very noticeable shock, but not a serious one. Some high powered resistivity meters, for very deep exploration, can have very dangerous voltages; these are not needed for archaeological surveys.

Generally, the hazards of geophysical survey are quite similar to those of general archaeological work. The safety practices of surveyors and petroleum geophysicists provide some guidance to geophysical surveys at archaeological sites (Tibbs 1987; Professional Surveyor 1992; International Association of Geophysical Contractors 1982). Because geophysical surveys can be done in the rain, it is important to know how to be safe when lightning might strike nearby (Lee 1977; Berger 1980).

The greatest hazard of a geophysical survey for passers-by is usually just tripping on all of the wires and ropes which are spread around the site. While guide ropes usually have to be staked and tight, wires can be slackened so that they cause little difficulty.

Most of the hazards which are encountered when doing geophysical surveys are just caused by common plants (Lampe 1984) and insects (Biery 1977). Poison ivy, whose leaves have a skin irritant, causes difficulty for geophysical surveys because of all of the wires, ropes, and instruments which are set or moved on the ground. These field items may pick up the irritating resins, which are later transferred to the unsuspecting geophysicist, perhaps at another site. If there is a field of clean grass nearby, it is a good practice to drag the equipment through this before it is packed up.

Dangerous animals are very uncommon, and normal practices are all that are needed (Klauber 1982). Non-dangerous animals cause the most difficulty. Dogs may try to run off with your ropes and cows will nibble on your instruments.

Special survey conditions

Geophysical surveys are most commonly done in quite civilized and pleasant locations. A small number of them are done in unusual or difficult circumstances of weather or location. Some references to procedures which might help you are given here. These emphasize the particular problems which are encountered in doing technical field work. General references to camping or survival are not listed.

Surveys can readily be done at remote locations from isolated field camps (Dillon 1989; Land 1978; Gordon 1975; Volunteers in Technical Assistance 1975; Farkas 1970; John 1965). Transportation of equipment and supplies is the major factor, so the light weight instruments may have first priority. Electrical power will be necessary for the instruments; if the survey will require a few weeks of field time, rechargeable batteries may be better than primary (or disposable) batteries. Photovoltaic and gasoline-powered electric generators can recharge these batteries.

If the area of field work is separate from the camp site, it can be best to leave the geophysical instruments at the work site overnight. If you do this, you may have to make sure that rain will not damage the equipment while you are away. Two layers of good plastic will provide all the protection you need. The equipment is set on one sheet, which is wrapped over the top of the pile. Then, a second sheet is wrapped around that and tucked below the first. This provides protection from both rainfall and also water washing along

the ground's surface. If there is a possibility of fire at the site; you will need to make precautions for that also. The foraging of wild animals is also a factor to consider.

Rather few modern authors have described the detailed considerations for doing scientific work like geophysics at remote sites, but their writings can provide valuable guidance (Rainey 1992; Rosendahl 1984; Mallowan 1974; Kielan-Jaworowska 1969; Ronne 1961).

Special practices are needed for cold or polar work (Professional Surveyor 1986; Griffith 1976; Perla and Martinelli 1976; MacDonald 1969; Bertram 1957). Radar surveys can be easier in the snow; the antenna sleds are easier to pull. Batteries can have a very short life; they may have to be kept inside the operator's clothing. The liquid crystal displays (LCDs) of some instruments, and computers, will not operate in cold weather. Some types of hand warmers are based on the heat generated by the rusting of iron powder in a saline solution; these cannot be used if you are doing a magnetic survey. Because of all of the clothing which is worn, it is much more difficult for the operator of a magnetometer to be nonmagnetic in the winter. If the ground is frozen, a resistivity and a seismic survey may not be practical. If you wish to survey a lake, it will be easiest to do when the water is frozen in the winter. Irritating insects are almost never found in the winter.

Geophysical surveys in hot weather are little different from other types of field work (Glen 1980; Adolph and Associates 1969). The primary difficulty is usually dust. If the recorders of a radar are lifted on tables to a height of 1 m or so, this will often provide good protection from some blowing dust. In very hot weather, the LCDs of some instruments will go completely black; these will need to be cooled in the shade. If the soil is very dry, resistivity surveys will give erratic and unreliable readings; if a half liter of water is poured on each electrode, adequate measurements may be possible.

In areas with a hot and humid climate, the humidity generally causes more difficulty for the equipment than the heat (Hyzer 1974; Porkert 1974). For longer surveys, fungus may grow on the instruments or supplies. High voltage difficulties might be found also; radar equipment and computer monitors are potential problems.

All of the geophysical surveys can be done in the rain. If bare soil is at the surface, resistivity, radar, and seismic surveys can be quite messy, for these surveys have equipment on the surface of the ground. The messiest surveys of all are done when there is freezing mud. If there are thorny bushes at the site, they will quickly rip most rain coats and other plastic sheets when you walk through the bushes. Be sure to keep waterproof writing paper available; normal paper will be useless.

I have never done a geophysical survey in a cave, but I do not believe that there are any limits past the difficulties of other cave work. Geophysical surveys can be done in cellars, buildings, and tunnels if wished.

Geophysical surveys can also be done at night easier than most other types of field work. While I have not tested it myself, the geomagnetic field is quieter at night (Parkinson 1983 p. 262), since the site is then shielded from the Sun by the Earth. If a survey finds interference from electrical machinery or traffic, a survey at night may be considered; seismic and conductivity surveys may be much improved.

Notes on the Figures

Detailed information on the surveys and interpretations is given in this section. This information is for reference, rather than reading. If you have a detailed question about the procedures of my work, the answer will probably be here.

Fig. B1: A test of this meter was made during the National Park Service course on archaeology and remote sensing which was held at Fort Laramie, Wyoming, in 1994. This test was done by a group composed of Lucy Johnson, Pete Gardner, Leslie Drucker, Bob Yohe, and Diana Yupe. A Gossen Geohm 3 resistivity meter indicated a resistivity of 310 ohm-m when connected to the four electrodes.

Fig. B2: The two seasonal soundings were done on line N85; they were centered at E0 and E65. The locations are slightly offset in the figure in order to distinguish them. The circles mark the electrode points at the greatest separation between the electrodes.

Fig. B3: The resistivity measurements for this map and all of the other resistivity maps here were made with a Gossen Geohm 3 earth resistance meter. The map is rather similar to that measured with the Geonics EM38 conductivity meter. The correction described with Fig. C72 has been applied to this map. The survey was done on 4 May 1992 (10:46 - 16:15), using the pole-pole configuration of electrodes; measurements were plotted at the midpoint between the two moving electrodes. Two ropes defined the line of each traverse; these calibrated ropes were placed along east-west lines 5 ft (1.5 m) apart. Measurements were made alternately with the array north-south, then east-west. For the north-south orientation, the two electrodes were placed at the same east coordinate on the two ropes. For the east-west orientation, the two electrodes were set along the same rope. For each new measurement, it was only necessary to move one electrode. Except for the correction of the north-south measurements, the map has not been smoothed. The reference electrodes were at the locations mapped in Fig. C157; the resistance between these electrodes was measured to be 6300 ohm. The direction of the north arrow on this contour map (and all of the other contour maps) is less accurate than the north arrows on the interpretation drawings; this is because the drawing of the arrow is pasted on the contour map, and there could be an error in its alignment.

Fig. B4: The lines of two pseudosections are shown in the figure. This is a 3x3 E-W striation smoothed version of Fig. B3.

Fig. B5: The northern-most line in the grid was measured three times, one after another. The differences between the surveys are primarily due to errors in location of the electrodes.

Fig. B6: The offset Wenner configuration had its middle electrode at E50 N85, and the electrode spacing was 1.5 m. Measurements were made at rotational increments of 5 degrees. The upper diagram plots the measurements with the contrasts exaggerated by assuming the middle of the circle has a resistivity of 350 ohm-m. The survey was done on 2 April 1993 (12:14 - 13:23) and the Gossen Geohm 3 was used. The broken line offset curve was measured with the array offset from the midpoint in the direction shown; the solid line is the average of the two offsets.

Fig. B7: The resistivity sounding shown in Fig. C74 is plotted with 5 circles to mark the greatest electrode spread. The line of the resistivity and EM profiles over a pipe is marked by a broken line at the top of the figure. The dotted pattern shows the estimated location of the fort.

Fig. B8: This survey was done on 8 September 1992 (9:42 - 13:57), using the same procedures as for the Taylor House survey. The electrode spacing was 5 ft (1.5 m) and the pole-pole configuration was used. Measurements were made with the array both north-south and east-west, with electrode pairs defining the edges of 5 ft squares. There were no bees at the southeast corner of the grid during this

survey, and this corner could be surveyed. The reference electrodes were located at their normal points for surveys on this side of the park road (the potential electrode was at E100 S500 and the current electrode was at E500 S600). Measurement traverses were made east-west with the aid of two ropes. It was found that the line averages with the array north-south were somewhat more irregular than with the array east-west, although the differences were much smaller than those at the Taylor House. For this survey area, the best correction for this error was found to be that of forcing the line averages of the measurements with the array north-south to be the same as the average of the averages of the lines to the north and south, which were measured with the array east-west. The interpretation of this data is given in Fig. A42.

Fig. B9: The high resistivity along the lines of some of the bombproof trenches is more apparent here. The northernmost trench was partly detected, as was the third from the north. The second trench was rather clearly detected, but the fourth trench was not detected. There is little correlation with the magnetic survey. This map has been smoothed from Fig. B8 with an east-west 3x3 striation filter.

Fig. B11: The 325 measurements of this map were measured on 7 September 1992 (14:19 - 16:02). The spacing between the electrodes was 5 ft (1.5 m) and the pole-pole array was oriented both north-south and east-west. The electrodes were placed at even 5 ft multiples in the grid and the measurements were recorded at the midpoint between the two electrodes. There were 11 one-point anomalies which appear to be measurement errors; these were primarily resistivity lows and the measurements were replaced by the average of the four adjacent points. Traverses were made along north-south lines and the measurements perpendicular to the guide ropes were only slightly greater than the measurements with the array parallel to the guide ropes. The averages with the array east-west were forced to the average of the averages of the adjacent lines with the array north-south.

Fig. B12: The line of a resistivity pseudosection is marked at S25. A 3x3 north-south striation smoothing has been applied to the original data to create this map.

Fig. B13: The 84 measurements of this survey were made on 7 September 1992 (17:02 - 17:30). The normal pole-pole array was used with an electrode spacing of 5 ft (1.5 m); traverses were north-south. As with the other resistivity surveys at Fort Morton, the average values on each line with the array perpendicular to the traverse were forced to the average of the adjacent lines, made with the electrodes along the line of the guide ropes. From the four resistivity maps made at this site, it was found that the resistivity measurements were always higher with the array perpendicular to the guide ropes than parallel to the guide ropes, by an average of 3.1%; this is equivalent to saying that the electrode spacing perpendicular to the two ropes was about 5 cm too small. This is a reasonable error; while it is readily corrected, it would generally be better to use a rigid bar to hold the electrode spacing correct whenever this is practical.

Fig. B14: The two profiles have a shift between them which is about 10 ohm-m or 6%. This is probably caused by a spacing error between the electrodes, and the measurements with the array parallel to the pipe are probably in error. The electrode spacing was intended to be 5 ft (1.5 m); this was set by two parallel ropes, but they must have been slightly too far apart. This survey was done on 7 September 1992 (16:20 - 16:36), making measurements with intervals of 2.5 ft (0.8 m). The Gossen Geohm 3 was used with the normal reference points.

Figure Notes

Fig. B15: A simple schematic of a resistivity meter is shown. A current is sent through the soil between the outer pair of electrodes. The resistivity meter also measures the voltage at the inner pair of electrodes; it then calculates the ratio of voltage (V) divided by current (I) and displays is as a resistance, in ohms. This resistance can be converted to the parameter, apparent resistivity, by multiplying resistance by the electrode spacing (S) and by twice pi.

Fig. B16: The vertical lines indicate a suggested sequence of the spacings between the electrodes of the sounding. For most of my soundings I use the sequence: 0.1, 0.15, 0.2, 0.3, 0.4, 0.5, 0.7, 1, 1.5, 2, 3, 4, 5 m. As you can see, the lines are then rather equally spaced along the horizontal, logarithmic axis of the graph, and this provides the most efficient sequence for analysis. For the 1979 sounding, the measurements were not quite as uniformly spaced along the graph. This analysis assumes that the soil interfaces are horizontal and abrupt; while most soil interfaces would be rather gradual, the approximation of abrupt changes is generally adequate.

Fig. B17: These are called two-layer curves; they are calculations which assume a simple and standardized upper stratum. It has a thickness of 1 m and a resistivity of 100 ohm-m. The different curves then plot how a resistivity sounding would look if the infinitely thick lower layer had a different, but constant value of resistivity. The ratio of the resistivity of the lower layer to the upper layer is indicated by the numbers at the right hand side of the graph. These graphs were calculated by the procedure given by Tagg (1964 p. 37).

Fig. B19: The details on this sounding are included with Fig. C159. The offset Wenner configuration was used for this sounding. With it, five electrodes are set along the line, but four of them are used at a time; these are the four on the left or the four on the right. For the offset configuration, the average of these two resistivity values is calculated. The procedure is further described in Volume C.

Fig. B20: The compass was rested on a wooden rod for support and the apparent angle to a distant stake was measured along a line which passed close to the buried iron object. The compass was a Suunto model KB-14, which can be read to a precision of 0.1 degree. Two separate traverses were made on the line and both show the same deflection. The survey was done on 23 October 1992, between 8:40 and 9:30. With the monopole model of Fig. C55, it is possible to calculate the deflection of a compass, and this agrees with the measurements. The difference is simply due to a calibration error of the compass.

Fig. B21: The maximum deflection is found next to the iron object.

Fig. B22: The numbers show the pattern of the changing strength of the Earth's magnetic field. Measurement traverses were made only going toward the north and parallel lines progresses toward the east. This survey was done as part of a training course coordinated by Steven De Vore, of the National Park Service. The students in the course measured this magnetic map. The magnetometer for the survey was loaned by Bob Sonderman and Barbara Little of the National Capital Area of the National Park Service. The E0 N0 point in the figure has an actual site coordinate of E40 N3. The Fredericksburg A-index on 9 June 1993 was 8; on the next day, it was 25.

Fig. B27: These two curves show the range of variability which was measured during this survey. The curve at the top is unusually quiet and smooth. The A-indices shown in the figure are from the magnetic observatory at Fredericksburg, Virginia. The base station curve for 25 June 1992 shows a larger irregularity than usual; there is a particularly large deviation at about hour 17. Both curves show

the typical decrease near noon. The measurements were made with a Geometrics G-856AX proton magnetometer; the coordinates of the sensor are shown in the figure. The sensor was always at an elevation of about 8 ft (2.4 m) in order to minimize the effect of objects near the surface; the sensor staff was tied to a tree trunk and the readout was set on the ground next to the tree. Local time is shown at the bottom of the figure; for the January record, this is Eastern Standard Time; it was Eastern Daylight Time for the June data.

Fig. B28: The object is assumed to be a dipole, with a moment of 0.3 Am^2. The Earth's field is assumed to have the parameters of Petersburg: strength = 53,200 nT, inclination = 66 degrees, declination = -7 degrees (grid angle).

Fig. B29: Each calculation area covers a 5 m square. The average half-width of each anomaly is about 1 m and the depth of the object is indeed 1 m below the elevation of the calculations. The source is a magnetic dipole with a moment of 0.31 Am^2; this approximates 1 kg of iron with only remanent magnetization. As with Fig. C43, three different types of magnetometers are shown at three magnetic latitudes. Note that since the moment is constant for each latitude, the magnetic anomaly decreases by about half at the equator. The anomaly patterns here are the same as those for the 1 m cube in Fig. C43; therefore the shape of that source cannot be resolved at this sensor elevation.

Fig. B30: For model #1, the sources are rectangular prisms with a total moment of 300 Am^2 for each span (this is the total length of the east-west and the north-south segments). For this model, the pipe is assumed to have only induced magnetization; the culvert below the park road has this magnetic pattern. The iron pipes near the former farm may be steel pipes which appear to show primarily remanent magnetization; these match model #2. For that model, the directions of magnetization of the dipoles, which were spaced by 12 ft (3.7 m), were chosen semi-randomly; each dipole has a moment of 20 Am^2.

Fig. B31: The general anomaly of the square slab at the top has its typical form. The small square inside is a hole in the middle of this magnetic slab. The high caused by the hole in the slab is lost in the gradient of the nearby low. These models are calculated at a 45 degree magnetic latitude. The slab is 6 m on a side and it has a 1 m hole in it. Its magnetic susceptibility is 0.01 and its thickness is 1/6 m; the top of the slab is 1 m below the sensor. For the overhead object, a dipole with a moment of 3.13 Am^2 is assumed (about 10 kg iron); this dipole is 3 m above the sensor and is located at the asterisk in the figure.

Fig. B32: The survey was done on 13 August 1991, during the period 15:20 - 16:55. The sensor height was 0.85 m and measurement traverses were made going to the east. The Gem GSM-19FG was set up to make measurements automatically at 1 second intervals, and the traverse speed was adjusted to pass 5 ft measurement points at this rate; a buzzer alerted that each measurement was made. A rope with marks at 5 ft intervals guided the lines of traverse. This rope was moved every 3 lines, since the 5 ft offset could be estimated. Due to a recording error, measurements were not made at the E50 point on each line. Base station measurements were made at 20 s intervals and the Fredericksburg A-index on this day was 9. A Geometrics model G-856AX proton magnetometer was used for all of the base station readings for these magnetic surveys. For the surveys at the Taylor House, the sensor was typically placed against a tree trunk at W132 N36 with the sensor at an elevation of 2.4 m. The correction for the temporal variation in the magnetic field was done by determining the time at which each spatial measurement was made and subtracting the base station measurement from it. The base station measurement was estimated by making a linear interpolation between the measurements

made before and after the spatial measurement. A high gradient at W115 N90 prevented a reading there. Because of the very strong magnetic low near W20 N20, the contour lines there are not completely drawn; the lowest contour lines has a value of -300 nT. A comparison of this map to the map in Fig. B33 (2.5 ft spacing) reveals errors in this map. At E25 N40, E35 N50, and E5 N65 there are magnetic lows which must be due to measurement errors during the magnetic survey. There is also a spurious magnetic high at W115 N90. The cause of these errors is not known. The contour lines are not complete at the high amplitude anomaly around W25 N20; blanks in the middle of other anomalies also indicate these very high amplitude anomalies.

Fig. B33: The spacing between measurements was 2.5 ft (0.8 m) in both the north-south and the east-west directions. The sensor height was 0.8 m. Traverses were made going to both the east and the west. The alignment rope was moved after every 5 traverses, since an offset of 5 ft could be estimated by eye. The survey was done on 27 January 1992, between about 14:15 and 16:00. The Fredericksburg A-index on the day of this survey was 18. The base station magnetometer was in the area of Fort Morton, at E499 S301. Two trains went by during this survey, but I was between lines of measurement then. The survey was probably done with polarization continuously on, and with an external trigger. The blank area near W20 N20 is due to the fact that the contour lines for very low anomalies were not drawn. The broken line contours are at intervals of 5 nT. When I mapped the original data, I found a slight amount of striations in the map. I determined that these were caused by a perspective or parallax error in my location of the magnetic sensor for each measurement; the sensor was far enough in front of me that I could not tell its exact location on the ground. I stopped slightly short of the desired point. I corrected the map by shifting alternate lines of measurement by 1 ft to the east or west.

Fig. B34: This survey was done during the period of 25 - 27 June 1992. The Gem GSM-19FG Overhauser magnetometer was operated with an external trigger with the sensor at the front end of a 8 ft (2.4 m) long bar; the height of this bar and the sensor was 0.85 m. Measurement traverses were made going toward the west. The Geometrics G-856AX proton magnetometer had its sensor against a tree trunk at W132 N36 on the west side of the grid. The interval between base station measurements was 15 s. The Fredericksburg A-indices on the three days were 16, 10, and 15. The survey was halted when any trains were passing on the tracks to the west. A thunderstorm began at the end of the survey. In the northern part of the map, from N104 - N120 there were 10 measurement spikes, visible as one point anomalies with an amplitude of about -38 nT (only 2 of the 10 spikes had a positive anomaly). These are almost certainly due to electrical interference from lightning. The errors were removed by averaging the 4 adjacent measurements. The base station did not appear to detect these lightning effects; this may be due to the orientation of its sensor.

Fig. B35: The solid line contours are at intervals of 10 nT (from -190 to +190 nT), while the broken line contours are at 5 nT intervals (these are at anomaly levels of -15 and -5 nT). This is an enlargement of the western third of Fig. B34. Note that there is an overlap on the three maps.

Fig. B38: Note that the vertical axis is the negative of the anomaly; distant objects always cause the magnetic field to be reduced. This analysis assumes that the measurements are not made near the equator and the elevation of the sensor and the objects are roughly the same. For a total field magnetometer, the magnitude of the anomaly decreases as the cube of the distance from the object; for a gradiometer it decreases as the fourth power of distance. This

explains the difference in the slopes of the two curves. For a total field magnetometer, the magnetic anomaly of distant objects is:

B = -100 * m / r^3

where B is the magnetic anomaly, in nT, and m is the magnetic moment of the object. The magnetic moments of vehicles which I have measured are: m (car) = 300 - 850 Am^2; m (train) = 9 - 17 (10^4) Am^2. At the magnetic equator, the magnetic anomaly of distant objects is different from what is found at other latitudes. To the east or west, the anomaly is negative; to the north or south, it is positive. At all latitudes, the change in anomaly with distance is the same for large distances.

Fig. B39: The survey was done with the Gem GSM-19FG, which can be operated as a base station, a total field magnetometer, or as a gradiometer. The lower sensor was at an elevation of 1.0 m and the upper sensor was at 2.0 m. Since I did the survey by myself, I fixed the two sensors on a triangular wooden frame which I pulled along the lines of the survey. The traverse directions were both to the east and to the west. The survey was done on 30 June 1992, between 10:08 and 14:27. The base station was the G-856AX, with measurements at 15 s intervals; the sensor was in the tree at W132 N36. The survey was stopped for a passing train (at a distance of 103 m) which caused a -15 nT anomaly. The Fredericksburg A-index was moderately high at 27. The Gem instrument makes simultaneous measurements at its two sensors. The base station measurements allowed the total field at both sensors to be corrected for the temporal change. The solid line contours are at intervals of 10 nT, while the broken line contours fill in parts of the map with 5 nT intervals. The linear magnetic low along N42.5, and just south of the foundation anomaly, is apparently a measurement error. The magnetic low near W25 N20 has not been fully contoured.

Fig. B40: This survey was done during the period of 22 - 27 June 1992. Measurement traverses were made going alternately to the east or west and parallel lines progressed to the north. Westward-going traverses were made along lines with line coordinates which were a multiple of 5. The instrument was the Gem GSM-19FG Overhauser magnetometer which had its sensor at an elevation of 0.8 m. The base station magnetometer measured the temporal change in the Earth's field at 60 s intervals; it was a Geometrics G-856AX proton magnetometer whose sensor was tied to a tree 2.5 ft southwest of E500 S300. At this distance, passing trains cause the magnetic field to drop by about 1.4 nT; spatial measurements were halted for these passing trains.

Fig. B42: The symbols mark the estimated location of the magnetic objects; the key to the different types of symbols is shown in Fig. A30. The upper number indicates the estimated mass of the object in kg, and assumes that it is iron with a magnetic moment of 0.3 Am^2/kg. The lower number of the pairs indicates the estimated depth of the object in meters. Dots without numbers indicate magnetic objects which were not interpreted. This is usually because it is likely that the object is caused by modern iron debris; in a few cases, the anomalies were not clear enough for interpretation. The lines connecting objects indicate the likely path of buried segments of iron pipe. The Fort Morton grid extends across the park road at the upper left corner, and no survey was done there.

Fig. B44: A total of 374 magnetic anomalies were interpreted for the analysis of the Fort Morton survey. The total iron mass was estimated to be 3512 kg and the average mass per object is 9.4 kg; the average depth of the objects is 0.67 m. Because of the large number of anomalies to be interpreted for this map, a computer-assisted approach was used. The program first located the peaks of all anomalies automatically, and then sorted them in order of their magnitude. Starting with the highest amplitude anomalies, the

program listed the peak value, and also the values radiating from the peak to the north, south, east, and west. This allowed me to estimate the background value. The program then calculated the radius of the anomaly to the four half amplitude points and displayed these. I would then accept those radii which were reasonable, and the program would calculate their average, and then double it to give me the half width of the anomaly. This value and the peak allowed the depth and mass of the object to be calculated. The mass was calculated from the equation m = Ba * W^3 / 56, in kg, where Ba is the peak anomaly and W is the half-width. The program also estimated the direction to the magnetic low from the local gradient of the field to a resolution of 45 degrees. I would check if this direction was reasonable, and then the program would locate the source of the anomaly a distance of 1 ft (0.3 m) in that direction. Since the magnetic map at Fort Morton was made with a measurement spacing of 2.5 ft, I did not make a detailed mathematical model for the analysis of each anomaly.

Fig. B46: It is possible that many of the objects with an interpreted depth of 0 could be modern iron trash just at the surface. While visible iron objects were moved from the survey area, leaves or grass could cover many objects. These shallow objects appear to be most common in the wooded or unmown areas, just where it is most likely that modern trash would accumulate.

Fig. B47: The broken line is a curve which shows likely interpretation errors. As an example, assume that an object has been interpreted as having a mass of 1 kg and a depth of 1 m. It is possible that the actual mass and depth are not those values, but the actual value of mass and depth would probably fall along the broken line curve. Points along this curve have the same anomaly amplitude. It is always most likely that depths and masses are estimated to be too large than too small. See also Fig. A99.

Fig. B48: While most of the map is contoured with an interval of 1 nT, the high anomaly amplitudes have a 5 nT interval; the abrupt shift in the density of contour lines reveals the change in the contour interval. The survey was done on 7 August 1992 with measurements spaced by 1 ft (0.3 m). The sensor height was 0.75 m and the sensor was carried on the horizontal staff. Traverses were made going toward the south, and parallel lines progressed to the east. The survey was stopped for three trains. The spatial map was corrected with the magnetic base station at E499 S301, making measurements at 30 s intervals. The magnetic field was moderately irregular on the day of this survey, with an A-index of 20 at Fredericksburg, Virginia. A value of 0.5 nT was added to the measurements on line E333 and 0.8 nT was subtracted from line E334 to correct for a striation. There were 17 one-point anomalies with an amplitude of about 4 nT; these appear to have been caused by lightning noise, and they were smoothed by averaging the adjacent four readings. The blank line at the bottom of the map is the result of a recording error in the magnetometer.

Fig. B49: The measurement at each point was replaced by the average of the nine measurements which surround the point; this is a 3x3 matrix smoothing. The striations in Fig. B48 are accentuated by the close spacing between measurements. While these striations do not have a serious effect on the interpretation of the data, the contour lines are rather jagged; this makes the patterns in the map more difficult to see.

Fig. B50: The shift between the 1 nT and 5 nT contours is seen by the change in the line spacing of the high amplitude anomalies. The sensor elevation was 0.75 m and the Gem GSM-19FG Overhauser magnetometer was operated with the sensor on a horizontal staff. The measurement spacing of this resurvey was 1 ft (0.3 m); traverses were made going toward the north and parallel lines progressed toward the

east. The survey was done on 6 August 1992 and the A-index at Fredericksburg, Virginia, was 19; the base station magnetometer was at E499 S301 and measurements were at 30 s intervals. Three trains passed during the survey; a magnetic shift on line E500 at S35 may be due to a train (not heard until it was close). Striations were reduced by adding constants to these lines: E471 = -0.8 nT; E472 = +0.5 nT; E474 = -0.7 nT; E475 = +0.5 nT; E483 = -1.0 nT. A total of 14 points had noise interference of about 2.5 nT; these points were replaced by the average of the 4 adjacent measurements. There is an overall gradient in the area of the magnetic map which is caused by the magnetic low of the large iron source near E525 S145.

Fig. B51: The maps on the left plot the measurements made at the upper and lower sensor of a total field gradiometer. This survey was done with the Gem GSM-19FG operating in its gradiometer mode. The calculated gradient from these two maps is plotted in the lower right corner. The contours of the gradient map are at 100 nT/m intervals, with additional 10 nT/m contours shown with broken lines. While this gradient map was measured on 21 October 1992, a separate total field map was measured on 27 June 1992 and this is plotted in the upper right of the figure. Base station magnetometers corrected the total field maps. On 21 October, the base station was at E499 S301 and measurements were at 15 s intervals; the A-index at Fredericksburg, Virginia, was 6. For the 27 June survey, the base station was at W132 N36 and measurements were at 15 s intervals; the A-index was 15.

Fig. B52: For each of the three cross-sections, the surface is at the top of the section. These three sections indicate that the conductivity reading will change if the depth of an interface changes, the thickness of a layer changes, or the concentration or density of a material changes laterally.

Fig. B53: This survey was done on 3 September 1992 and measurements were spaced by 1 ft (0.3 m); with this close spacing, the shape of the curves is quite accurate. The bar was at its normal height of 1 m. The width of the negative-going anomaly (at the background level of about 8.3 mS/m) is 3.6 m; this is about the coil spacing of the EM31.

Fig. B54: This survey was also done on 3 September 1992; after it was finished, the standard deviation of the EM noise was 0.13 mS/m. The pipe at about E275 S130 was also traversed with the bar parallel to the pipe and it also revealed a sharp low immediately over the pipe. At other sites, the EM31 has indicated only a high conductivity over a pipe when the EM31 is parallel to it; perhaps this may be due to the lower spatial resolution of those other surveys.

Fig. B55: This survey was done on 5 September 1992, at about 11:25; Fig. B93 is a plot of the noise which was measured just before the start of this survey. The EM38 was at an elevation of 1.25 ft (0.4 m) and the data have not been adjusted for elevation. The dipoles were vertical and the measurement spacing was 1 ft (0.3 m).

Fig. B56: The metal plate was iron, with a thickness of 1.1 mm. The metal mesh was made of soldered or welded iron wire; the square holes in the mesh had sides of 0.5 inch (1.3 cm) and the wire diameter was 1.3 mm. The loop was a shorted one-turn square coil of wire; the diameter of the wire was 1.3 mm also. All of these objects were insulated from the ground. The measurements were made on 8 October 1992 in my yard, and the soil conductivity is seen to be about 6 mS/m. The measurement interval was 1 ft (0.3 m). For this test, the "depth" of the objects is 0.4 times the intercoil spacing of the EM31.

Fig. B57: The half-widths of these anomaly highs are all about the same, with an average of 1.1 m; this is less than the distance of the objects from the EM38. For this test, the "depth" of the objects

is 1.5 times the intercoil spacing. This test, like that plotted in Fig. B58, was done on 8 October 1992.

Fig. B58: Both were the same size: 14 cm squares. Measurements were made at intervals of 0.25 ft (7.6 cm).

Fig. B59: These tests were done on 20 October 1992 near the visitors' center of the park. The EM38 was hung from the branch of a tree with its bottom edge 0.8 m above the ground. The four iron artifacts were moved below the instrument, making measurements at intervals of 0.1 m along a line below the length of the EM38. The thickness or height of the artifacts has not been subtracted from the "apparent depth" of the objects below the EM38.

Fig. B60: The same aluminum foil used in Fig. B58 was used for this test. The EM38 was hung in a tree at an elevation of 0.5 m and the foil was moved below the instrument in a grid pattern with measurements at intervals of 0.1 m; the area of the test is a rectangle of 1.2 by 1.8 m. The dipoles of the EM38 were vertical. A background value of 2.3 mS/m has been subtracted from all of the measurements. The map should be symmetrical in each quadrant; the differences are due to errors resulting from noise, tilt of the EM38, and mispositioning. This test was also done in my yard, on 10 October 1992. A defect in the contouring program, Surfer, causes one contour line (at -5) to be missing its tick marks.

Fig. B61: This is an enlargement of a section of Fig. B98. This object was detected on east-going traverses with both the 180 MHz and the 315 MHz radar antennas; the depth from the radar profiles was either 0.4 or 0.5 m. An analysis of the high resolution magnetic map indicates an object at a depth of 0.45 m at this point.

Fig. B62: For this very fast survey, the traverses were done quickly, without averaging the measurements with the data logger. The survey was done on 11 August 1991, between 10:10 and 11:40; this survey was done immediately after the main survey of this grid (at a spacing of 2 ft) was completed. After this survey was finished, the noise standard deviation was measured to be 0.05 mS/m. The EM31 bar was east-west, as was the traverse direction; parallel lines progressed to the north. The integration time of the EM31 (1 s) caused the measurements to be striated; this was removed by shifting alternate lines to the east or west by 4 ft (1.2 m). The shifting was done by resampling along the lines using a quadratic interpolation of three adjacent measurements.

Fig. B63: This survey also had a 5 ft (1.5 m) measurement spacing, but it was done more carefully than the survey plotted in Fig. B62. It was done on 9 October 1991, between 13:00 and 14:45. No adjustment or lateral shifting was needed for this survey. The traverses were made with westward traverses only, and parallel lines progressed toward the south. As before, the bar of the EM31 was east-west. After the end of the survey the standard deviation of repeated measurements was measured to be 0.03 mS/m.

Fig. B64: The measurement spacing was 2 ft (0.6 m) for this survey. This survey was done during the period 8 - 9 August 1991. Traverses were made going to the east and west. The Metrosonics data logger (dl-712) was set to sample the EM31 at intervals of 0.5 s and to average for a period of about 5 s (or 9 samples) The bar height was about 1 m. On 8 August 1991, the standard deviation of stationary repeated measurements was 0.10 mS/m. Parallel lines progressed toward the north.

Fig. B65: This map is quite similar to that of Fig. B64, with the bar east-west; the measurement spacing was also 2 ft for this survey. The survey was done during the period of 9 - 11 August 1991. The sampling was done the same as with the survey shown in Fig. B64. Traverses were still made to the east and west, but the EM31 was put in a wooden pack frame for this perpendicular orientation; the instrument height was then about 1.1 m. Parallel lines progressed to

the south. Fig. B92 illustrates two noise tests which were done during this survey. On 11 August, the EM31 noise had a standard deviation of 0.04 mS/m. A total of 4386 measurements are in this map; the same number generated Fig. B64. Unlike the Fort Morton grid, no adjustment of the measurements was needed for this survey.

Fig. B67: Contours are drawn for the range -2 to 2 mS/m.

Fig. B68: The measurements of Fig. B66 have been smoothed with a 3x3 matrix averaging in order to simplify the map. The high values in the far background are in a general area of debris.

Fig. B69: The survey was done on 8 March 1992 between 12:08 and 14:32, or about 2.5 hours. The height of the bar was 2.5 ft (0.8 m) and it was aligned east-west. Traverses were made east and west, and parallel lines progressed toward the north. The Metrosonics dl-712 sampled at 0.5 s intervals and averaged for about 3 s (or about 5 samples per measurement). After the survey was finished, the standard deviation of the EM38 noise was 0.03 mS/m, although a 5 s averaging period was used for that test. The measurements were converted to approximate the measurements at the surface by multiplying them by 1.54. No smoothing has been done to the data.

Fig. B70: The measurement spacing was 2 ft (0.6 m). Traverses were made going to the east and west and parallel lines progressed to the north. The EM38 bar was oriented east-west also; since the coils are at the ends of the bar, the line between the coils was east-west also. The dipoles were vertical and the instrument was lifted 2.25 ft (0.7 m) in the air. The EM38 was encased in a Styrofoam plastic thermal shell; this was the first survey which I used this insulation. A triangular frame of plastic pipes supported the EM38. The Metrosonics dl-712 data logger recorded the measurements; it was programmed to sample the EM38 values at 0.5 s intervals and to average for about 5 s (9 samples) for each recorded measurement. The survey was done during the period of 3 - 5 October 1991. Standard deviations of the values of stationary measurements were as follows: 3 October 1991 = 0.02 mS/m; 4 October = 0.04 mS/m. The original data showed level shifts of 0.5 mS/m in the apparent conductivity after I restarted the survey after stopping to download data to a computer or at the start of a new day. Three perpendicular test lines (W120, W34, and E50) done at the end of the survey provided a correction for the level shifts of the EM38 from line to line. A correction for the elevation of the instrument was made by multiplying all measurements by a factor of 1.54 in order to approximate the readings which would be measured with the instrument on the surface. Except for these corrections, no smoothing has been done to the measurements. The contour range is 0 - 15 mS/m and the two blank areas have higher conductivity.

Fig. B71: The differences between Fig. B70 and Fig. B71 are primarily the result of measurement and positional errors. This survey was done the same as that shown in Fig. B70, except that the bar of the EM38 was oriented north-south. The traverses were still done in an east-west direction, but the parallel lines progressed toward the south. The survey was done during the period of 5 - 7 October 1991. The measurement noise was 0.03 mS/m on each of these days. The east-west line averages were forced to be the same as those from the survey shown in Fig. B70.

Fig. B72: The average of Fig. B70 and Fig. B71 is plotted here. The difference between the two figures was also calculated, but it revealed primarily noise.

Fig. B73: A 3x3 matrix smoothing was done on Fig. B72 to get this figure.

Fig. B75: Measurements were made at 5 ft (1.5 m) intervals along the lines. On 24 January 1991, I made the measurements at even multiples of 50 ft (such as S100 and S150); on 16 March 1991, I added lines at intermediate 25 ft intervals, such as S25, S75. All of

these lines were remeasured later during the full survey of this area.

Fig. B76: This survey was done with the Geonics EM31 during the period of 27 April - 2 May 1991. The dipoles of the instrument were vertical, as is normal. The long bar of the EM31 was oriented east-west and was at a height of about 1 m. Traverses were made in an east-west direction and parallel lines progressed toward the north. Measurements were made at 5 ft intervals; at each measurement point, the EM31 was sampled at a rate of 2/s with a Metrosonics dl-712 data logger; the logger averaged for a period of about 2 s, for a total of about 5 samples in the recorded average at each point. The conductivity of the soil is typically in the range of 6 - 9 mS/m. The standard deviation of the temporal noise was measured to be 0.03 mS/m on 30 April and 0.08 mS/m on 1 May 1991. The contours are drawn in the range of 2 - 17 mS/m; blank areas have apparent conductivity which is either more or less than this range.

Fig. B78: Contour lines are drawn at +0.2 and -0.2 mS/m. While there are other ways of isolating small-area anomalies, this method is suitable for this area.

Fig. B79: The survey was done 20 - 25 June 1991 with the Geonics EM38. The instrument was raised by 1 ft (0.3 m) above the ground, partly to reduce the effect of small metal objects and partly to simplify the survey in the wooded area. The EM38 was tied to a triangular frame of plastic pipe to hold it at the correct height. The dipoles of the EM38 were vertical; the length of the EM38 was east-west, the same as the traverse direction. The survey began at the south end of the area and parallel lines progressed toward the north; the entire 600 ft (181 m) length of the area was surveyed in one continuous line. The measurements were recorded in a Metrosonics dl-712 data logger. This logger was programmed to sample the EM38 values at intervals of 0.5 s; these samples were averaged for a period of about 5 s at each measurement point, and therefore about 11 samples were averaged for each recorded measurement. The 11,828 measurements are plotted in the map. The standard deviation of the measurement noise was monitored on two of the survey days: 22 June = 0.25 mS/m (see Fig. B94); 24 June = 0.07 mS/m. This survey was done before a thermal shell was constructed for the EM38, and there were changes in the measurements as the temperature of the instrument changed. As with the EM31 survey, four check lines were measured after the survey was finished. These check lines went perpendicular to the direction of the original survey, on lines E100, 300, 500, and 700. These check lines were used to correct for the drift of the instrument's readings along each line by forcing the along-traverse slopes of the original measurements to these lines. These check lines also adjusted for the line-to-line drift of the instrument, as was done for the EM31 survey. The measurements have been approximately corrected from the elevation of 1 ft down to the surface by multiplying each of them by 1.16. The complexity of the contours prevents line labels in the map; contours are drawn in the range of 8 - 18 mS/m.

Fig. B80: The many metallic objects caused a large number of abrupt measurement changes; this made the map more difficult to smooth. First, the measurements were truncated to hold them within a range of 0 - 15 mS/m. Then the 740 most anomalous points were replaced by the average of their 4 neighbors. Finally, a striation smoothing was applied to the data. For this striation smoothing, the points along the line of traverse are given a weight of 2, while the points along the lines to the north and south are given a weight of 1; the sum of the 9 numbers is divided by 12, the sum of the weights.

Fig. B81: This figure is done the same as Fig. B78. It is the difference of Fig. B79 and Fig. B80. Only the two contour lines of

+1 and -1 mS/m are drawn. The hachured lines indicate conductivity lows.

Fig. B82: The main part of this survey was done on 9 August 1992. Traverses went to the north or south and parallel lines progressed to the east. The dipoles were vertical and the bar was aligned north-south; the measurement spacing was 1 ft (0.3 m). The Metrosonics data logger was set to sample at 2/s, average two samples for each measurement, and automatically store the measurements at 1 s intervals. The traverse speed was adjusted to 1 ft/s so that the measurements were registered in time and distance. A tree and a bumblebee nest at the southeast corner prevented readings there. On 3 September 1992, lines E405 - 425 were resurveyed because of the interference found there on the original survey; the 0.15 mS/m shift in the measurements on the two days was corrected. A north-south 3x3 striation filter was used to smooth the measurements.

Fig. B83: While the contours are at intervals of 0.5 mS/m, it was not practical to include the conductivity levels on the contours, because of their complexity. The survey was done on 11 August 1992 (9:04 - 15:00) and the standard deviation of the noise during the survey was rather high at 0.24 and 0.37 mS/m. The sferic noise increased during the day, and parallel lines progressed to the east, where noise is more evident. The EM38 was encased in the Styrofoam shell and tied to a pair of 2.4 m long boards to make a travois. The bottom of the instrument was at an elevation of about 1.25 ft (0.4 m) and the dipoles were vertical. Traverses were made to the south, and measurements were made at 1 ft and 1 s intervals; the dl-712 data logger was programmed to sample at 0.5 s intervals and average 2 samples. The logger was about 1.1 m from the nearest coil of the EM38. The data were corrected to the surface by multiplying the measurements by 1.25, however, no line-to-line adjustments were needed for the data, and the measurements are not smoothed.

Fig. B84: Some of the trends in the data are apparent in this 3x3 striation smoothed map. Both this figure and Fig. B83 have a hachure error on a contour line near E375 S235. The lowest contour is at a level of 5 mS/m; the strongest low values have blanks at their middles.

Fig. B85: The breadth of the lows indicates the clarity (amplitude and width) of the small-area anomalies; a greater breadth may also indicate that the object has a larger size and a shallower depth. This map is a difference: Fig. B83 - Fig. C60. The contour line is at a level of -1 mS/m on the map. This map could also have been generated by a high pass filter map of the original data, rather than subtracting the low pass filtered data from the original map.

Fig. B86: For this map, wherever values were found to be less than -0.3 mS/m, the values were replaced by the average of nearby measurements. A 3x3 striation smoothing was also applied to the measurements for this map. While the low pass filtered map of Fig. C60 rather enlarges the area of the anomalies, the anomaly sizes have not been changed much in this map.

Fig. B87: The survey shown here was done on 3 September 1992 (11:30 - 13:47); the noise was 0.04 mS/m before the survey and 0.07 mS/m after the survey. Measurements were made at 1 ft (0.3 m) intervals along south-going traverses; parallel lines progressed to the east. The EM31 bar was north-south at a height of about 1 m, and the dipoles were vertical. The measurements were 1 s averages of two samples, and the traverse speed was 1 ft/s. An earlier survey was done on 9 August 1992 (16:02 - 18:25), but the noise at the end of the survey was 0.13 mS/m and the data were not usable. A 3x3 striation smoothing filter has been applied to the original measurements for the data in the figure.

Fig. B88: This map averages the measurements of three separate surveys with the EM38. Two surveys with the bar of the instrument

north-south were averaged. These surveys were done on 5 September 1992 (8:36 - 11:14) and 3 December 1992 (8:07 - 10:49). The EM38 was in the insulating shell and mounted on the wooden travois, at a height of 1 - 1.25 ft. Traverses were made going north-south, with measurements at intervals of 1 ft and 1 s; the Metrosonics dl-712 was operated in its autocycling mode. The noise at the end of both surveys was 0.10 mS/m. The third survey was averaged with the first two; this survey, made with traverses to the east, was done on 21 October 1992 (8:19 - 11:58) but otherwise used the same procedures as the other two surveys. The standard deviation of the noise of stationary measurements was found to be 0.09 mS/m at the end of this survey. The measurements in the map have been corrected to the ground surface, and have had line-to-line adjustments for instrument drift, but have not been smoothed.

Fig. B89: A 3x3 matrix smoothing has be done on the data.

Fig. B90: Four different surveys are mapped in the figure; two of the surveys were done with the EM31 and two with the EM38. The EM31 survey was done once with the instrument's bar north-south and once with it east-west. The two surveys are averaged in the upper left map, while the difference (east - north) is plotted at the upper right. With a single orientation of the EM bar, the low is an oval which is elongated in the direction of the bar; the averaged map eliminates this elongation. The EM38 magnetic susceptibility map, on the right, is rather similar to the EM38 conductivity map. The contour interval of the susceptibility map is 0.25 ppt, which is a susceptibility of 0.00025 in SI units; note that the interior contours of two strong lows are not completed. The spacing between measurements for all surveys was 1 ft (0.3 m); therefore, each map is created from 961 measurements. The Metrosonics dl-712 data logger recorded all the measurements. It was set to automatically store measurements at 1 s intervals; the logger sampled the data at 0.5 s intervals and two samples were averaged for each recorded measurement. The first EM31 survey was done on 27 June 1992; traverses were made going toward the east, and the bar was east-west. The second EM31 survey was done on 4 September 1992; traverses were made going toward the north and the bar was oriented north-south. The EM31 was also operated in its susceptibility mode on 10 August 1992 over the iron anomaly; since the map of that data is almost identical to the conductivity map, it is not included here. The EM38 conductivity survey was done on 10 August 1992 (15:39 - 16:59); the dipoles were vertical, the bar was east-west, and traverses were made to the east. The instrument was carried in its thermal shell with the aid of a shoulder strap, holding it at an elevation of 1 ft above the ground. The measurements were corrected to indicate the values at the ground surface. The EM38 susceptibility survey was done on 4 September 1992 (15:29 - 16:45). The dipoles were vertical; the bar was east-west, and traverses were made to the west. The readings of apparent conductivity were converted to magnetic susceptibility.

Fig. B92: The EM31 was operated with its dipoles vertical.

Fig. B95: The noise is measured by the standard deviation of repeated measurements, with the instrument stationary.

Fig. B97: This survey was done on 5 May 1992.

Fig. B98: This survey was done on 11 December 1991, with the dipoles vertical and the bar east-west. The normal dl-712 operating procedure was used with a 5 s average.

Fig. B99: These tests were made by three profiles along line N85 at the Taylor House on 21 October 1992.

Fig. B100: The resistivity has usually been determined from resistivity soundings; in a few cases, the resistivity has been determined by EM measurements or from a resistivity map or a measurement with a single electrode spacing. The average resistivity is determined from a depth model of the resistivity soundings; the

resistivity for each layer (within the depth range of the radar) is multiplied by its thickness and the resulting sum of products is divided by the maximum depth of radar echoes.

Fig. B101: This and the following three profiles were made across the width of the Taylor cellar. This is line E10, and the survey was done on 22 October 1992. For every profile in this report, the tick marks at the tops of the profile are at 5 ft (1.5 m) intervals; double tick marks indicate 50 ft multiples in the coordinate system along the line of traverse. This profile was made with a model 3055 antenna, which had a model 705D transceiver. Since this antenna was not found to be generally the best for this site, not very much effort was made to optimize the range gain setting with this antenna. It is likely that the major cause of the greater apparent depth with this antenna is simply the fact that the upper part of the echo from the cellar floor has a very low amplitude and is not detected in this profile.

Fig. B102: This is a model 3105 antenna. The 180 MHz on the figure indicates the predominant frequency in the spectrum of the radar pulse; this is determined by the width of the black echo bands.

Fig. B103: This is a model 3102 antenna; the manufacturer calls this a 500 MHz antenna, but I have found the predominant frequency to be about 315 MHz in average soil. The gray echo bands below an apparent depth of 1.4 m are caused by reverberations in the radar system; they do not indicate soil strata.

Fig. B104: This profile was made with a model 3101 antenna.

Fig. B105: These profiles are made along line E400 and all were made on 22 October 1992.

Fig. B106: This 180 MHz antenna was found to be generally the most suitable for the survey at this site.

Fig. B107: Note that this antenna separates the echoes from the trenches almost completely from the horizontal echo bands caused primarily by the surface of the soil. This allows the depth of the interfaces to be clearly determined. However, note that the echo from the third trench from the right (at S240) is quite faint.

Fig. B108: The northern trench, at S200, still causes a very distinct echo. This must mean that the soil contrast at its base is very large and sharp.

Fig. B109: Both of these profiles are along Taylor House line N80 and both are profiles made with the model 3105 (180 MHz) antenna; the survey was done on 2 September 1992.

Fig. B110: These profiles were made on 28 June 1992 along line N90 at the Taylor House, and both were made with the model 3105 (180 MHz) antenna.

Fig. B111: These are profiles of line S200 at Fort Morton, surveyed with the model 3102 (315 MHz) antenna. During the period of 6 - 8 March 1992, there was 7.4 cm (2.9 inch) of rain at the site; there was no rain on March 4, 5, or 9 and the rain ended before the morning survey of March 8. The ground was still soggy on March 9.

The lower frequency model 3105 (180 MHz) antenna shows similar effects. Similar tests at the Taylor house on these two days showed little difference in those profiles.

Fig. B112: These are profiles of line S200 at Fort Morton; the survey was done with the model 3102 (315 MHz) antenna. The August 6 profile was made at 12:45 pm; an hour earlier there was heavy rain at the site. The rain began slowly early in the morning and ended at about mid-day. While the rainfall at the site is not known, at Hopewell, there was 1.9 cm of rain on the 6th. There was no rain at the site on August 7 or 8. The complex radar pattern on August 6 may be caused by lenses of soil which have different moisture content; these are indicated by the distinct oblique echo lines in the profile. While all of the Fort Morton depth scales assume a pulse velocity of 0.09 m/ns, the apparent depth of these features is

clearly dependent on soil moisture, and the apparent depth is greatest on 9 March at the Taylor house (see Fig. B111), when the soil moisture content must have been its greatest.

Fig. B113: Line N32.5 was surveyed on 1 May 1992 with the model 3102 antenna; this object was detected with several antennas and on perpendicular profiles. Line N72.5 was surveyed on 4 April 1993 with the model 3101 antenna; the traverse speed with this antenna was 16 s per 5 ft. The horizontal scale applies to the profile with the model 3101 (900 MHz) antenna.

Fig. B114: Note that one-way echo delay times are used for this calculation. Often the time scale of a radar profile will show the full, or two-way, delay time. If the reflector is large or is extended in a direction which is not perpendicular to the line of the radar traverse, a more complicated analysis is needed; see Volume C.

Fig. B116: It is also possible that some reverberations may be due to the length of a metallic object. During my 1979 survey at this site, I studied the reverberations from metal objects, trying to find out if there was any important information in the frequency of the reverberations, but I found none.

Fig. B117: This survey was done only with the low resolution or 120 MHz, model 3055, radar antenna. The symbols which I used to mark the radar echoes were somewhat different for that survey, and I have not changed them to make them consistent with the symbols from this later survey. For that survey, the radar profiles were made primarily along east-west lines. After the cellar floor was detected, I made separate short profiles along north-south lines there in order to define its shape better.

Fig. B118: Only the profiles from the 1991 - 1993 surveys are located here. The profiles with the 900 MHz antenna were only made close to the Taylor House cellar. While only one line was profiled with the 120 MHz antenna, this was the same antenna which I was used for the 1979 survey here.

Fig. B119: The average distance between the start of echoes is 14.8 ft. This echo spacing is much smaller than that at Fort Morton. This survey was done during the period of 29 April - 2 May 1992, and a total field time of 34 hours was needed.

Fig. B120: The profiles in this area were measured on 30 April 1992 with the model 3105 antenna. Numbers indicate depths, in dm. There were 69 lines profiled, with a total length of 6900 ft; there are 454 echoes mapped in the figure.

Fig. B121: This survey was done with the model 3105 antenna during 29 - 30 April 1992. The numbers show echo depth, in decimeters. With 41 profile lines, a total length of 6970 ft was profiled for this map; there are 553 echoes located on it.

Fig. B123: The survey was done on 2 May 1992 with the model 3102 antenna. The numbers indicate the depths of the echoes, in dm. For the 69 lines of profile, there were 370 echoes mapped on a total length of 6900 ft.

Fig. B124: Using the model 3102 antenna, this survey was done entirely on 1 May 1992. The numbers show the depth of the echoes, in dm. The traverse direction was to the east. There are 41 profile lines, for a total length of 6970 ft. There are 501 echoes mapped in the figure.

Fig. B125: The two depth calculations should give the same number; any difference indicates an error either in location or with the assumed velocity of the radar pulse.

Fig. B126: The solid lines mark the profiles which were made with the 180 MHz antenna, while the dashed lines show the profiles with the 315 MHz antenna. Some of the lines are slightly offset from their true path, so they do not obscure other lines.

Fig. B127: Survey with a 180 MHz antenna on 29 April 1992. This profile closely follows the southern wall of the cellar, although the

wall is at a slight angle to the line of traverse. The shallower echoes at the far ends of the cellar could be caused by the tops of the cellar walls. The radar detects moderately complex and irregular fill within the cellar, but few objects can be isolated.

Fig. B128: The survey was done on 30 April 1992 with a model 3105 (180 MHz) antenna. The halves of two arcs are visible at a depth of about 0.6 m on the left at right sides of the cellar; it is possible that these are caused by echoes from the brick side walls of the cellar. The depth scale assumes that the velocity of the radar pulse is 9.4 cm/ns; this velocity has been assumed for all of the profiles in the area of the Taylor House, independent of the survey date or the radar antenna. Depth actually means range. The mapped echoes are plotted at the bottom of the profile and the numbers indicate their depth, in m. Tick marks at the top of the profile indicate 5 ft intervals; these marks were placed by pushing a button on the handle of the radar antenna whenever the midpoint of the antenna passed a 5 ft mark on the guide rope. Double tick marks indicate 50 ft intervals in the grid system. The traverse speed of the radar antenna was 8 s per 5 ft; this was controlled by an electronic metronome which beeped at 1 s intervals. Unless otherwise stated, all profiles made with the model 3105 antenna have this same traverse speed. The radar was set to measure depth scans (vertical lines) at a rate of 12.8 scans per s; therefore, the line spacing between depths scans was 1.5 cm. These scans are faintly visible as vertical lines in the profiles; only every other scan is printed in these illustrations. The traversing direction of the radar antenna was to the north here, as is conventional; the left side of a profile was always measured earlier than the right side.

Fig. B129: Both traverse directions of the model 3102 antenna are included in the statistics. There are a total of 539 echoes from west of W10, and 306 echoes from the east side. Each side is normalized to those sums to give the fractions which are plotted; all echoes within each depth interval of 0.1 m are added.

Fig. B130: The survey was done on 29 April 1992 with the 180 MHz antenna. This echo was similarly detected on line N65; however, on line N62.5, there was a shallow reverberation in this area. The echo was not detected at all on the north-going traverses. This evidence suggests that there is a metal object like a pipe or wire which goes along a north-south line in this area. This object was clearly detected by the 1979 radar survey also, and it is illustrated in Figure 2 of the publication (Bevan, Orr, and Blades 1984); however, the depth of the object listed there (1.4 m) was incorrectly too large because the low frequency model 3055 antenna could not detect the shallow echo at 0.6 m.

Fig. B131: Note that depths are in cm here; depths in the other radar maps are in dm. The radar survey was done during 2 hours on 4 April 1993 with the model 3101C antenna. For the 13 lines, a total length of 780 ft was profiled and 48 echoes were mapped.

Fig. B132: The lines which were surveyed with the low frequency, model 3055 (120 MHz) antenna are slightly offset and are indicated as a long-short dash line. Note that the primary survey was done only with the 180 MHz antenna. Since this antenna and the 315 MHz antennas were both about equally suitable here, only one was used.

Fig. B133: The map is the result of radar profiles with a total traverse length of 34,560 ft. There are 1365 echoes mapped here, which indicates that the separation from the start of one echo to the start of the next averages 25.3 ft. A total of 43 hours of field work was needed to generate the profiles of this map.

Fig. B134: This survey was done with the model 3105 (180 MHz) antenna during the period of 6 - 8 December 1991. A total length of 19,155 ft was profiled on 68 lines, and 785 echoes are mapped here.

Figure Notes

The spacing between the lines of profile was 10 ft and the traverses were made going toward the east. The maximum length of the profiles was 300 ft, and long profiles were broken at the E400 ft point. The fine-lined print of this figure is needed because of the small details of the echoes and the closely-spaced numbers.

Fig. B135: The numbers indicate depths in decimeters (dm); in some cases, a range of depths indicates the actual range of the echoes. This survey was done with the model 3105 (180 MHz) antenna during the period of 8 - 10 December 1991. A length of 15,405 ft was profiled on 62 lines, and 580 echoes are mapped in the figure. The spacing between the profile lines was 10 ft and the direction of traverse was to the south; this direction is backward from the typical and standard direction because it allowed the traverses to go from the grassy area into the wooded area, and this is much easier than the opposite. Long traverses were broken into two spans: from S0 to S300 and S300 to S450. The profile spans were interpreted separately, and the interpretation symbol can change at the junction between the two segments of a traverse.

Fig. B136: The profiles with the 180 MHz antenna are marked with a solid line, while the 315 MHz profiles are indicated with a broken line.

Fig. B137: Survey on 26 June 1991. The traversing speed of the radar antenna was 12 s per 5 ft; this is 0.13 m/s or 0.46 km/hour. Since the scan rate of the antenna was set for 12.8 scans per second, the scan lines were spaced by 1.0 cm; this printout has every other scan on it, so the spacing between vertical scan lines here is 2 cm.

Fig. B138: The bombproof trench is the third from the north. To the east of E450, the profile crosses the unmown area of the site; the profile shows no difficulty there. The survey was done on 8 December 1991 with the 180 MHz antenna.

Fig. B139: Survey 6 December 1991 with the 180 MHz antenna.

Fig. B140: The iron pipe causes a strong echo at E359. Survey 6 December 1991 with the 180 MHz antenna.

Fig. B141: Both profiles were made with the 180 MHz antenna; the profile of line S70 was made on 6 December 1991, while line E250 was profiled on 9 December 1991. It is possible that this wire goes from about E263 S10 to E250 S80. The very distinct echo on the right hand side of the E250 profile is caused by an iron pipe there.

Fig. B142: The distinct echo at E160 is caused by an isolated object in front of the fort. A perpendicular profile was not made here. Survey 7 December 1994 with the 180 MHz antenna.

Fig. B143: There is an indication of reverberation on the right hand half of the road echo. Survey 7 December 1991; 180 MHz antenna.

Fig. B144: Solid lines indicate the lines profiled with the 180 MHz antenna, while broken lines show the path of the 315 MHz antenna.

Fig. B145: This map reveals how the clarity of an echo pattern can change along the length of a trench. Some of the echoes appear to extend from one trench to another along the north-south lines; this is partly caused by the indistinct boundaries on some of the patterns. This map was generated from a total profile length of 12,155 ft. A total of 513 echoes are plotted here, indicating an average spacing between the starting points of echoes to be 23.7 ft. A total of 25 hours of field work was required to make the profiles for this map.

Fig. B146: The survey was done on 5 August 1992 with the model 3102 antenna. For the 42 lines of profile, with a total length of 4070 ft, a total of 174 echoes were mapped. The numbers show echo depth in dm.

Fig. B147: This survey was done of 5 and 6 August 1992 with the model 3105 antenna. For the 40 lines of profile, a total of 170 echoes were mapped in the length of 3985 ft. East-going traverses were made with the model 3105 antenna later in the day of August 6;

the rain that afternoon reduced the quality of these profiles and they were not interpreted. The numbers show the depth of the echoes in decimeters, dm (10 dm = 1 m).

Fig. B148: The field work for this map was done on 2 September 1992, using the model 3102 antenna. This survey was done shortly after a relic hunter had excavated holes in this area. The total profile length of 4100 ft was done with 41 traverses; a total of 169 echoes are mapped. The numbers show the echo depth, in dm.

Fig. B149: The cross-sectional diagram is included with the historical map of Fort Morton, Fig. A72. It has been registered with the radar echoes. Survey 6 August 1992 with the 315 MHz antenna.

Fig. B150: The lines for the model 3102 (315 MHz) antenna are offset from the actual line of traverse so that these lines may be distinguished from the lines of the 180 MHz antenna.

Fig. B151: The survey was done during 9 hours of field work on 8 August 1992. A total profile length of 4900 ft was generated along 86 lines. There are 248 echoes mapped in the figure.

Fig. B152: This survey was done on 8 August 1992 with the model 3102 antenna. The spacing between profile lines is 2.5 ft and most were made with east-going traverses. Only three lines were made with south-going traverses, and these echoes are mapped here also. The numbers show echo depth, dm; the orientation shows traverse direction.

Fig. B153: This is also the model 3105 antenna, and the survey continued on 8 August 1992. The numbers show echo depth, dm.

Fig. B154: This survey was done with the model 3105 antenna on 8 August 1992.

Fig. B155: Survey 8 August 1992 with the 180 MHz antenna. The radar profiles indicate a line of echo arcs along E485; these are plotted in Fig. B152. At first I thought that this marked the line of a buried pipe or wire; since the conductivity and magnetic surveys do not detect this, there must be another cause. The line of echoes is probably caused by the bottom corner of the fortification trench; this is acting like a corner reflector; corners are also strongly detected by airborne radars.

Fig. B156: Some of these apparent pits may also be bays into the side of the trench, but most are isolated pits. Survey 8 December 1991 using the 180 MHz antenna.

Fig. B157: The field work required about 3 hours on 28 June 1992. A total of 26 lines were profiled, with a total length of 780 ft. A total of 66 echoes are mapped, and the numbers next to the echoes show their depth in decimeters. Note that the 3l5 MHz antenna was only used for profiles to the east and the 180 MHz only profiled to the south.

Fig. B158: The two profiles are along perpendicular lines and are made with two different antennas. Note that the depth of the feature here is about 0.4 m, less than that from the interpretation of other geophysical data; this suggests that part of the metallic mass is at a shallow depth, while the major part of the feature must begin at a greater depth. Survey 28 June 1992.

Fig. B159: The survey area of the Iron detail is located just behind the main fortification trench at the fort.

Fig. B160: The survey was done on 1 December 1992 (16:22 - 16:37). Only a single pair of these pots were prepared for this test, so no adjustment of the differences between pots was needed. The upper 2 - 3 cm of the grass turf was scraped away, and the moving pot was set on the surface of the soil. The resistance between the pair of pots was measured to be 9000 ohm, much lower than for the Ag-AgCl electrodes. The measurements were made at 30 s intervals, and the voltage dropped by about 2 mV during that period. After the measurement traverse to the east was finished, the point at E510 was

measured again and the difference between the two readings was only 0.2 mV.

Fig. B161: This survey was done on 25 October 1992, using the large-surface electrodes. The first survey was done by just setting the electrodes on the surface of the ground; about half of the surface was covered by rather dry grass. While the voltage changed with pressure, it was measured with no pressure on the electrodes. The first survey was done during 12:25 - 12:46, while the second survey was done 13:19 - 13:49. For the second survey, the grass was scraped from the surface at each electrode location in order to expose the bare soil. In two locations, a slight excavation of the grass roots was made, and this raised the voltage at the electrode. The voltage of these Tinker and Rasor electrodes drops by about 1.5 mV when sunlight shines into the transparent inspection window on the side of the electrodes.

Fig. B162: Stainless steel electrodes were driven to a depth of about 13 cm and measurements were made at 30 s intervals. During that 30 s, the voltage usually rose by about 0.15 V; this large rise may account for much of the irregularity of the measurements. The survey was done 1 December 1992 (15:43 - 15:58).

Fig. B163: The 25 October 1992 survey was done during 10:45 - 11:18 with the six Ag-AgCl electrodes; electrode #0 was the reference negative. The resistances between the electrodes were measured relative to electrode #0 before the start of the survey, and while the electrodes were in a KCl bath; these values (in kilohms) were: #1 = 60; #2 = 85; #3 = 55; #4 = 23; #5 = 50. All measurements were made with a Fluke model 8060A digital voltmeter. After the first 5 electrodes were placed in the soil, the sequence was as follows, assuming the measurements move to the right: Measure the voltage at the left electrode; move the voltmeter to the next location to the right; core a hole on the right and remove the plug of soil; pull the left electrode; wash it in water and place it in the new hole on the right. The electrode numbers cycled 1234512345 ... and the electrode number was recorded along with the voltage. The inter-electrode resistance, with the electrodes in the soil, was measured only two times during the survey; both values were about 110,000 ohms. It was found that the voltages changed by about 3 mV when the electrodes were moved about the bottom of the cored holes. The voltage at an electrode increased by about 4 mV in a minute after it was placed in a hole; the measurement sequence above allowed this voltage to stabilize before it was recorded. The inter-electrode differences were adjusted by subtracting constants from the measurements with each electrode; these constants were: #1 = 37 mV; #2 = 45 mV; #3 = 33 mV; #4 = -1 mV; #5 = 24 mV. On 2 December 1992, the measurements were made between 10:06 - 10:52. The procedures were the same as with the earlier survey. However, for this survey, measurements were made at exact one minute intervals, in order to make the temporal drift of the electrodes in the holes about the same. It was easier to push the soil corer into the earth in December than it was in October.

Fig. B164: The survey was done on 2 December 1992 (11:27 - 12:17). The procedures described with Fig. B163 were applied except that the measurement interval was fixed at 30 s per measurement.

Fig. B165: The survey was done on 25 October 1992 (14:52 - 15:45). The procedures were the same as for the survey illustrated in Fig. B163. The voltages would change by 3 - 10 mV when the electrode was moved across the bottom of the 1 inch (2.5 cm) diameter cored holes, which were about 13 cm deep. At E479, the corer dropped abruptly, so there is probably the tunnel of a rodent there.

Fig. B166: These measurements are just as noisy as all of the other measurements with the Ag-AgCl electrodes. The survey was done on 2 December 1992 (13:39 - 14:37), making measurements at 30 s intervals with the procedures described with Fig. B163.

Figure Notes

Fig. B167: This was the only SP map which was made; all of the other surveys were single, isolated lines. Measurements were made at 2 ft (0.6 m) intervals for this map. The original measurements are plotted in the upper left corner of the figure. The 256 measurements were made on 26 October 1992 (9:40 - 14:12). Traverses were made to the east and west, and parallel lines progressed toward the south. The 6 Ag-AgCl electrodes were used in sequential order, and measurements were made at intervals of 1 minute. The negative reference point was at E510 S130. Normal procedures for soil coring were used, and about 10% of the holes encountered fragments of brick. Possible rodent tunnels were found at two points along line S160: at E510 and E534.

Fig. B168: This test was made on 25 October 1992 (10:33 - 10:44) just at the start of the measurements shown in Fig. B163, and the moving electrode was at E411.

Fig. B169: Six Ag-AgCl electrodes were placed together in a water basin containing a solution of KCl for these tests. Electrode #1 was selected for the reference negative electrode and the voltages of all of the other electrodes were measured relative to this one electrode. A broken line separates two groups of numbers. The numbers below the line were measured in the field during the SP surveys; the numbers above the line were measured inside, in the laboratory and with the electrodes continuously in a bath, before the survey was started. On 14 October 1992, at 5:30 pm, there is a large change in the voltages; I measured the inter-electrode resistances before this. Electrodes #1 - #5 are Ag-AgCl double junction pH reference electrodes; they have a porous Teflon tip and an epoxy body. Before this survey, an algae-like growth was removed from some of the electrodes. Electrode #0 is a single junction electrode with a glass body; I bought this surplus. During all of these tests, the average voltage change of the electrodes was 13 mV.

Fig. B170: As with Fig. B169, the measurements shown below the broken line were measured in the field, while the measurements above were measured in the laboratory, where the changes in temperature and light were much smaller. The inter-electrode voltages were measured with the electrodes grouped together in a bath of copper sulfate in water. While the Geoex electrodes were bought in 1980, the Tinker and Rasor electrodes were bought in 1987. Unlike the Ag-AgCl electrodes, no growths appeared on these electrodes after long term storage; this is probably because CuSO4 is toxic to organisms. Both the Tinker and Rasor and the Geoex electrodes have a copper rod which dips into the saturated solution of copper sulfate in water.

Fig. B171: Measurements were recorded with the Metrosonics dl-712 data logger; it averaged samples for an interval of 30 s and the samples were taken at either 1 or 15 s intervals.

Fig. B172: The central point of the SP anomaly is estimated to be at E525.8 S144.8 and the distances from this point to all of the original measurements, shown in the upper left part of Fig. B167, are plotted along with the measured voltages. While a bipole model (with poles at depths of 4.3 and 11 m) gave a poorer fit to the measurements, the data are so noisy that these models cannot be reliably distinguished.

Fig. B173: The data for this figure, and also Fig. B174, Fig. B175, Fig. B176, and Fig. B177 was kindly sent to me by Brooke Blades. No samples were taken in the northwest corner. The chemistry of these samples was measured by the Soil Testing Laboratory of the Agronomy Department of the University of Maryland in July 1979. I do not know what are the units of these measurements.

Fig. B177: High pH means that the soil is more acidic.

References

35th Regiment, 1884, History of the Thirty-Fifth Regiment Massachusetts Volunteers, Mills, Knight (Boston).

36th Regiment, 1884, History of the Thirty-Sixth Regiment Massachusetts Volunteers, Rockwell and Churchill (Boston).

Abbot, Henry L., 1868, Siege Artillery in the Campaigns Against Richmond, Van Nostrand (New York), reprinted 1986 by Dean Thomas (Arendtsville, Pennsylvania).

Abrahamsen, N., 1992, "Evidence for church orientation by magnetic compass in twelfth-century Denmark", Archaeometry 34(2): 293 - 303.

Ackermann, Hans D., Leroy W. Pankratz, and Danny Dansereau, 1986, "Resolution of ambiguities of seismic refraction traveltime curves" Geophysics, 51(2): 223 - 235.

Acworth, R. I., and D. H. Griffiths, 1985, "Simple data processing of tripotential apparent resistivity measurements as an aid to the interpretation of subsurface structure", Geophysical Prospecting, 33(6): 861 - 887.

Adams, John S., and Paolo Gasparini, 1970, Gamma-Ray Spectrometry of Rocks, Elsevier (Amsterdam).

Adolph, E. F., and associates, 1969, Physiology of Man in the Desert, Hafner (New York).

Aitken, M. J., 1974, Physics and Archaeology, second edition, Clarendon Press (Oxford).

Aitken, M. J., 1959, "Test for correlation between dowsing response and magnetic disturbance", Archaeometry, 2: 58, 59.

Albert, Allen D. (editor), 1912, History of the Forty-Fifth Regiment, Pennsylvania Veteran Volunteer Infantry 1861-1865, Grit Publishing Co. (Williamsport, Pennsylvania).

Aldridge, David F., and Douglas W. Oldenburg, 1992, "Refractor imaging using an automated wavefront reconstruction method", Geophysics, 57(3): 378 - 385.

Allen, George H., 1887, Forty-Six Months With the Fourth R.I. Volunteers, Reid (Providence, Rhode Island).

Allen, J. H., C. C. Abston, E. P. Kharin, N. E. Papitashvili, and V. O. Papitashvili, 1982, International Catalog of Geomagnetic Data, report UAG-86, Environmental Data and Information Service (Boulder, Colorado).

Ambrose, William S., 1976, An interpretive Earthworks Preservation Guide for Petersburg National Battlefield, M. S. thesis, Clemson University (Clemson, South Carolina).

American Society of Photogrammetry, 1985, Close-Range Photogrammetry and Surveying: State of the Art, American Society of Photogrammetry (Falls Church, Virginia).

American Foundrymen's Association, 1944, Cast Metals Handbook, American Foundrymen's Association (Chicago).

Ames, Nelson, 1900, History of Battery G, First Regiment New York Light Artillery, Marshall Printing (Marshalltown, Iowa).

Anderson, John, 1896, The Fifty-Seventh Regiment of Massachusetts Volunteers in the War of the Rebellion, Stillings (Boston).

Andrews, Harry C., 1970, Computer Techniques in Image Processing, Academic Press (New York).

Annan, A. P. and S. W. Cosway, 1992, "Ground penetrating radar survey design", p. 329 - 351 in: Symposium on the Application of Geophysics to Engineering and Environmental Problems, Society of Engineering and Mineral Exploration Geophysicists (Golden, Colorado).

Apparao, A., T. Gangadhara Rao, R. Sivarama Sastry, and V. Subrahmanya Sarma, 1992, "Depth of detection of buried conductive targets with different electrode arrays in

resistivity prospecting", Geophysical Prospecting, 40(7): 749 - 760.

Arandjelovic, Dusan, 1986, "Resistivity method applied to the investigation of earth embankments", First Break, 4(3): 19 - 23.

Arcone, Steven A., 1984, "Field observations of electromagnetic pulse propagation in dielectric slabs", Geophysics, 49(10): 1763 - 1773.

Arkani-Hamed, J., and D. W. Strangway, 1986, "Magnetic susceptibility anomalies of lithosphere beneath Eastern Europe and the Middle East", Geophysics, 51(9): 1711 - 1724.

Aspinall, A., and J. T. Lynam, 1970, "An induced polarization instrument for the detection of near-surface features", Prospezioni Archeologiche, 5: 67 - 75.

Badekas, John (editor), 1975, Photogrammetric Surveys of Monuments and Sites, North-Holland (Amsterdam).

Bankoff, H. Arthur, and Frederick A. Winter, 1979, "A house-burning in Serbia", Archaeology, 32(5): 8 - 14.

Banks, Richard, 1991, "Contouring algorithms", Geobyte, 6(5): 15 - 23.

Barker, R. D., 1989, "Depth of investigation of collinear symmetrical four-electrode arrays", Geophysics, 54(8): 1031 - 1037.

Barker, R. D., 1981, "The offset system of electrical resistivity sounding and its use with a multicore cable", Geophysical Prospecting, 29(1): 128 - 143.

Basokur, A. T., 1983, "Transformation of resistivity sounding measurements obtained in one electrode configuration to another configuration by means of digital linear filtering", Geophysical Prospecting, 31(4): 649 - 663.

Baxter, W. M., 1963, The Sun and the Amateur Astronomer, Norton (New York).

Bates, C. Richard, David Phillips, and James Hild, 1992, "Studies in P-wave and S-wave seismics", p. 261 - 274 in: Symposium on the Application of Geophysics to Engineering and Environmental Problems, Society of Engineering and Mineral Exploration Geophysicists (Golden, Colorado).

Battelle Laboratories, 1981, Computer-Enhanced Geophysical Survey Techniques for Location of Underground Objects and Structures, Battelle Pacific Northwest Laboratories.

Beard, L. P., and A. C. Tripp, 1994, "Investigating the resolution of resistivity arrays using inverse theory", p. 803 - 815 in: Symposium on the Application of Geophysics to Engineering and Environmental Problems, edited by Ronald S. Bell and C. Melvin Lepper, Environmental and Engineering Geophysical Society (Englewood, Colorado).

Bearss, Edward C., 1950 (estimated), Spring Garden Overlook: Before the Explosion, Petersburg National Battlefield, report on file at the Petersburg National Battlefield).

Berger, K., 1980, "Suggestions for the protection of persons and groups of people against lightning hazards", p. 221 - 227 in: Thunderstorms, by Choji Magono, Elsevier (Amsterdam).

Bertram, Colin, 1957, Arctic and Antarctic, Heffer (Cambridge).Bevan, Bruce W., David G. Orr, and Brooke S. Blades, 1984, "The discovery of the Taylor House at the Petersburg National Battlefield", Historical Archaeology, 18(2): 64 - 74.

Bevan, Bruce W., 1984, "Looking backward: Geophysical location of historic structures", p. 284 - 302 in: The Scope of Historical Archaeology, edited by David G. Orr and Daniel G. Crozier, Temple University (Philadelphia).

Bevan, Bruce, 1993, "Technical report: Selecting a resistivity meter", SAS Bulletin 16(3): 2 - 7.

Bevan, Bruce, 1991, "Technical report: Selecting a magnetometer", SAS Bulletin, 14(4): 2 - 5.

References

Beyer, Bernd Fahmel, 1992, "Evidence for the use of a magnetic compass at Monte Alban: 400 B.C. - A.D. 830", abstract of a talk at the 28th International Symposium on Archaeometry, Los Angeles.

Bhattacharyya, B. K., 1964, "Magnetic anomalies due to prism-shaped bodies with arbitrary polarization", Geophysics, 29(4): 517 - 531.

Bhattacharyya, B. K., and K. C. Chan, 1977, "Reduction of magnetic and gravity data on an arbitrary surface acquired in a region of high topographic relief", Geophysics, 42(7): 1411 - 1430.

Billings, John D., 1909, The History of the Tenth Massachusetts Battery of Light Artillery in the War of the Rebellion, Arakelyan Press, Boston.

Bird, Christopher, 1979, The Divining Hand, Dutton (New York).

Biery, Terry L., 1977, Venomous Arthropod Handbook, U.S. Air Force School of Aerospace Medicine, AFP 161-43, U. S. Government Printing Office (Washington).

Bisdorf, Robert J., and Adel A. R. Zohdy, 1990, IBM PC Programs for Automatic Processing and Interpretation of Wenner Sounding Curves, Open File Report 90-211, U. S. Geological Survey (Denver, Colorado).

Bishop, I., and P. Styles, 1990, "Seismic tomographic imaging of a buried concrete target" Geophysical Prospecting, 38(2): p. 169 - 188; see also comment on this paper, by C. R. I. Clayton, V. S. Hope, and S. J. Howe, 1991, Geophysical Prospecting, 39(5): 711 - 718.

Blades, Brooke S., 1993, Archaeological Excavations at the Taylor House Site, Petersburg National Battlefield, Virginia, National Park Service (Philadelphia).

Blakely, Richard J., 1995, Potential Theory in Gravity and Magnetic Applications, Cambridge University Press (Cambridge).

Blakely, Richard J., and Robert W. Simpson, 1986, "Approximating edges of source bodies from magnetic or gravity anomalies", Geophysics, 51(7): 1494 - 1498.

Blakely, R. J., 1985, "The effect of topography on aeromagnetic data in the wavenumber domain", p. 102 - 109 in: Potential Fields in Rugged Topography, proceedings of a meeting, IGL Bulletin 7, University of Lausanne (Lausanne, Switzerland).

Blau, L. W., 1936, "Black magic in geophysical prospecting", Geophysics, 1(1): 1 - 8.

Blizkovsky, M., 1979, "Processing and applications in microgravity surveys", Geophysical Prospecting, 27(4): 848 - 861.

Bogorodsky, V. V., C. R. Bentley, and P. E. Gudmandsen, 1985, Radioglaciology, D. Reidel (Dordrecht).

Bondar, Istvan, 1992, "Seismic horizon detection using image processing algorithms", Geophysical Prospecting, 40(7): 785 - 800.

Bourke, Paul D., 1987, "A contouring subroutine", Byte, 12(6): 143 - 146, 148, 150. See also comments in 12(11): 14, 16, 20.

Bozorth, Richard M., 1978, Ferromagnetism, IEEE Press (Piscataway, New Jersey).

Breiner, S., 1973, Applications Manual for Portable Magnetometers, Geometrics (Sunnyvale, California).

Breiner, Sheldon, and Michael D. Coe, 1972, "Magnetic exploration of the Olmec civilization", American Scientist, 60(5): 566 - 575.

Brigham, E. Oran, 1988, The Fast Fourier Transform and Its Applications, Prentice Hall, (Englewood Cliffs, New Jersey).

Bristow, C., 1966, "A new graphical resistivity technique for detecting air-filled cavities", Studies in Speleology, 1: 204 - 227.

References

Brock, James, and Steven J. Schwartz, 1991, "A little slice of heaven: Investigations at Rincon Cemetery, Prado Basin, California", Historical Archaeology, 25(3): 78 - 90.

Broome, H. John, 1990, "Generation and interpretation of geophysical images with examples from the Rae Province, northwestern Canada shield", Geophysics, 55(8): 977 - 997.

Brown, A. G., 1992, "Slope erosion and colluviation at the floodplain edge", p. 77 - 87 in: Past and Present Soil Erosion, edited by Martin Bell and John Boardman, Oxbow (Oxford).

Brothwell, Don, and Eric Higgs, 1969, Science in Archaeology, second edition, Thames and Hudson (London).

Brouwer, Jan, and Vincent Nijhof, 1994, "The use of geophysical techniques for the detection of partially collapsed mine shafts", p. 593 - 604 in: Symposium on the Application of Geophysics to Engineering and Environmental Problems, Environmental and Engineering Geophysical Society (Englewood, Colorado).

Bruckl, E., 1987, "The interpretation of traveltime fields in refraction seismology", Geophysical Prospecting, 35(9): 973 - 992.

Burger, H. Robert, 1992, Exploration Geophysics of the Shallow Subsurface, Prentice Hall (Englewood Cliffs, New Jersey).

Burr, S. V., 1982, A Guide to Prospecting by the Self-Potential Method, Miscellaneous Paper 99, Ontario Geological Survey (Toronto).

Cain, J. C., S. J. Hendricks, R. A. Langel, and W. V. Hudson, 1967, "A proposed model for the international geomagnetic reference field - 1965", Journal of Geomagnetism and Geoelectricity, 19: 335 - 355.

Carr, Christopher, 1982, Handbook on Soil Resistivity Surveying, Center for American Archeology Press (Evanston, Illinois).

Catton, Bruce, 1952, Glory Road, Pocket Books (New York).

Challands, Adrian, 1992, "Field magnetic susceptibility measurement for prospection and excavation", p. 33 - 41 in: Geoprospection in the Archaeological Landscape, Oxbow (Oxford).

Chapra, Steven C., and Raymond P. Canale, 1988, Numerical Methods for Engineers, second edition, McGraw-Hill (New York).

Chen, Chih-Wen, 1986, Magnetism and Metallurgy of Soft Magnetic Materials, Dover (New York).

Choubert, G., and A. Faure-Muret (General co-ordinators), 1976, Geological World Atlas, UNESCO (Paris).

Christensen, Nikolas I., 1982, "Seismic velocities", p. 1 - 228 in: Handbook of Physical Properties of Rocks, volume 2, edited by Roberts S. Carmichael, CRC Press (Boca Raton, Florida).

Clark, Anthony, 1969, "Resistivity surveying", p. 695 - 707 in: Science in Archaeology, 2nd edition, edited by Don Brothwell and Eric Higgs, Thames and Hudson (London).

Clark, Anthony J., 1986, "Archaeological geophysics in Britain", Geophysics, 51(7): 1404 - 1413.

Clark, Anthony, 1990, Seeing Beneath the Soil, B. T. Batsford (London).

Clough, John W., 1976, "Electromagnetic lateral waves observed by earth-sounding radars", Geophysics, 41(6A): 1126 - 1132.

Coffin, Millard F., and Olav Eldholm, 1993, "Large igneous provinces", Scientific American, 269(4): 42 - 49.

Conniff, Richard, 1994, "The mole has a way of undermining our assumptions", Smithsonian 24(12): 52 - 63.

Cook, John C., and Stanley L. Carts, Jr., 1962, "Magnetic effects and properties of typical topsoils", Journal of Geophysical Research, 67(2): 815 - 828.

References

Cordell, Lindrith, and A. E. McCafferty, 1989, "A terracing operator for physical property mapping with potential field data", Geophysics, 54(5): 621 - 634.

Cordell, Lindrith, and V. J. S. Grauch, 1982, "Reconciliation of the discrete and integral Fourier transforms", Geophysics, 47(2): 237 - 243.

Cordell, Lindrith, Jeffrey D. Phillips, and Richard H. Godson, 1992, Potential-Field Geophysical Software, Open File Report 92-18, U. S. Geological Survey (Denver, Colorado).

Corry, Charles E., Gregory T. DeMoully, and Michael T. Gerety, 1983, Field Procedure Manual for Self-Potential Surveys, Zonge Engineering and Research Organization (Tucson, Arizona).

Corwin, Robert F., 1990, "The self-potential method for environmental and engineering applications", p. 127 - 145 in: Geotechnical and Environmental Geophysics, Vol. 1, Review and Tutorial, edited by Stanley H. Ward, Society of Exploration Geophysicists (Tulsa, Oklahoma).

Corwin, Robert F., and Donald B. Hoover, 1979, "The self-potential method in geothermal exploration", Geophysics, 44(2): 226 - 245.

Cuffel, Charles A., 1903, History of Durell's Battery in the Civil War, (Philadelphia).

Cullen, Joseph P., 1970, The Siege of Petersburg, Eastern Acorn Press (Harrisburg, Pennsylvania).

Dahlin, Torleif, Sam Johansson, and Ola Landin, 1994, "Resistivity surveying for planning of infrastructure", p. 509 - 528 in: Symposium on the Application of Geophysics to Engineering and Environmental Problems, Environmental and Engineering Geophysical Society (Englewood, Colorado).

Dalan, Rinita A., 1991, "Defining archaeological features with electromagnetic surveys at the Cahokia Mounds State Historic Site", Geophysics, 56(8): 1280 - 1287.

Dalan, Rinita A., 1993, Landscape Modification at the Cahokia Mounds Site: Geophysical Evidence of Culture Change, PhD dissertation, University of Minnesota (Minneapolis).

Danbom, S. H., and S. N. Domenico, 1986, Shear-Wave Exploration, Society of Exploration Geophysicists (Tulsa, Oklahoma).

Daniels, Jeffrey J., 1989, "Fundamentals of ground penetrating radar", p. 62 - 142 in: Symposium on the Application of Geophysics to Engineering and Environmental Problems, Society of Engineering and Mineral Exploration Geophysicists (Golden, Colorado).

d'Arnaud Gerkens, J. C., 1989, Foundation of Exploration Geophysics, Elsevier (Amsterdam).

Das, U. C., and S. K. Verma, 1980, "Digital linear filter for computing type curves for the two-electrode system of resistivity sounding", Geophysical Prospecting, 28(4): 610 - 619.

Davidson, Thomas E., 1986, "Computer-correcting historical maps for archaeological use", Historical Archaeology 20(2): 27 - 37.

Davis, William C., 1986, Death in the Trenches, Time-Life Books (Alexandria, Virginia).

Davis, Raymond E., Francis S. Foote, James M. Anderson, and Edward M. Mikhail, 1986, Surveying Theory and Practice, McGraw-Hill (New York).

Degauque, Pierre, Quoc The Nguyen, and Michel Cauterman, 1984, "Simulation of the high-frequency response of a heterogeneous ground through the finite difference technique", IEEE Transactions on Geoscience and Remote Sensing, 22(4): 368 - 374.

Dentith, M. C., A. Trench, and M. Jones, 1993, "Geophysical exploration for Archaean gold: A case study from the Southern Cross Greenstone Belt, Western Australia", Journal of Applied Geophysics, 30(3): 175 - 186.

References

Deuel, Leo, 1969, Flights Into Yesterday, St. Martin's Press (New York).

Dey, A., and H. F. Morrison, 1979, "Resistivity modeling for arbitrarily shaped three-dimensional structures", Geophysics, 44(4): 753 - 780.

Dillon, Brian D., 1989, Practical Archaeology, Institute of Archaeology, University of California (Los Angeles).

Dischinger, James B., Jr., 1987, Late Mesozoic and Cenozoic stratigraphic and structural framework near Hopewell, Virginia, U. S. Geological Survey Bulletin 1567, U. S. Government Printing Office (Washington).

Dobrin, Milton B., and Carl H. Savit, 1988, Introduction to Geophysical Prospecting, Fourth edition, McGraw-Hill (New York).

Dods, S. D., D. J. Teskey, and P. J. Hood, 1985, "The new series of 1:1 000 000-scale magnetic anomaly maps of the Geological Survey of Canada: Compilation techniques and interpretation", p. 69 - 87 in: The Utility of Regional Gravity and Magnetic Anomaly Maps, edited by William J. Hinze, Society of Exploration Geophysicists (Tulsa, Oklahoma).

Dohr, Gerhard P., 1985, Seismic Shear Waves, Part B: Applications, Geophysical Press (London).

Doolittle, James A., and Mary E. Collins, 1995, "Use of soil information to determine application of ground penetrating radar", Journal of Applied Geophysics, 33(1-3): 101 - 108.

Dresen, Lothar, 1978, "Locating and mapping of cavities at shallow depths by the seismic transmission method", p. 149 - 171 in: Rock Dynamics and Geophysical Aspects, edited by G. W. Borm, Balkema (Rotterdam).

Drouin, Pierre, 1991, "Thunder and powder: May they never meet! Lightning conductors at the Esplanade powder magazine, Quebec City", Northeast Historical Archaeology, 20: 37 - 50.

Duch, Peter M., and Kurt I. Sorensen, 1994, "When is 1D 2D? Interpretation of geoelectrical sections", p. 967 - 976 in: Symposium on the Application of Geophysics to Engineering and Environmental Problems, Environmental and Engineering Geophysical Society (Englewood, Colorado).

Duffett-Smith, Peter, 1988, Practical Astronomy with Your Calculator, third edition, Cambridge University Press (Cambridge).

Eden, R. C., 1865, The Sword and Gun, a History of the 37th Wis. Volunteer Infantry, Atwood and Rublee (Madison, Wisconsin).

Ehrenhard, John E., William P. Athens, and Richard E. Johnson, 1984, "A practical deployment array for the Geohm 3 soil resistivity meter", CRM Bulletin, 7(3): 3, 5, 6.

Eidt, Robert C., 1985, "Theoretical and practical considerations in the analysis of anthrosols", p. 155 - 190 in: Archaeological Geology, edited by George Rapp, Jr., and John A. Gifford, Yale University Press (New Haven, Connecticut).

Ehrat, Rolf, 1992, Magnetic Survey Correction Techniques, Scintrex Technical Information (Concord, Ontario).

Elgin, Richard L., David R. Knowles, and Joseph H. Senne, 1994, Celestial Observation Handbook and Ephemeris, Lietz (Box 2934, Overton Park, Kansas)

Embleton, Clifford, and Cuchlaine A. M. King, 1975, Periglacial Geomorphology, second edition, Wiley (New York).

Environmental Protection Agency, 1973, Manual of Individual Water Supply Systems, U. S. Government Printing Office (Washington).

Ernstson, Kord, and H. Ulrich Scherer, 1986, "Self-potential variations with time and their relation to hydrogeologic and meteorological parameters", Geophysics, 51(10): 1967 - 1977.

Evans, Ulick R., 1926, The Corrosion of Metals, Edward Arnold (London).

References

Fabiano, E. B., N. W. Peddie, D. R. Barraclough, and A. K. Zunde, 1983, International Geomagnetic Reference Field 1980 - Charts and Grid Values, circular 873, U. S. Geological Survey (Denver, Colorado).

Fabiano, E. B., N. W. Peddie, and A. K. Zunde, 1983, The Magnetic Field of the Earth, 1980, five maps showing declination, inclination, horizontal and vertical intensity, and total field, Map I-1457 through I-1461, U. S. Geological Survey (Denver, Colorado).

Farkas, L. L., 1970, Management of Technical Field Operations, McGraw-Hill (New York).

Fedi, Maurizio, Giovanni Florio, and Antonio Rapolla, 1994, "A method to estimate the total magnetization direction from a distortion analysis of magnetic anomalies", Geophysical Prospecting, 42(3): 261 - 274.

Fink, James B., Ben K. Sternberg, Edgar O. McAlister, and W. Gordon Wieduwilt, 1990, Induced Polarization Applications and Case Histories, Society of Exploration Geophysicists (Tulsa, Oklahoma).

Fisher, Elizabeth, George A. McMechan and A. Peter Annan, 1992, "Acquisition and processing of wide-aperture ground-penetrating radar data", Geophysics, 57(3): 495 - 504.

Fitzpatrick, R. W., 1988, "Iron compounds as indicators of pedogenic processes: Examples from the southern hemisphere", p. 351 - 396 in: Iron in Soils and Clay Minerals, edited by J. W. Stucki, B. A. Goodman, and U. Schwertmann, D. Reidel (Dordrecht).

Frantov, G. S., and A. A. Pynkevich, 1966, Geophysics for Archaeology, Nedra (St. Petersburg), in Russian.

Frassanito, William A., 1983, Grant and Lee, the Virginia Campaigns 1864 - 1865, Scribner's (New York).

Frederick, Charles D., and James T. Abbott, 1992, "Magnetic prospection of prehistoric sites in an alluvial environment: Examples from NW and west-central Texas", Journal of Field Archaeology, 19(2): 139 - 153.

Gardner, Martin, 1964, "Mathematical games", Scientific American, 211(4): 118 - 120, 125, 126.

Gay, S. Parker, Jr., 1992, "Epigenetic versus syngenetic magnetite as a cause of magnetic anomalies", Geophysics, 57(1): 60 - 68.

Gay, S. Parker, Jr., 1986, "The effects of cathodically protected pipelines on aeromagnetic surveys", Geophysics, 51(8): 1671 - 1684.

Gibbon, John, 1860, The Artillerists's Manual, reprinted in 1970 by Benchmark Publishing (Glendale, New York).

Gibbs, Betty L., 1991, "A review of public domain mapping software", p. 80 - 88 in: GeoTech/GeoChautauqua '91 Proceedings, Denver GeoTech (Denver).

Gibson, Terrance H., 1986, "Magnetic prospection on prehistoric sites in Western Canada", Geophysics, 51(3): 553 - 560.

Giles, Albert W., 1918, The Country about Camp Lee, Virginia, Virginia Geological Survey, Bulletin number 16, (Charlottesville, Virginia).

Glen, Simon and Jan, 1980, Sahara Handbook, Roger Lascelles (London).

Goell, Theresa, 1969, "The Nemrud Dagh (Turkey) geophysical surveys of 1964", p. 61 - 81 in: National Geographic Society Research Reports, National Geographic Society (Washington).

Goforth, Tom, and Chris Hayward, 1992, "Seismic reflection investigations of a bedrock surface buried under alluvium", Geophysics, 57(9): 1217 - 1227.

Goldstein, N. E., and S. H. Ward, 1966, "The separation of remanent from induced magnetism in situ", Geophysics, 31(4): 779 - 796.

Goodman, Dean, 1994, "Ground-penetrating radar simulation in engineering and archaeology", Geophysics, 59(2): 224 - 232.

References

Goodman, D., Y. Nishimura, T. Uno, and T. Yamamoto, 1994, "A ground radar survey of medieval kiln sites in Suzu City, western Japan", Archaeometry, 36(2): 317 - 326.

Gould, Joseph, 1908, The Story of the Forty-Eighth, Alfred M. Slocum.

Goulty, N. R., and A. L. Hudson, 1994, "Completion of the seismic refraction survey to locate the vallum at Vindobala, Hadrian's Wall", Archaeometry, 36(2): 327 - 335.

Gordon, John Steele, 1975, Overlanding, Harper and Row (New York).

Gramly, Richard M., 1970, "Use of a magnetic balance to detect pits and postmolds", American Antiquity, 35(2): 217 - 220.

Grant, F. S., and G. F. West, 1965, Interpretation Theory in Applied Geophysics, McGraw-Hill (New York).

Grauch, V. J. S., and Lindrith Cordell, 1987, "Limitations of determining density or magnetic boundaries from the horizontal gradient of gravity or pseudogravity data", Geophysics, 52(1): 118 - 121.

Gray, Donald H., 1969, "Prevention of moisture rise in capillary systems by electrical short circuiting", Nature, 223(5204): 371 - 374.

Griffith, Fred, 1976, "Some notes on Antarctic photography", Photomethods, p. 21, 46 - 48.

Griffiths, D. H., J. Turnbull, and A. I. Olayinka, 1990, "Two-dimensional resistivity mapping with a computer-controlled array", First Break, 8(4): 121 - 129.

Griffiths, D. H., and J. Turnbull, 1985, "A multi-electrode array for resistivity surveying", First Break, 3(7): 16 - 20.

Grumman, David L., Jr., and Jeffrey J. Daniels, 1995, "Experiments on the detection of organic contaminants in the vadose zone", Journal of Environmental and Engineering Geophysics, 0(1): 31 - 38.

Guerin, Roger, Alain Tabbagh, and Pierre Andrieux, 1994, "Field and/or resistivity mapping in MT-VLF and implications for data processing", Geophysics, 59(11): 1695 - 1712.

Gunn, P. J., 1975, "Linear transformations of gravity and magnetic fields", Geophysical Prospecting, 23(2): 300 - 312.

Haanel, Eugene, 1904, On the Location and Examination of Magnetic Ore Deposits by Magnetometric Measurements, Department of the Interior (Ottawa).

Habberjam, G. M., 1979, Apparent Resistivity Observations and the Use of Square Array Techniques, Gebruder Borntraeger (Berlin).

Habberjam, G. M., 1969, "The location of spherical cavities using a tripotential resistivity technique", Geophysics, 34(5): 780 - 784.

Haeni, F. P., 1988, Application of Seismic-Refraction Techniques to Hydrologic Studies, Techniques of Water-Resources Investigations, Book 2, Chapter D2, U. S. Geological Survey (Denver, Colorado).

Hagerman, Edward H., 1965, The Evolution of Trench Warfare in the American Civil War, Ph.D. dissertation, Duke University (Durham, North Carolina).

Hansen, Richard O., and Marc Simmonds, 1993, "Multiple-source Werner deconvolution", Geophysics, 58(12): 1792 - 1800.

Harbaugh, A. W., 1990, A Simple Contouring Program for Gridded Data, Open File Report OF 90-144, U. S. Geological Survey (Denver).

Harknett, M. R., 1969, "A proton magnetometer with solid state switching", Archaeometry, 11: 173 - 177.

Harmuth, Henning F., 1981, Nonsinusoidal Waves for Radar and Radio Communication, Academic Press (New York).

Hawkes, H. E., 1957, Principles of Geochemical Prospecting, U. S. Geological Survey Bulletin 1000-F, U. S. Government Printing Office (Washington).

References

Hawkins, L. V., 1961, "The reciprocal method of routine shallow seismic refraction investigations", Geophysics, 26(6): 806 - 819.

Haydon, R. Stansbury, 1941, Aeronautics in the Union and Confederate Armies, John Hopkins Press (Baltimore).

Heimmer, Don H., 1992, Near-Surface, High Resolution Geophysical Methods for Cultural Resource Management and Archaeological Investigations, National Park Service (Denver, Colorado).

Helbig, K., and C. S. Mesdag, 1982, "The potential of shear-wave observations", Geophysical Prospecting, 30(4): 413 - 431.

Herbich, Thomasz, 1993, "The method of estimation of the extent of the mining field of flint mines through observation of the arrangement of surface layers", Archeologia Polski, 38: 23 - 35.

Herkommer, Mark A., 1986, "Techniques devised to improve contour mapping by microcomputer", Geobyte, 1(2): 38 - 41.

Hesse, A., 1990, "Resistivity prospecting", p. 307 - 374 in: Archaeological Prospecting and Remote Sensing, by I. Scollar, A. Tabbagh, A. Hesse, and I. Herzog, Cambridge University Press (Cambridge).

Hesse, A., 1967, "Mesures et interpretation en prospection geophysique des sites archeologiques du Nil", Prospezioni Archeologiche, 2: 43 - 48.

Hesse, Albert, 1970, "Introduction geophysique et notes techniques" (in French), p. 51 - 121 in: Mirgissa I, volume 1, edited by J. Vercoutter, Paul Geuthner (Paris).

Hildenbrand, Thomas G., 1983, FFTFIL: A Filtering Program Based on Two-Dimensional Fourier Analysis of Geophysical Data, Open File Report 83-237, U. S. Geological Survey (Denver, Colorado).

Hill, David A., 1988, "Electromagnetic scatter by buried objects of low contrast", IEEE Transactions on Geoscience and Remote Sensing, 26(2): 195 - 203.

Hill, Patricia L., 1991, Bibliographies and Location Maps of Publications on Aeromagnetic and Aeroradiometric Surveys, Open File Report 91-370 (6 publications divided by region), U. S. Geological Survey (Denver, Colorado).

Hinze, William J., 1990, "The role of gravity and magnetic methods in engineering and environmental studies", p. 75 - 126 in: Geotechnical and Environmental Geophysics, Volume 1: Review and Tutorial, edited by Stanley H. Ward, Society of Exploration Geophysicists (Tulsa, Oklahoma).

Hinze, William J. (editor), 1985, The Utility of Regional Gravity and Magnetic Anomaly Maps, Society of Exploration Geophysicists (Tulsa, Oklahoma).

Hogan, Gregory, 1988, "Migration of ground penetrating radar data: A technique for locating subsurface targets", p. 164 - 179 in: Second International Symposium on Geotechnical Applications of Ground-penetrating Radar, University of Florida, Institute of Food and Agricultural Sciences (Gainesville, Florida).

Holcombe, H. Truman, and George R. Jiracek, 1984, "Three-dimensional terrain corrections in resistivity surveys", Geophysics, 49(4): 439 - 452.

Howe, Sandra L. (editor), 1976, NBS Time and Frequency Dissemination Services, NBS Special Publication 432, U. S. Government Printing Office (Washington).

Howell, Benjamin F., Jr., 1959, Introduction to Geophysics, McGraw-Hill (New York).

Hyzer, William G., 1974, "Protecting film and cameras from typical tropical climates", Photomethods, 17(10): 60 - 64.

Imai, Tsuneo, Hideo Fumoto, and Koichiro Yokota, 1976, P- and S-Wave Velocities in Subsurface Layers of Ground in Japan, Oyo Technical Note RP-460, Oyo Corporation (Saitama, Japan).

References

Imai, Tsuneo, and Masayoshi Yoshimura, The Relation of Mechanical Properties of Soils to P- and S-Wave Velocities for Soil Ground in Japan, Oyo Technical Note RP-447, Oyo Corporation (Saitama, Japan).

Imai, Tsuneo, Toshihiko Sakayama, and Takashi Kanemori, 1987, "Use of ground-probing radar and resistivity surveys for archaeological investigations", Geophysics, 52(1): 137 - 150.

International Association of Geophysical Contractors, 1982, Safety Manual for Geophysical Field Operations, IAGC (Houston).

Jahn, Alfred, 1971, Problems of the Periglacial Zone, translated from Polish, U. S. Department of Commerce (Springfield, Virginia).

Janke, N. C., 1972, "Field measurements with common equipment", Photogrammetric Engineering, 38(1): 37 - 47.

John, D. H. O., 1965, Photography on Expeditions, Focal Press (London).

Johnson, Robert Underwood, and Clarence Clough Buel (editors), 1956, The Way to Appomattox, Battles and Leaders of the Civil War, reprinted by Castle Books (New York).

Johnston, H. F., J. A. Fleming, and H. E. McComb, 1945, "Magnetic instruments", p. 59 - 109 in: Terrestrial Magnetism and Electricity, edited by J. A. Fleming, Dover (New York).

Johnston, Ronald H., F. N. Trofimenkoff, and James W. Haslett, 1987, "Resistivity response of a homogeneous earth with a finite-length contained vertical conductor", IEEE Transactions on Geoscience and Remote Sensing, 25(4): 414 - 421.

Jones, Thomas A., David E. Hamilton, and Carlton R. Johnson, 1986, Contouring Geologic Surfaces With a Computer, Van Nostrand Reinhold (New York).

Jones, Virgil Carrington, and Harold L. Peterson, 1971, U.S.S. Cairo, the Story of a Civil War Gunboat, U.S. Government Printing Office (Washington).

Keller, George V., 1968, "Discussion on 'An inverse slope method of determining absolute resistivity'", Geophysics, 33(5): 843 - 845.

Keller, George V., and Frank C. Frischknecht, 1966, Electrical Methods in Geophysical Prospecting, Pergamon Press (Oxford).

Kelly, M. A., P. Dale, and J. G. B. Haigh, 1984, "A microcomputer system for data logging in geophysical surveying", Archaeometry, 26(2): 183 - 191.

Kerr, Julian, 1990, "Drying out flood-damaged equipment", Popular Electronics, (January), p. 45, 46, 94.

Kielan-Jaworowska, Zofia, 1969, Hunting for Dinosaurs, MIT Press (Cambridge, Massachusetts).

Kilty, Kevin T., 1983, "Werner deconvolution of profile potential field data", Geophysics, 48(2): 234 - 237.

King, Julia A., Bruce W. Bevan, and Robert J. Hurry, 1993, "The reliability of geophysical surveys at historic period cemeteries: An example from the Plains Cemetery, Mechanicsville, Maryland", Historical Archaeology, 27(3): 4 - 16.

Kirk, Hyland C., 1890, Heavy Guns and Light: A History of the 4th New York Heavy Artillery, Dillingham (New York).

Kirk, Keith G., and Eberhard Werner, 1981, Handbook of Geophysical Cavity-Locating Techniques, U. S. Department of Transportation, Implementation Package FHWA-IP-81-3.

Klauber, Laurence M., 1982, Rattlesnakes, University of California Press (Berkeley).

Koefoed, O., 1968, The Application of the Kernel Function in Interpreting Geoelectrical Resistivity Measurements, Gebruder Borntraeger (Berlin).

Koefoed, Otto, 1979, Geosounding Principles, 1, Resistivity Sounding Measurements, Elsevier (Amsterdam).

References

Krum, Glenn L., and Thomas A. Jones, 1992, "Pitfalls in computer contouring", Geobyte, 7(3): 30 - 35.

Kumar, Rakesh, 1974, "Direct interpretation of two-electrode resistivity soundings", Geophysical Prospecting, 22(2): 224 - 237.

Kunaratnam, K., 1981, "Simplified expressions for the magnetic anomalies due to vertical rectangular prisms", Geophysical Prospecting, 29(6): 883 - 890.

Kunetz, Geza, 1966, Principles of Direct Current Resistivity Prospecting, Gebruder Borntraeger (Berlin).

Lakshmanan, Jacques, and Jacques Montlucon, 1987, "Microgravity probes the Great Pyramid", The Leading Edge, 6(1): 10 - 17.

Lampe, Kenneth F., 1984, Common Poisonous and Injurious Plants, U. S. Department of Health, and Human Services, FDA 81-7006, U. S. Government Printing Office (Washington).

Lancaster, Donald E., 1966, "Electronic metal detectors", Electronics World, December, 39 - 42, 62.

Land, Tony (editor), 1978, The Expedition Handbook, Butterworths (London).

Lange, Arthur L., 1965, "Cave detection by magnetic surveys", Cave Notes, 7(6): 41 - 54.

Langel, R. A., 1987, "The main field", p. 249 - 512 in: Geomagnetism, volume 1, edited by J. A. Jacobs, Academic Press (London).

Langel, R. A., 1992, "International Geomagnetic Reference Field, 1991 revision", Geophysics, 57(7): 956 - 959.

Lankston, Robert W., 1990, "High-resolution refraction seismic data acquisition and interpretation", p. 45 - 73 in: Geotechnical and Environmental Geophysics, volume 1, edited by Stanley H. Ward, Society of Exploration Geophysicists (Tulsa, Oklahoma).

Lankston, Robert W., 1989, "The seismic refraction method: A viable tool for mapping shallow targets into the 1990s", Geophysics, 54(12): 1535 - 1542.

Lasfargues, Pierre, 1957, Prospection Electrique par Courants Continus, in French, Masson (Paris).

Lattin, B. C., 1977, "Continuous pipe-to-soil potential surveys", p. 145 - 149 in: Proceedings of the 22nd Annual Appalachian Underground Corrosion Short Course, West Virginia University (Morgantown, West Virginia).

Layne, Charles, 1995, "Geomagnetism and surveying", Professional Surveyor, 15(2): 38 - 40.

Leao, Jorge W. D., and Joao B. C. Silva, 1989, "Discrete linear transformations of potential field data", Geophysics, 54(4): 497 - 507.

Lee, W. R., 1977, "Lightning injuries and death", p. 521 - 543 in: Lightning, volume 2, edited by R. H. Golde, Academic Press (London).

Leerburger, Benedict A., (editor), 1977, The Battle of Petersburg, Kraus Reprint (Millwood, New York), a part of the Report of the Joint Committee on the Conduct of the War, 1863 - 1866, conducted by the U.S. Congress.

Linington, Richard E., 1963, "The application of geophysics to archaeology", American Scientist, March, p. 48 - 70.

Liu, Ce, and Liang C. Shen, 1991, "Numerical simulation of subsurface radar for detecting buried pipes", IEEE Transactions on Geoscience and Remote Sensing, 29(5): 795 - 798.

Logachev, A. A., and V. P. Zajarov, 1978, Exploracion Magnetica (in Spanish), Editorial Reverte (Barcelona).

Logan, Kirk H., 1945, Underground Corrosion, National Bureau of Standards Circular C450, U. S. Government Printing Office (Washington).

References

Lomnitz, Cinna, and J. Adauto de Souza, 1990, "Discussion on: 'Observations of the air-coupled waves as a function of depth'", Geophysics, 55(6): 791.

Lourenco, Jose Seixas, and H. Frank Morrison, 1973, "Vector magnetic anomalies derived from measurements of a single component of the field", Geophysics, 38(2): 359 - 368.

Low, Steven R., and Roy J. Greenfield, 1990, "Response of a cylindrical target: Implications for ground penetrating radar", p. 424 - 427 in: Expanded Abstracts of the Technical Program, 60th annual international meeting, Society of Exploration Geophysicists (Tulsa, Oklahoma).

Lowry, Tony, and Peter N. Shive, 1990, "An evaluation of Bristow's method for the detection of subsurface cavities", Geophysics, 55(5): 514 - 520.

Maag, Russell C., Jerry M. Sherlin, and Rollin P. Van Zandt, 1976, Observe and Understand the Sun, Astronomical League (Washington).

MacDonald, Edwin A., 1969, Polar Operations, U. S. Naval Institute (Annapolis, Maryland).

MacMahan, Horace, Jr., 1972, Stereogram Book of Contours, Hubbard Press (Northbrook, Illinois).

Macurda, D. Bradford, Jr., and H. Roice Nelson, Jr., "Interactive interpretation of a submarine fan, offshore Ireland: A case history", The Leading Edge, 7(10): 28 - 34.

Mahan, D. H., 1836, A Complete Treatise on Field Fortifications, reprinted 1968 by Greenwood Press (New York).

Mallowan, Agatha Christie, 1974, Come, Tell Me How You Live, Dodd, Mead (New York).

Mannheim, L. A. (principal editor), 1971, The Focal Encyclopedia of Photography, McGraw-Hill (New York).

Manzanilla, L., L. Barba, R. Chavez, A. Tejero, G. Cifuentes, and N. Peralta, 1994, "Caves and geophysics: An approximation to the underworld of Teotihuacan, Mexico", Archaeometry, 36(1): 141 - 157.

Mares, Stanislav, 1984, Introduction to Applied Geophysics, D. Reidel (Dordrecht).

Martin, William A., James E. Bruseth, and Robert J. Huggins, 1991, "Assessing feature function and spatial patterning of artifacts with geophysical remote-sensing data", American Antiquity, 56(4): 701 - 720.

Mason, Randall J., 1984, "An unorthodox magnetic survey of a large forested historic site", Historical Archaeology, 18(2): 54 - 63.

Masuda, Hideo, 1975, Seismic Refraction Analysis for Engineering Study, Oyo Technical Note TN-10, Oyo Corporation (Saitama, Japan).

McGovern, P. J., 1981, "The Baqah Valley, Jordan: Test soundings of cesium magnetometer anomalies", MASCA Journal, 1(7): 214 - 217.

McIntosh, Patrick S., and Murray Dryer, 1972, Solar Activity Observations and Predictions, MIT Press (Cambridge, Massachusetts).

McPherron, Alan, and Elizabeth K. Ralph, 1970, "Magnetometer location of Neolithic houses in Yugoslavia", Expedition, 12(2): 10 - 17.

McManamon, Francis P., 1984, "Discovering sites unseen", p. 223 - 292 in: Advances in Archaeological Method and Theory, vol. 7, edited by Michael B. Schiffer, Academic Press (New York).

McNeill, J. D., 1980, Electromagnetic Terrain Conductivity Measurement at Low Induction Numbers, Technical note TN-6, Geonics Limited (Mississauga, Ontario).

McNeill, J. D., and V. F. Labson, 1991, "Geological mapping using VLF radio fields", p. 521 - 640 in: Electromagnetic Methods in Applied Geophysics, volume 2, edited by Misac N. Nabighian, Society of Exploration Geophysicists (Tulsa, Oklahoma).

References

Meek, John W., 1973, "Three-dimensional model - Gulf of Mexico", Geophysics, 38(2): 295 - 300.

Miller, Francis Trevelyan (editor), 1957, Forts and Artillery, The Photographic History of the Civil War, reprint by Castle Books (New York).

Milsom, John, 1989, Field Geophysics, Wiley (New York).

Mironov, V. S., 1980, Kurs Gravirazvedki (in Russian), Nedra (Moscow); also translated into Spanish as: Curso de Prospeccion Gravimetrica, Editorial Reverte (Barcelona).

Mixon, R. B., C. R. Berquist, Jr., W. L. Newell, G. H. Johnson, D. S. Powars, J. S. Schindler, and E. K. Rader, 1989, Geological map and generalized cross sections of the coastal plain and adjacent parts of the piedmont, Virginia, U. S. Geological Survey Map I-2033 (Denver, Colorado).

Moik, Johannes G., 1980, Digital Processing of Remotely Sensed Images, National Aeronautics and Space Administration SP-431, U. S. Government Printing Office (Washington).

Molano, C. E., M. Salamanca, and R. A. van Overmeeren, 1990, "Numerical modelling of standard and continuous vertical electrical soundings", Geophysical Prospecting, 38(7): 705 - 718.

Monkhouse, F. J., and H. R. Wilkinson, 1971, Maps and Diagrams, (third edition), Methuen (London).

Mooney, Harold M., 1977, Handbook of Engineering Geophysics, Bison Instruments (Minneapolis, Minnesota).

Moore, R. Woodward, 1952, "Geophysical methods adapted to highway engineering problems", Geophysics, 17(3): 505 - 530.

Morey, Rexford M., 1974, "Continuous subsurface profiling by impulse radar", p. 213 - 232 in: Subsurface Exploration for Underground Excavation and Heavy Construction, American Society of Civil Engineers (New York).

Morgan, Frank Dale, Janet E. Simms, W. P. Aspinall, and J. B. Shepherd, 1990, "Volume determination of buried sand using DC resistivity: An engineering geophysics case history", p. 470 - 471 in Expanded Abstracts of the Technical Program, 60th annual meeting, Society of Exploration Geophysicists (Tulsa, Oklahoma).

Morrison, Frank, Jose Benavente, C. W. Clewlow, Jr., and R. F. Heizer, 1970, "Magnetometer evidence of a structure within the La Venta Pyramid", Science, 167: 1488 - 1490.

Musgrave, Albert W. (editor), 1967, Seismic Refraction Prospecting, Society of Exploration Geophysicists (Tulsa, Oklahoma).

Nabighian, Misac, (editor), 1987, 1991, Electromagnetic Methods in Applied Geophysics, 3 volumes, Society of Exploration Geophysicists (Tulsa, Oklahoma).

Nelson, Christopher, 1992, Mapping the Civil War, Starwood Publishing (Washington).

Nelson, J. Bradley, 1988, "Calculation of the magnetic gradient tensor from total field gradient measurements and its application to geophysical interpretation", Geophysics, 53(7): 957 - 966.

Newhall, Beaumont, 1969, Airborne Camera, Hastings House (New York).

Oimoen, Daniel C., 1987, "Evaluation of a tablet digitizer for analytical photogrammetry", Photogrammetric Engineering and Remote Sensing, 53(6): 601 - 603.

Olhoeft, Gary R., 1988, "Selected bibliography on ground penetrating radar", p. 462 - 520 in: Symposium on the Application of Geophysics to Engineering and Environmental Problems, Society of Engineering and Mineral Exploration Geophysicists (Golden, Colorado).

Olsen, Herbert, 1954, Dating the Destruction of the Taylor House, National Park Service, report on file at the Petersburg National Battlefield.

References

Orellana, Ernesto, 1982, Prospeccion Geoelectrica en Corriente Continua, (in Spanish), Paraninfo (Madrid).

Orellana, Ernesto, 1973, Prospeccion Geoelectrica por Campos Variables, (in Spanish), Paraninfo (Madrid).

Orellana, Ernesto, and Harold M. Mooney, 1972, Two and Three Layer Master Curves and Auxiliary Point Diagrams for Vertical Electrical Sounding using Wenner Arrangement, Interciencia (Madrid).

Palfrey, Francis Winthrop, 1878, Memoir of William Francis Bartlett, Houghton, Osgood (Boston).

Palmer, Derecke, 1986, Refraction Seismics, Geophysical Press (London).

Pan, Jeng-Jong, 1989, "Spectral analysis and filtering techniques in digital spatial data processing", Photogrammetric Engineering and Remote Sensing, 55(8): 1203 - 1207.

Pan, Jeng-Jong, and Julia O. Domingue, 1990, "Differentiator design and performance for edge sharpening", Photogrammetric Engineering and Remote Sensing, 56(5): 573 - 578.

Parasnis, D. S., 1986, Principles of Applied Geophysics, fourth edition, Chapman and Hall (London).

Park, S. K., and G. P. Van, 1991, "Inversion of pole-pole data for 3-D resistivity structure beneath arrays of electrodes", Geophysics, 56(7): 951 - 960.

Parker, Thomas H., 1869, History of the 51st Regiment of P.V. and V.V., King and Baird (Philadelphia).

Parkinson, W. D., 1983, Introduction to Geomagnetism, Elsevier (Edinburgh).

Paterson, Norman R., and Colin V. Reeves, 1985, "Applications of gravity and magnetic surveys: The state-of-the-art in 1985", Geophysics, 50(12): 2558 - 2594.

Patra, H. P., and K. Mallick, 1980, Geosounding Principles, 2, Time-Varying Geoelectric Soundings, Elsevier (Amsterdam).

Pattantyus-A., M., 1986, "Geophysical results in archaeology in Hungary", Geophysics, 51(3): 561 - 567.

Peddie, Norman W., 1983, "International geomagnetic reference field - Its evolution and the difference in total field intensity between new and old models for 1965 - 1980", Geophysics, 48(12): 1691 - 1696.

Pelton, W. H., L. Rijo, and C. M. Swift, Jr., 1978, "Inversion of two-dimensional resistivity and induced-polarization data", Geophysics, 43(4): 788 - 803.

Perla, Ronald I., and M. Martinelli, Jr., 1976, Avalanche Handbook, U. S. Department of Agriculture, Agriculture Handbook 489, U. S. Government Printing Office (Washington).

Peschel, G., 1967, "A new favourable combination of resistivity sounding and profiling in archaeological surveying", Prospezioni Archeologiche, 2: 23 - 28.

Peters, Leon, Jr., and Jonathan D. Young, 1986, "Applications of subsurface transient radar", p. 296 - 351 in: Time-Domain Measurements in Electromagnetics, edited by Edmund K. Miller, Van Nostrand Reinhold (New York).

Petersen, Carol A., 1992, "Publicly available mapping programs and test data sets", Geobyte, 7(3): 22 - 23.

Petkov, A. T., M. I. Georgiev, D. H. Georgiev, and M. K. Kanartchev, 1989, "Geophysical prospecting of 'Zelenka' Tumulus", p. 427 - 434 in: Archaeometry, edited by Y. Maniatis, Elsevier (Amsterdam).

Porkert, Manfred, 1974, "When lenses steam up", Leica Fotografie, 3: 117, 119.

Powers, Michael H., Steven K. Duke, Arlie C. Huffman III, and Gary R. Olhoeft, 1992, GPRmodel: One-Dimensional Full Waveform Forward

Modeling of Ground Penetrating Radar Data, Open File Report 92-532, U. S. Geological Survey (Denver, Colorado).

Press, Frank, 1966, "Seismic velocities", p. 195 - 218 in: Handbook of Physical Constants, revised edition, edited by Sydney P. Clark, Jr., Geological Society of America (New York).

Probstein, Ronald F., and R. Edwin Hicks, 1993, "Removal of contaminants from soils by electric fields", Science, 260: 498 - 503.

Professional Surveyor, 1986, "Living with hostile weather", Professional Surveyor, 6(5): 6, 9 - 12.

Professional Surveyor, 1992, "Keeping an eye on safety", Professional Surveyor, 12(3): 10 - 13.

Pullan, S. E., J. A. Hunter, and K. G. Neave, 1990, "Shallow shear-wave reflection tests", p. 380 - 382 in: Expanded Abstracts of the Technical Program, 60th annual international meeting, Society of Exploration Geophysicists (Tulsa, Oklahoma).

Rainey, Froelich, 1969, "The location of archaic Greek Sybaris", American Journal of Archaeology, 73: 260 - 273.

Rainey, Froelich, 1992, Reflections of a Digger, University of Pennsylvania Museum (Philadelphia).

Ralph, E. K., 1973, "Magnetometer survey at Malkata, Egypt", MASCA Newsletter, 9(2): 3 - 5.

Randi, James, 1980, Flim-Flam, Lippincott and Crowell (New York).

Rangarajan, G. K., 1989, "Indices of geomagnetic activity", p. 323 - 384 in: Geomagnetism, volume 3, edited by J. A. Jacobs, Academic Press (London).

Rao, D. Bhaskara, and N. Ramesh Babu, 1991, "A rapid method for three-dimensional modeling of magnetic anomalies", Geophysics, 56(11): 1729 - 1737.

Ray, Richard D., 1985, "Correction of systematic error in magnetic surveys: An application of ridge regression and sparse matrix theory", Geophysics, 50(11): 1721 - 1731.

Redpath, Bruce B., 1973, Seismic Refraction Exploration for Engineering Site Investigations, National Technical Information Service AD-768 710, U. S. Department of Commerce (Springfield, Virginia).

Reid, A. B., 1980, "Aeromagnetic survey design", Geophysics, 45(5): 973 - 976.

Reiter, E. C., M. N. Toksoz, and G. M. Purdy, 1993, "A semblance-guided median filter", Geophysical Prospecting, 41(1): 15 - 41.

Riddihough, R. P., 1971, "Diurnal corrections to magnetic surveys - An assessment of errors", Geophysical Prospecting, 19(4): 551 - 567.

Ritter, Paul, 1987, "A vector-based slope and aspect generation algorithm", Photogrammetric Engineering and Remote Sensing, 53(8): 1109 - 1111.

Roberts, Roger, Jeffrey J. Daniels, and Mark Vendl, 1991, "Seasonal variations and ground-penetrating radar data repeatability", p. 486 - 489 in: Expanded Abstracts of the Technical Program, 61st international meeting, Society of Exploration Geophysicists (Tulsa, Oklahoma).

Robinson, Edwin S., and Cahit Coruh, 1988, Basic Exploration Geophysics, Wiley (New York).

Roemer, Jacob, 1897, Reminiscences of the War of the Rebellion, estate of Jacob Roemer (Flushing, NY).

Roest, Walter R., and Mark Pilkington, 1993, "Identifying remanent magnetization effects in magnetic data", Geophysics, 58(5): 653 - 659.

Roest, Walter R., Jacob Verhoef, and Mark Pilkington, 1992, "Magnetic interpretation using the 3-D analytic signal", Geophysics, 57(1): 116 - 125.

Ronne, Finn, 1961, Antarctic Command, Bobbs-Merrill (Indianapolis).

References

Roosevelt, Anna Curtenius, 1991, Moundbuilders of the Amazon, Academic Press (San Diego, California).

Rosendahl, Bruce R., 1984, "The Nyanja chronicles", The Leading Edge, 3(2): 18 - 24.

Rosenfeld, Azriel, and Avinash C. Kak, 1976, Digital Picture Processing, Academic Press (New York).

Roy, A., and A. Apparao, 1971, "Depth of investigation in direct current methods", Geophysics, 36(5): 943 - 959.

Rudloff, Willy, 1981, World-Climates, Wissenschaftliche Verlagsgesellschaft (Stuttgart).

Sakayama, Toshihiko, and Tetsuo Hara, 1982, "Subsurface exploration using ground probing radar, #2, WARR sounding", paper presented at the fall meeting of the Society of Exploration Geophysicists of Japan (Sapporo).

Sandberg, Stewart K., 1990, Microcomputer Software for Individual or Simultaneous Inverse Modeling of Transient Electromagnetic, Resistivity, and Induced Polarization Soundings, Open-File Report 90-1, New Jersey Geological Survey (Trenton, New Jersey).

Saraoja, E. K., 1977, "Lightning earths", p. 577 - 598 in: Lightning, volume 2, edited by R. H. Golde, Academic Press (London).

Schwertmann, U., 1988, "Occurrence and formation of iron oxides in various pedoenvironments", p. 267 - 308 in: Iron in Soils and Clay Minerals, edited by J. W. Stucki, B. A. Goodman, and U. Schwertmann, D. Reidel (Dordrecht).

Scollar, Irwin, A. Tabbagh, A. Hesse, and I. Herzog, 1990, Archaeological Prospecting and Remote Sensing, Cambridge University Press (Cambridge).

Scott, James H., and Richard D. Markiewicz, 1990, "Dips and chips: PC programs for analyzing seismic refraction data", p. 175 - 200 in: Symposium on the Application of Geophysics to Engineering and Environmental Problems, Society of Engineering and Mineral Exploration Geophysicists (Golden, Colorado).

Scott, Stuart D., Patricia Kay Scott, James W. F. Smith, and James MacLeay, 1991, "Reorientation of historical maps of Old Fort Niagara using computer-assisted cartography", Journal of Field Archaeology 18(3): 319 - 343.

Shaffer, Gary D., 1993, "An archaeomagnetic study of a wattle and daub building collapse", Journal of Field Archaeology, 20(1): 59 - 75.

Shapiro, Gary, 1984, "A soil resistivity survey of 16th-century Puerto Real, Haiti", Journal of Field Archaeology, 11(1): 101 - 110.

Sharma, P. V., 1986, Geophysical Methods in Geology, second edition, Elsevier (New York).

Sheriff, Robert E., 1989, Geophysical Methods, Prentice Hall (Englewood Cliffs, New Jersey).

Shima, Hiromasa, 1990, "Two-dimensional automatic resistivity inversion technique using alpha centers", Geophysics, 55(6): 682 - 694.

Siegel, Frederic R., 1974, Applied Geochemistry, Wiley-Interscience (New York).

Simms, J. E., and F. D. Morgan, 1992, "Comparison of four least-squares inversion schemes for studying equivalence in one-dimensional resistivity interpretation", Geophysics, 57(10): 1282 - 1293.

Sinnott, Roger W., 1989, "A jam-jar magnetometer as 'aurora detector'", Sky and Telescope, (October), p. 426 - 432.

Sirles, Phil C., and Andy Viksne, 1990, "Site-specific shear wave velocity determinations for geotechnical engineering applications", p. 121 - 131 in: Geotechnical and Environmental Geophysics, volume 3, edited by Stanley H. Ward, Society of Exploration Geophysicists (Tulsa, Oklahoma).

References

Sjogren, Bengt, 1984, Shallow Refraction Seismics, Chapman and Hall (London).

Skomal, Edward N., 1978, Man-Made Radio Noise, Van Nostrand Reinhold (New York).

Smekalova, T. N., 1994, "The use of magnetic prospecting in archaeology", notes for the course: Remote Sensing/Geophysical Techniques for Cultural Resource Management, edited by Steven L. De Vore, National Park Service (Denver, Colorado).

Smekalova, T. N., and A. A. Maslennikov, 1993, "Cadaster of geophysical maps of Bospor sites in the coast of Asov Sea", p. 27 - 35 in: Geophysical Exploration of Archaeological Sites, edited by Andreas Vogel and Gregory N. Tsokas, Vieweg (Wiesbaden).

Smekalova, T. N., V. L. Myts, and A. V. Melnikov, 1993, "Magnetometric investigation of medieval pottery centers in the mountainous Crimea", p. 37 - 44 in: Geophysical Exploration of Archaeological Sites, edited by Andreas Vogel and Gregory N. Tsokas, Vieweg Publishing (Wiesbaden).

Spector, A., and B. K. Bhattacharyya, 1966, "Energy density spectrum and autocorrelation function of anomalies due to simple magnetic models", Geophysical Prospecting, 14(3): 242 - 272.

Steponaitis, Vincas P., and Jeffrey P. Brain, 1976, "A portable differential proton magnetometer", Journal of Field Archaeology, 3: 455 - 463.

Strongman, K. B., 1992, "Forensic applications of ground penetrating radar", p. 203 - 211 in: Ground Penetrating Radar, edited by J. Pilon, Paper 90-4, Geological Survey of Canada (Ottawa).

Sumner, J. S., 1976, Principles of Induced Polarization for Geophysical Exploration, Elsevier (Amsterdam).

Swanson, C. O., 1936, "The dip needle as a magnetometer", Geophysics, 1(1): 48 - 96.

Syberg, F. J. R., 1972, "A Fourier method for the regional-residual problem of potential fields", Geophysical Prospecting, 20(1): 47 - 75.

Tabbagh, Alain, 1986, "Applications and advantages of the Slingram electromagnetic method for archaeological prospecting", Geophysics, 51(3): 576 - 584.

Tabbagh, A., 1984, "On the comparison between magnetic and electromagnetic prospection methods for magnetic features detection", Archaeometry, 26(2): 171 - 182.

Tabbagh, Alain, Albert Hesse, and Rejean Grard, 1993, "Determination of electrical properties of the ground at shallow depth with an electrostatic quadrupole: Field trials on archaeological sites", Geophysical Prospecting, 41(5): 579 - 597.

Tagg, G. F., 1964, Earth Resistances, Pitman (New York).

Tarchova, A. G., 1980, Elektrorazvedka, in Russian, Nedra (Moscow).

Taylor, Robert W., and Anthony H. Fleming, 1988, "Characterizing jointed systems by azimuthal resistivity surveys", Ground Water, 26(4): 464 - 474.

Teifke, Robert H., 1973, "Stratigraphic units of the lower Cretaceous through Miocene series", p. 5 - 78 in: Geologic Studies, Coastal Plain of Virginia, Virginia Division of Mineral Resources Bulletin 83 (Charlottesville, Virginia).

Telford, W. M., L. P. Geldart, and R. E. Sheriff, 1990, Applied Geophysics, second edition, Cambridge University Press (Cambridge).

Thomas, Dean S., 1985, Cannons, An Introduction to Civil War Artillery, Thomas Publications (Gettysburg, Pennsylvania).

Thorarinsson, Freyr, Stefan G. Magnusson, and Axel Bjornsson, 1988, "Directional spectral analysis and filtering of geophysical maps", Geophysics, 53(12): 1587 - 1591.

References

Thurston, Jeffrey B., and R. James Brown, 1994, "Automated source-edge location with a new variable pass-band horizontal-gradient operator", Geophysics, 59(4): 546 - 554.

Tibbs, Judith, 1987, "Watch out!", Professional Surveyor, 7(3): 26, 27, 30.

Tidball, John C., 1891, Manual of Heavy Artillery Service, Chapman (Washington).

Timofeev, V. M., A. W. Rogozinski, J. A. Hunter, and M. Douma, 1994, "A new ground resistivity method for engineering and environmental geophysics", p. 701 - 715 in: Symposium on the Application of Geophysics to Engineering and Environmental Problems, Environmental and Engineering Geophysical Society (Englewood, Colorado).

Tinney, Larry R, John R. Jensen, and John E. Estes, 1977, "Mapping archaeological sites from historical photography", Photogrammetric Engineering and Remote Sensing 43(1): 35 - 44.

Tite, M. S., 1972, Methods of Physical Examination in Archaeology, Seminar Press (London).

Toms, Francis R., 1929, A Report Concerning the Historical Fortifications Around Petersburg, University of North Carolina, (Chapel Hill, North Carolina).

Tonouchi, Keiji, Toshihiko Sakayama, and Tsuneo Imai, 1983, "S wave velocity in the ground and the damping factor", p. 327 - 333 in: Bulletin of the International Association of Engineering Geology, number 26 - 27.

Tripp, A. C., G. W. Hohmann, and C. M. Swift, Jr., 1984, "Two-dimensional resistivity inversion", Geophysics, 49(10): 1708 - 1717.

Trudeau, Noah Andre, 1991, The Last Citadel, Little, Brown (Boston).

Tsokas, G. N., A. Giannopoulos, P. Tsourlos, G. Vargemezis, J. M. Tealby, A. Sarris, C. B. Papazachos, and T. Savopoulou, 1994, "A large scale geophysical survey in the archaeological site of Europos (northern Greece)", Journal of Applied Geophysics, 32(1): 85 - 98.

Tsokas, G. N., and R. O. Hansen, 1995, "Comparison of inverse filtering and multiple source Werner deconvolution for model archaeological problems", Archaeometry, 37(1): 185 - 193.

Tsuboi, Chuji, 1983, Gravity, George Allen and Unwin (London).

Tucker, Paul M., 1952, "High magnetic effect of lateritic soil in Cuba", Geophysics, 17(4): 753 - 755.

Turner, Greg, 1994, "Subsurface radar propagation deconvolution", Geophysics, 59(2): 215 - 223.

Ulriksen, C. Peter F., 1982, Application of Impulse Radar to Civil Engineering, doctoral thesis, Lund University of Technology (Lund, Sweden).

Urquhart, Ted, 1988, "Decorrugation of enhanced magnetic field maps", p. 371 - 372 in: Expanded Abstracts of the Technical Program, 58th annual international meeting, Society of Exploration Geophysicists (Tulsa, Oklahoma).

Urquhart, W. E. S., and D. W. Strangeway, 1985, "Interpretation of part of an aeromagnetic survey in the Matagami area of Quebec", p. 426 - 438 in: The Utility of Regional Gravity and Magnetic Anomaly Maps, edited by William J. Hinze, Society of Exploration Geophysicists (Tulsa, Oklahoma).

U.S. Department of Commerce, 1975, Electric Current Abroad, U. S. Government Printing Office (Washington).

Vacquier, Victor, 1972, Geomagnetism in Marine Geology, Elsevier (Amsterdam).

van Dam, J. D., and J. J. Meulenkamp, 1975, Standard Graphs for Resistivity Prospecting, Swets and Zeitlinger (Lisse, The Netherlands).

References

Van Nostrand, Robert G., and Kenneth L. Cook, 1966, Interpretation of Resistivity Data, U. S. Geological Survey Professional Paper 499, U. S. Government Printing Office (Washington).

van Overmeeren, R. A., and I. L. Ritsema, 1988, "Continuous vertical electrical sounding", First Break, 6(10): 313 - 324.

Van Santvoord, C., 1894, The One Hundred and Twentieth Regiment New York State Volunteers, Kingston Freeman (Rondout, New York).

Vodjanitskij, Ju. N., 1981, "The formation of ferromagnetics in turf-podzol soils", (in Russian), Pochvovedenie, 5: 114 - 123.

Vogt, Evon Z., and Ray Hyman, 1959, Water Witching U.S.A., University of Chicago Press (Chicago).

Volunteers in Technical Assistance, 1975, Village Technology Handbook, VITA (Mt. Rainier, Maryland).

Wait, James R., 1971, Electromagnetic Probing in Geophysics, Golem Press (Boulder, Colorado).

Wait, James R., 1982, Geo-Electromagnetism, Academic Press (New York).

Wait, James R., 1983, "Resistivity response of a homogeneous earth with a contained vertical conductor", IEEE Transactions on Geoscience and Remote Sensing, 21(1): 109 - 113.

Wallace, Lee A., Jr., 1954, "Study of the Taylor House Remains", report at the Petersburg National Battlefield.

Wallace, Lee A., Jr., 1956 (approximate) History of Petersburg National Military Park, National Park Service, undated report at the Petersburg National Battlefield. Ward, Stanley H., 1990, "Resistivity and induced polarization methods", p. 147 - 189 in: Geotechnical and Environmental Geophysics, vol. 1, edited by Stanley H. Ward, Society of Exploration Geophysicists (Tulsa, Oklahoma).

Watkins, Joel S., Richard H. Godson, and Kenneth Watson, 1967, Seismic Detection of Near-Surface Cavities, U. S. Geological Survey Professional Paper 599-A, U.S. Government Printing Office (Washington).

Webster, J. G., (editor), 1990, Electrical Impedance Tomography, Adam Hilger (Bristol).

Wensink, W. A., J. Hofman, and J. K. Van Deen, 1991, "Measured reflection strengths of underwater pipes irradiated by a pulsed horizontal dipole in air: Comparison with continuous plane-wave scattering theory", Geophysical Exploration, 39(4): 543 - 566.

Weymouth, John W., 1986, "Geophysical methods of archaeological site surveying", p. 311 - 396 in: Advances in Archaeological Method and Theory, edited by Michael B. Schiffer, Academic Press (New York).

Weymouth, J. W., and Y. A. Lessard, 1986, "Simulation studies of diurnal corrections for magnetic prospection", Prospezioni Archeologiche, 10: 37 - 47.

Weymouth, John W., and Robert Nickel, 1977, "A magnetometer survey of the Knife River Indian villages", Plains Anthropologist, memoir 13, p. 104 - 118.

Weymouth, John W., and Robert Huggins, 1985, "Geophysical surveying of archaeological sites", p. 191 - 235 in Archaeological Geology, edited by George Rapp, Jr., and John A. Gifford, Yale University Press (New Haven, Connecticut).

Whalen, Michael E., 1990, "Defining buried features before excavation: A case from the American southwest", Journal of Field Archaeology 17(3): 323 - 331.

Whitwell, J. B., and K. F. Wood, 1969, "Three pottery kiln sites in Lincolnshire, located by proton gradiometer (Maxbleep) survey and confirmed by excavation", Prospezioni Archeologiche, (4): 125 - 129.

Wilkinson, Warren, 1990, Mother, May You Never See the Sights I Have Seen, Harper Collins (New York).

References

Williams, J. C. C., 1969, Simple Photogrammetry, Academic Press (London).

Williams, J. Mark, 1984, "A new resistivity device", Journal of Field Archaeology, 11(1): 110 - 114.

Williamson, James R., and Michael H. Brill, 1990, Dimensional Analysis Through Perspective, Kendall/Hunt (Dubuque, Iowa).

Wilson, D. R. (editor), 1975, Aerial Reconnaissance for Archaeology, Research Report Number 12, Council for British Archaeology (London).

Wilson, John H., 1931, "Brunton compass attachment for measurement of horizontal magnetic intensity", Transactions of the Society of Petroleum Geophysicists, 15(11, 12): 1391 - 1397.

Wolf, Paul R., 1974, Elements of Photogrammetry, McGraw-Hill (New York).

Won, I. J., and Michael Bevis, 1987, "Computing the gravitational and magnetic anomalies due to a polygon: Algorithms and Fortran subroutines", Geophysics, 52(2): 232 - 238.

Woodbury, Augustus, 1867, Major General Ambrose E. Burnside and the Ninth Army Corps, Sidney S. Rider (Providence, Rhode Island).

Wren, A. E., 1975, "Contouring and the contour map: A new perspective", Geophysical Prospecting, 23(1): 1 - 17.

Wright, James L., 1988, VLF Interpretation Manual, EDA Instruments (Toronto, Canada).

Wright, Winfield G., and John D. Powell, 1990, "Preliminary investigation of soil and ground-water contamination at a U.S. Army petroleum training facility, Fort Lee, Virginia, September - October 1989", U. S. Geological Survey Open File Report 90-387, (Denver, Colorado).

Wynn, Jeffrey C., and Susan I. Sherwood, 1984, "The self-potential (SP) method: An inexpensive reconnaissance and archaeological mapping tool", Journal of Field Archaeology, 11(2): 195 - 204.

Yakubovski, U. V., and L. L. Lyachov, 1988, Elektrorazvedka, in Russian, Nedra (Moscow); also in Spanish as Exploracion Electrica from Editorial Reverte (Barcelona).

Yarger, Harold L., Robert R. Robertson, and Robert L. Wentland, 1978, "Diurnal drift removal from aeromagnetic data using least squares", Geophysics, 43(6): 1148 - 1156.

Zietz, Isidore, 1982, Composite Magnetic Anomaly Map of the United States, Map GP-954A, U. S. Geological Survey (Denver, Colorado).

Zohdy, A. A. R., 1989, "A new method for the automatic interpretation of Schlumberger and Wenner sounding curves", Geophysics, 54(2): 245 - 253.

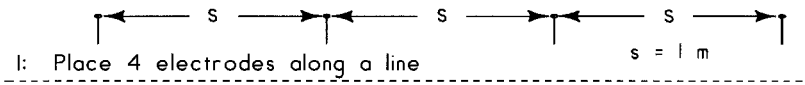

1: Place 4 electrodes along a line

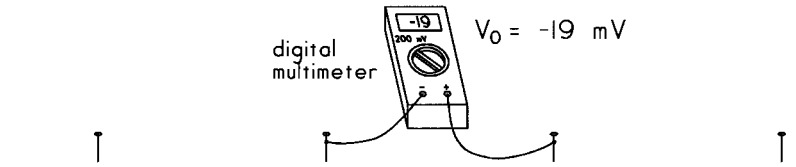

2: Measure the voltage between the middle pair of electrodes

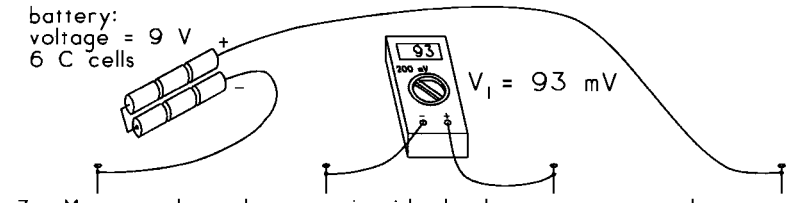

3: Measure the voltage again with the battery connected

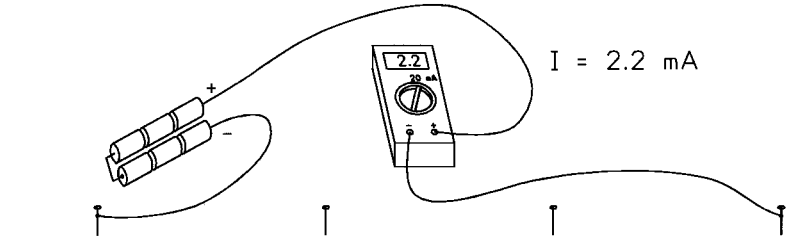

4: Measure the current between the outer pair of electrodes

5: Calculate resistance $R = \frac{V_1 - V_0}{I} = \frac{93 - (-19)}{2.2} = 51$ ohm

6: Calculate resistivity $\rho = 2\pi s\ R = 2\ (3.14)\ 1\ (51) = 320$ ohm-m

Fig. B1: A do-it-yourself resistivity meter. While this meter is very inexpensive, it will give you good measurements even though it is slow to operate.

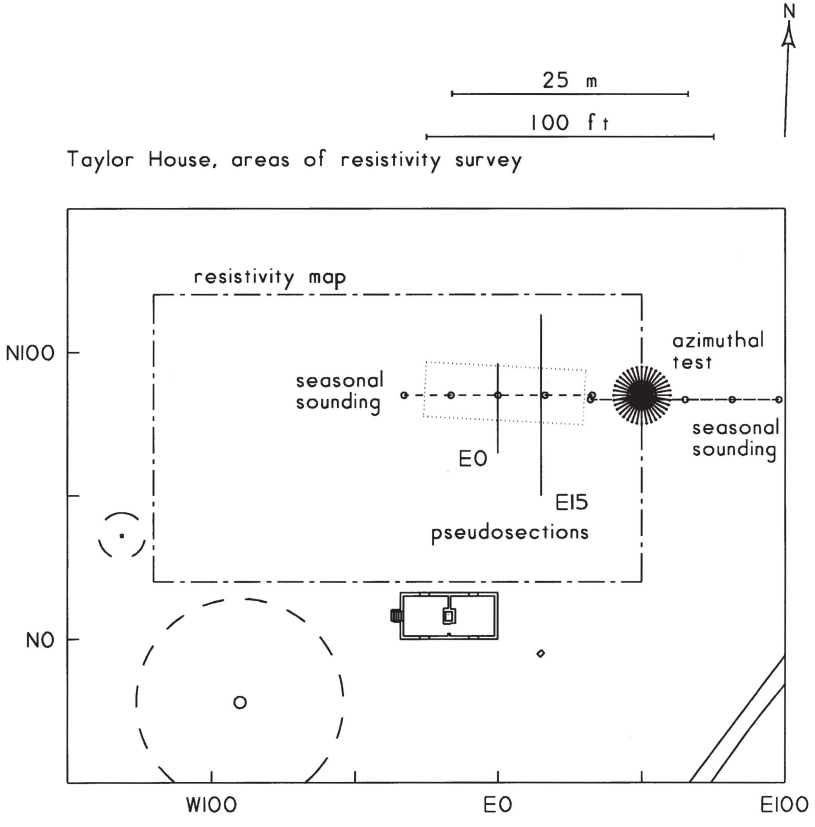

Fig. B2: The areas of resistivity survey near the Taylor House. The foundation of the cellar is marked with a dotted line. The brick shell of the Taylor kitchen is on the south side of the grid.

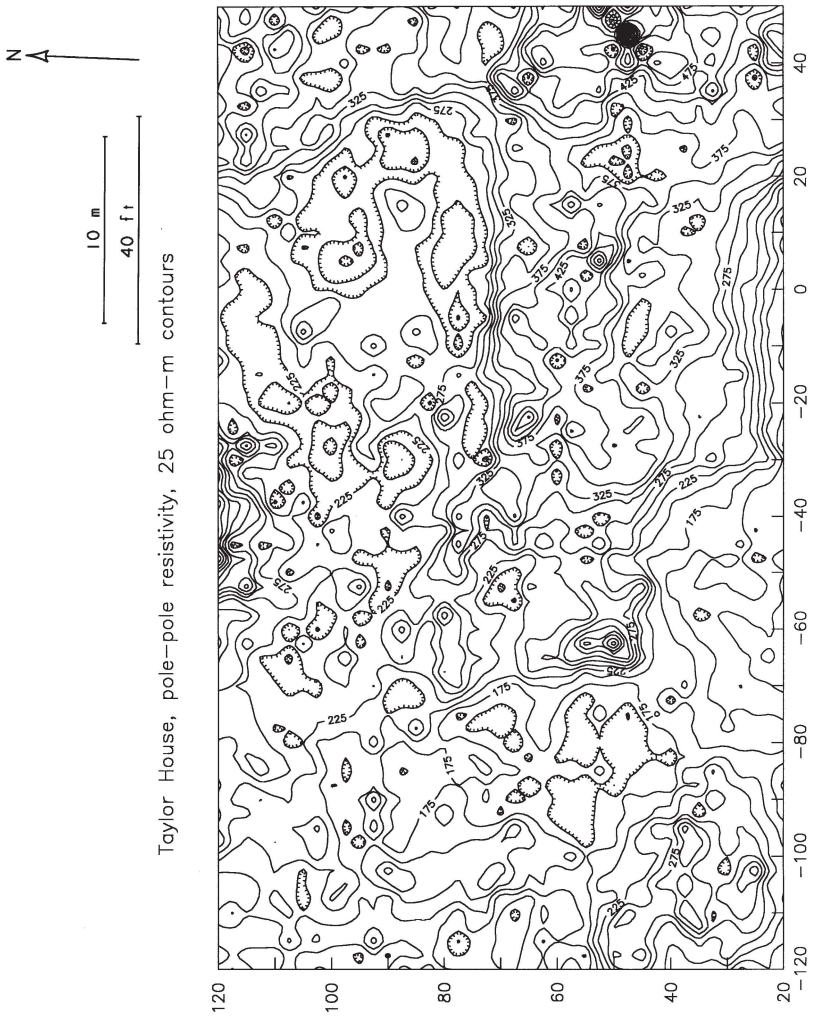

Fig. B3: The electrical resistivity of the soil at the Taylor House. It was measured with an electrode spacing of 5 ft (1.5 m).

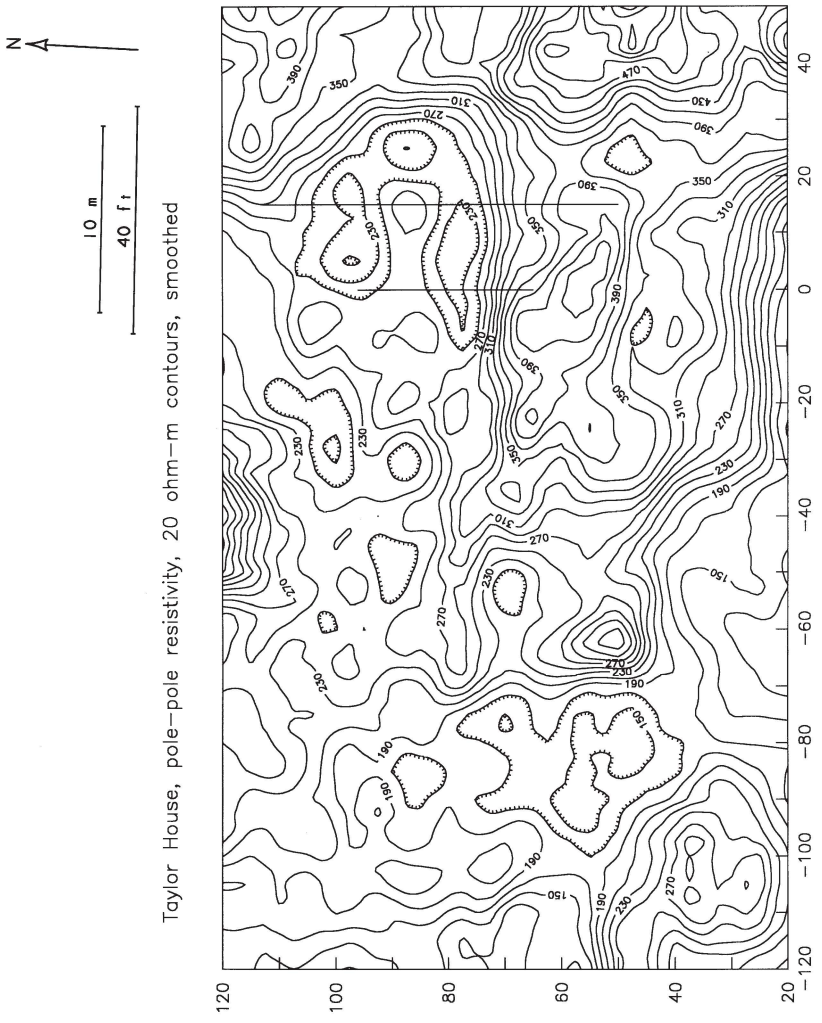

Fig. B4: A smoothed resistivity map. The eastern side of the Taylor House cellar is an arc of low resistivity near E10 N85.

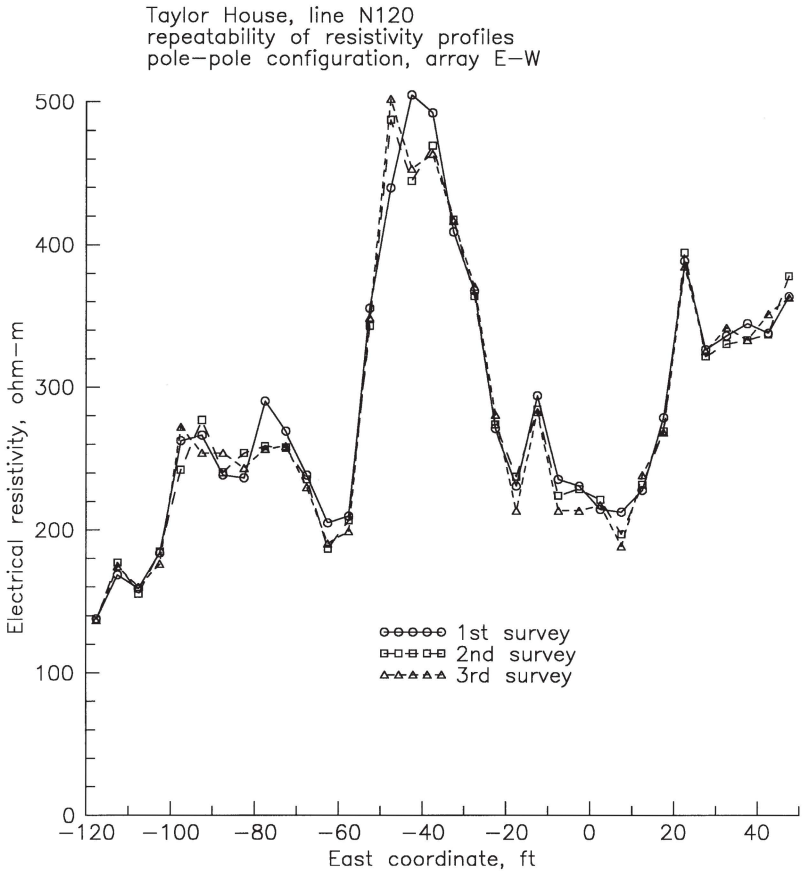

Fig. B5: An indication of the errors of resistivity measurement. The same line was measured three times.

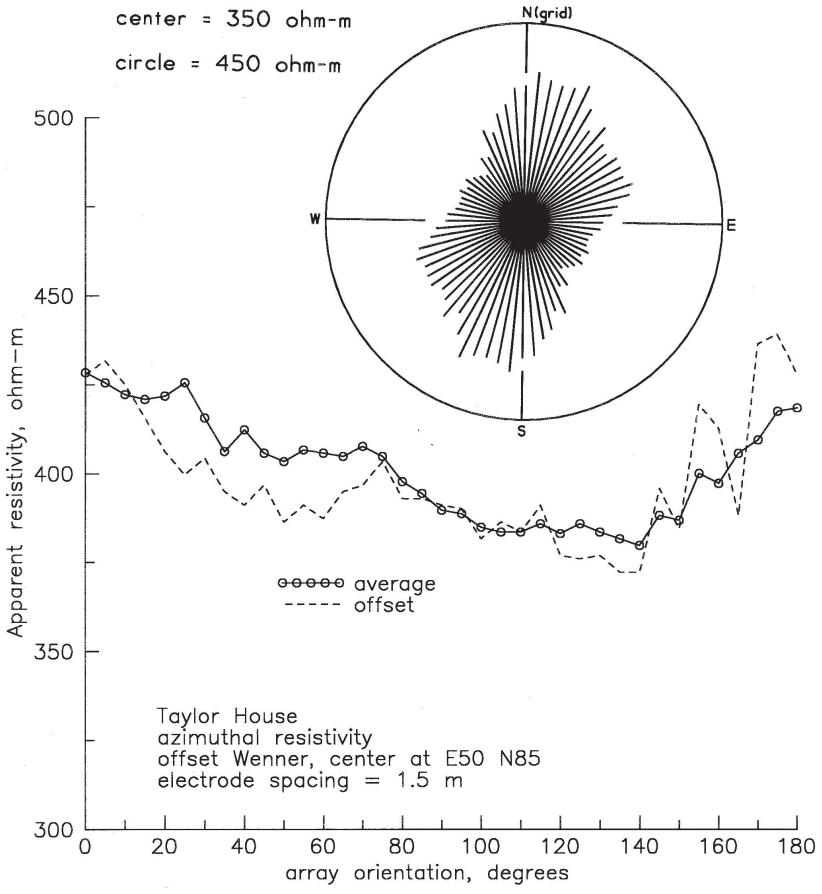

Fig. B6: Directional changes in electrical resistivity. It is highest with the array in a north-south direction.

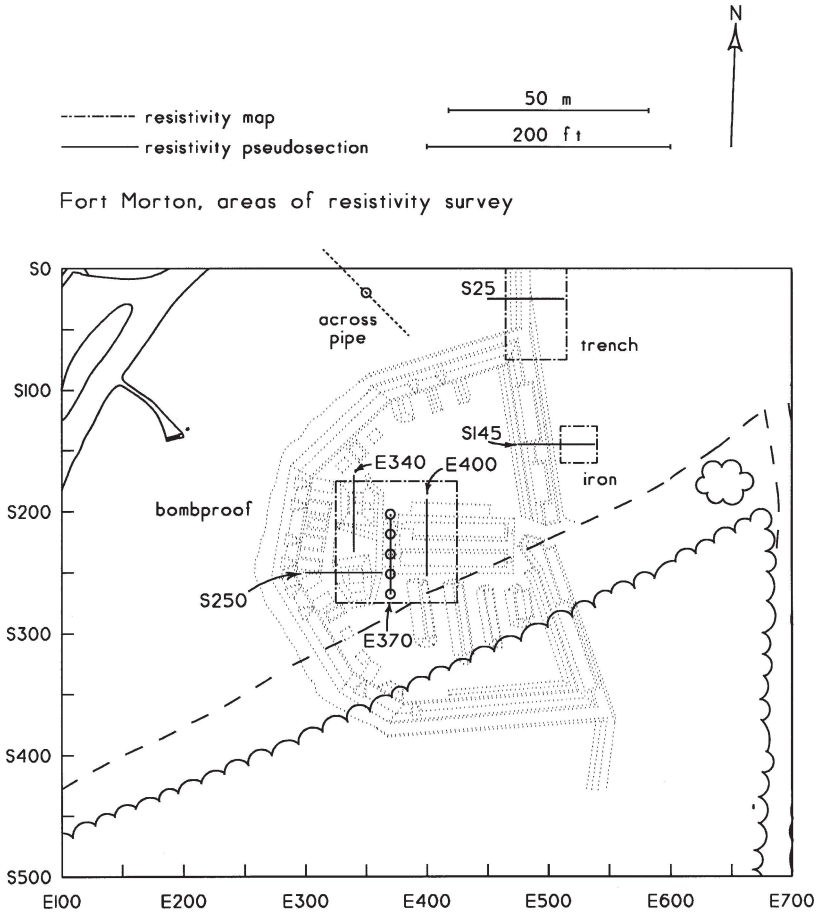

Fig. B7: The locations of the different resistivity surveys in the area of Fort Morton.

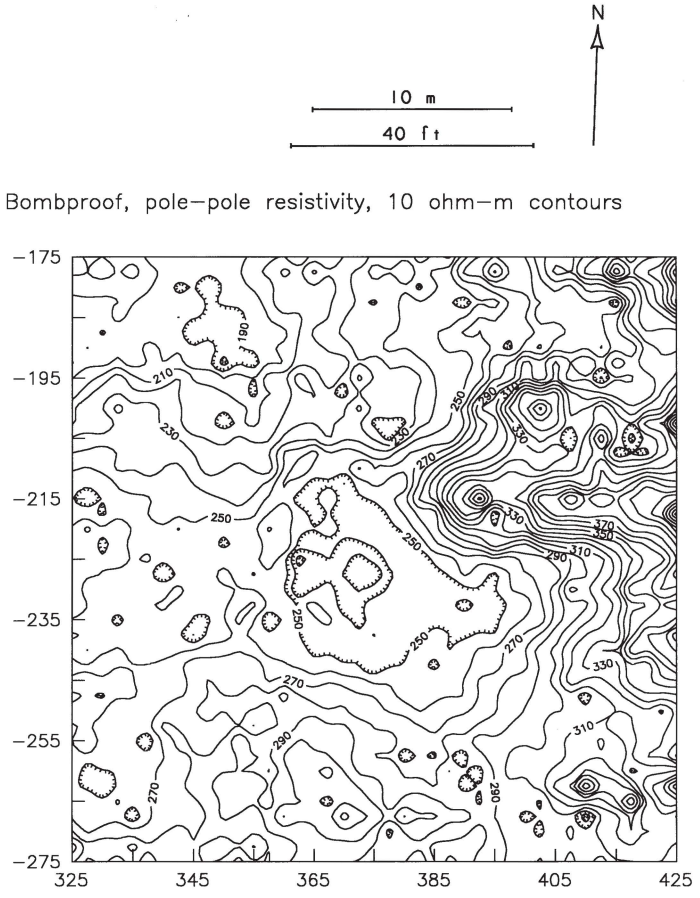

Fig. B8: The electrical resistivity of the Bombproof detail. The spacing between electrodes was 5 ft (1.5 m). One of the trenches causes the east-west line of high resistivity near S215.

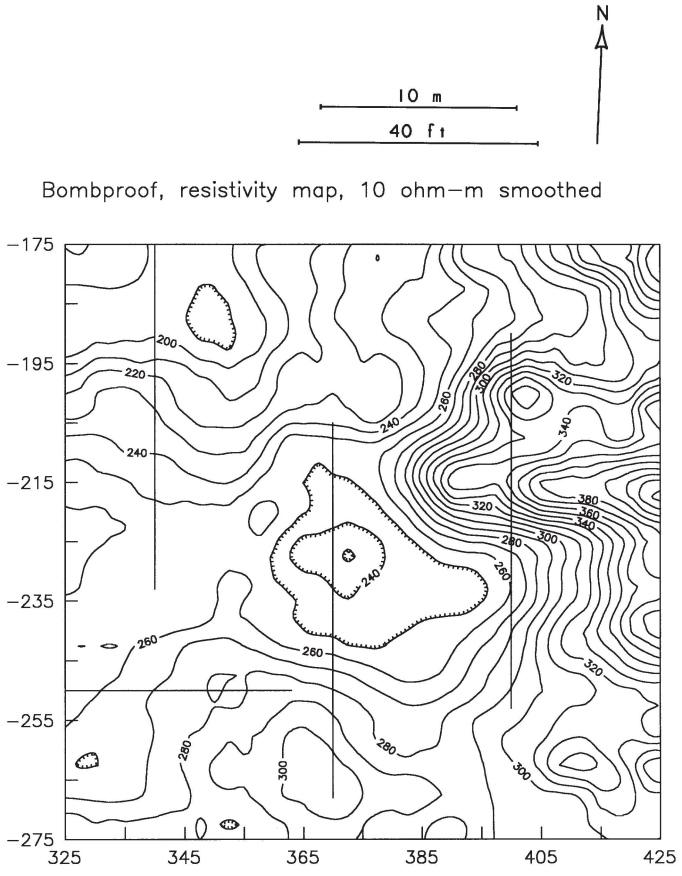

Fig. B9: A smoothed resistivity map of the Bombproof detail. It reveals the patterns more clearly. The straight lines mark the span of resistivity pseudosections.

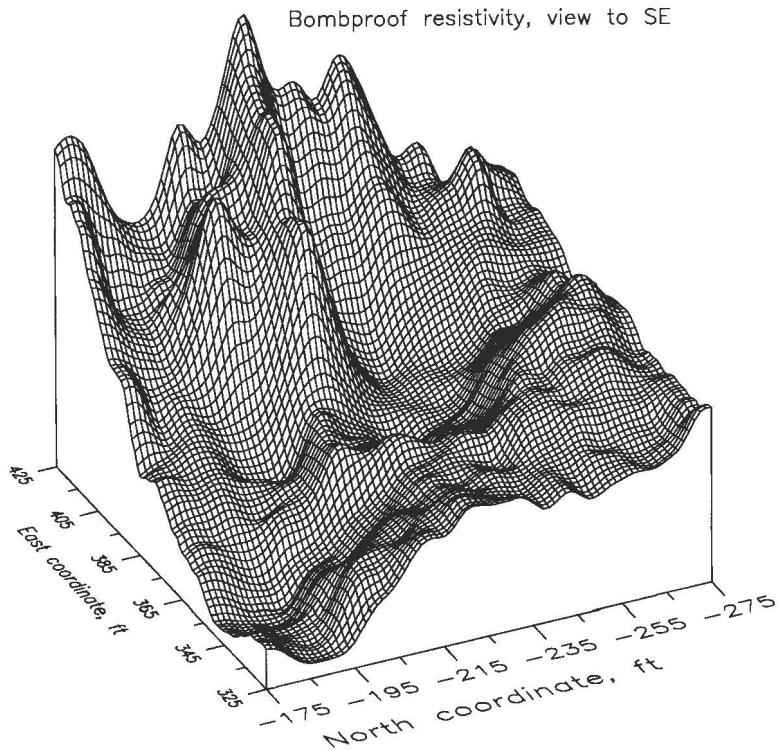

Fig. B10: A surface map of electrical resistivity. The major ridge in the background marks the line of one of the trenches of the bombproof.

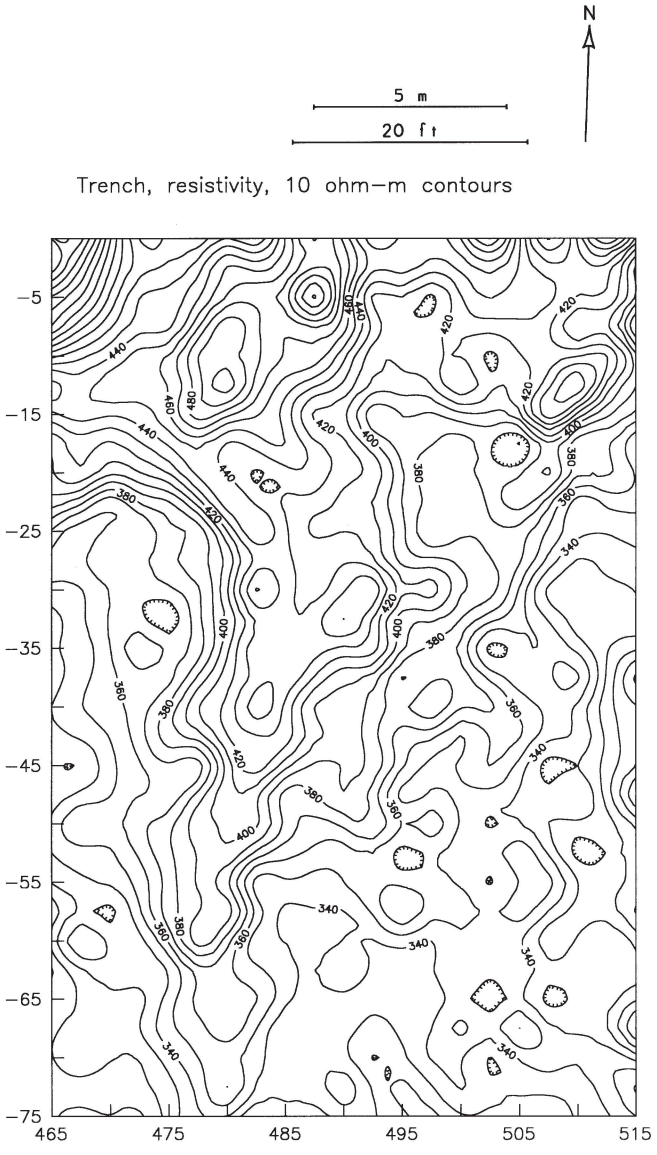

Fig. B11: A pole-pole resistivity map of the Trench detail.

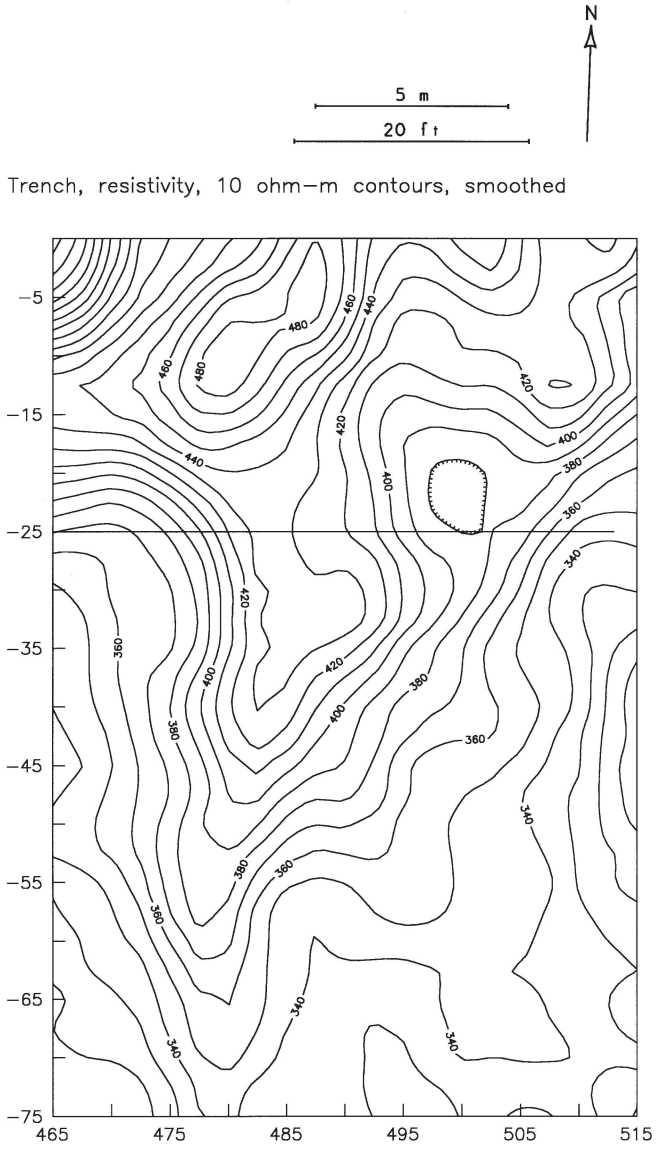

Fig. B12: A smoothed map of the Trench detail. It shows a line of high resistivity along the main fortification trench at E480.

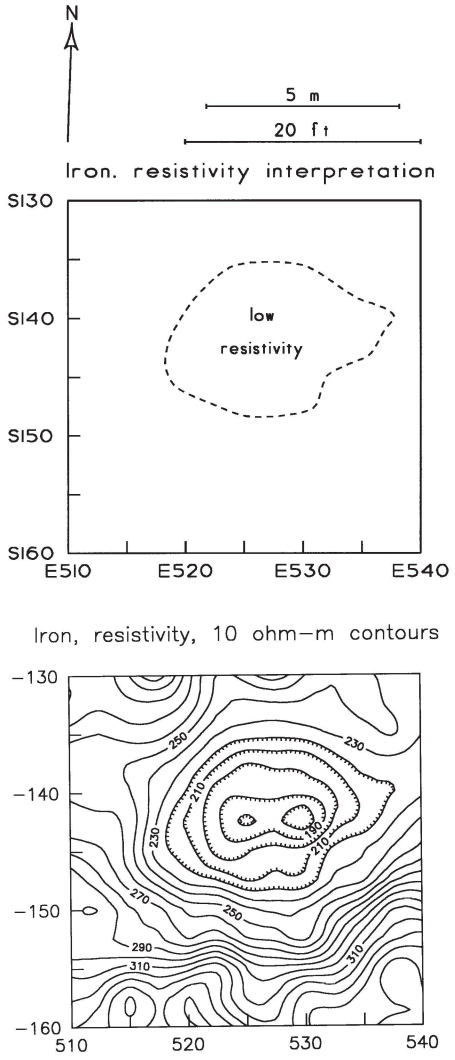

Fig. B13: A resistivity low centered on the massive iron object.

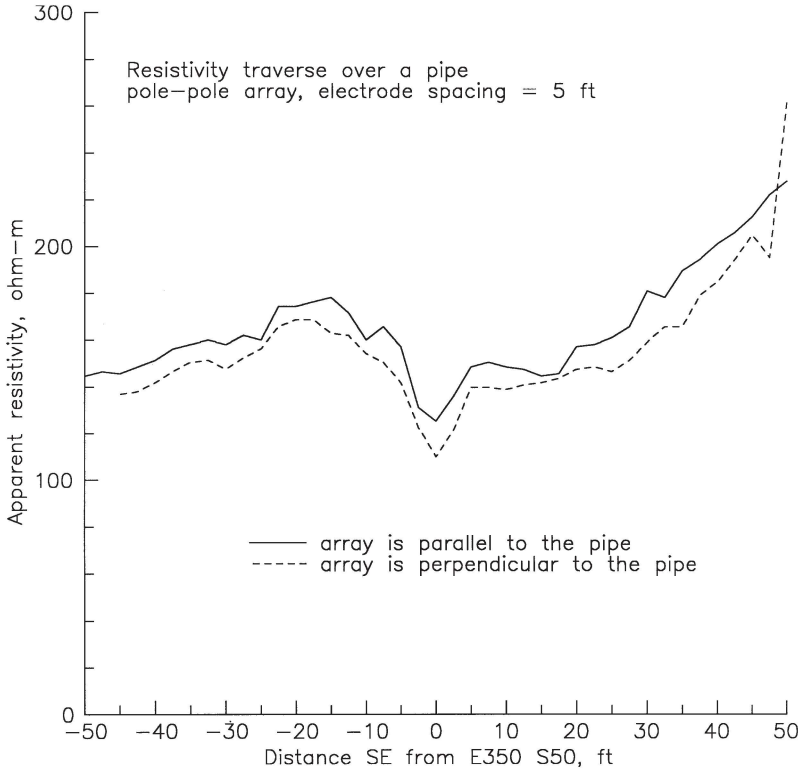

Fig. B14: Resistivity profiles over a pipe. The pipe crosses perpendicular to the survey line at the zero point and it gives a weak low resistivity.

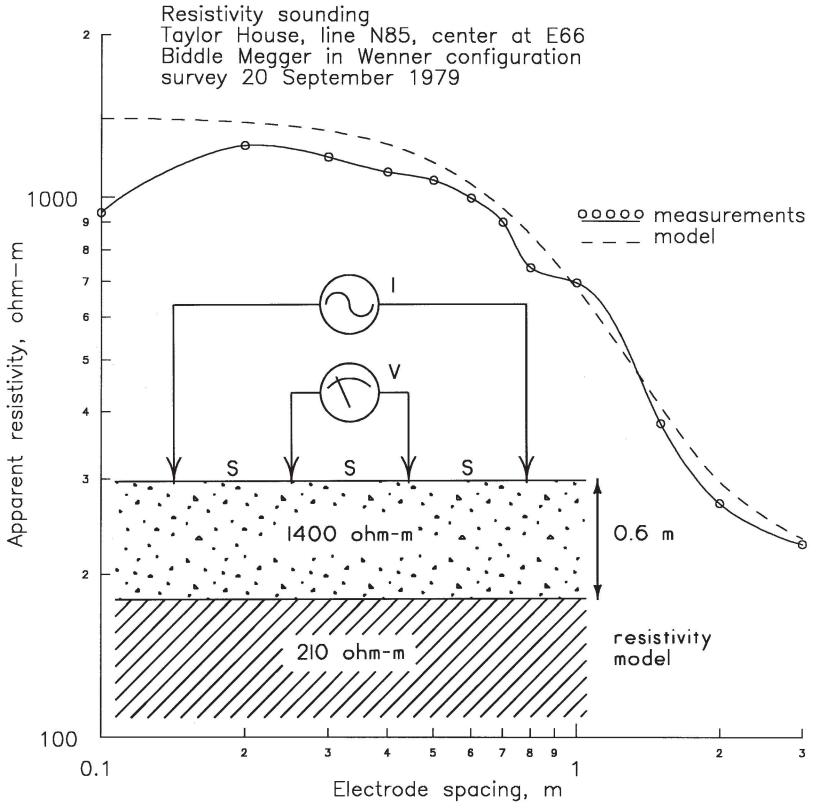

Fig. B15: The first resistivity sounding at the site, and its analysis. The measurements show that there are only two distinct soil layers; the upper layer is about 0.6 m thick and is very sandy.

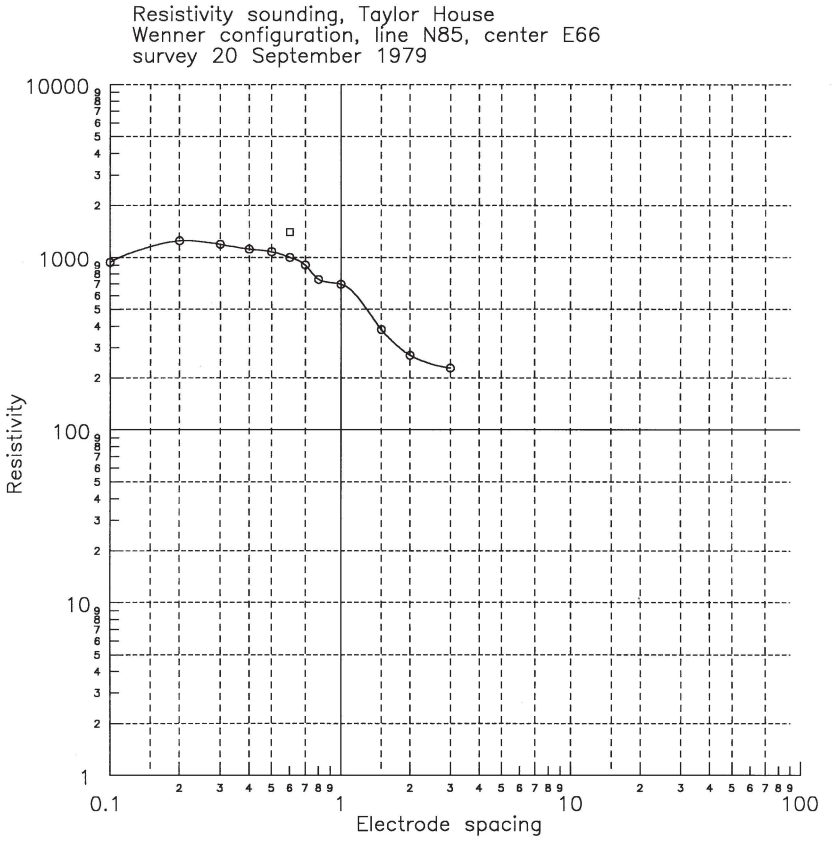

Fig. B16: Another resistivity plot. The measurements shown in Fig. B15 are replotted on a standard graph.

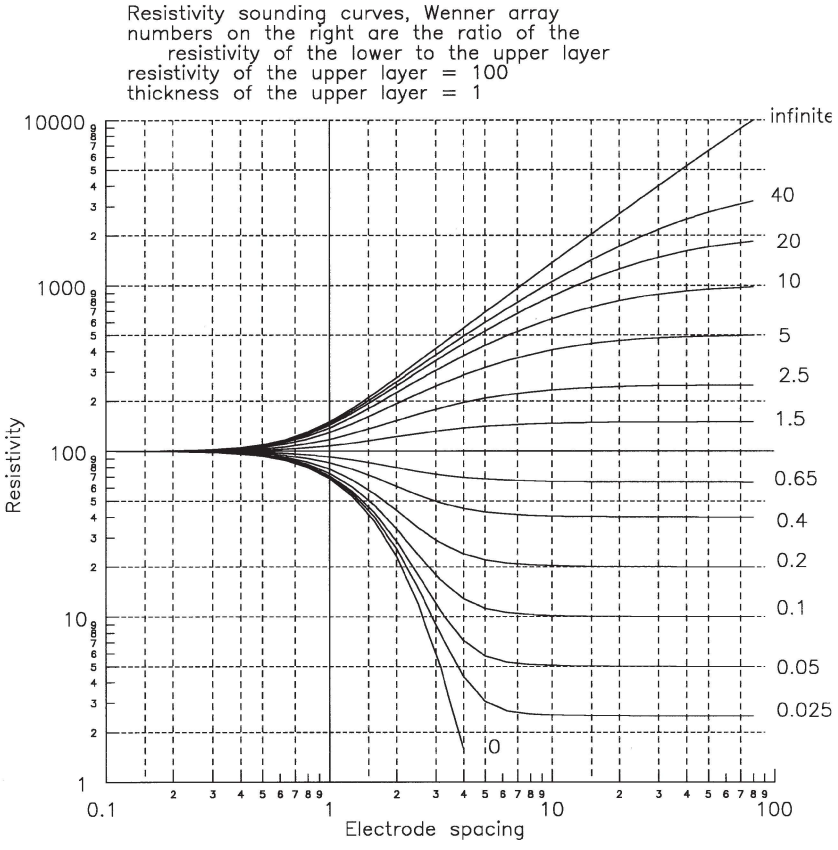

Fig. B17: Calculated resistivity soundings for two layers. The measurements are compared to these calculated curves and the best match between them is determined.

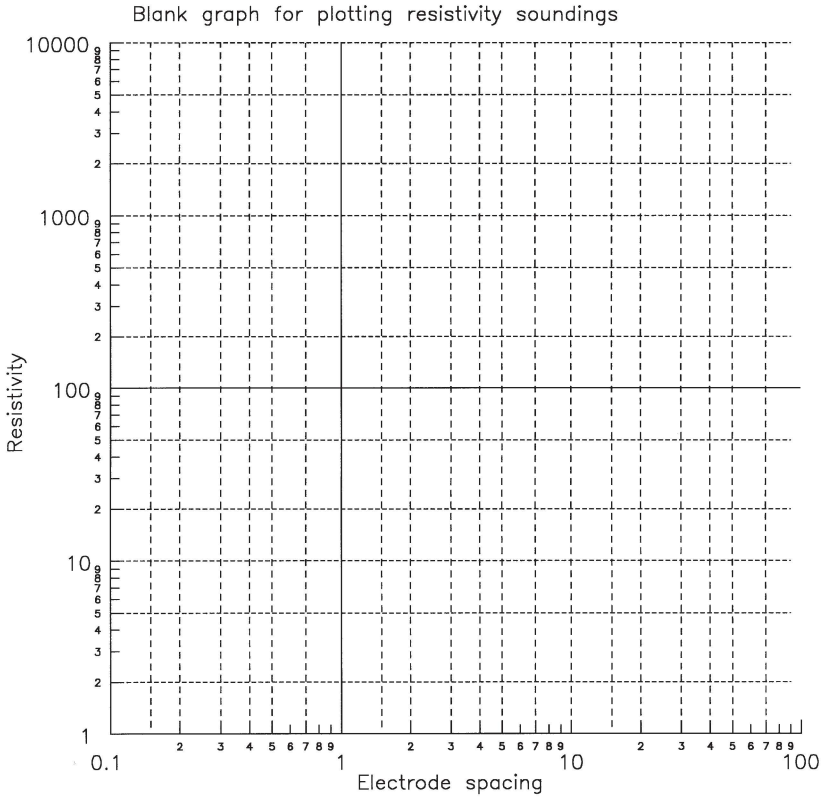

Fig. B18: A blank graph for your analysis. The vertical lines in this figure show suggested spacings for the electrodes of your sounding, although you do not need to use the entire range.

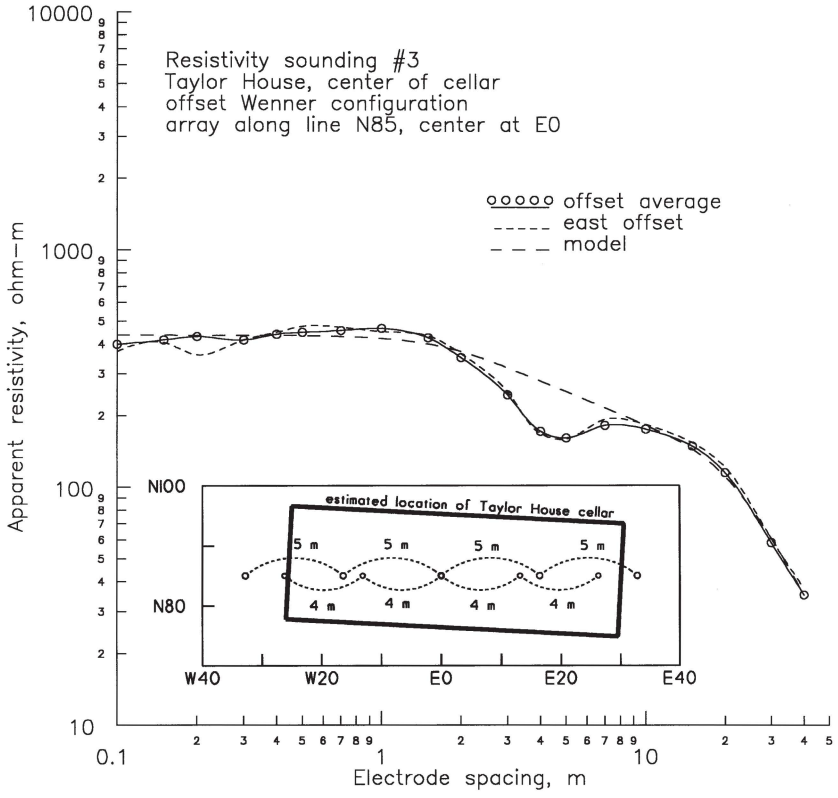

Fig. B19: A resistivity sounding over the Taylor House cellar. The measurements were affected when the electrodes crossed the east and west walls of the cellar, causing a dip in the readings.

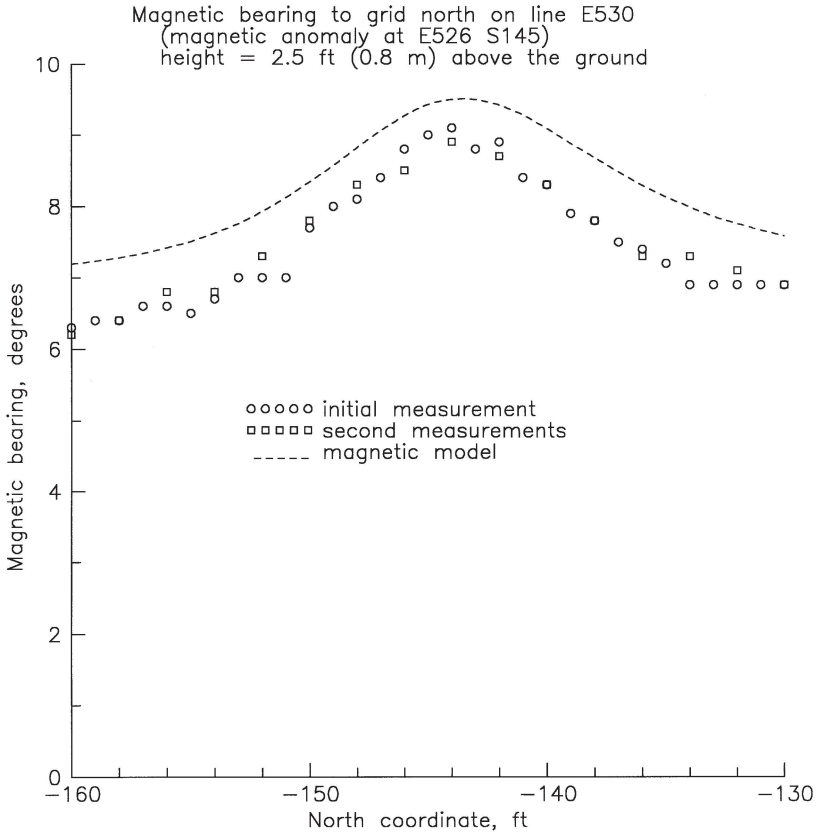

Fig. B20: A magnetic compass traverse. The needle is deflected by about 2 degrees in passing the massive iron object. This object is interpreted to be a well filled with iron.

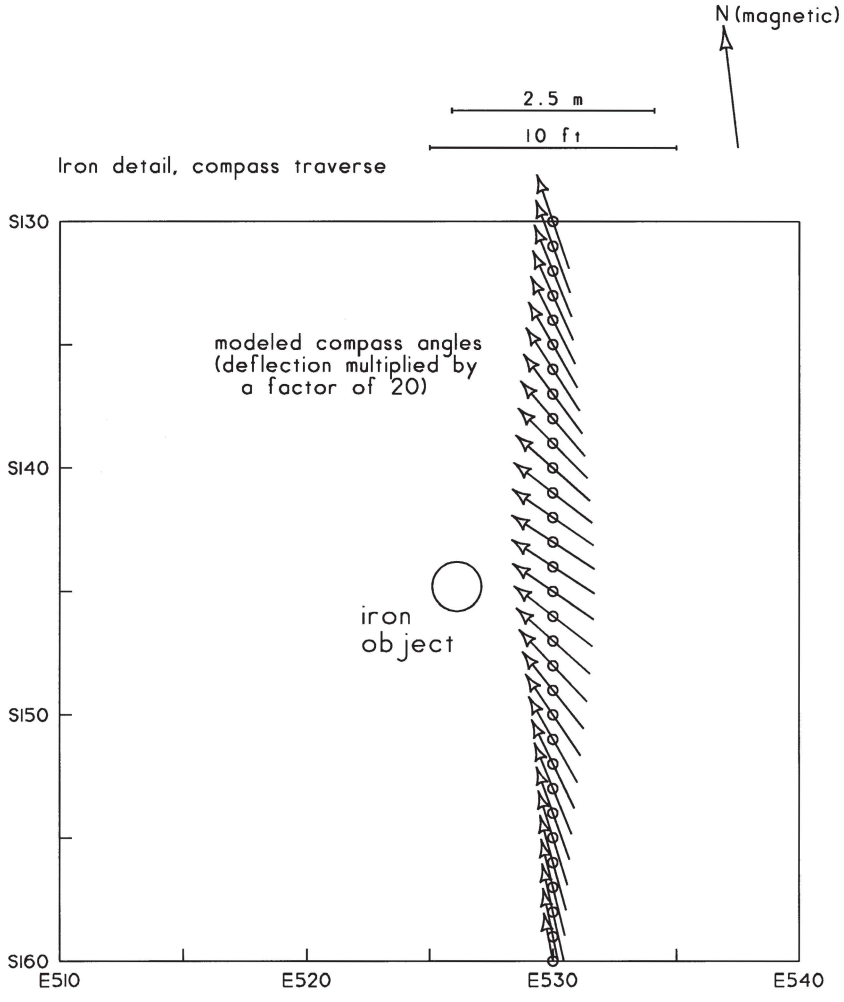

Fig. B21: The deflection of a compass. While an exaggeration, this illustrates the changing direction near the iron object.

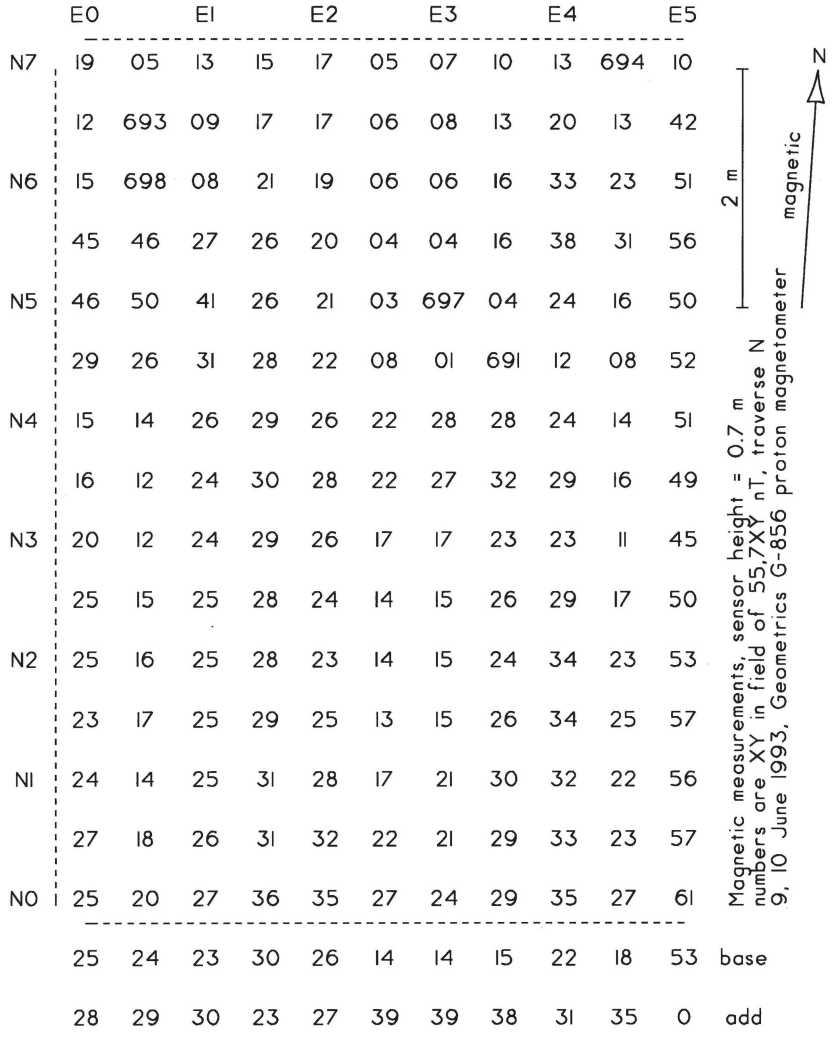

	E0		E1		E2		E3		E4		E5	
N7	19	05	13	15	17	05	07	10	13	694	10	
	12	693	09	17	17	06	08	13	20	13	42	
N6	15	698	08	21	19	06	06	16	33	23	51	
	45	46	27	26	20	04	04	16	38	31	56	
N5	46	50	41	26	21	03	697	04	24	16	50	
	29	26	31	28	22	08	01	691	12	08	52	
N4	15	14	26	29	26	22	28	28	24	14	51	
	16	12	24	30	28	22	27	32	29	16	49	
N3	20	12	24	29	26	17	17	23	23	11	45	
	25	15	25	28	24	14	15	26	29	17	50	
N2	25	16	25	28	23	14	15	24	34	23	53	
	23	17	25	29	25	13	15	26	34	25	57	
N1	24	14	25	31	28	17	21	30	32	22	56	
	27	18	26	31	32	22	21	29	33	23	57	
N0	25	20	27	36	35	27	24	29	35	27	61	
	25	24	23	30	26	14	14	15	22	18	53	base
	28	29	30	23	27	39	39	38	31	35	0	add

Fig. B22: The original measurements of a magnetic survey. This survey was done by students of a National Park Service course.

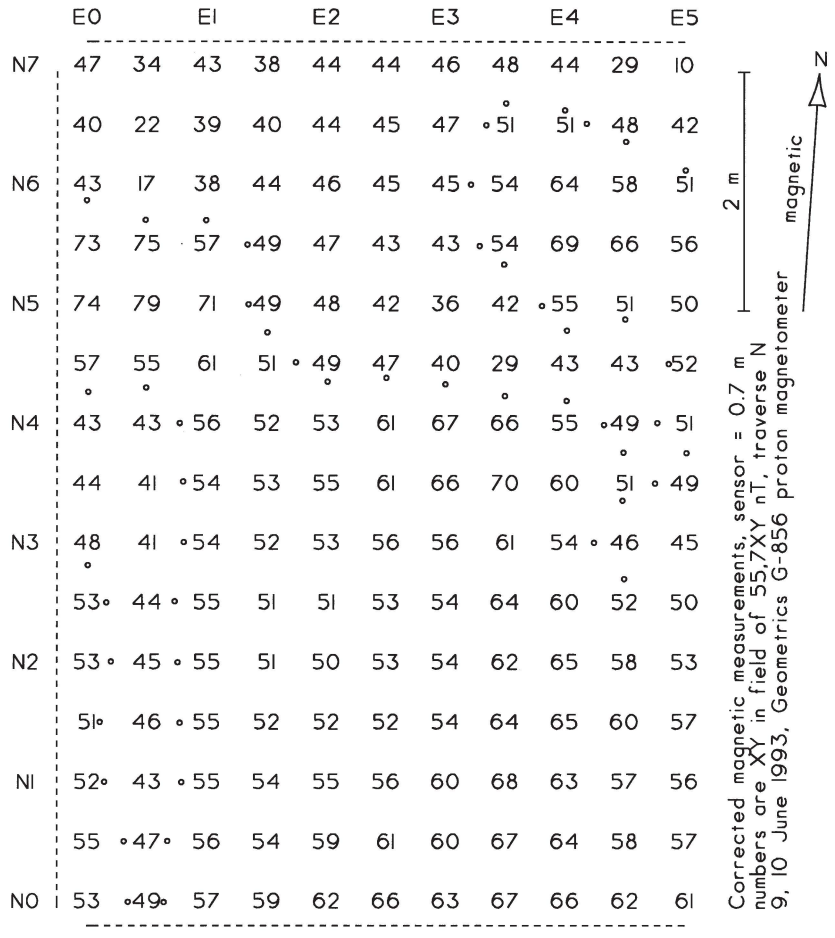

Fig. B23: The corrected magnetic measurements. The effect of the change in the Earth's field has been mostly eliminated.

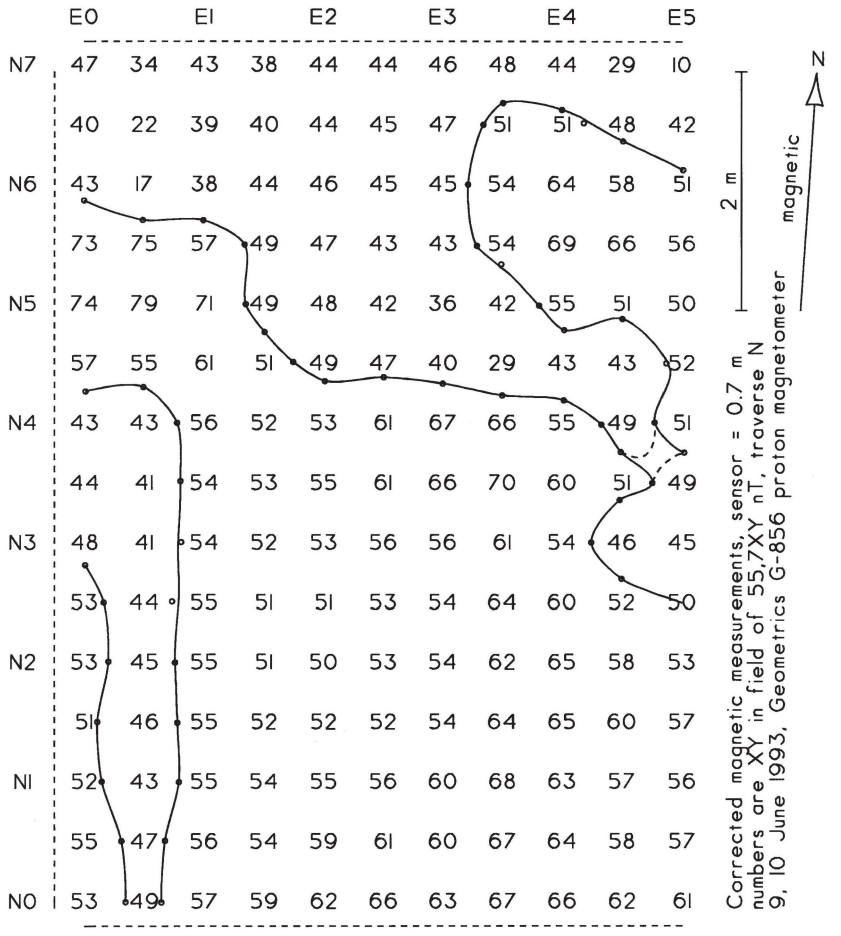

Fig. B24: The first contour line. The broken lines show two alternative line segments which would be just as valid as the solid lines. This part of the map is called a saddle surface, for the shape is similar to a horse saddle.

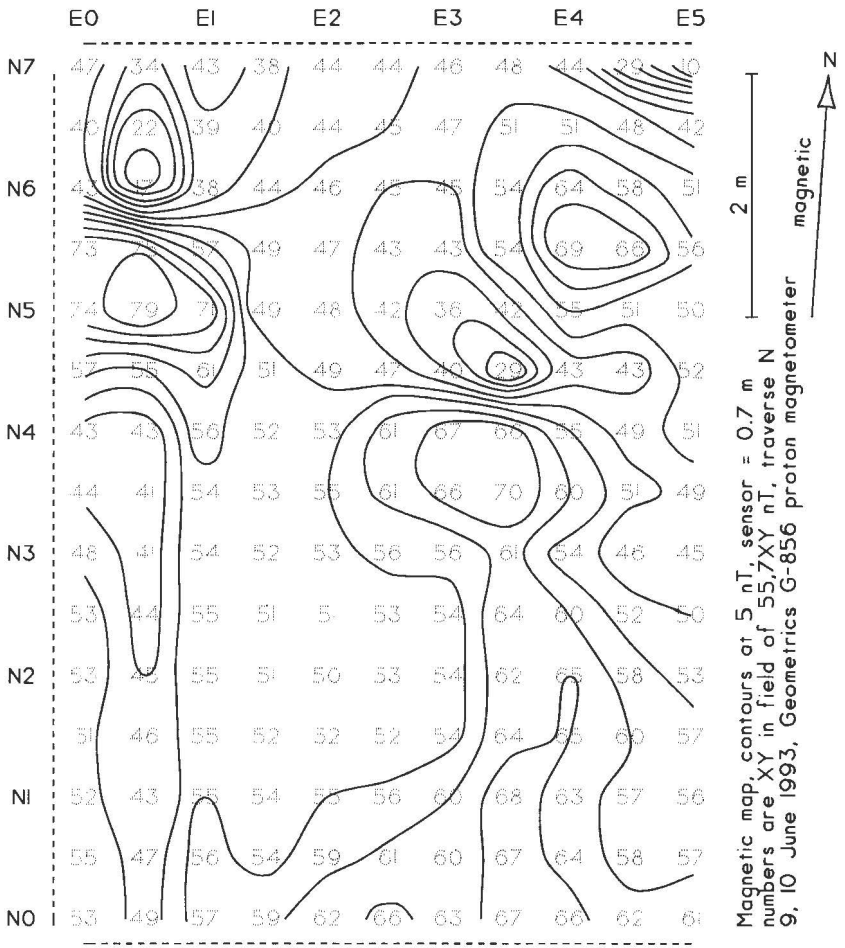

Fig. B25: The completed contour map. The contour lines are drawn at intervals of 5 nT.

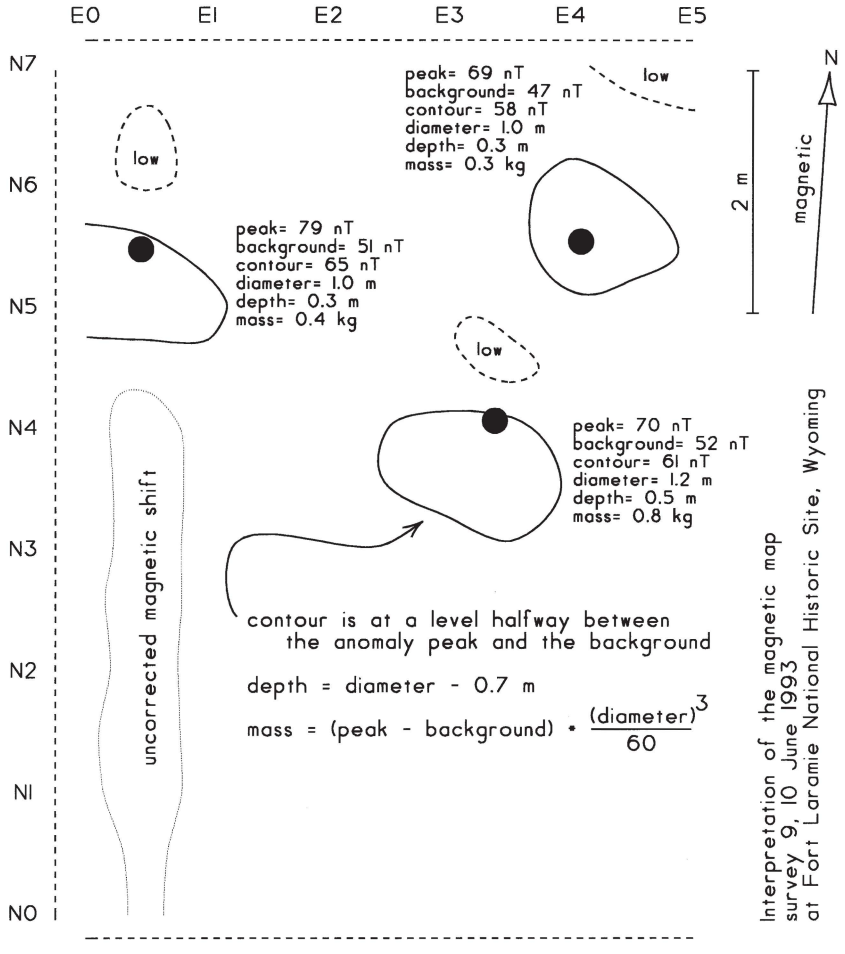

Fig. B26: The interpretation of the magnetic map. This shows estimates of the location, depth, and mass of the features.

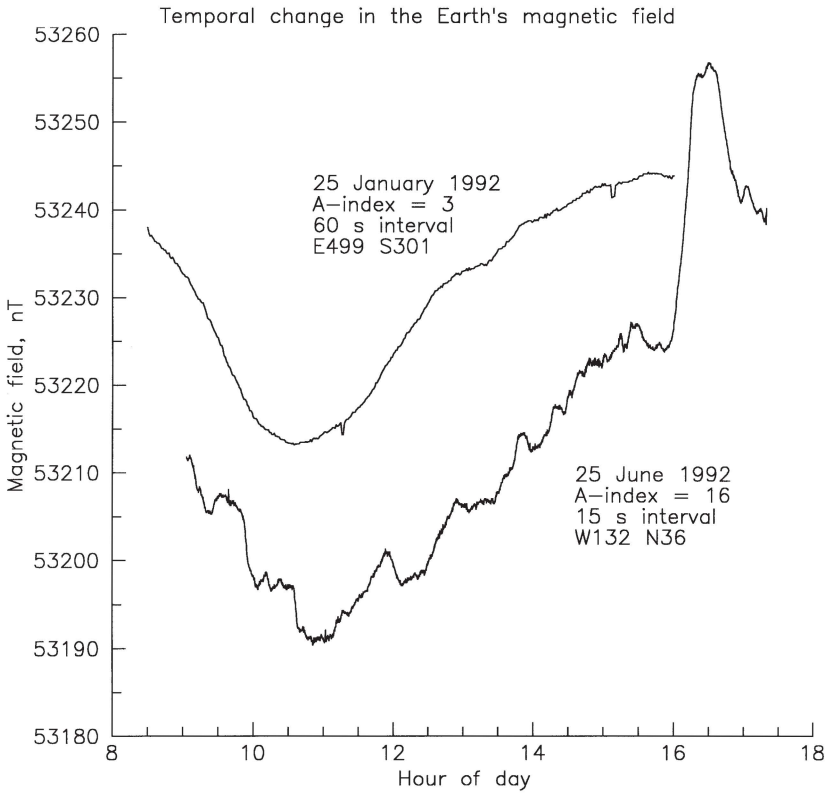

Fig. B27: A pair of magnetic base station recordings. One day was magnetically quiet; the other was noisy. Two trains passed at a distance of about 250 m on 25 January 1992, causing the two small dips.

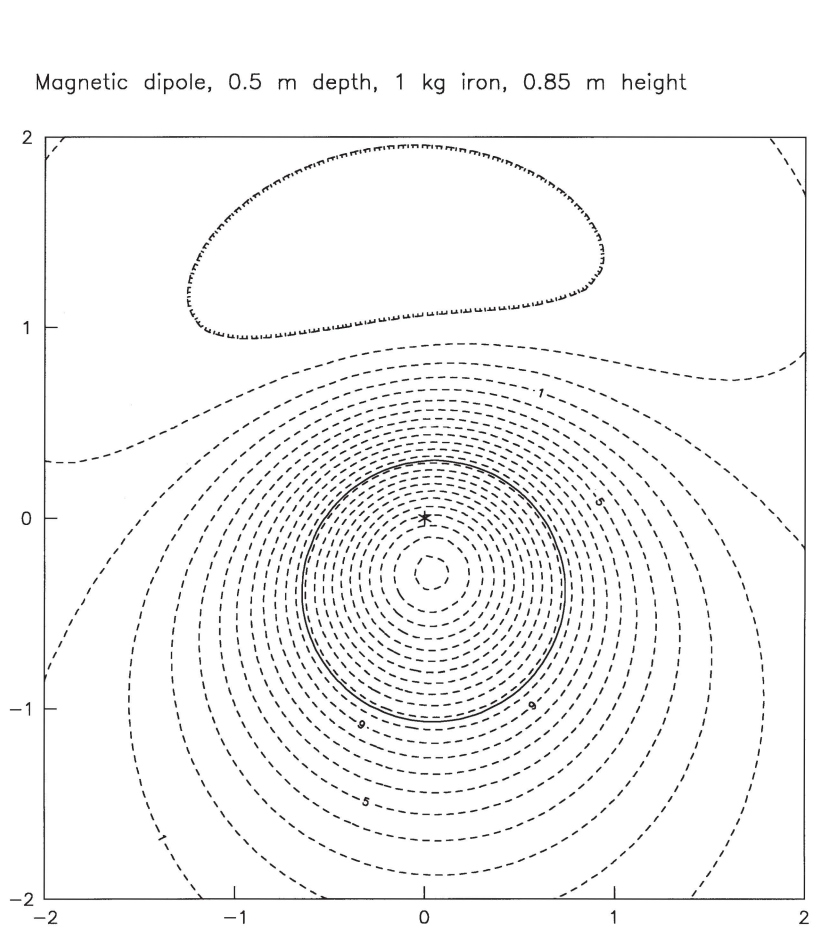

Fig. B28: The magnetic anomaly caused by 1 kg of iron. This is an idealized pattern, based on a calculation. The object is located at the middle of the figure, at a depth of 0.5 m. Contour lines are at intervals of 1 nT, and the solid line contour is at an amplitude which is half the peak value of the anomaly. The diameter of that solid line contour is equal to the sum of the height of the sensor added to the depth of the feature. This is the half-width rule.

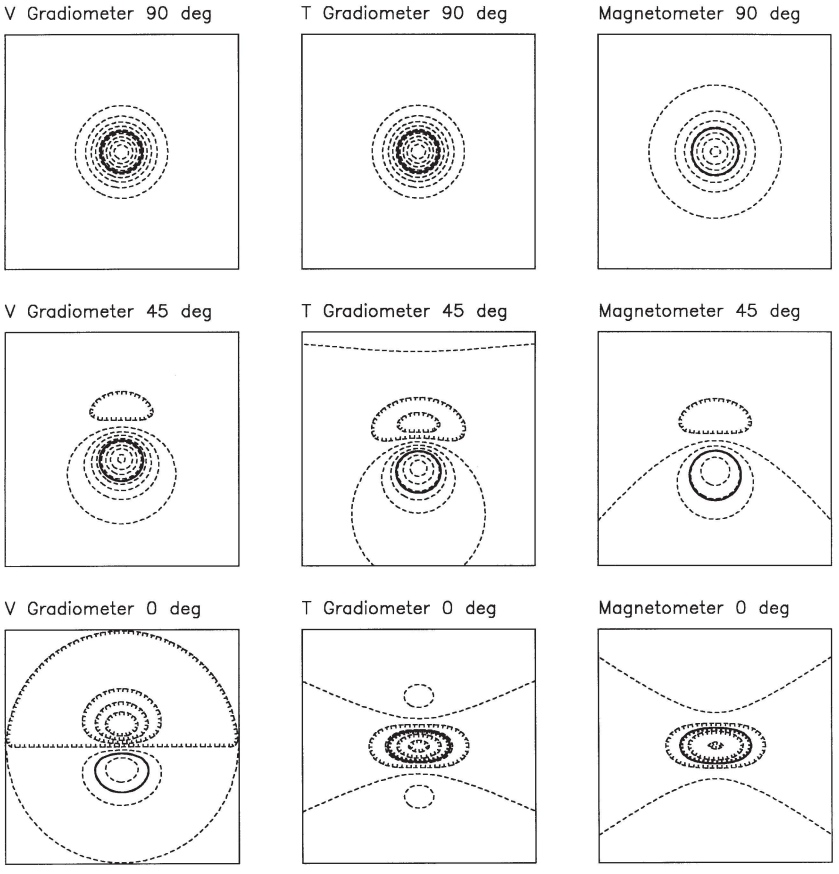

Fig. B29: The generality of the half-width rule. Each solid line contour is at an amplitude which is half of the peak amplitude. The maps of vertical component and total field gradiometers are plotted on the left side. The inclination of the Earth's field is listed with each map.

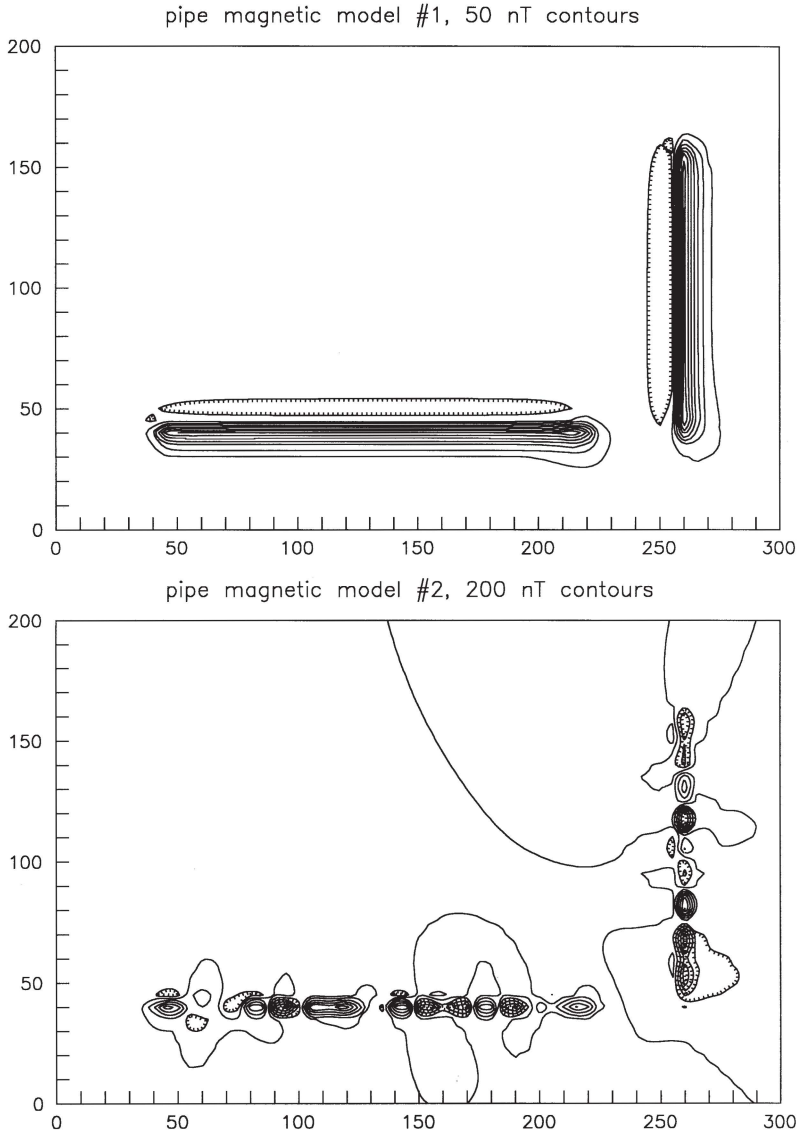

Fig. B30: Magnetic models of pipes. These approximate the patterns of two pipes which were found in the area of Fort Morton.

Magnetic map of a hole in a slab

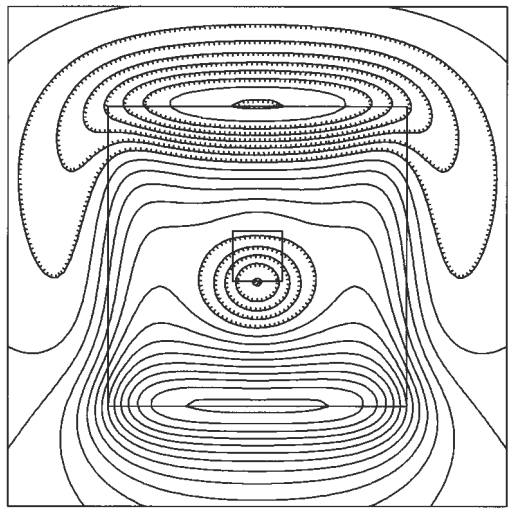

Magnetic map of an overhead object

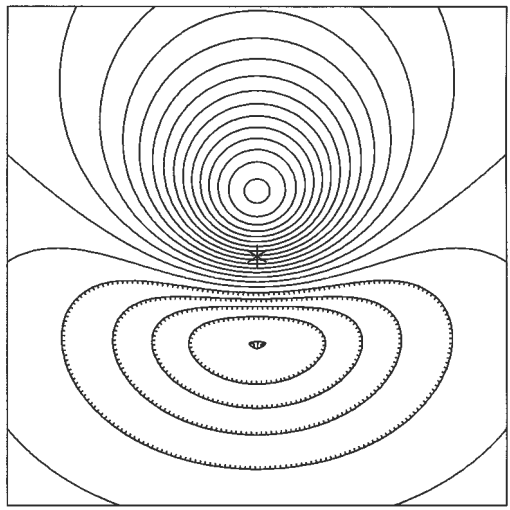

Fig. B31: Two special examples of magnetic models.

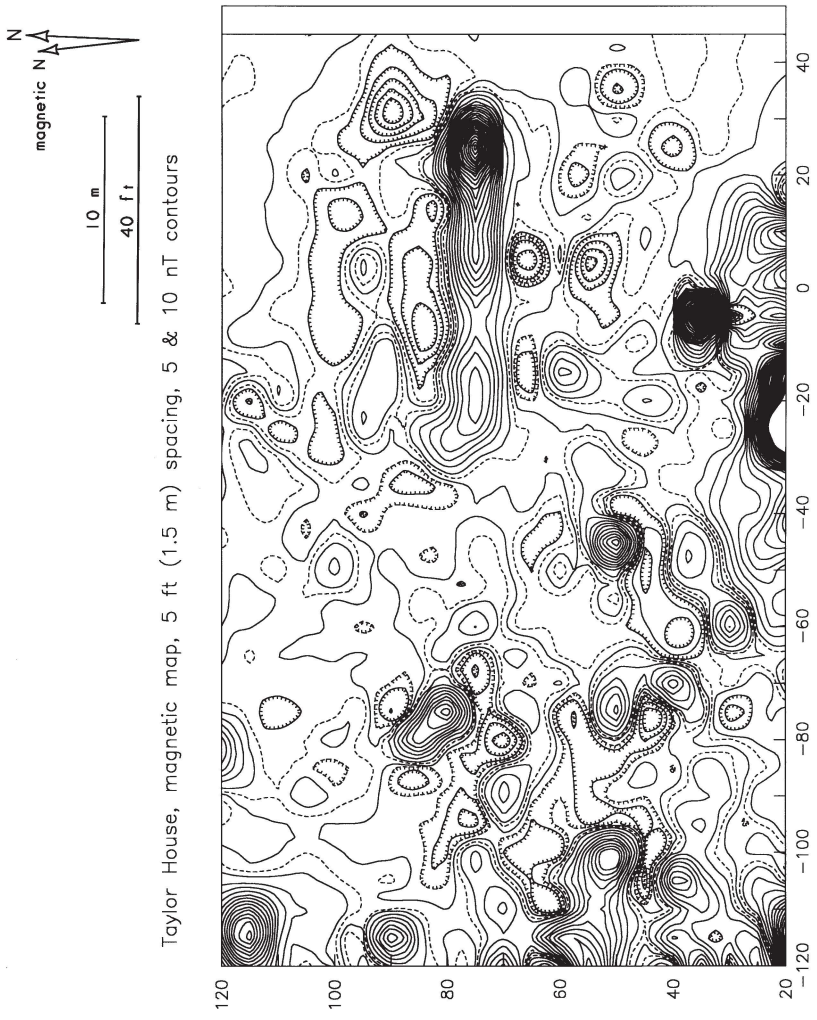

Fig. B32: A fast, low resolution magnetic survey of the Taylor House.

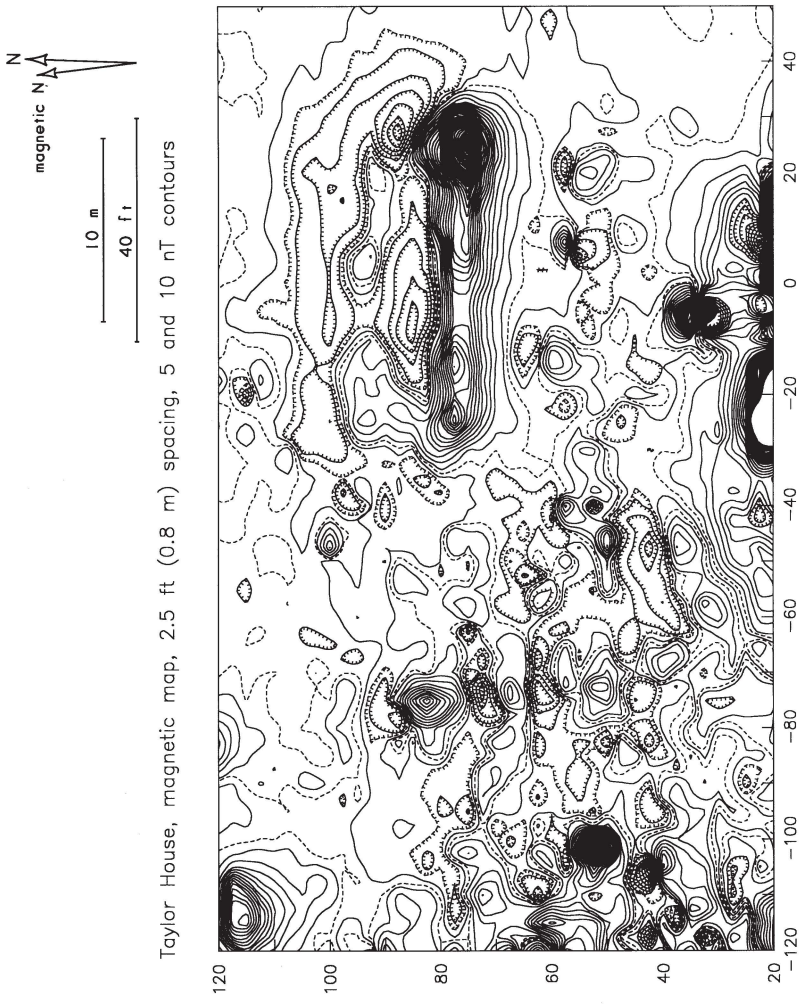

Fig. B33: A higher resolution magnetic map of the Taylor House.

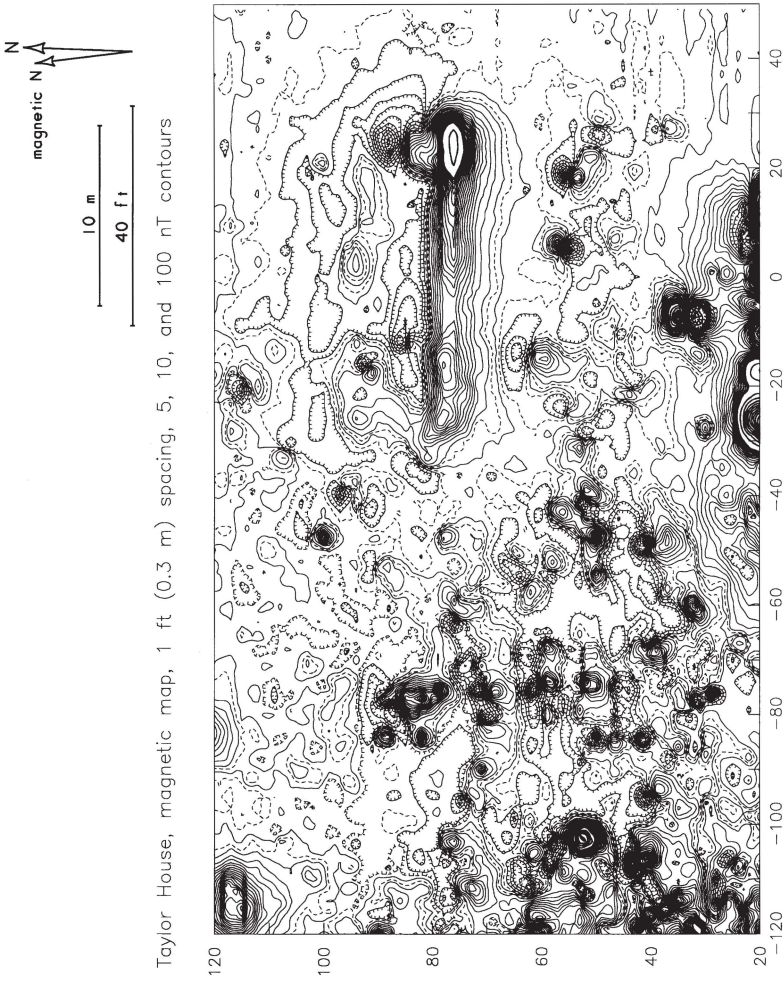

Fig. B34: A very detailed magnetic map. The measurement spacing was 1 ft (0.3 m) for this survey.

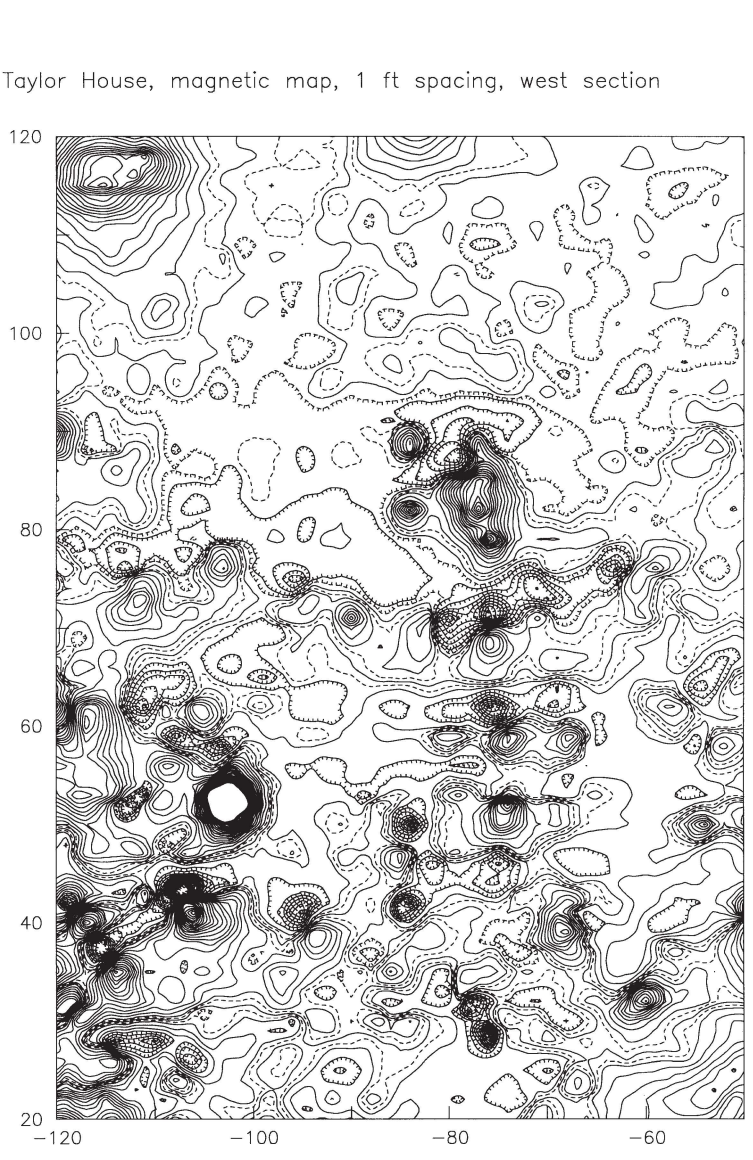

Fig. B35: An enlargement of the magnetic map. The detailed magnetic map of the Taylor House is divided between this figure and the following two.

Taylor House, magnetic map, 1 ft spacing, central section

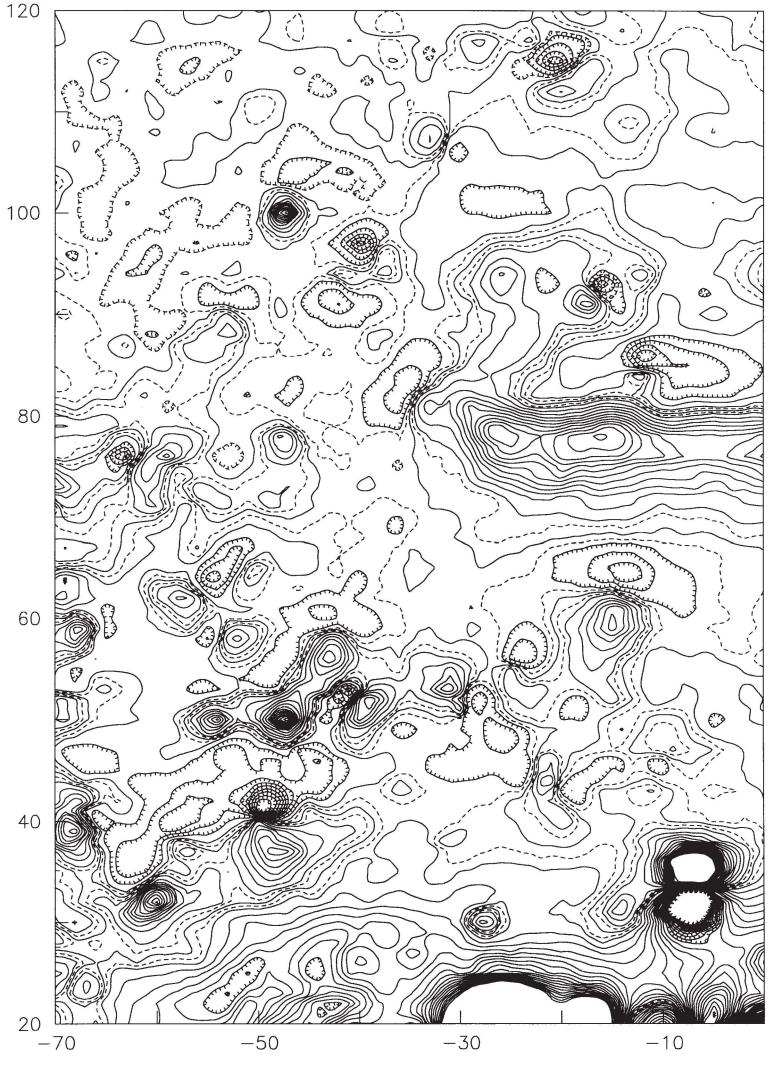

Fig. B36: The central section of the magnetic map.

Taylor House, magnetic map, 1 ft spacing, east section

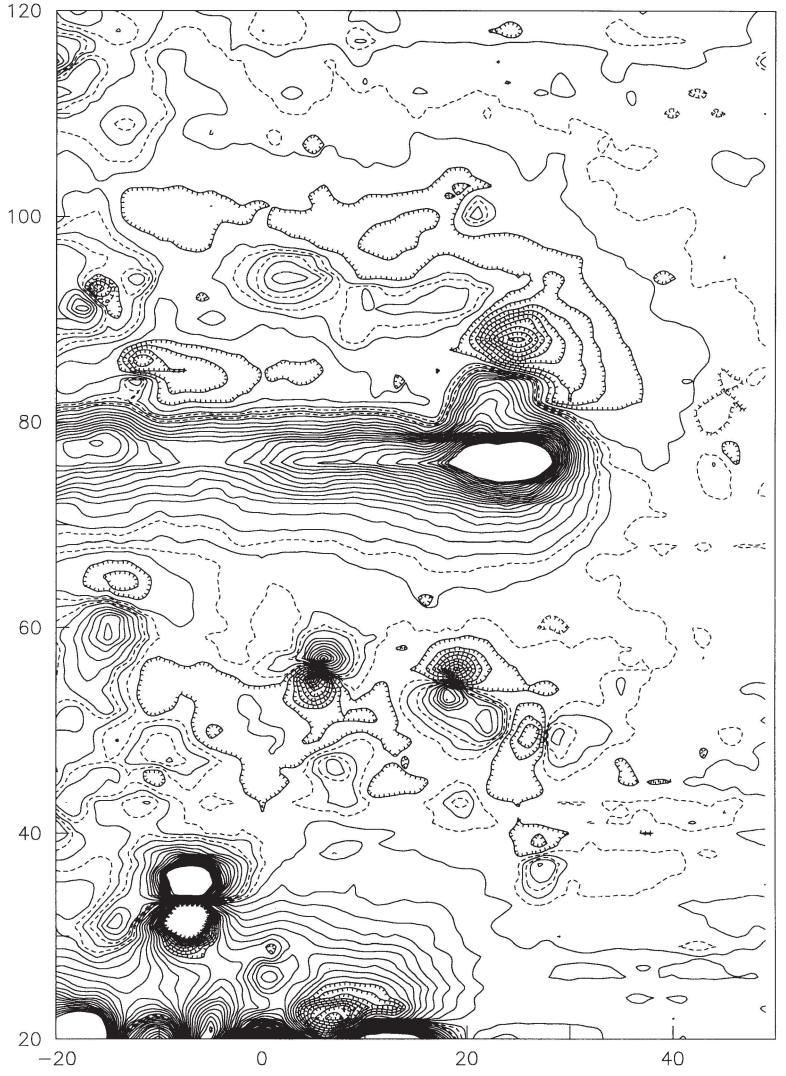

Fig. B37: The eastern third of the map.

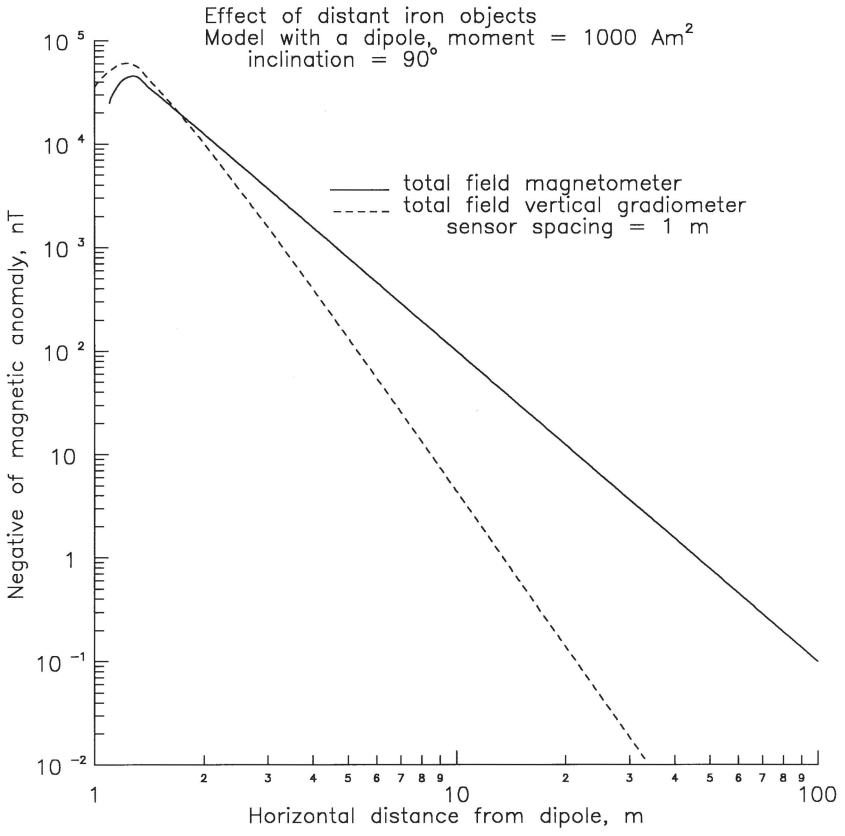

Fig. B38: A comparison of a magnetic gradiometer with a total field magnetometer. The gradiometer greatly reduces the effect of distant magnetic objects.

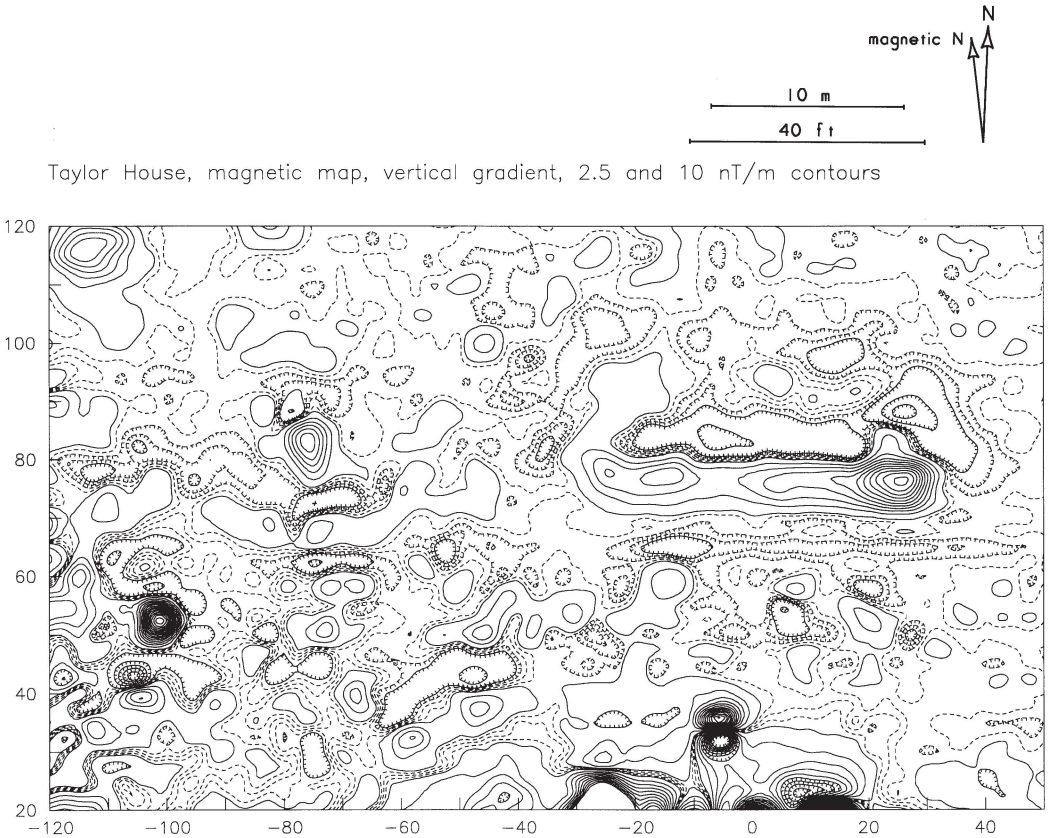

Fig. B39: A map measured with a magnetic gradiometer.

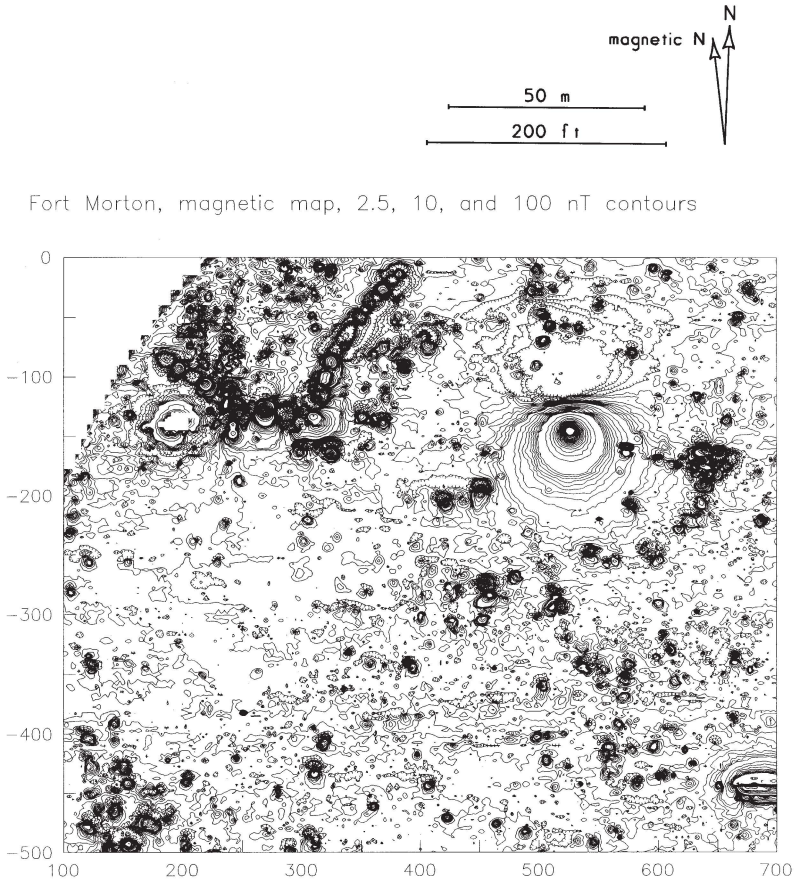

Fig. B40: The Fort Morton magnetic survey. In addition to a few pipes, the magnetic map shows many other iron objects.

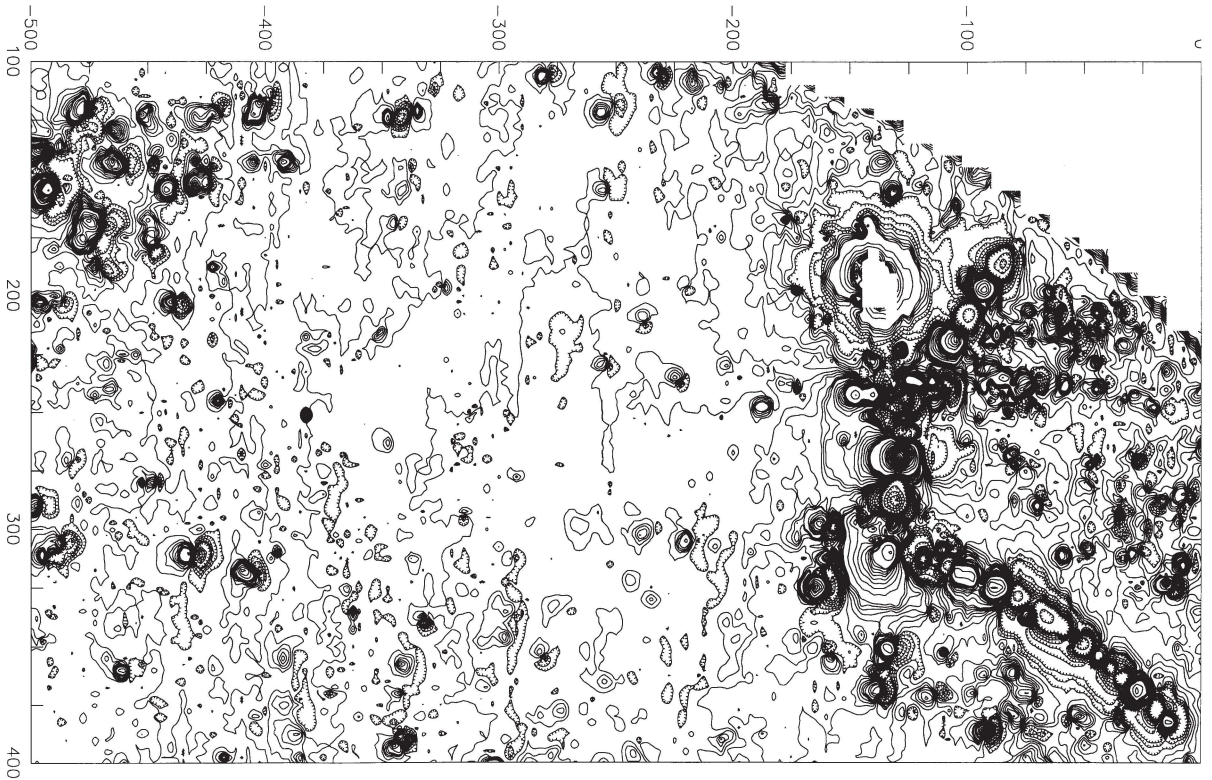

Fort Morton, magnetic map, western half, 2.5, 10, and 100 nT contours

Fig. B41: The western half of the magnetic survey.

Fort Morton, interpretation of magnetic survey, western half, showing iron mass (kg) and depth (m)

Fig. B42: An interpretation of half of the magnetic map.

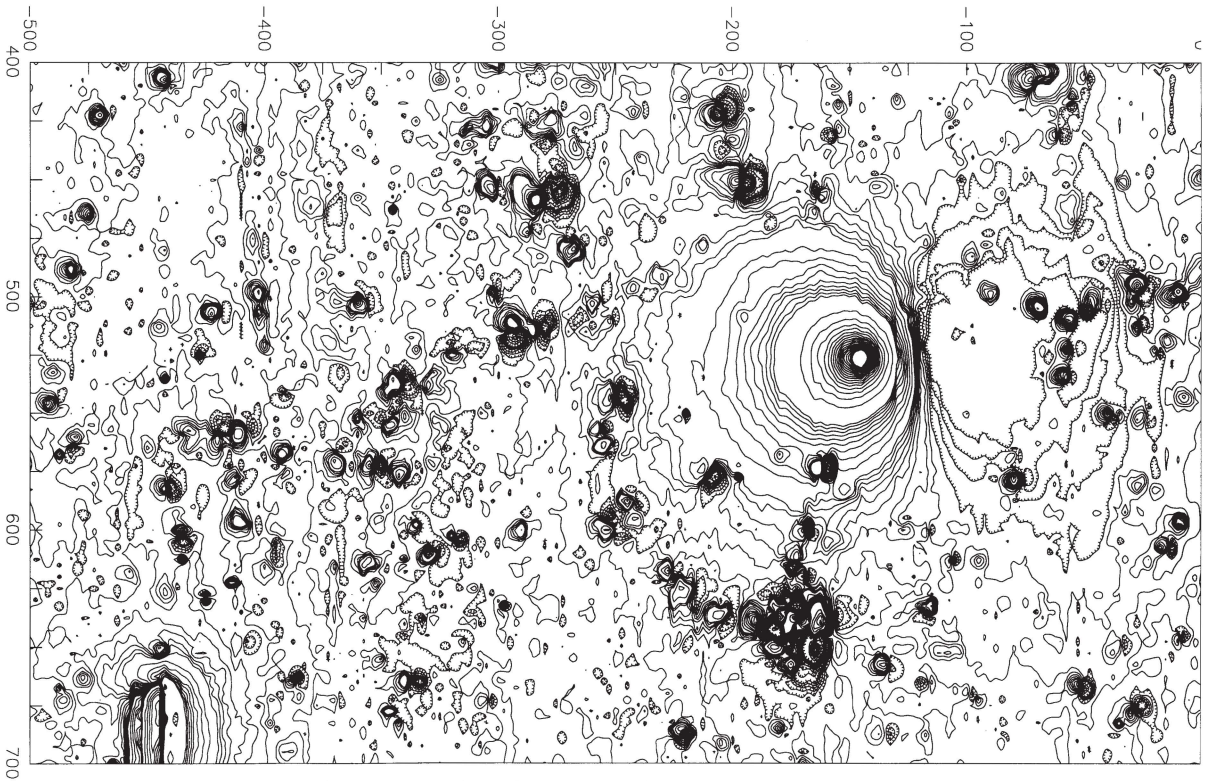

Fort Morton, magnetic map, eastern half, 2.5, 10, and 100 nT contours

Fig. B43: The eastern half of the Fort Morton survey.

Fig. B44: An interpretation of the eastern half.

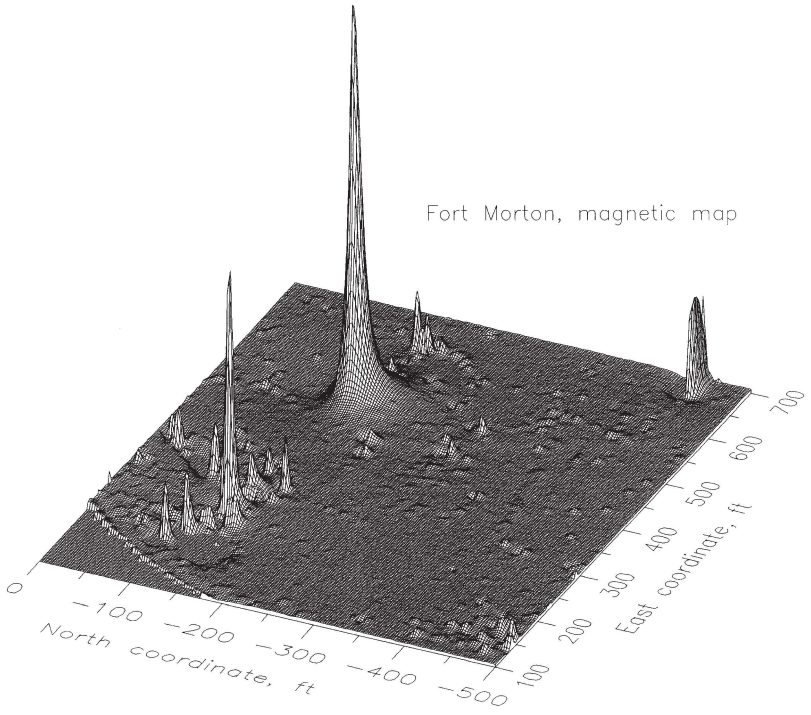

Fig. B45: A surface plot of the magnetic field. The highest peak is caused by an iron-filled well. Pipes cause other high values on the left and right side of the map.

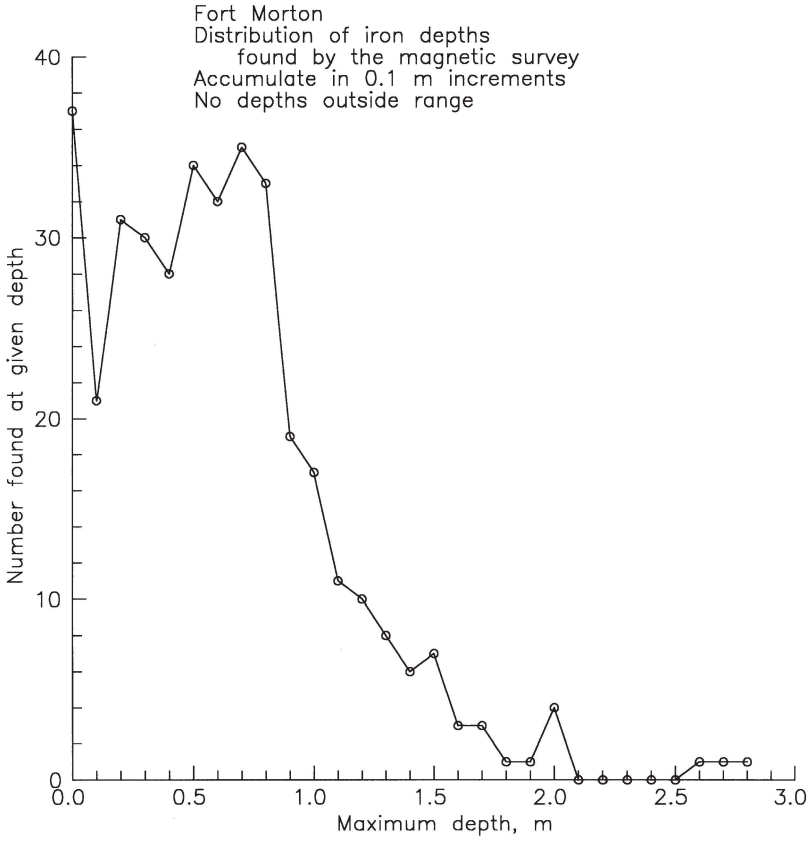

Fig. B46: Iron depth at Fort Morton. The interpretation of the magnetic map indicates that most objects are less than 0.9 m underground.

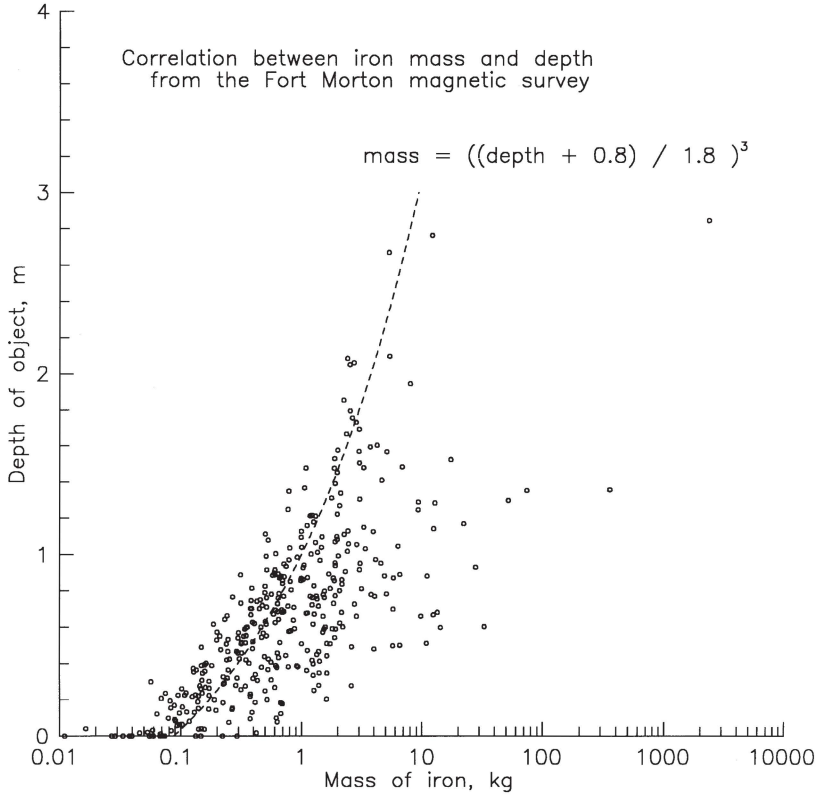

Fig. B47: Iron depth and mass. The most massive iron objects are deeper underground.

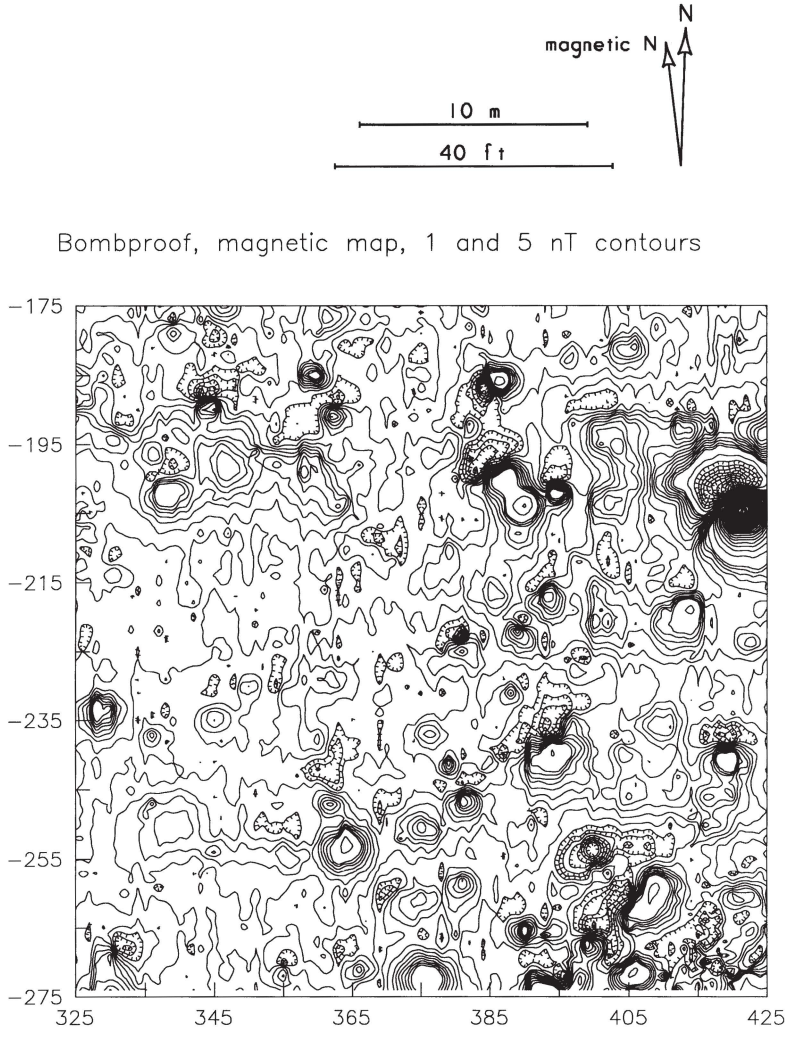

Fig. B48: A magnetic map of the Bombproof detail. The measurement spacing was 1 ft (0.3 m).

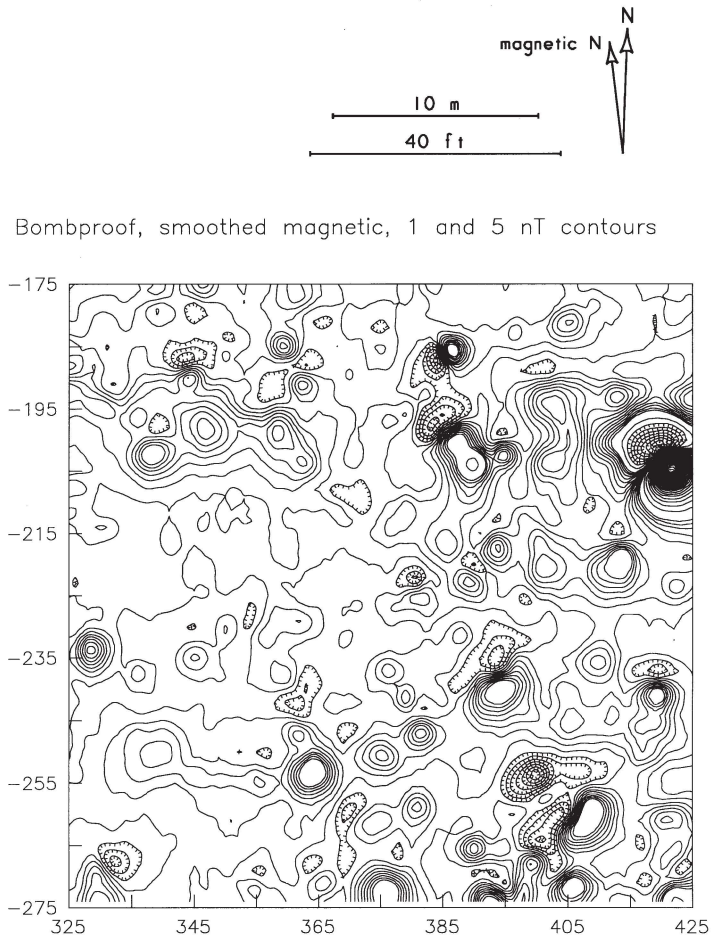

Fig. B49: A smoothed magnetic map. This clarifies the map of Fig. B48. Two different contour intervals are used; high amplitude anomalies are contoured at an interval of 5 nT.

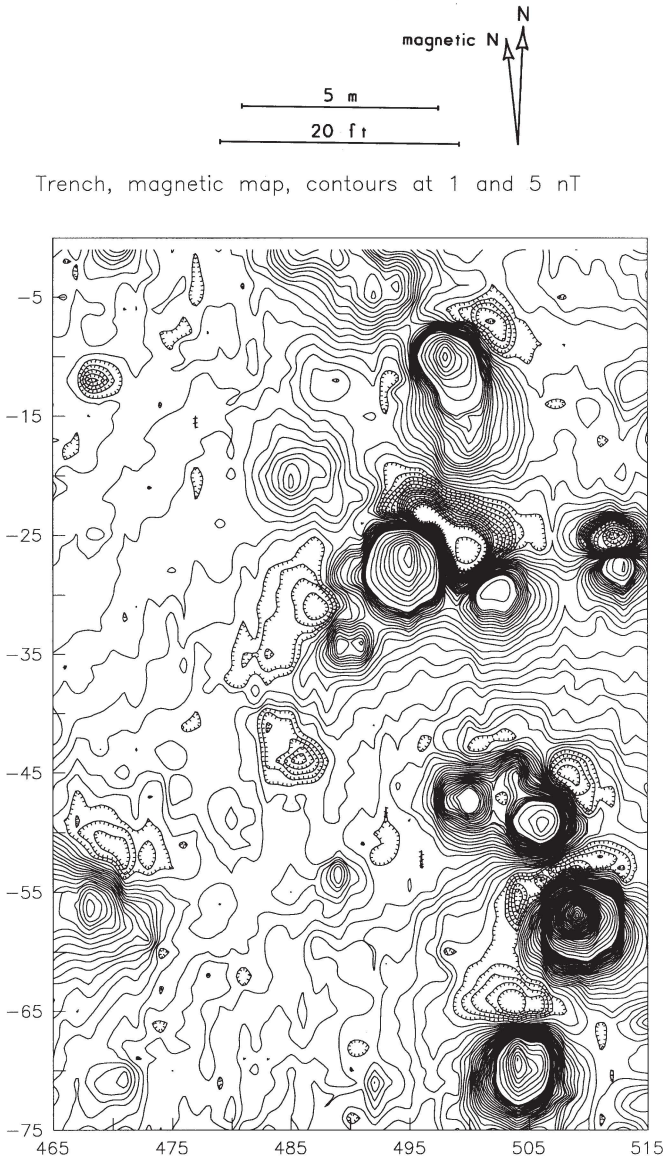

Fig. B50: Objects behind the main fortification trench.

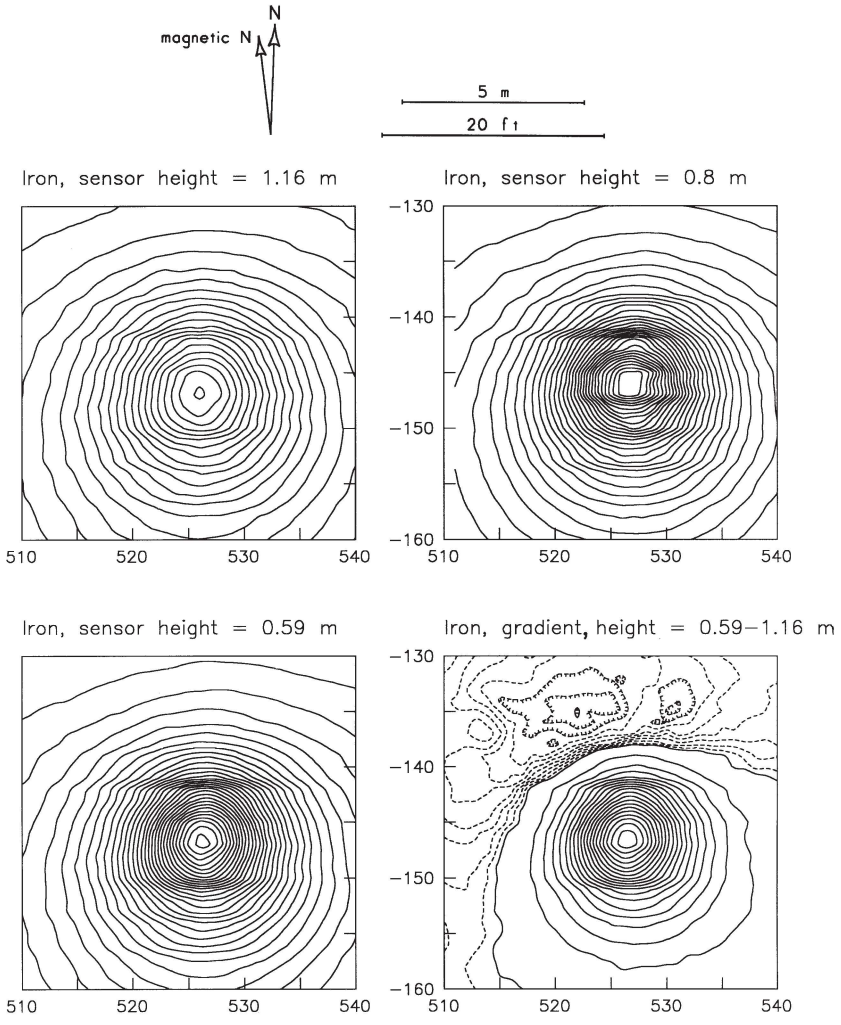

Fig. B51: The Iron detail. The three total field maps have a contour interval of 100 nT. The gradient map has contours at intervals of 100 nT/m and 10 nT/m (broken lines).

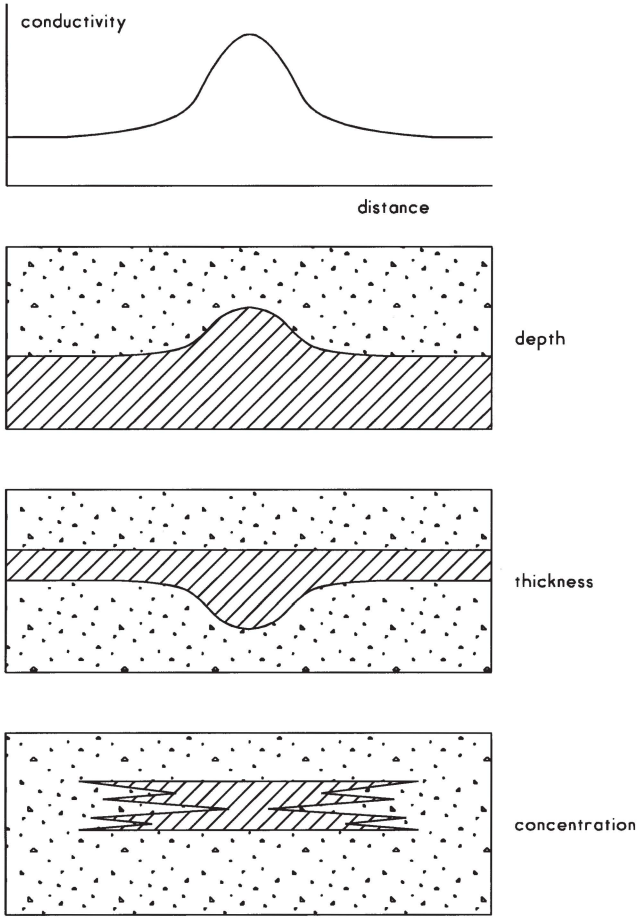

Fig. B52: A conductivity profile. Each of these different soil cross-sections can result in the same conductivity measurements. The dotted areas indicate low conductivity, while the hachured areas mark strata with high conductivity.

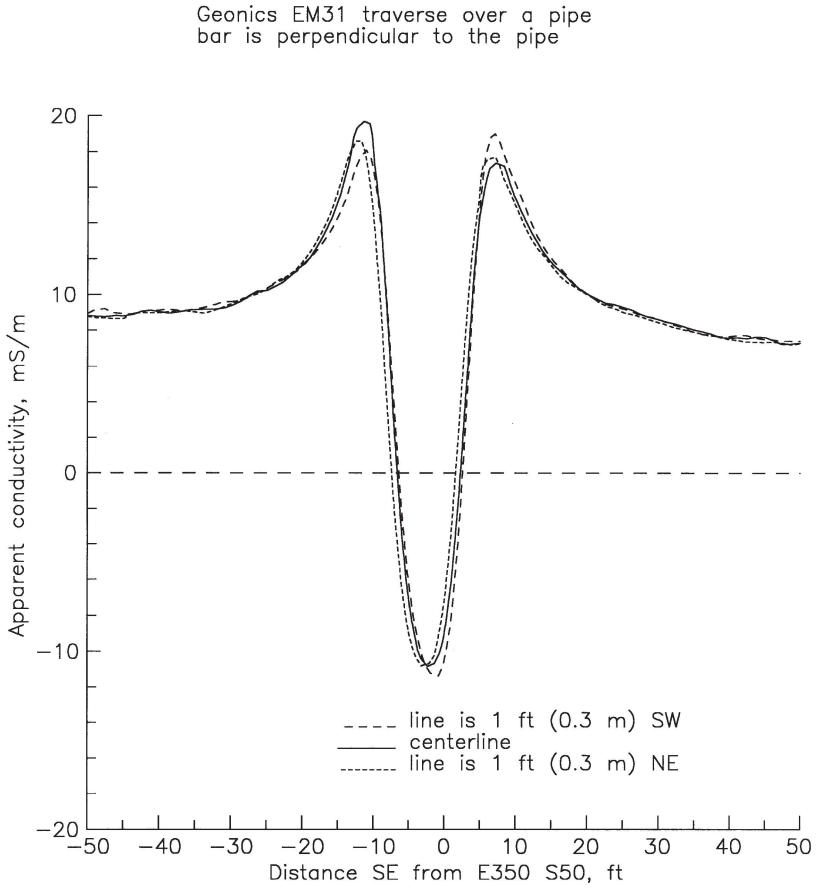

Fig. B53: The conductivity anomaly of a buried pipe. Note that the values are negative over the pipe.

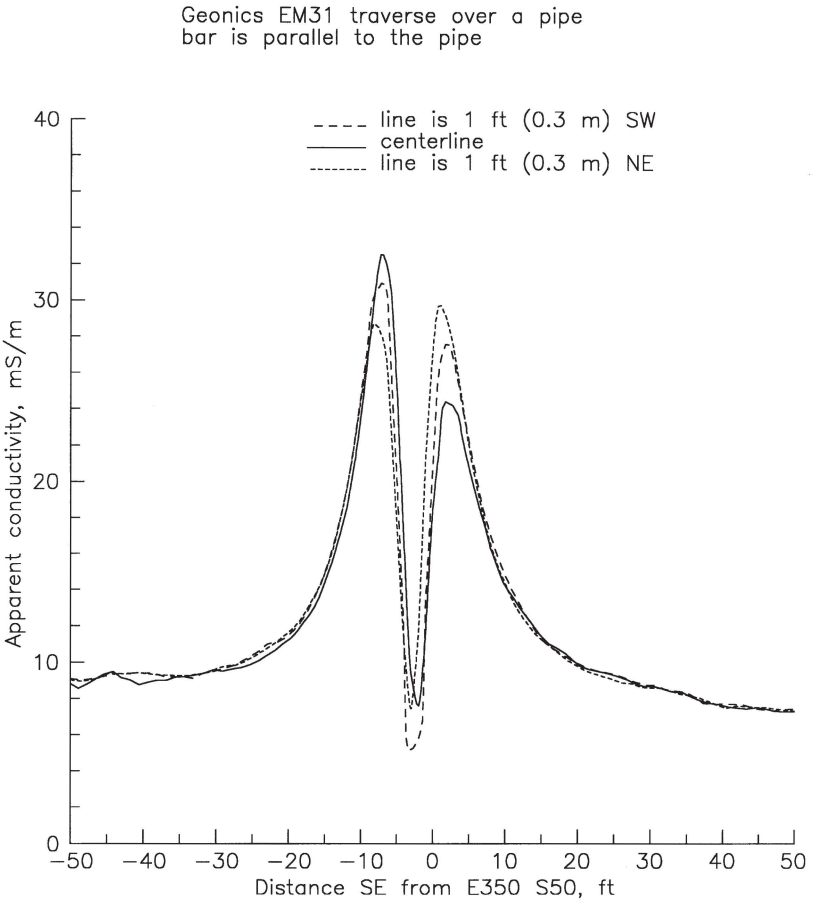

Fig. B54: Additional pipe measurements. With the bar of the EM31 parallel to the pipe, the anomaly is quite different.

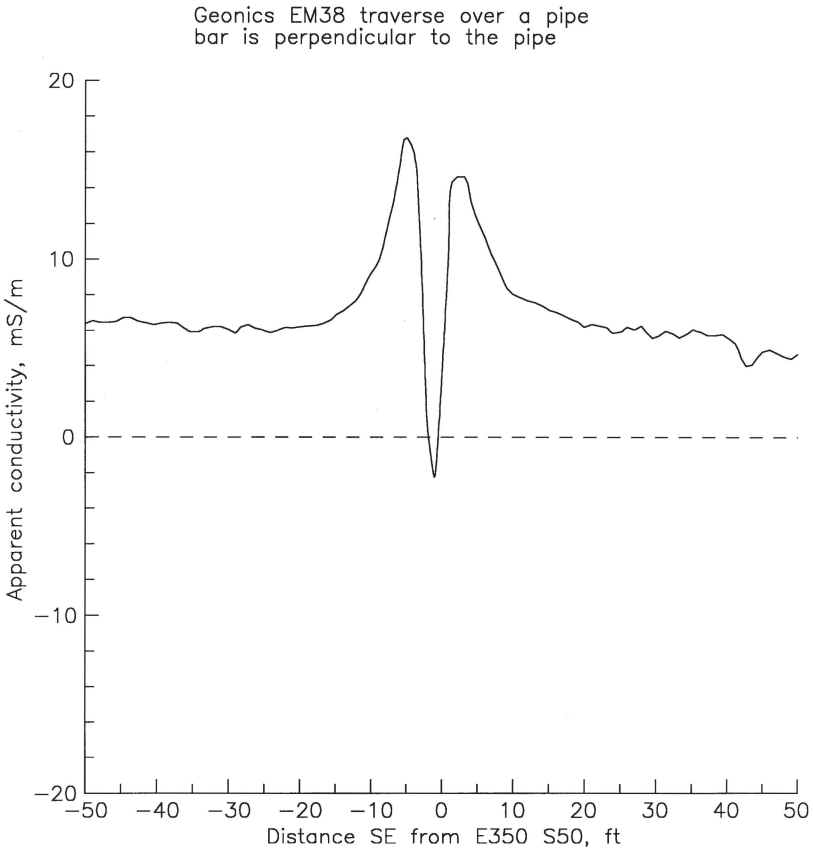

Fig. B55: An EM38 profile across the pipe. It is detected for a shorter span with this instrument.

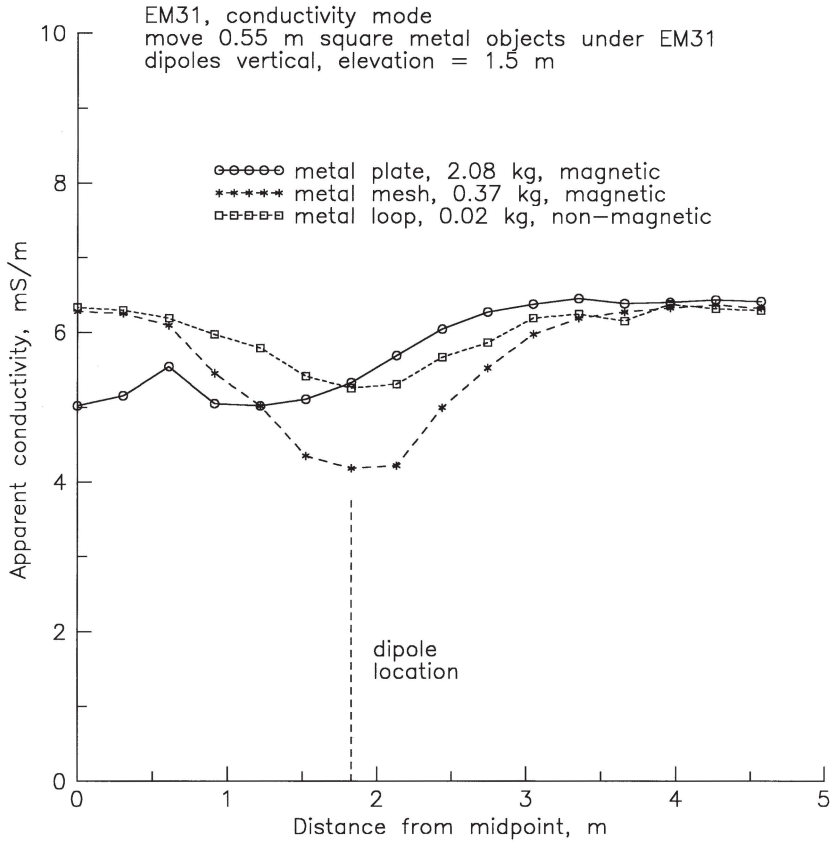

Fig. B56: Tests of the EM31 with large metal objects. While they are all the same size, they give different anomalies.

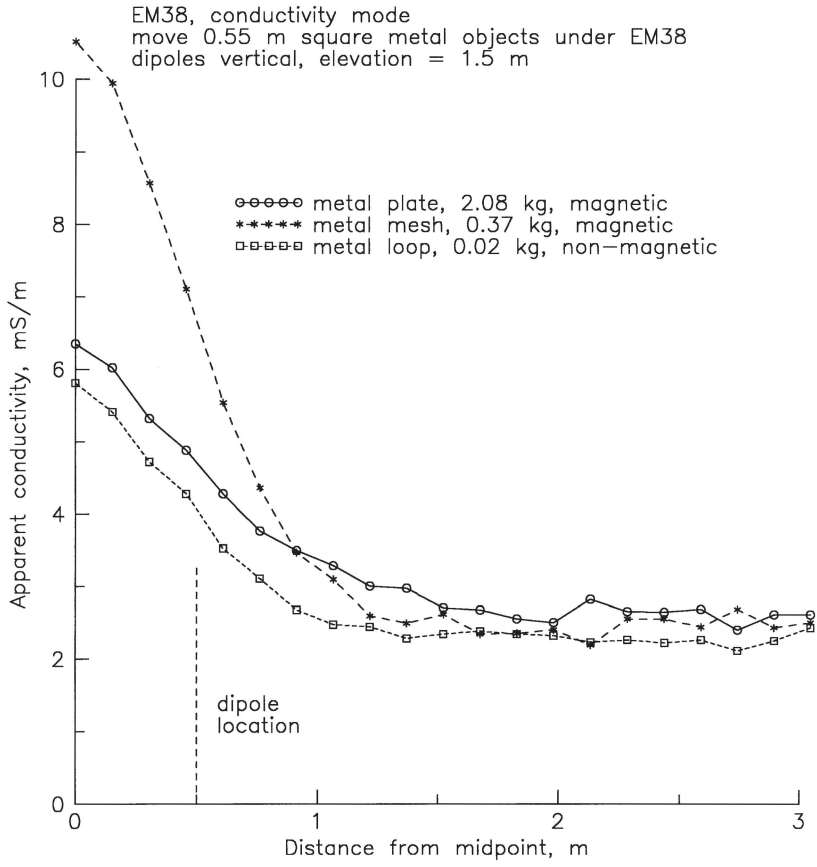

Fig. B57: The EM38 response to large metal objects. The EM38 gives high anomalies rather than lows; these are the same objects as those in Fig. B56 and the instrument elevation is the same.

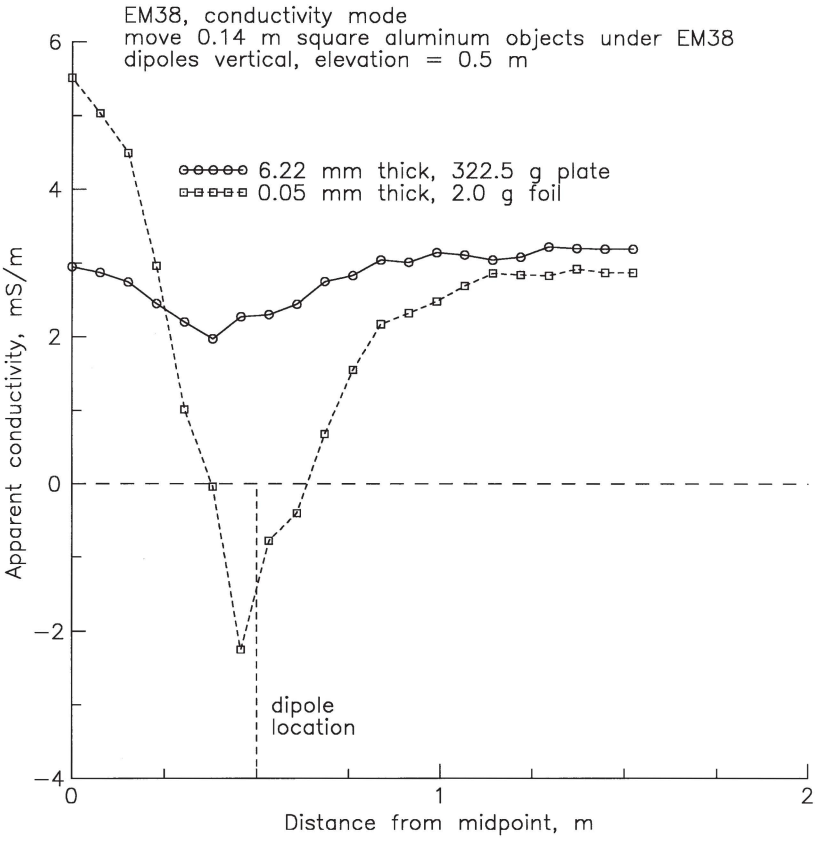

Fig. B58: EM38 response to small metal objects. A thin foil gives a larger anomaly than a plate.

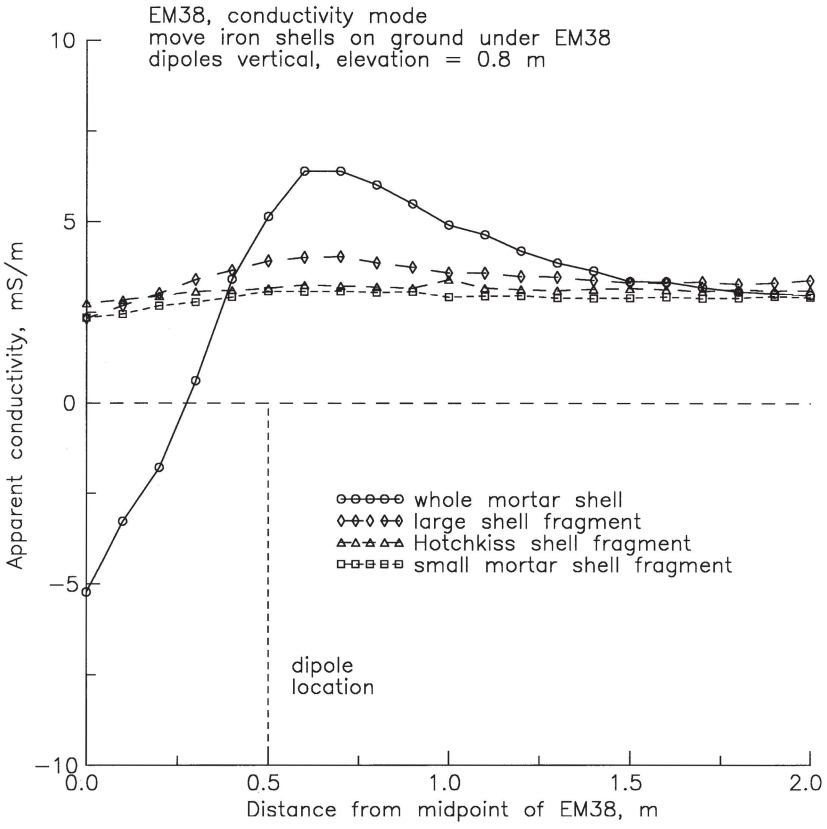

Fig. B59: The conductivity effect of military artifacts. These projectiles from the Civil War are sketched in Fig. C41.

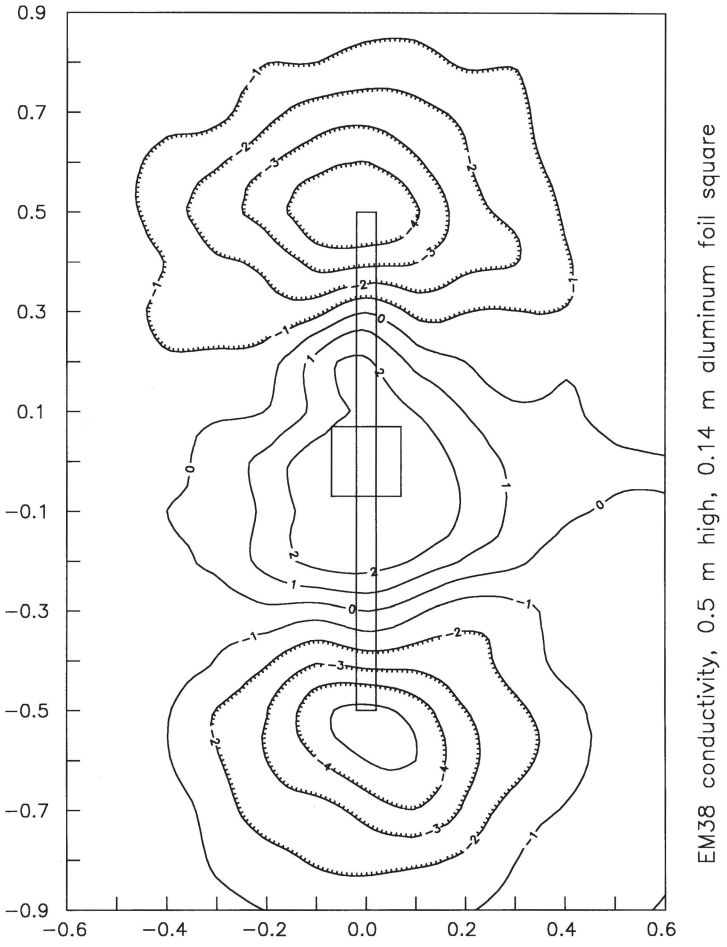

Fig. B60: A conductivity map of a metal object. Notice the change from low to high to low along the length of the anomaly.

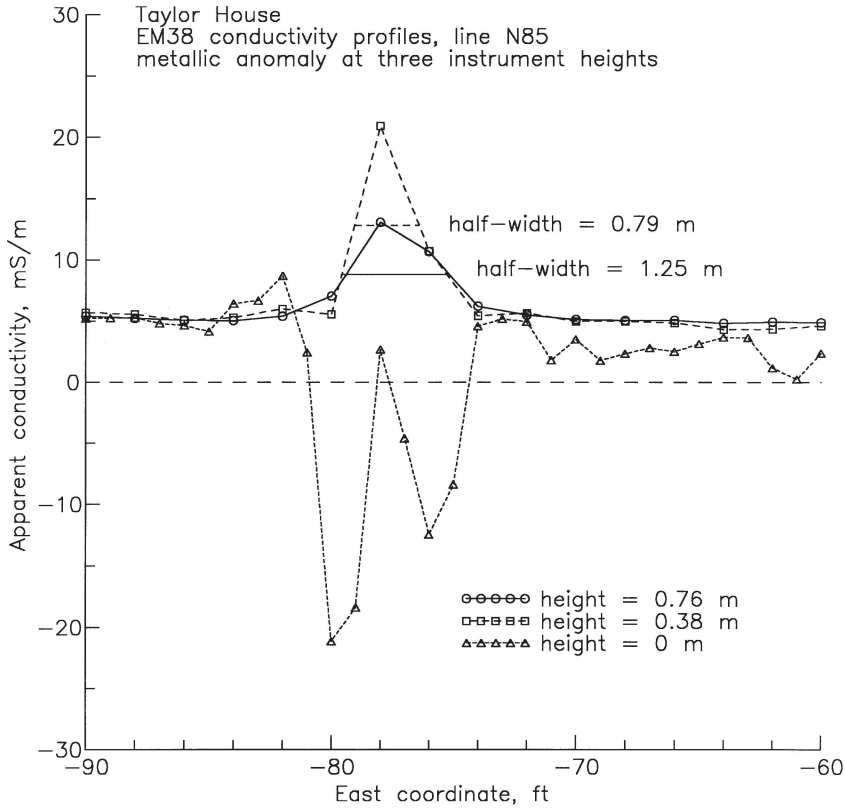

Fig. B61: A metal object in the Taylor House grid. The conductivity profiles were made with the instrument at three elevations above the ground.

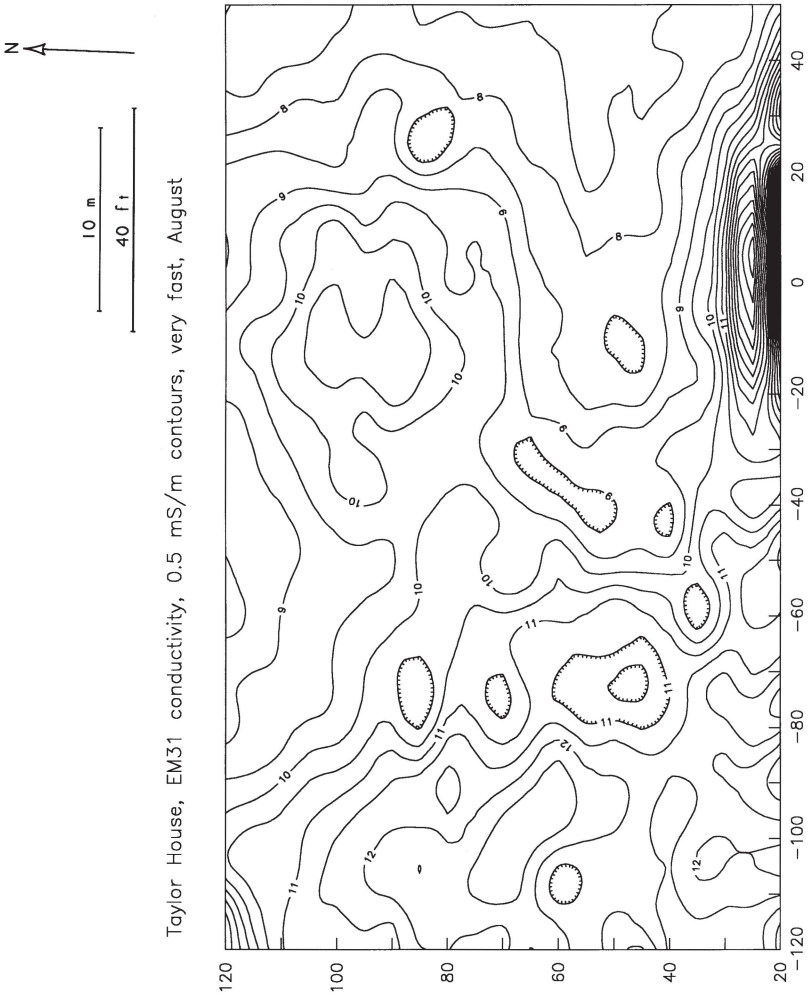

Fig. B62: A very fast conductivity survey. The measurement spacing was 5 ft (1.5 m).

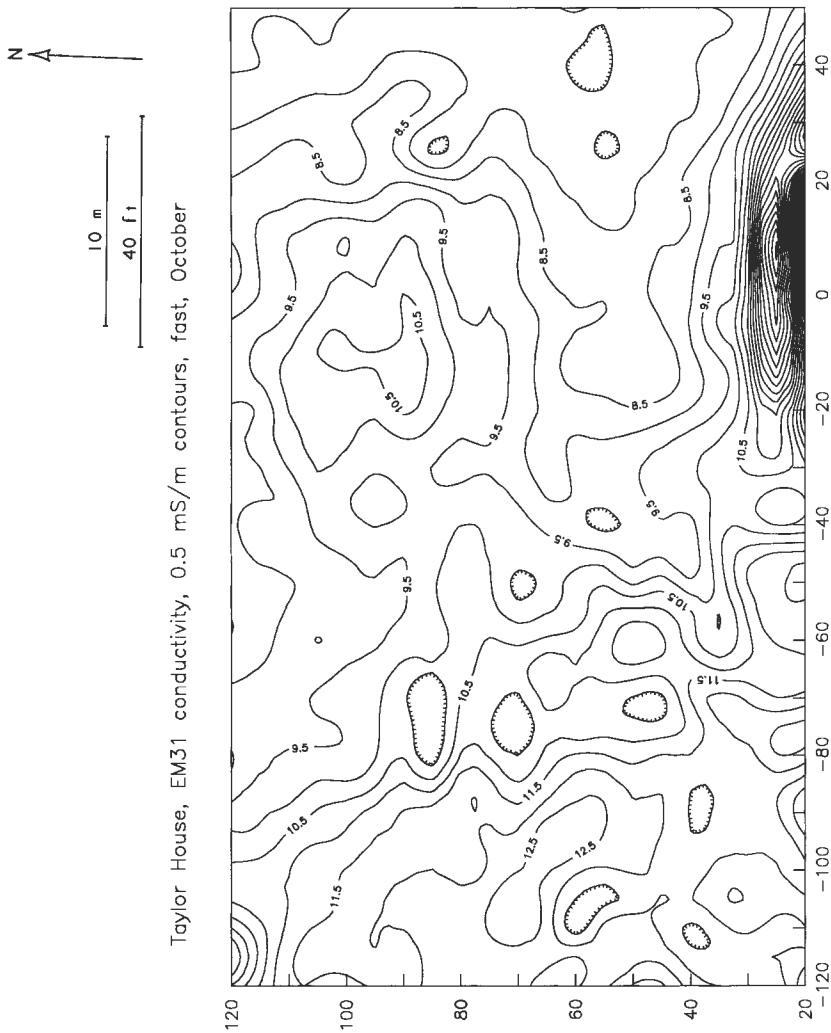

Fig. B63: A second, fast survey of the Taylor House.

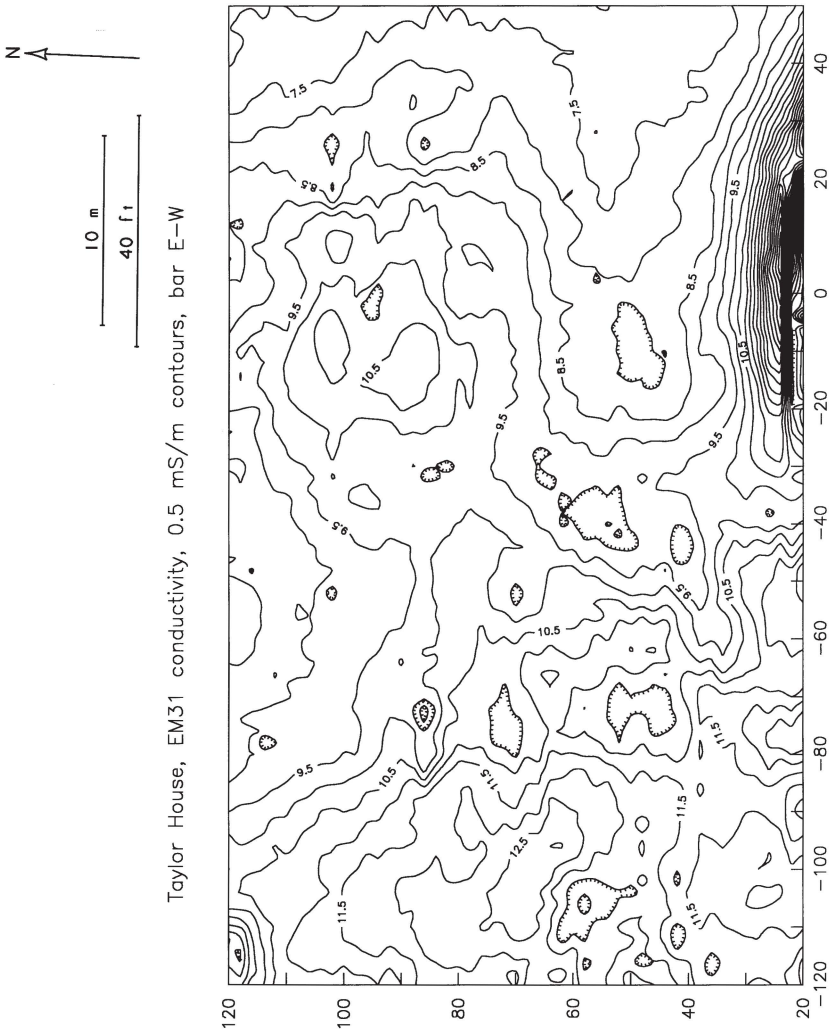

Fig. B64: Conductivity with the EM31 oriented east-west.

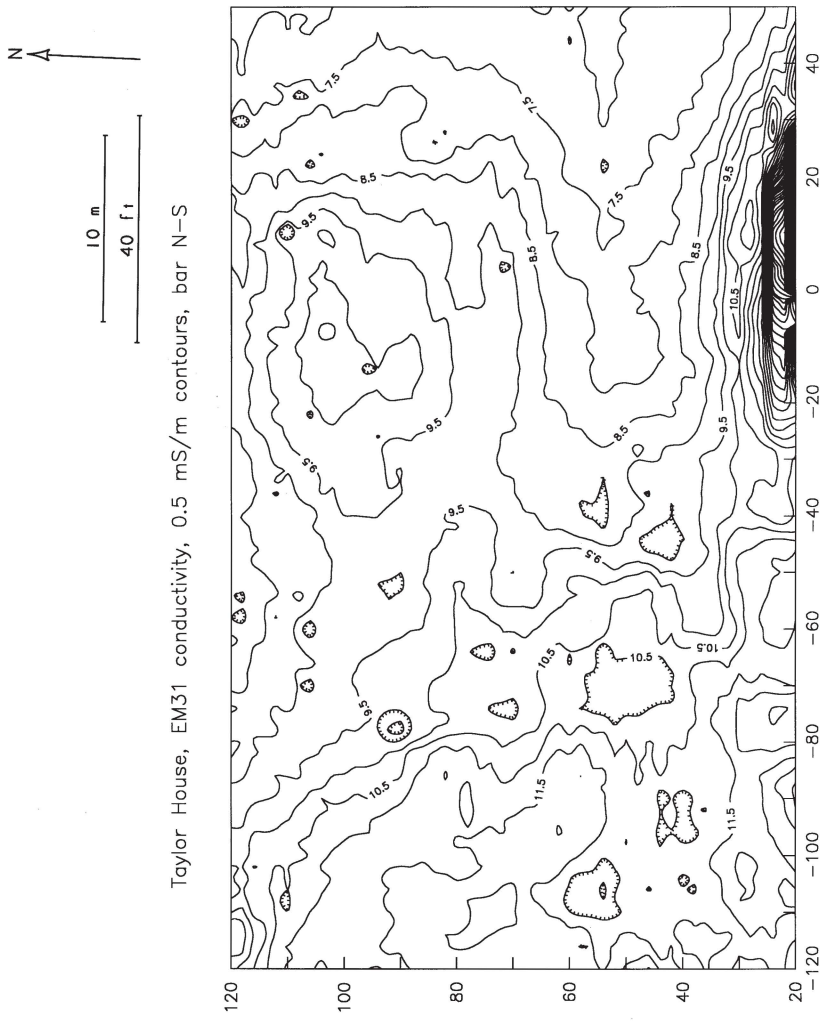

Fig. B65: Conductivity with the bar of the EM31 north-south.

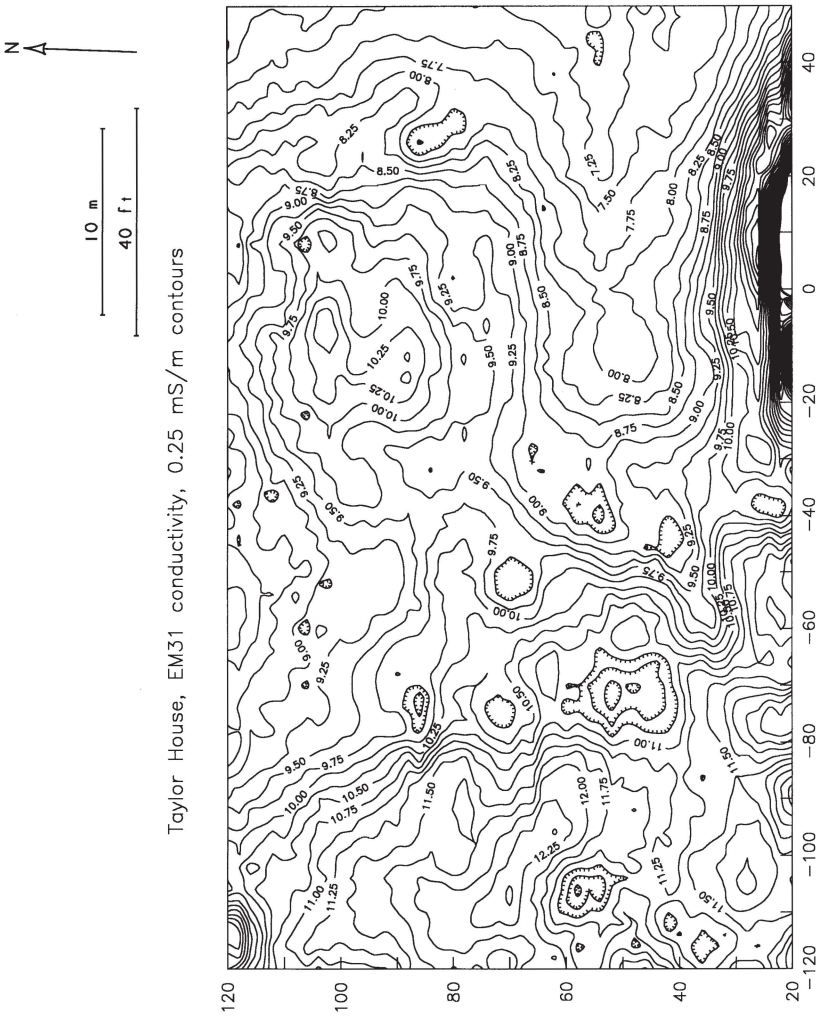

Fig. B66: An average of the two EM31 surveys. This somewhat smooths the map. A high conductivity anomaly is at W10 N100.

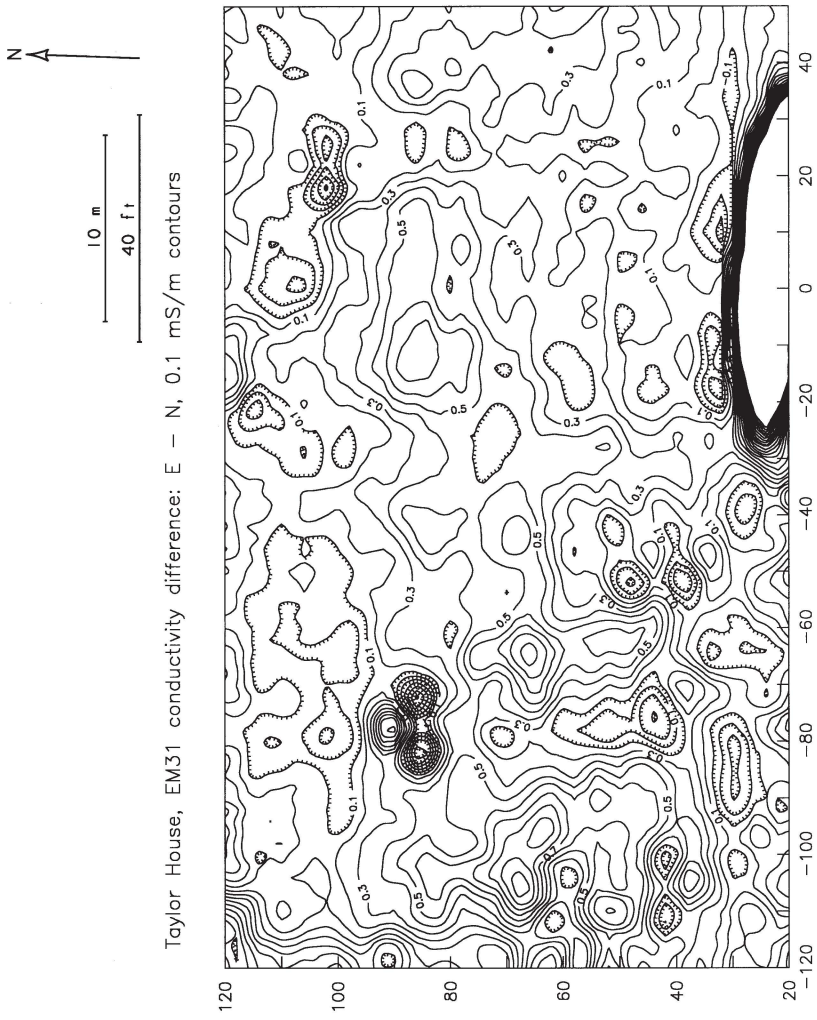

Fig. B67: The differences between the two EM31 orientations.

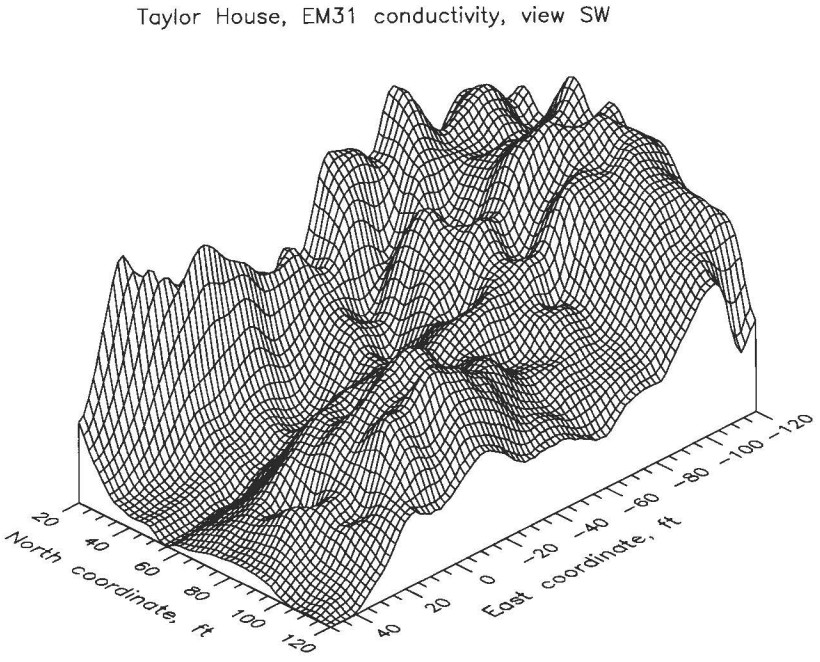

Fig. B68: A surface map of EM31 conductivity. The high conductivity at the Taylor House cellar is in the foreground of this illustration. A pipe causes the high values at the left rear.

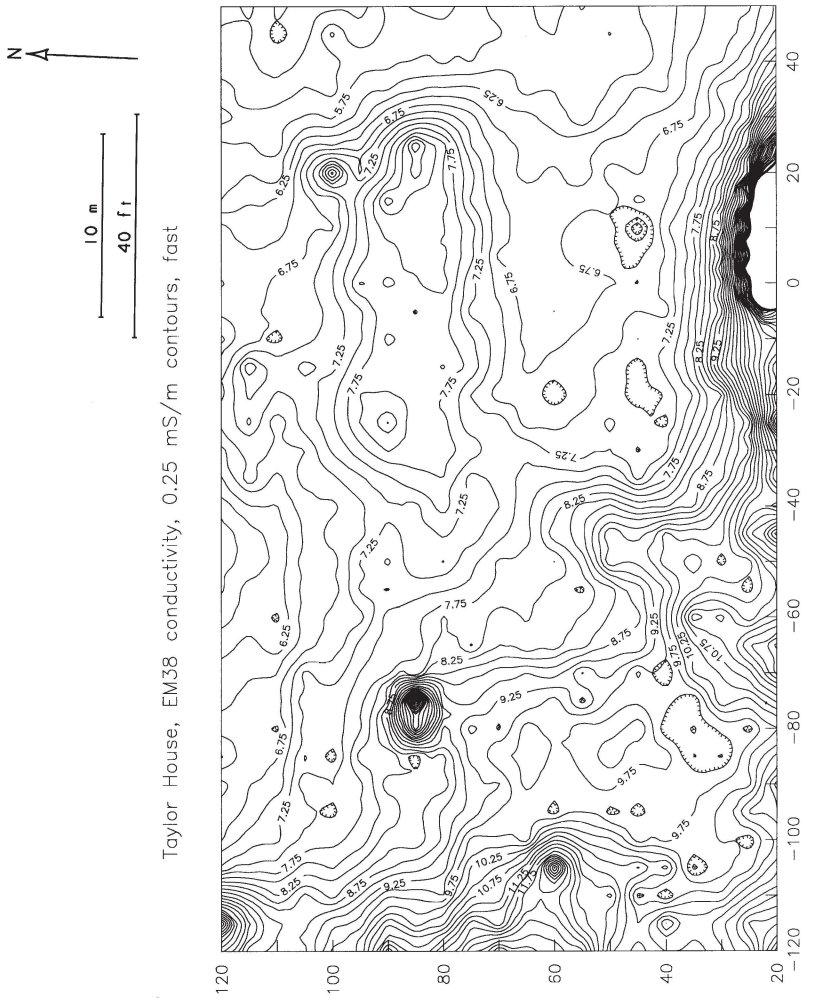

Fig. B69: A fast EM38 survey with a moderately low resolution.

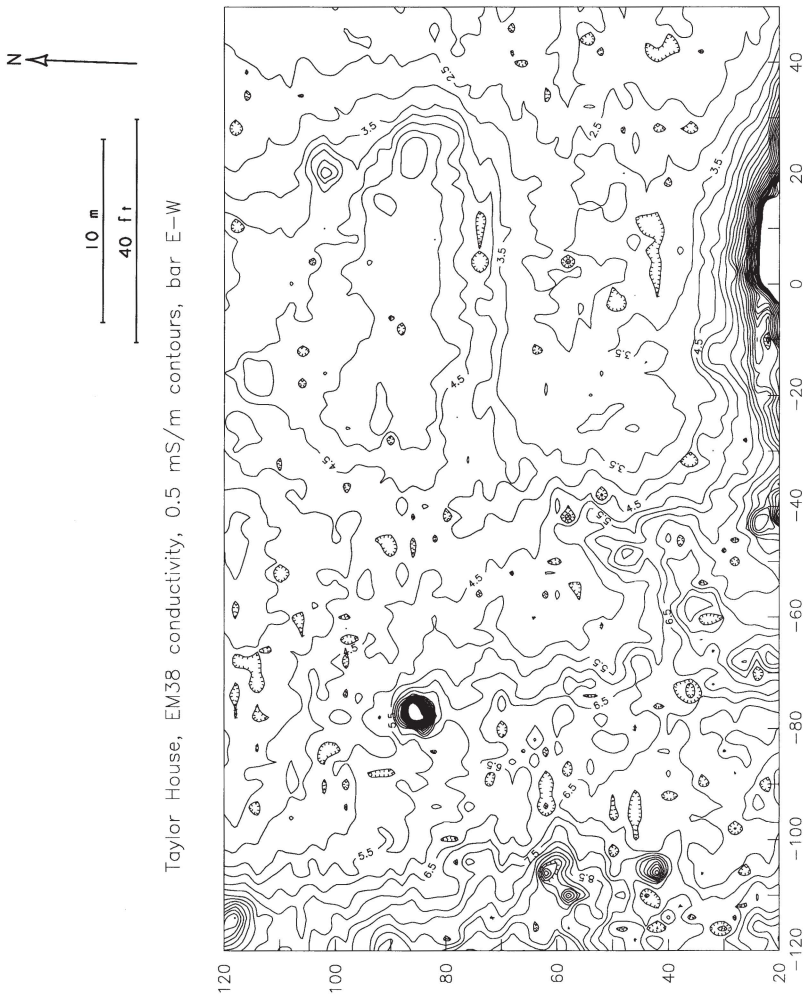

Fig. B70: A high resolution EM38 survey with the bar east-west.

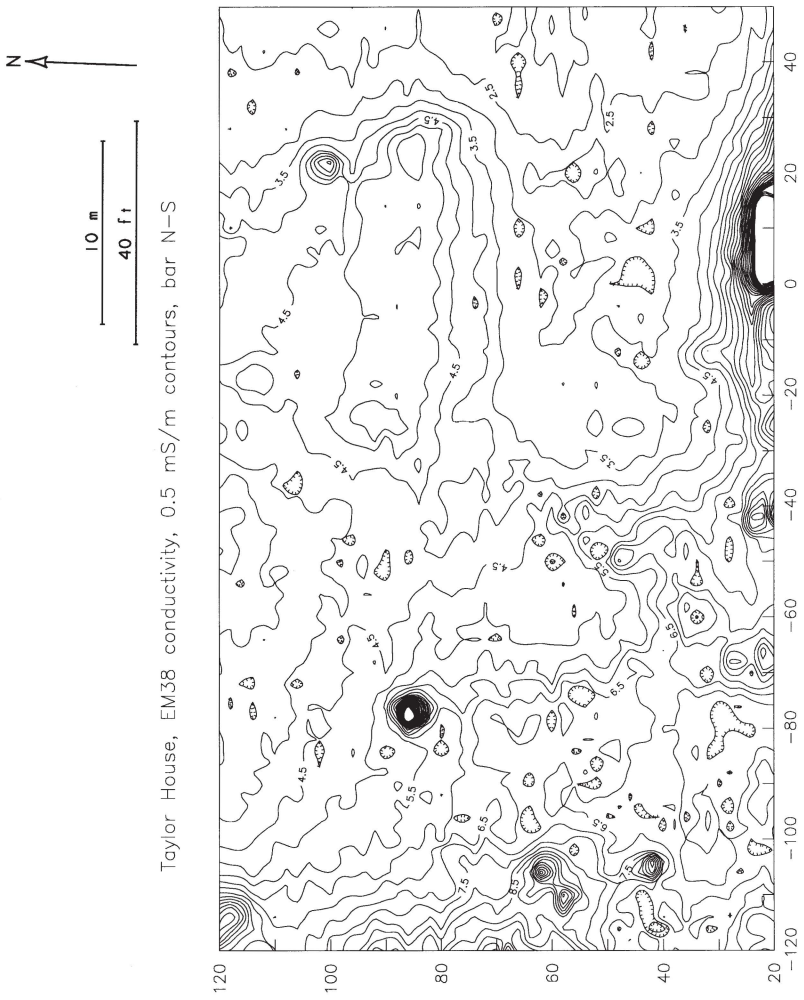

Fig. B71: A second survey with the bar of the EM38 north-south.

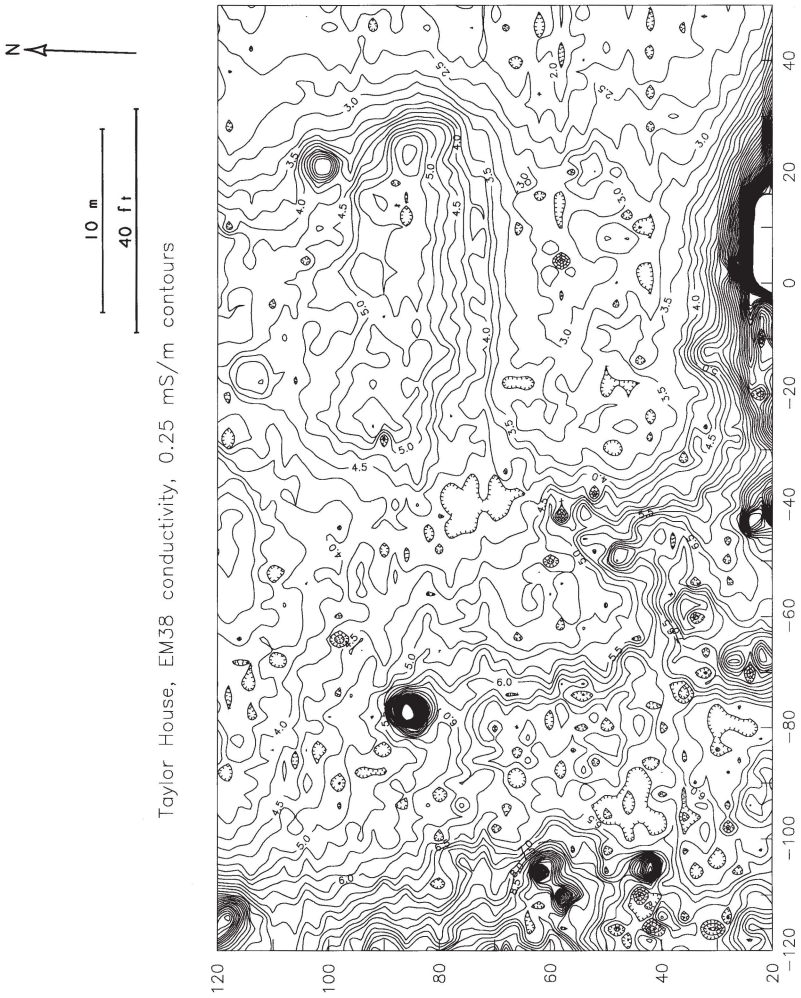

Fig. B72: The average of the two EM38 conductivity surveys.

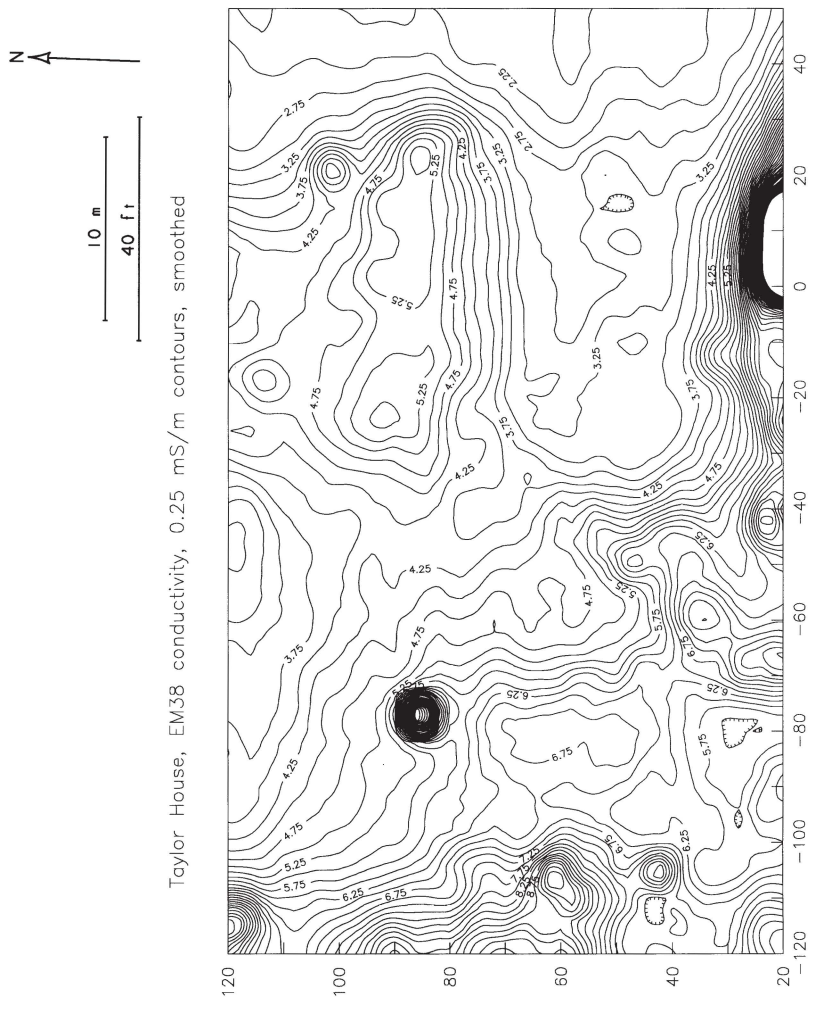

Fig. B73: A smoothed EM38 conductivity map of the Taylor House.

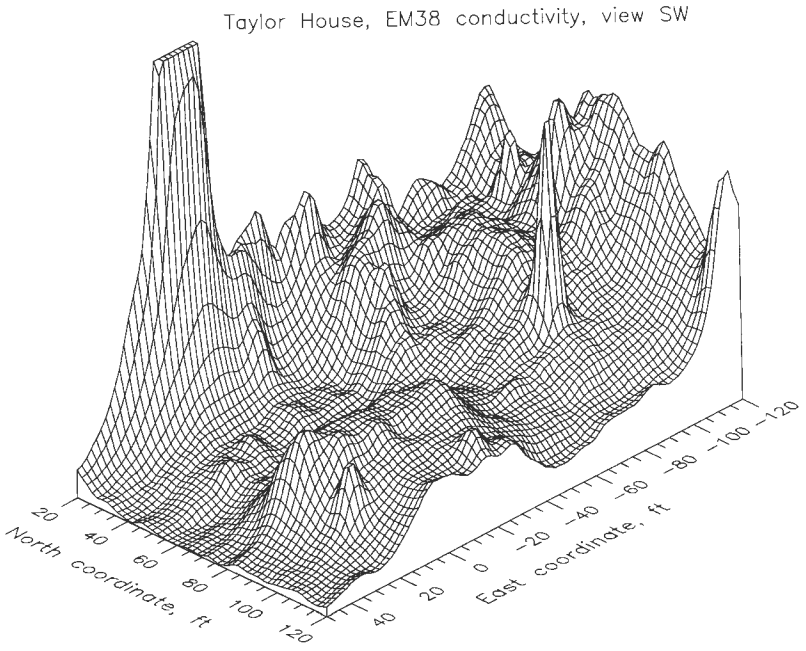

Fig. B74: A surface map of the EM38 conductivity. The rise near the front corner of this view is located at the Taylor House cellar.

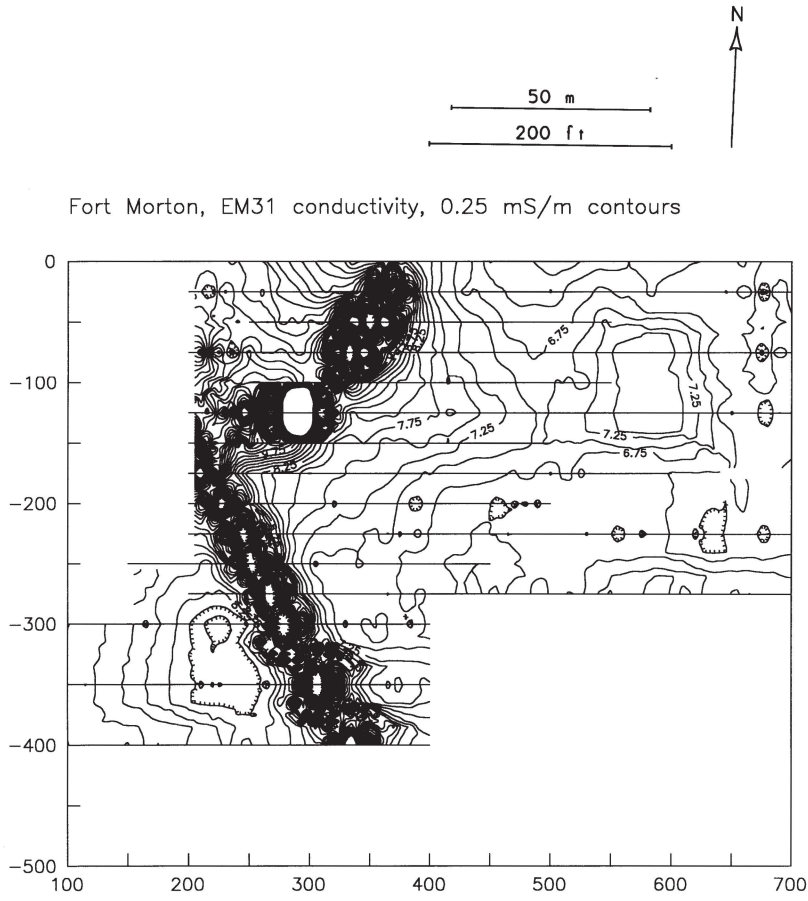

Fig. B75: Initial EM31 test lines in the Fort Morton area. The actual lines of survey are marked with straight lines.

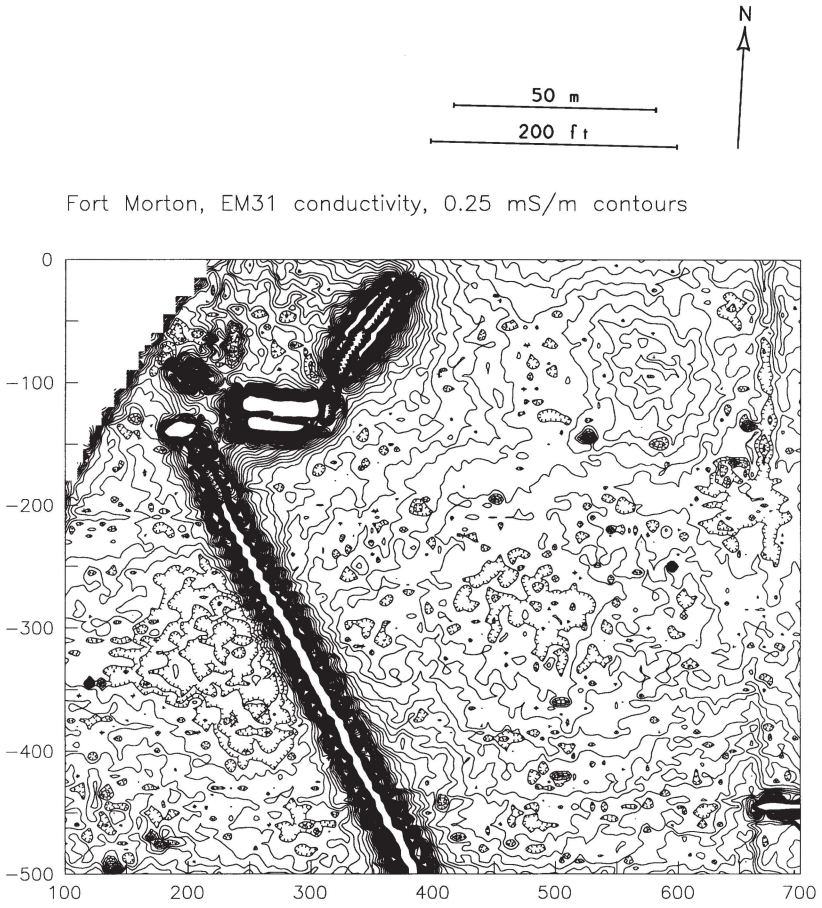

Fig. B76: The deep conductivity at Fort Morton. The strong linear patterns are caused by buried pipes and a wire.

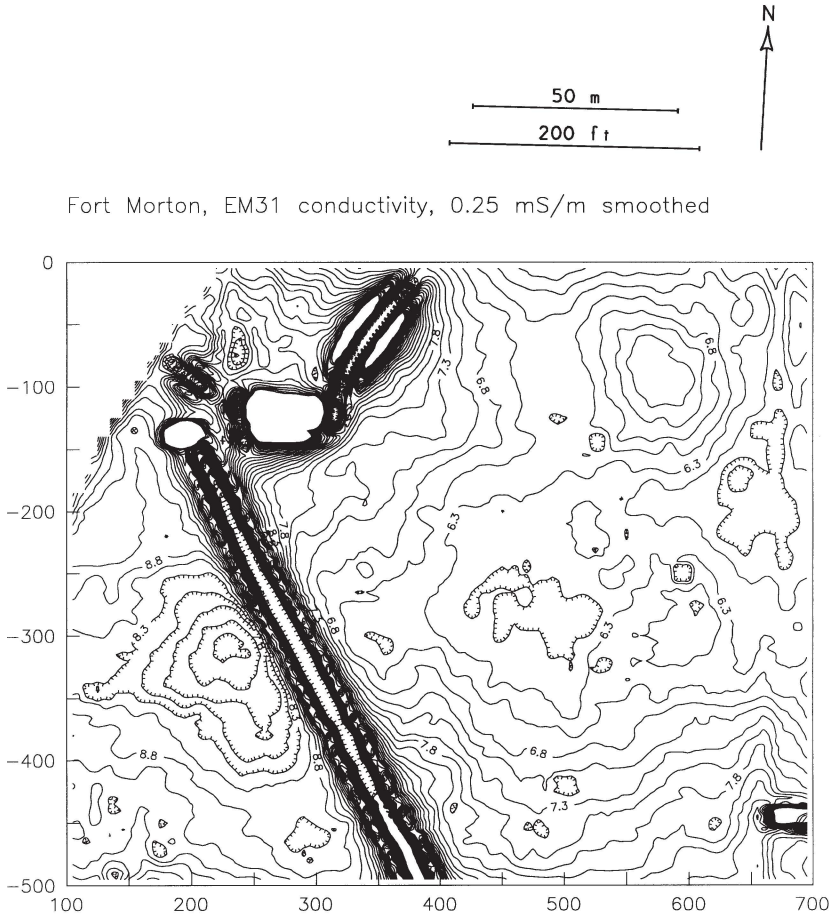

Fig. B77: A smoothed contour map. This clarifies the large patterns in the EM31 conductivity map.

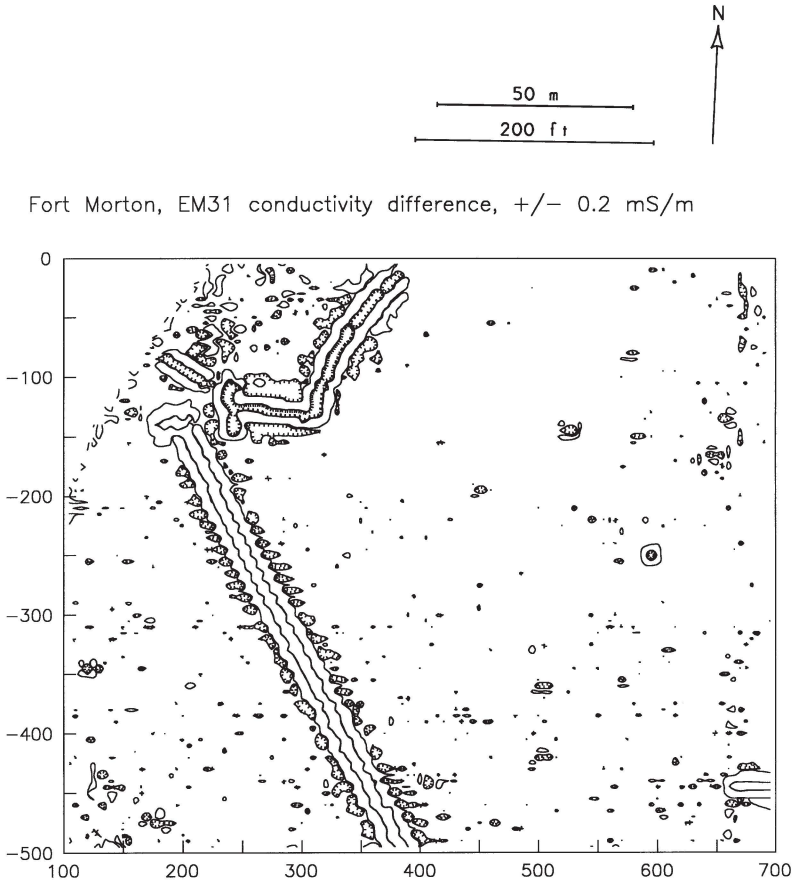

Fig. B78: A difference map. This map isolates many of the metallic objects in the area; the difference between Fig. B76 and Fig. B77 is plotted here.

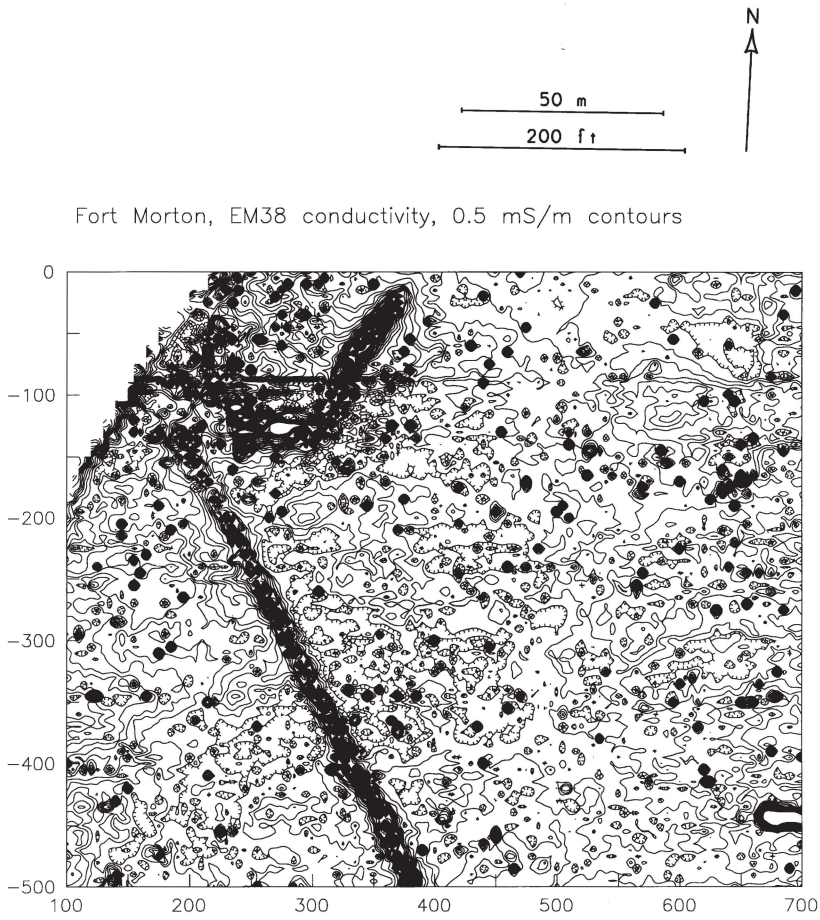

Fig. B79: Shallow conductivity features at Fort Morton. This map was measured with the EM38 instrument.

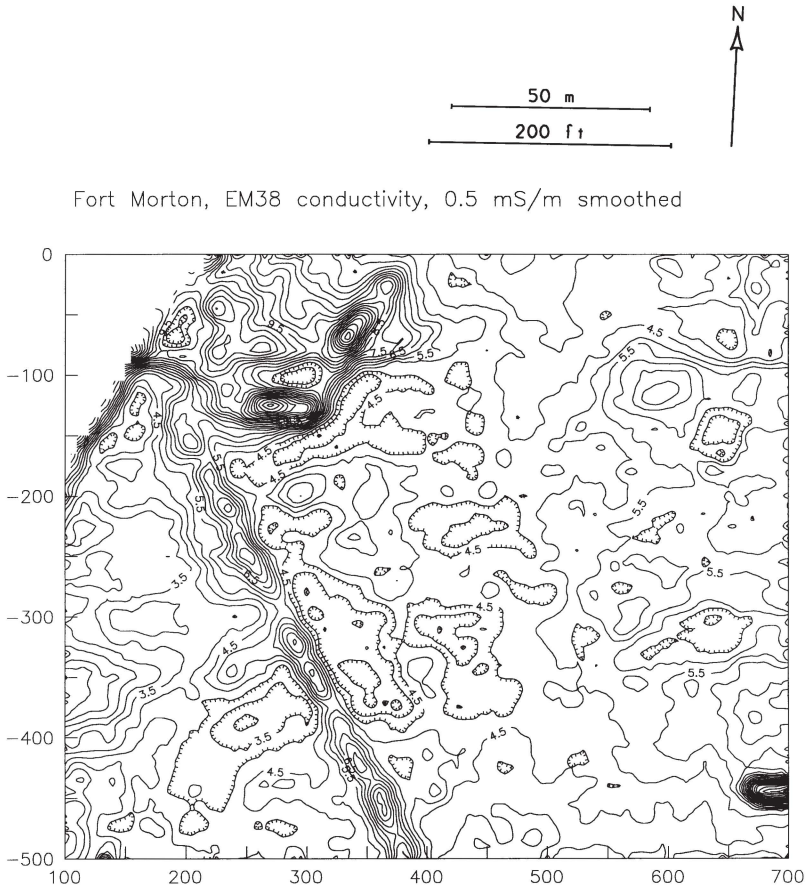

Fig. B80: A smoothed EM38 conductivity map. While the effects of small metal objects have disappeared, the large patterns are now very clear.

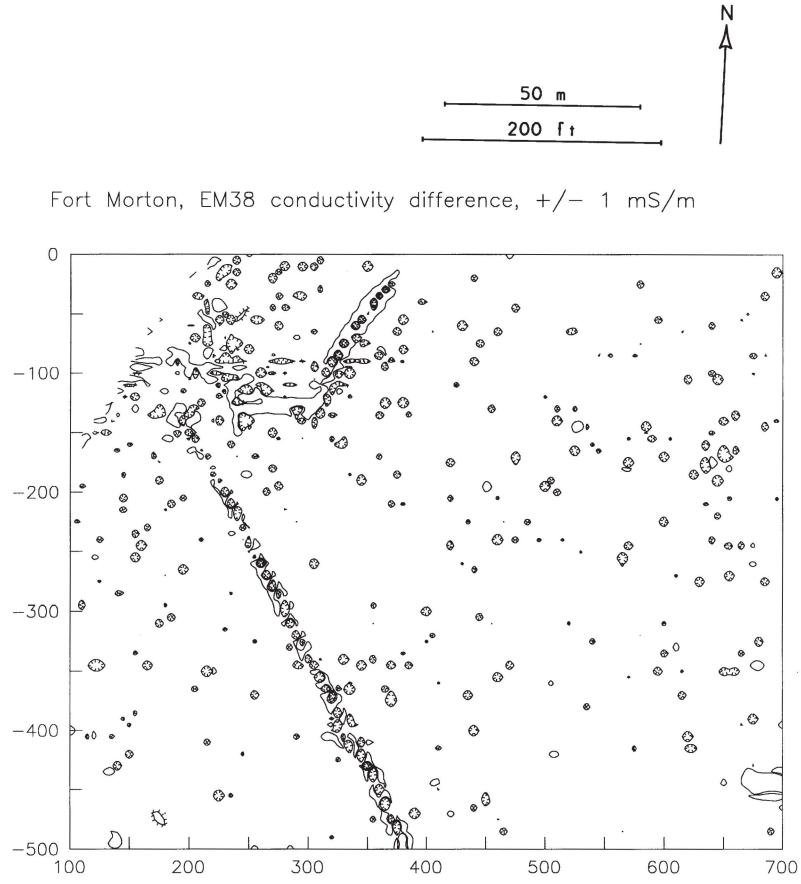

Fig. B81: Small metal objects in the Fort Morton grid. They are revealed by the circular patterns in this map.

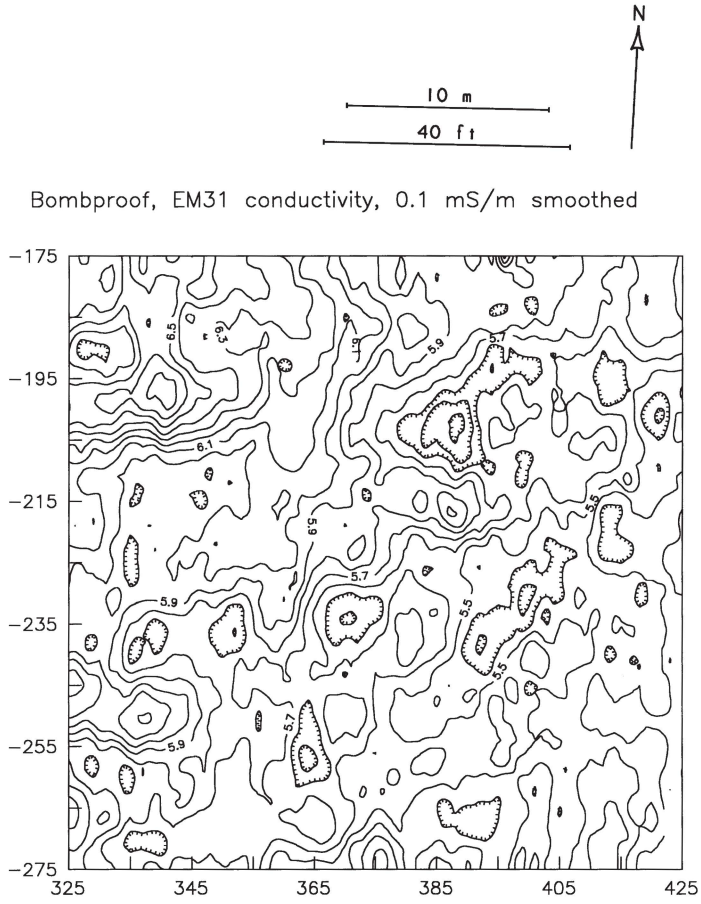

Fig. B82: The deep conductivity in the Bombproof detail. It shows high conductivity values at the two powder magazines near the left side of the survey area.

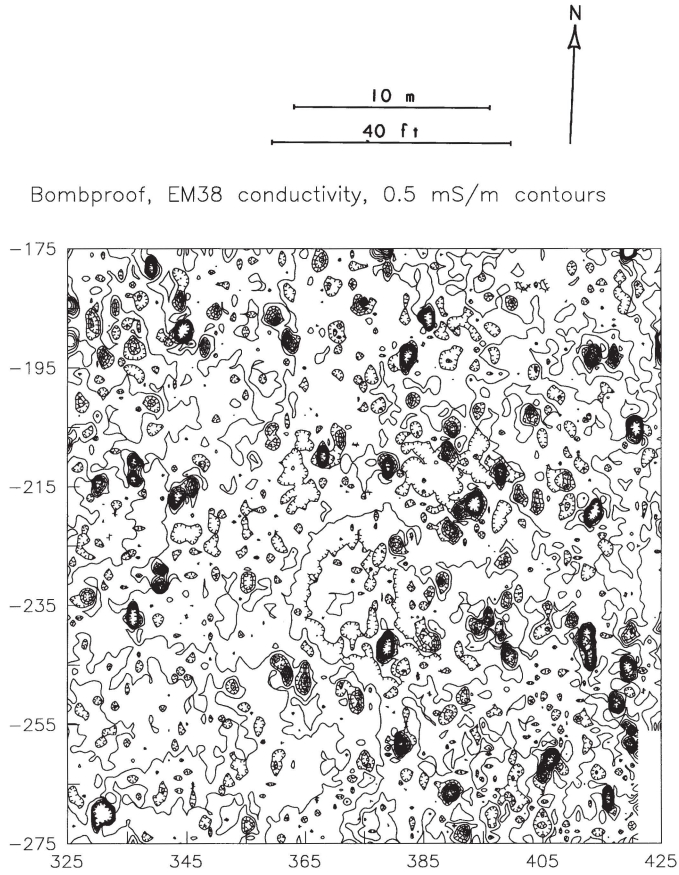

Fig. B83: The EM38 conductivity within the Bombproof detail. It is likely that shallow metal objects are the cause of the many oval anomalies.

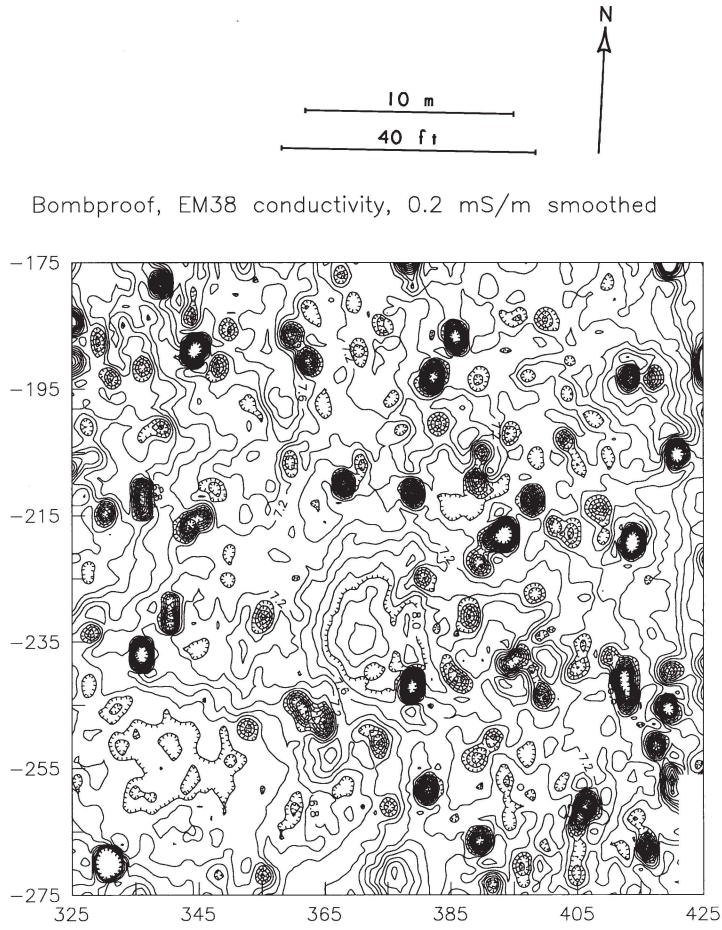

Fig. B84: A smoothed EM38 map. Some of the anomalies with a larger area are clearer in this map.

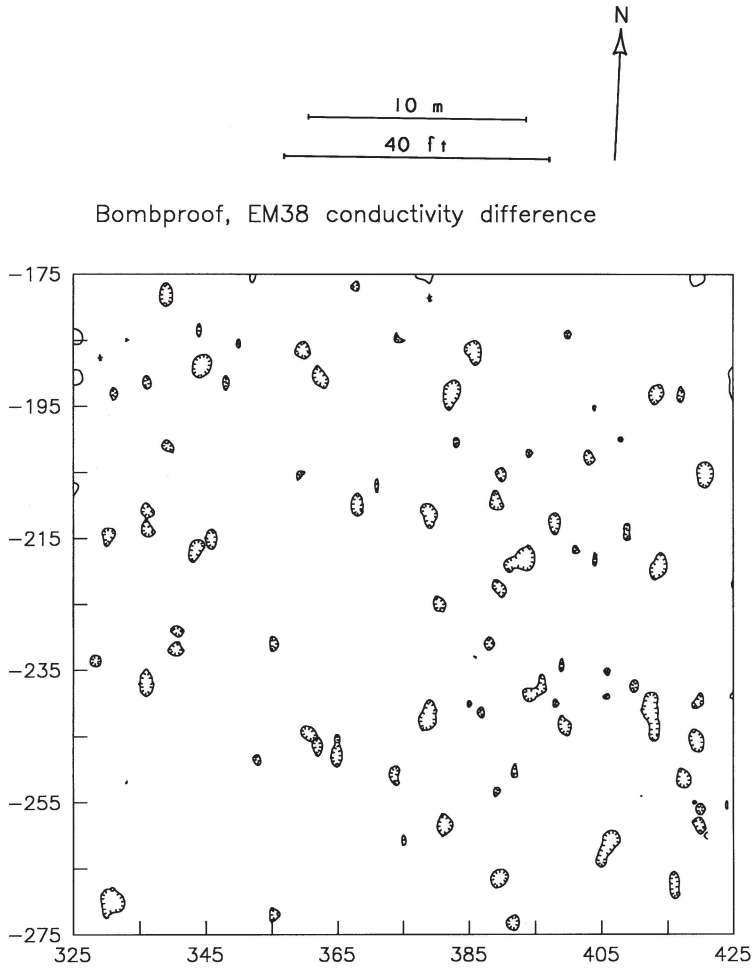

Fig. B85: A conductivity difference map. Small features, primarily metal objects, are located by this map as low values.

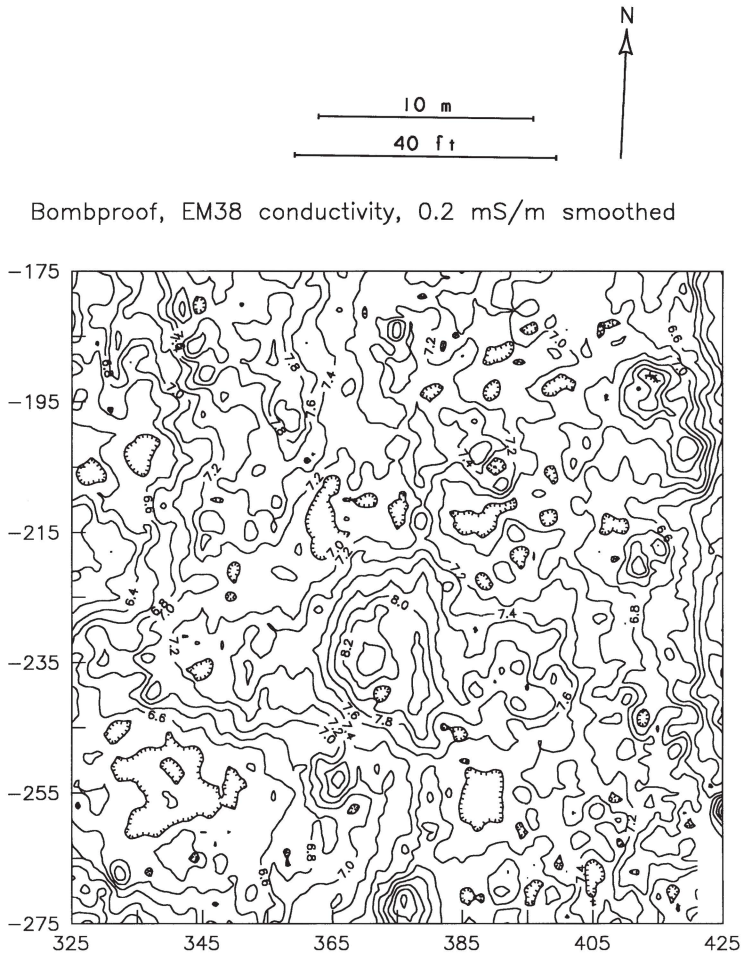

Fig. B86: After removal of the small-area anomalies. The patterns which remain are caused by larger or deeper features.

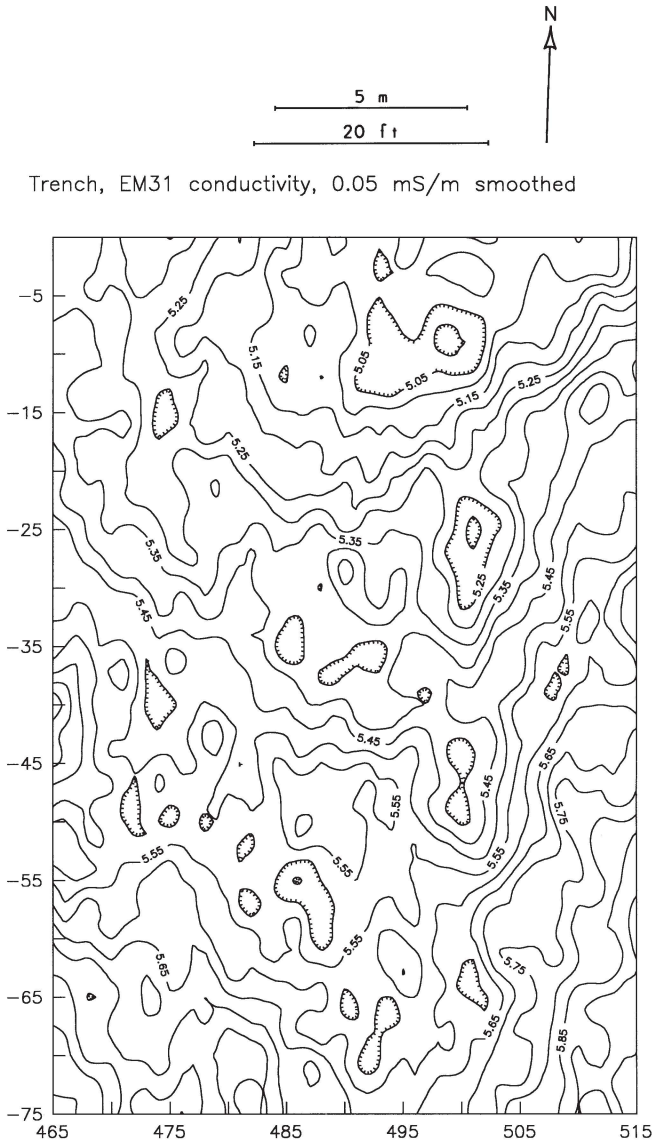

Fig. B87: The EM31 conductivity of the Trench detail. This map reveals a lateral gradient and a line of lows near E500.

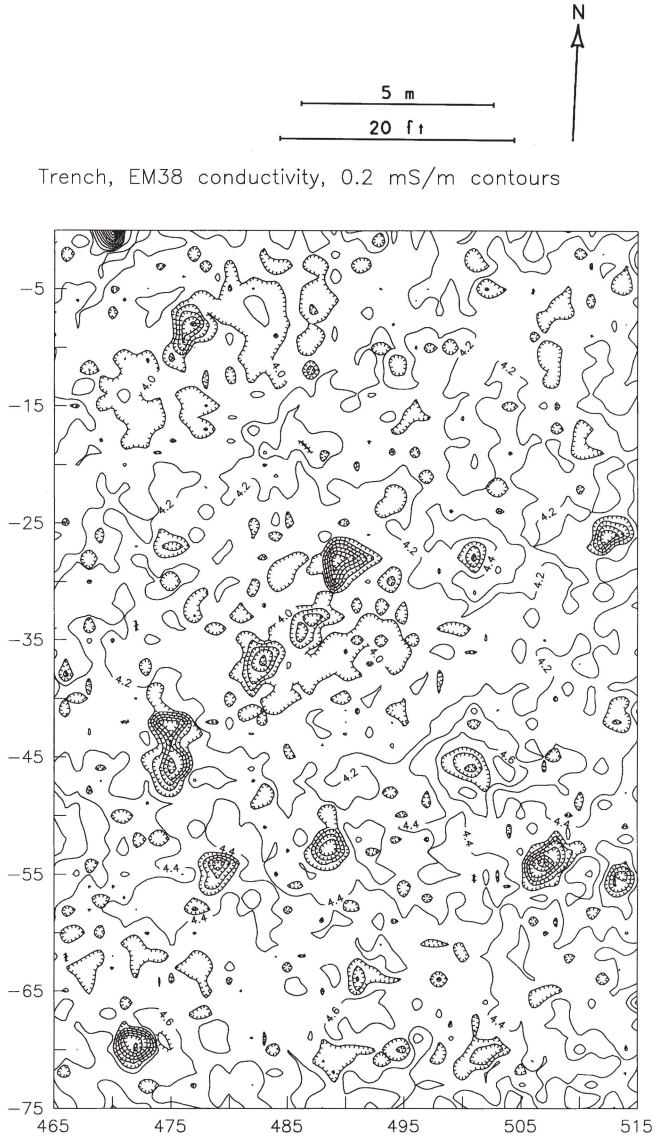

Fig. B88: An EM38 conductivity map of the Trench detail. It is likely that many metal objects are revealed here.

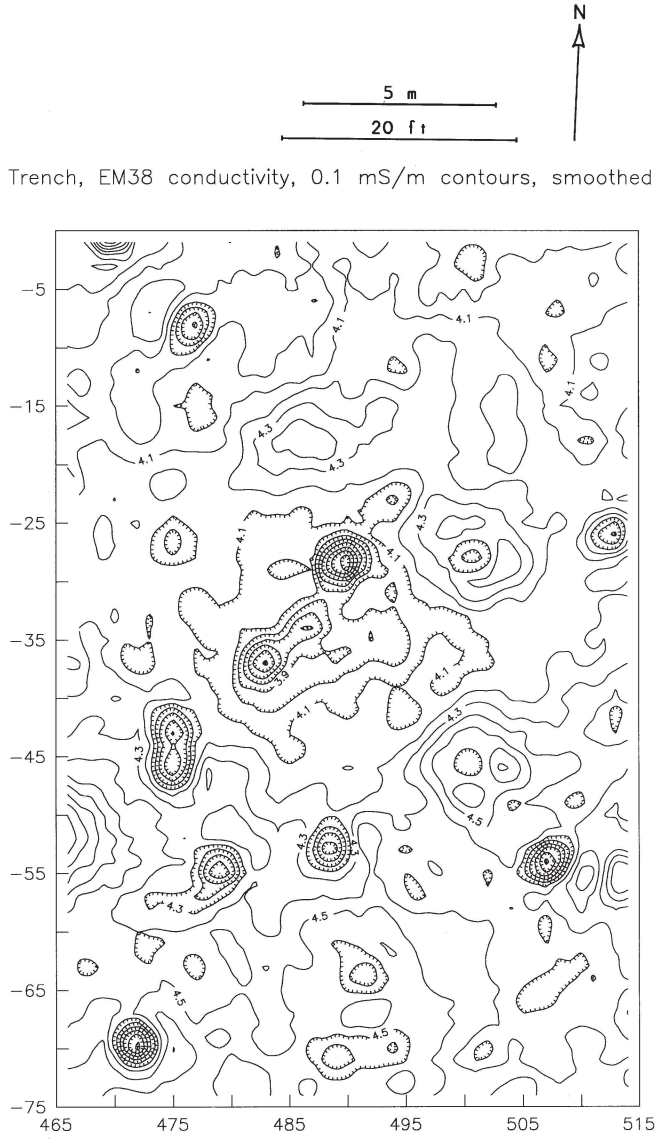

Fig. B89: The smoothed measurements of EM38 conductivity. This shows some patterns more clearly.

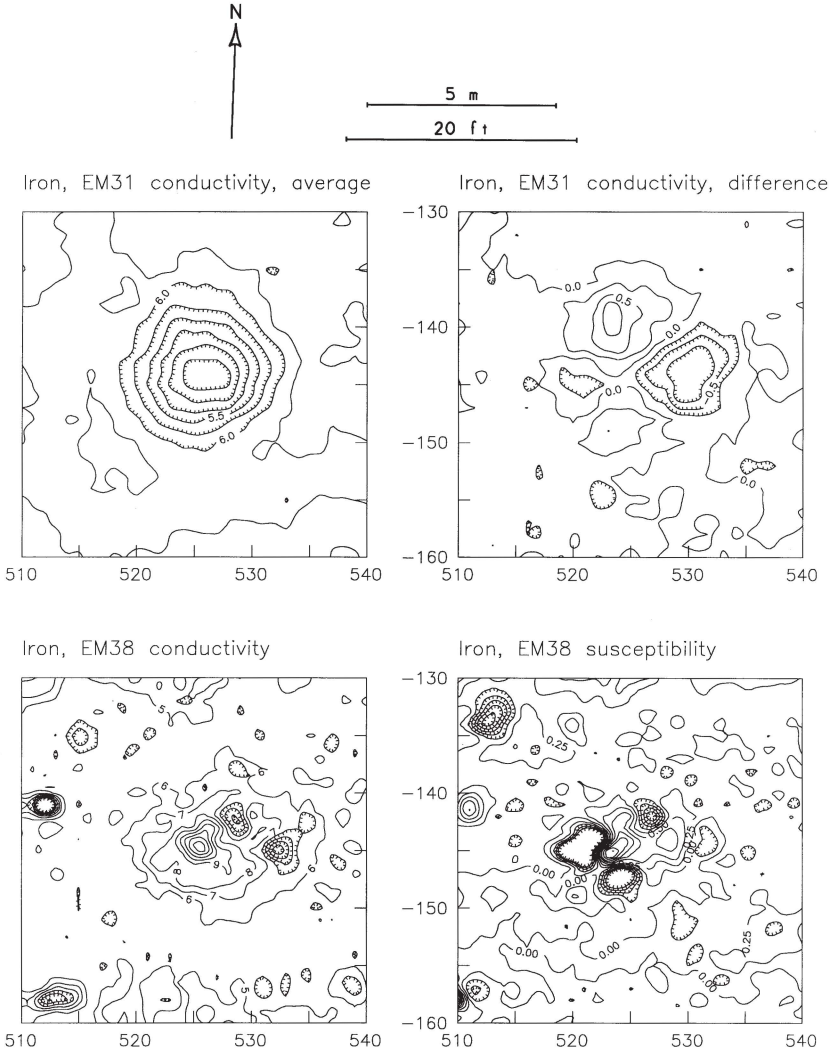

Fig. B90: EM31 and EM38 maps of the small Iron detail.

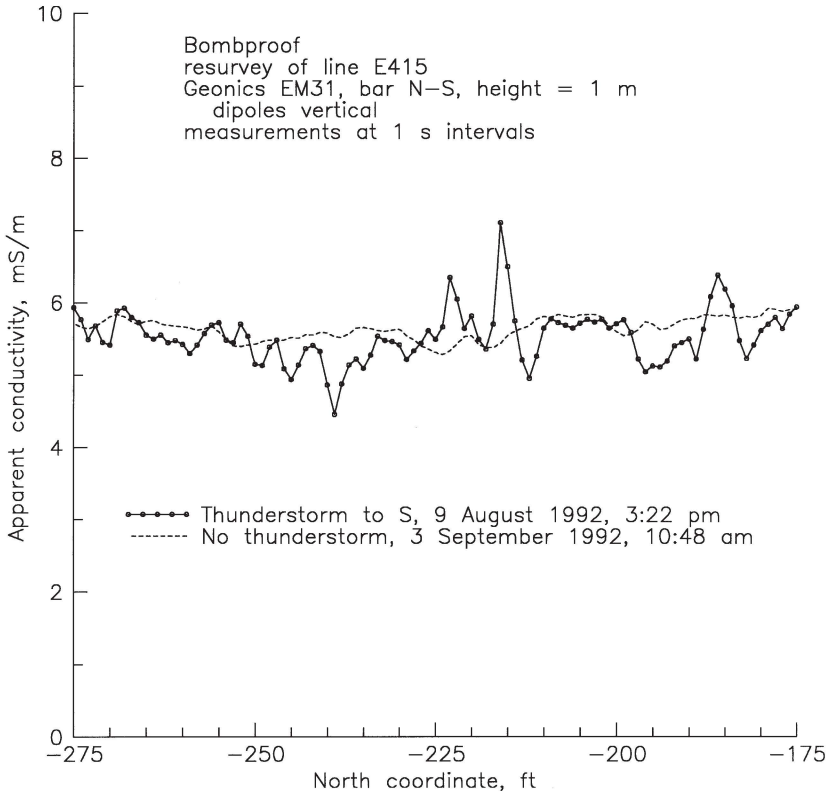

Fig. B91: Lightning noise. It can make it impossible to do EM surveys. The measurements with a nearby thunderstorm are unusable.

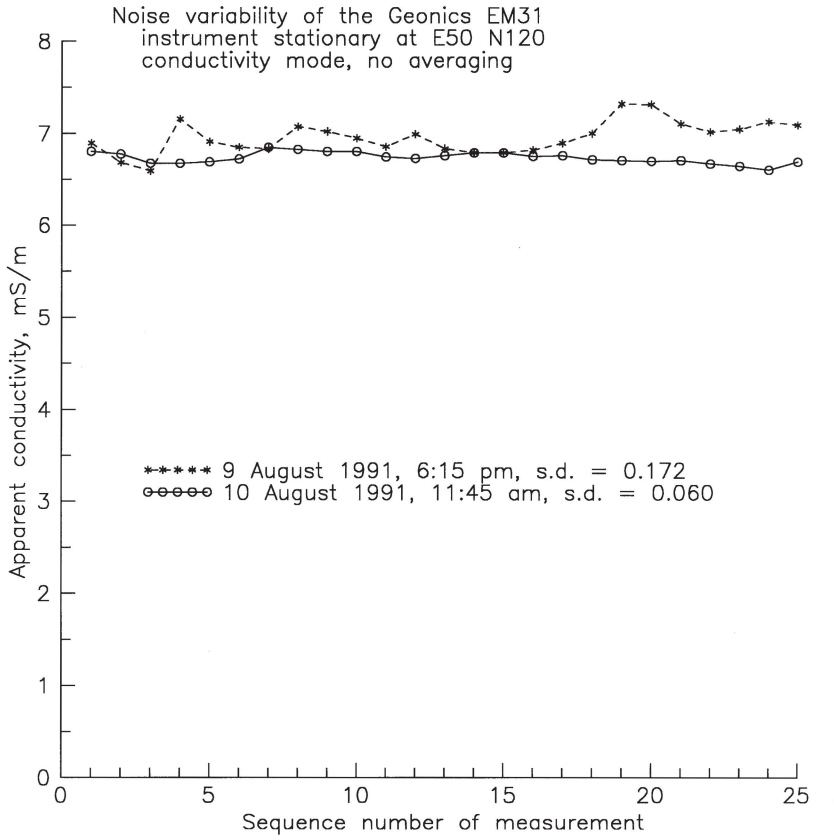

Fig. B92: Noisy and quiet measurements with the EM31 conductivity meter. The standard deviation of the measurements are listed.

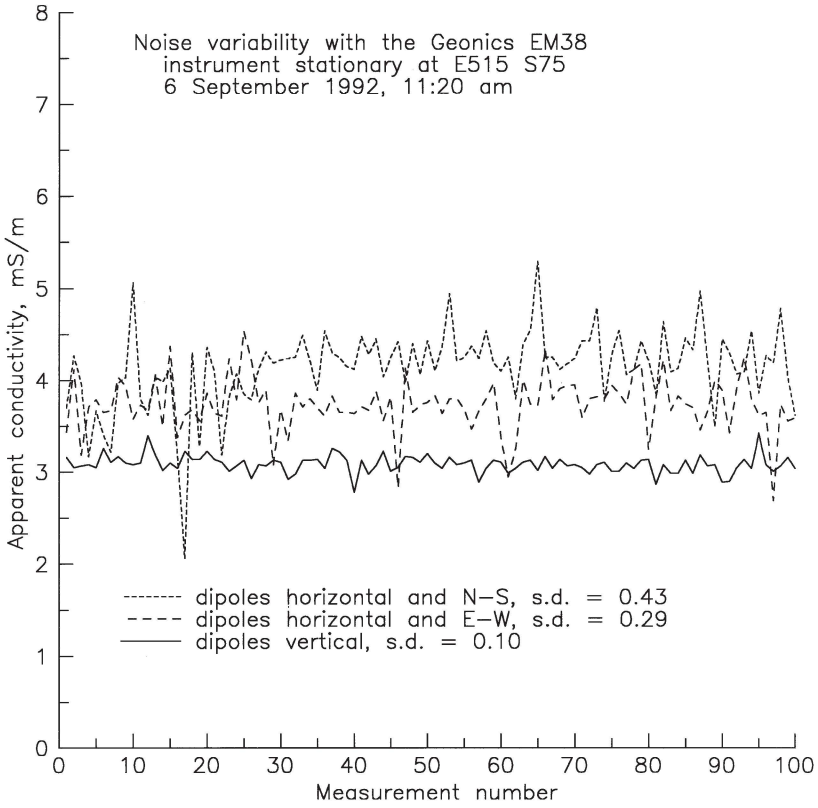

Fig. B93: EM38 noisiness on a rather typical day. It can be affected by the orientation of the instrument.

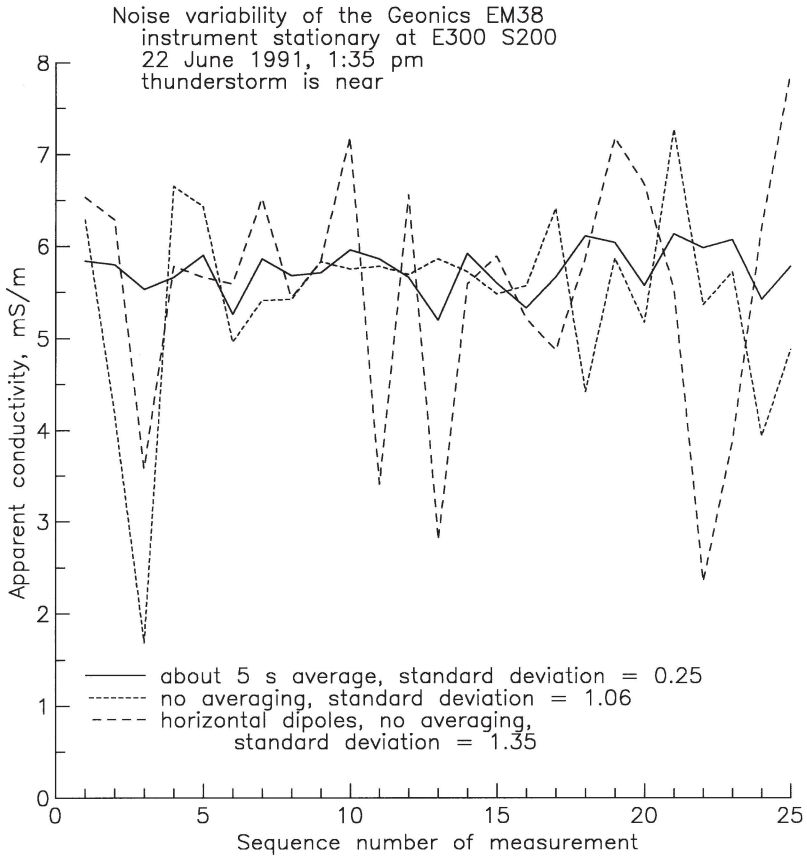

Fig. B94: EM38 noise detected when there was a thunderstorm nearby. The noise is reduced by averaging several measurements.

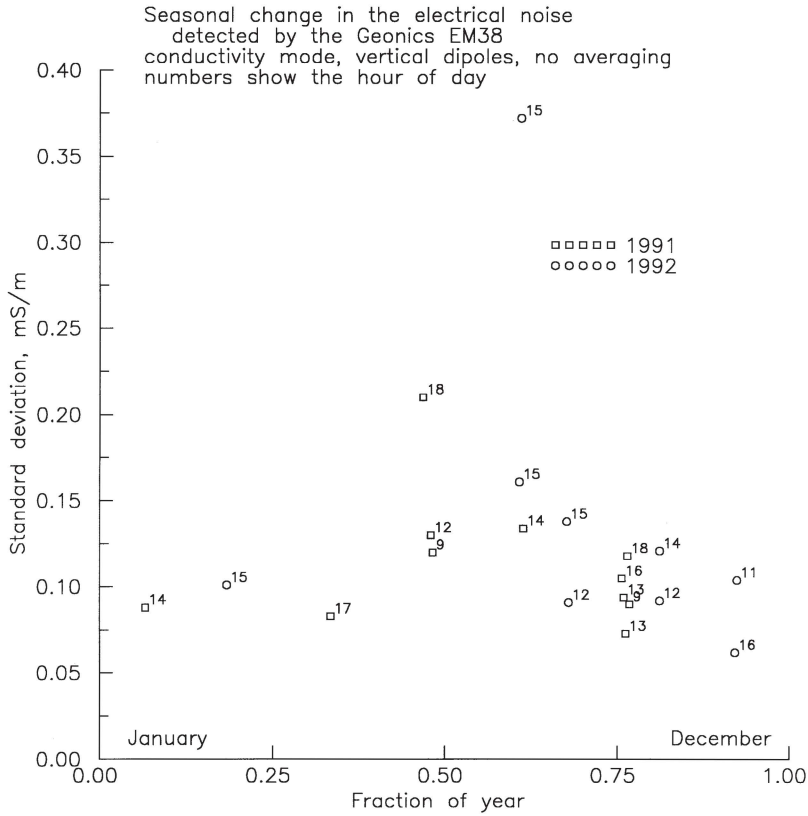

Fig. B95: Electrical noise detected by the EM38. It was highest in the summer months when thunderstorms are most frequent.

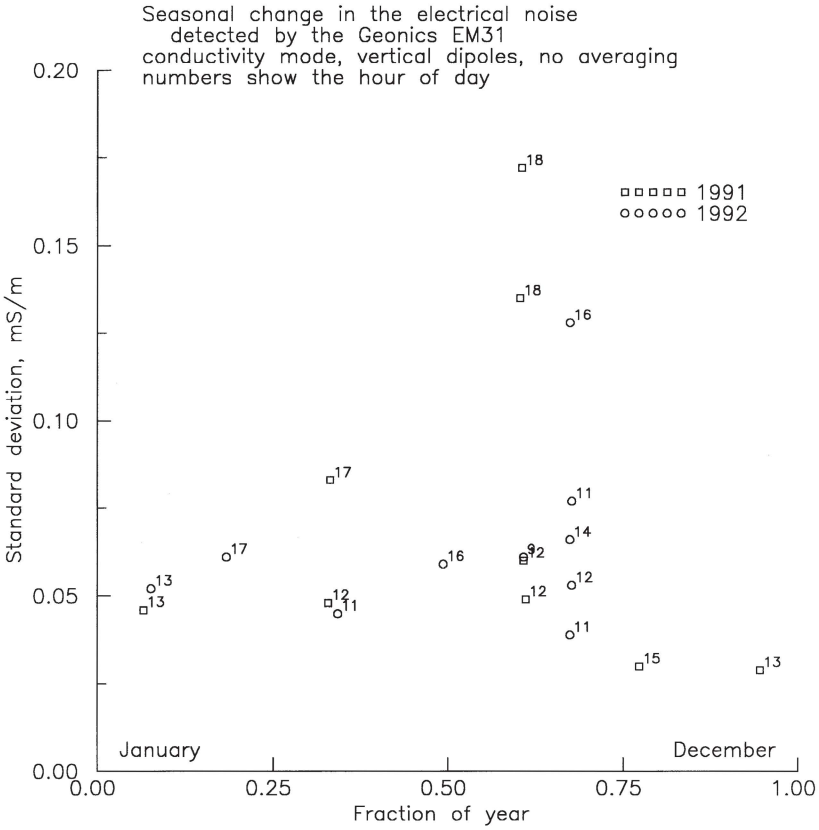

Fig. B96: Seasonal effect of noise detected by the EM31. While it is about half that found with the EM38, it is also highest in the summer.

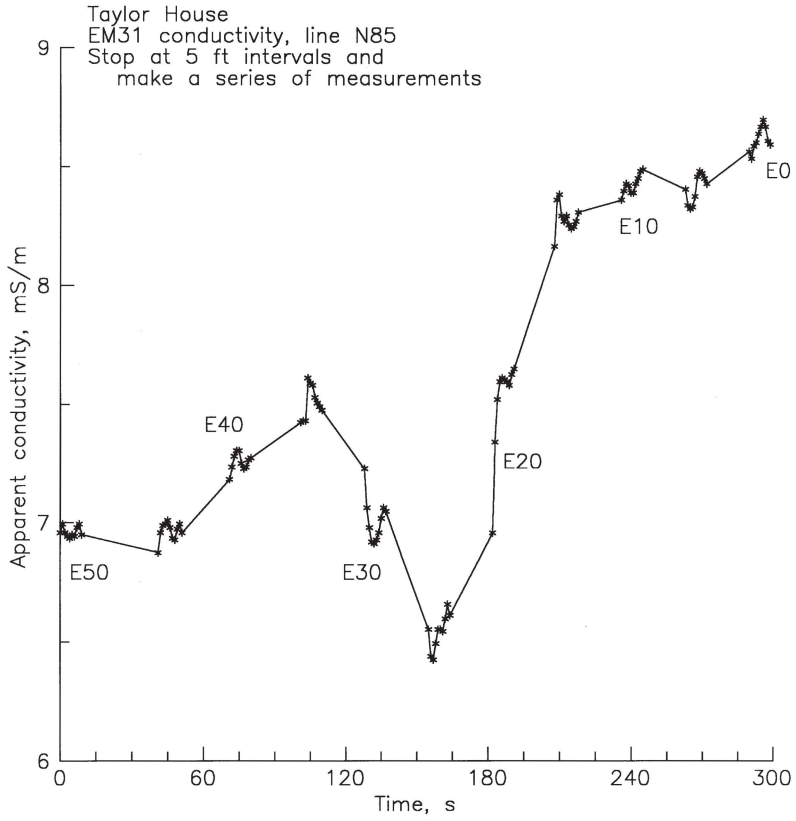

Fig. B97: Measurement lag with the EM31. After stopping to make a measurement with the EM31 conductivity meter, the measurements will change as the instrument's reading stabilizes to the correct value.

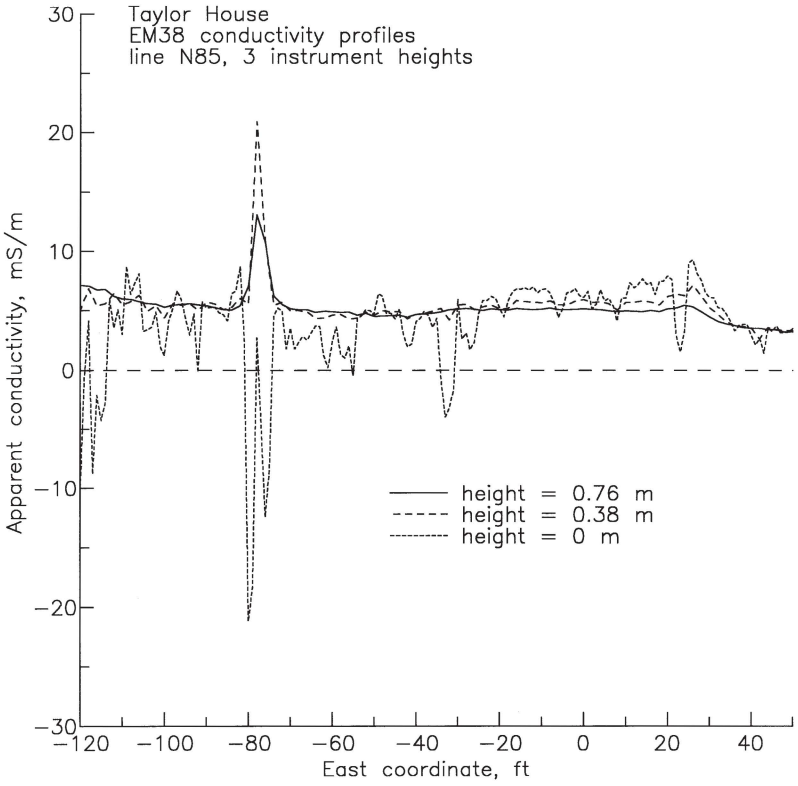

Fig. B98: The effect of elevation on the EM38. With increasing height, the reading of apparent conductivity decreases, as does the detection of small and shallow features.

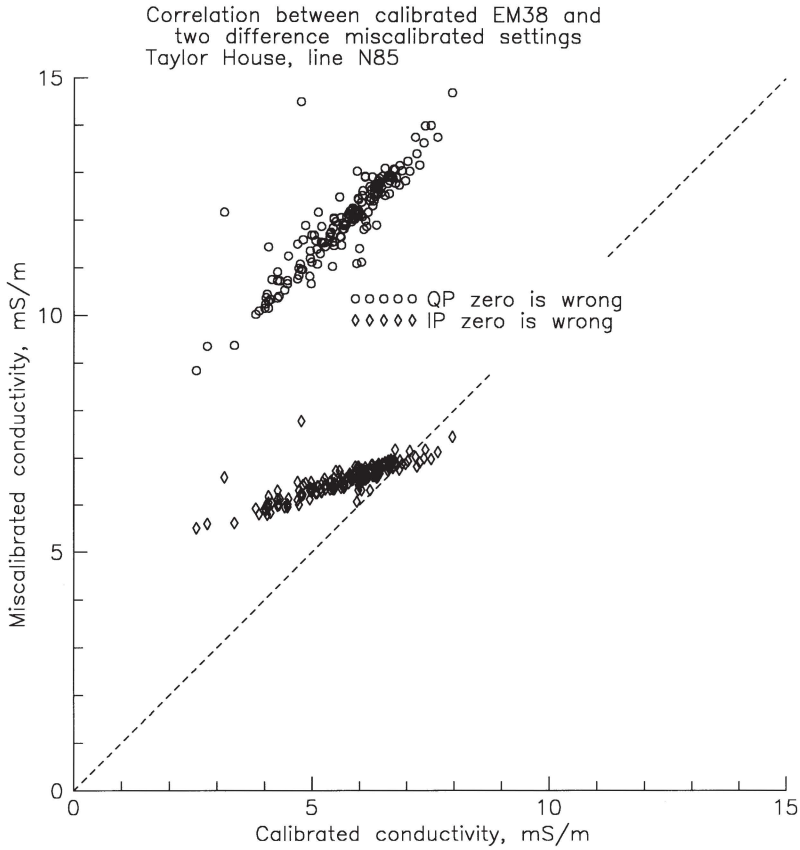

Fig. B99: The effect of the two calibration controls on the EM38. One adds a constant to the readings; the other multiplies them by a constant.

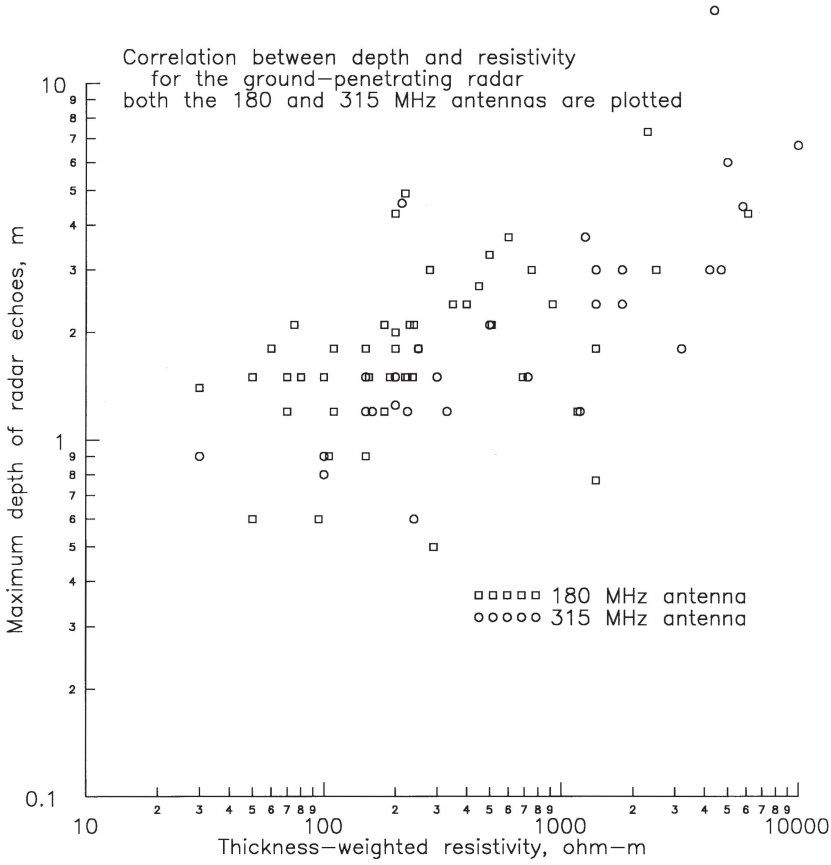

Fig. B100: The profiling depth of the radar, compared to soil resistivity. Higher resistivity means a greater profiling depth.

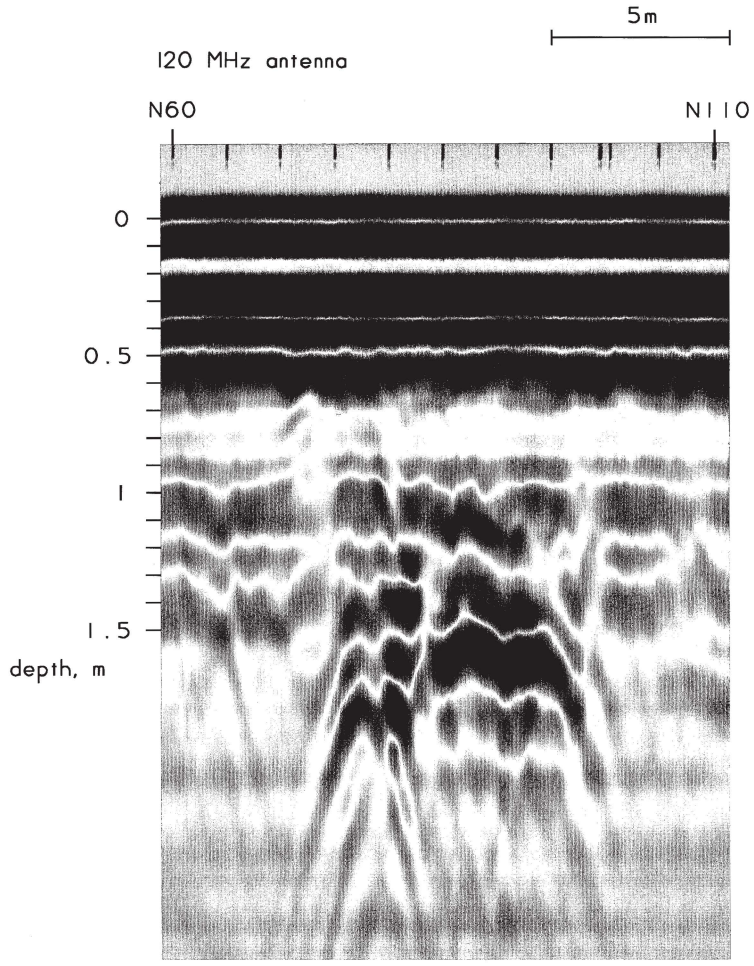

Fig. B101: A comparison of radar antennas. This profile was made over the Taylor House cellar with a low frequency antenna.

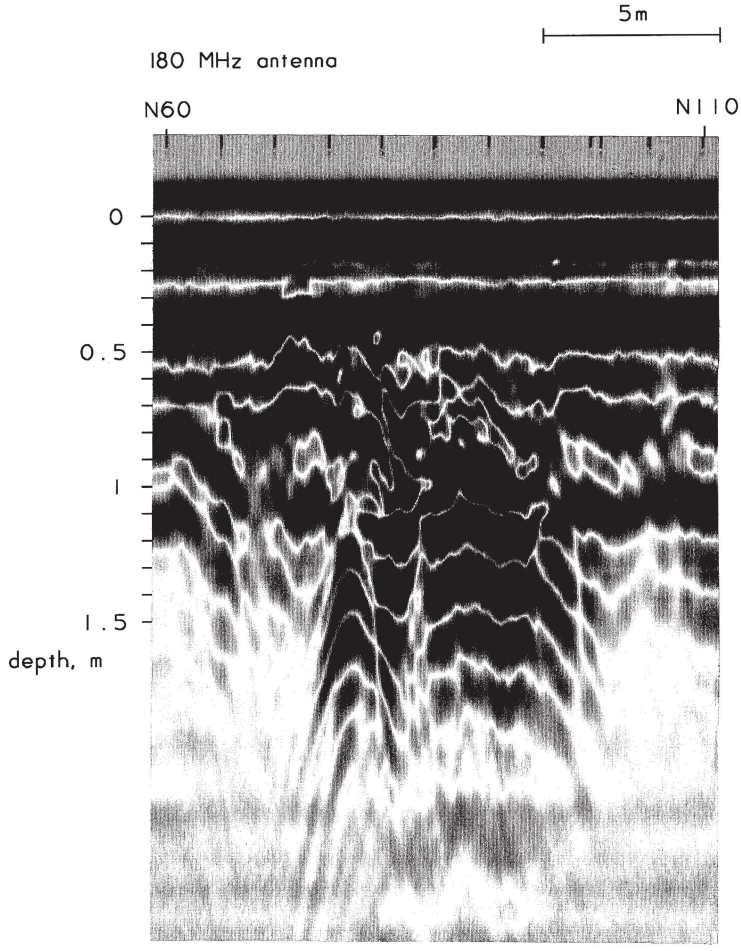

Fig. B102: A medium frequency antenna. It detects smaller and shallower features, although little in the upper 0.5 m of the soil.

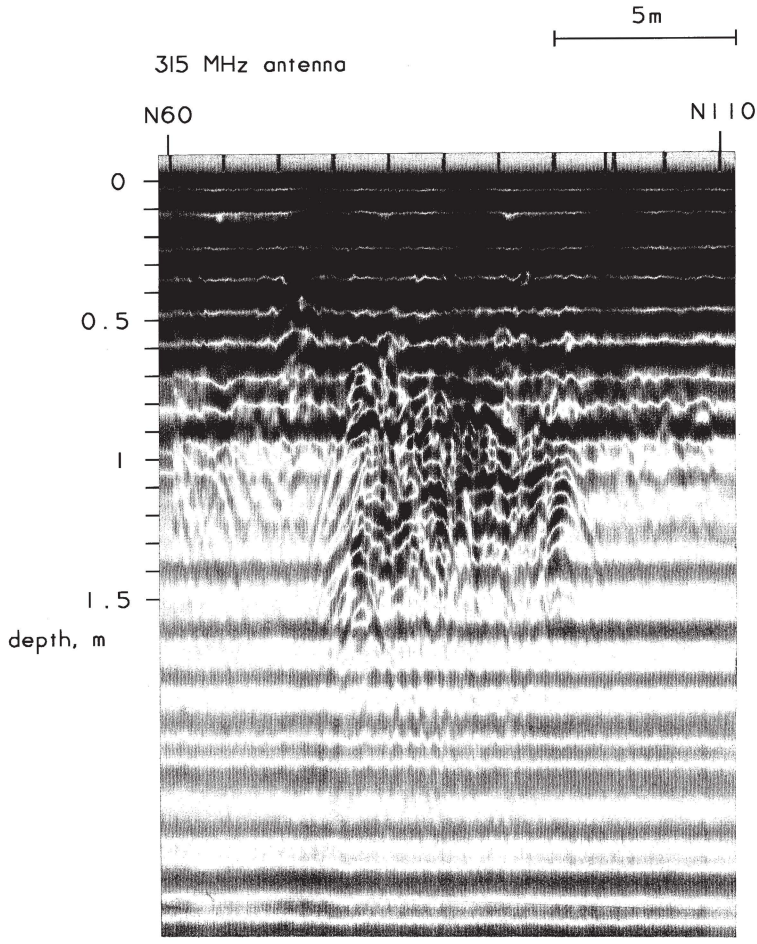

Fig. B103: A high frequency radar antenna. Quite small and shallow objects can be detected with it.

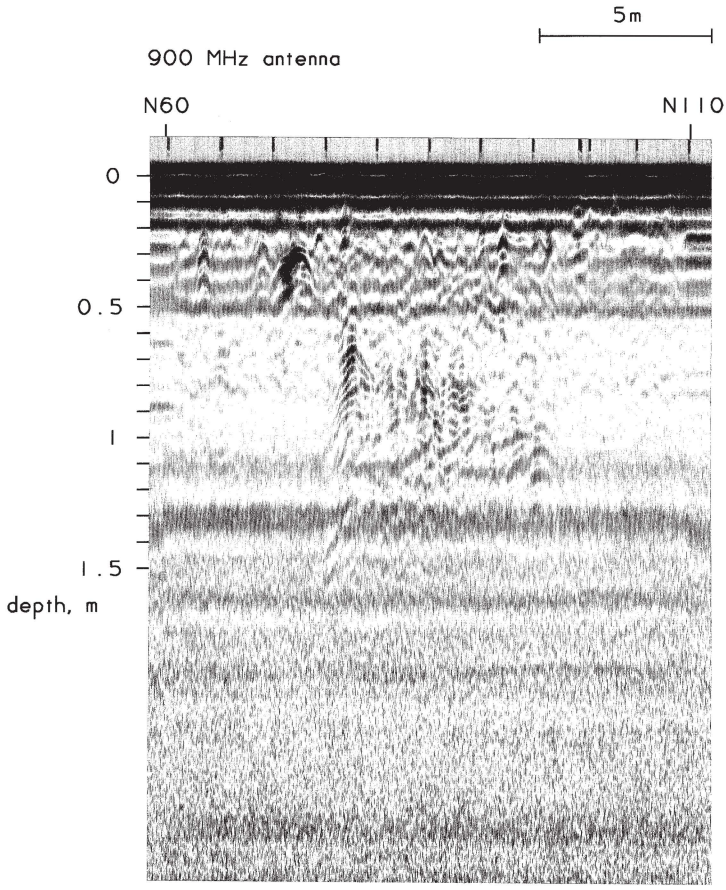

Fig. B104: A very high frequency antenna. While it readily detects very shallow features, deeper echoes are weak or missing. The grainy pattern at the bottom of the figure is caused by noise.

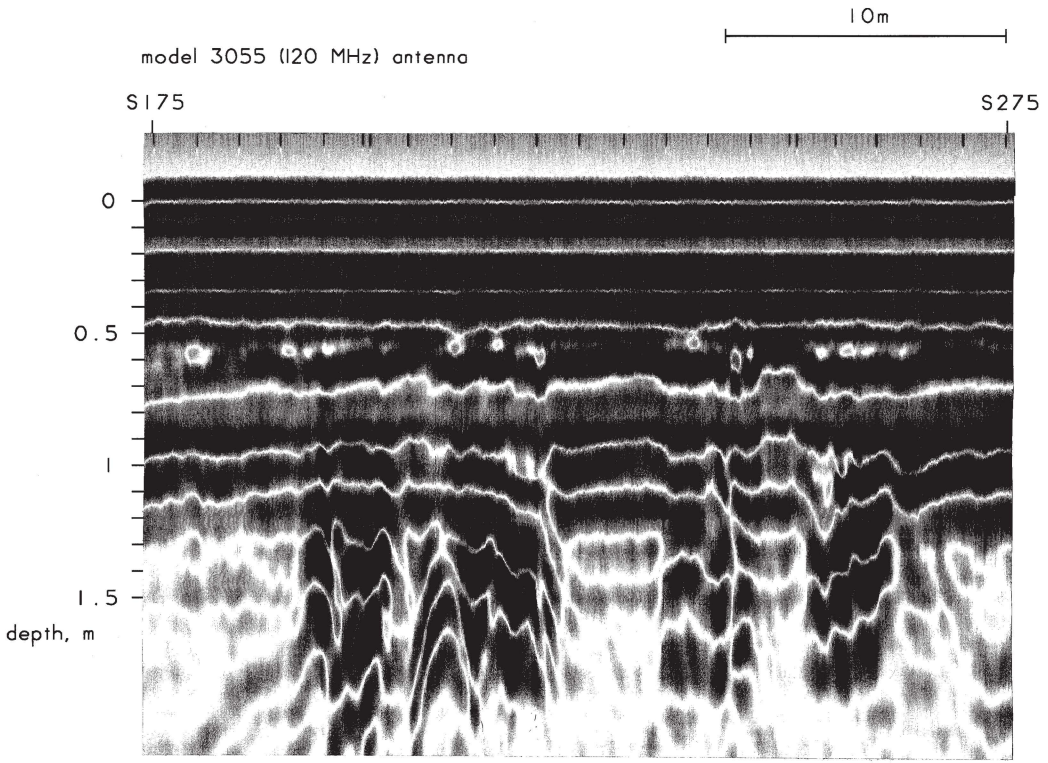

Fig. B105: An antenna test over the trenches of the bombproofs at Fort Morton. This is the lowest frequency antenna.

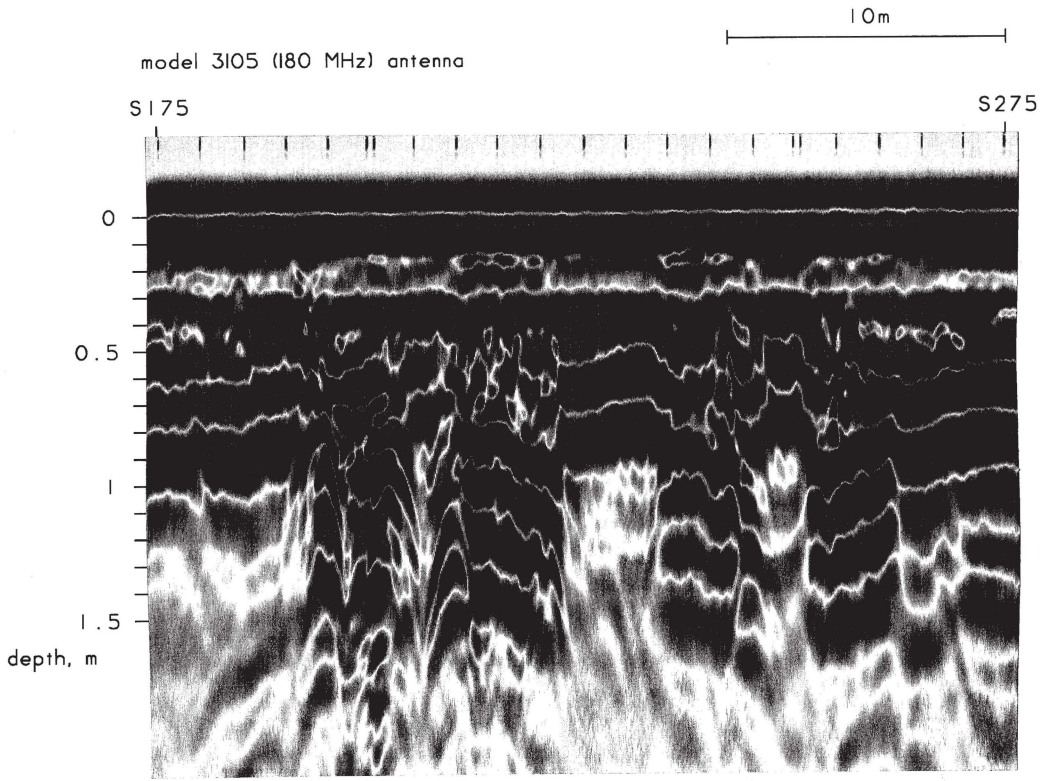

Fig. B106: A medium resolution radar profile. It shows distinct echoes from the bottoms of the four trenches along this line.

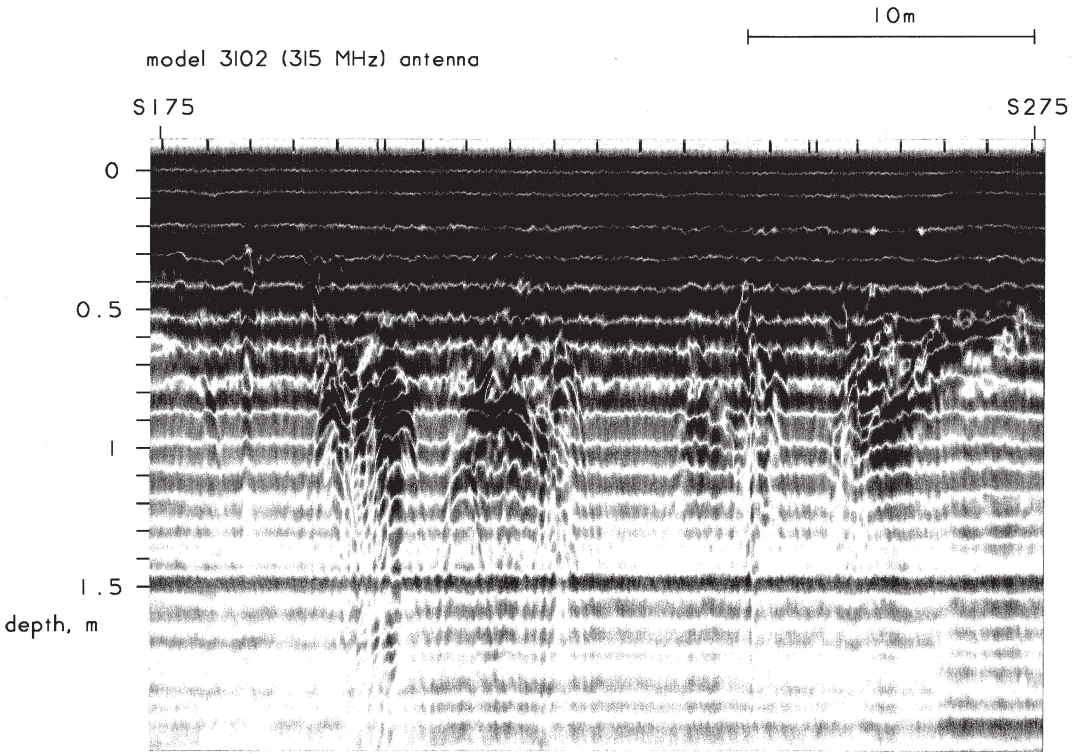

Fig. B107: A profile made with a high frequency antenna. It allows a greater resolution of the buried trenches.

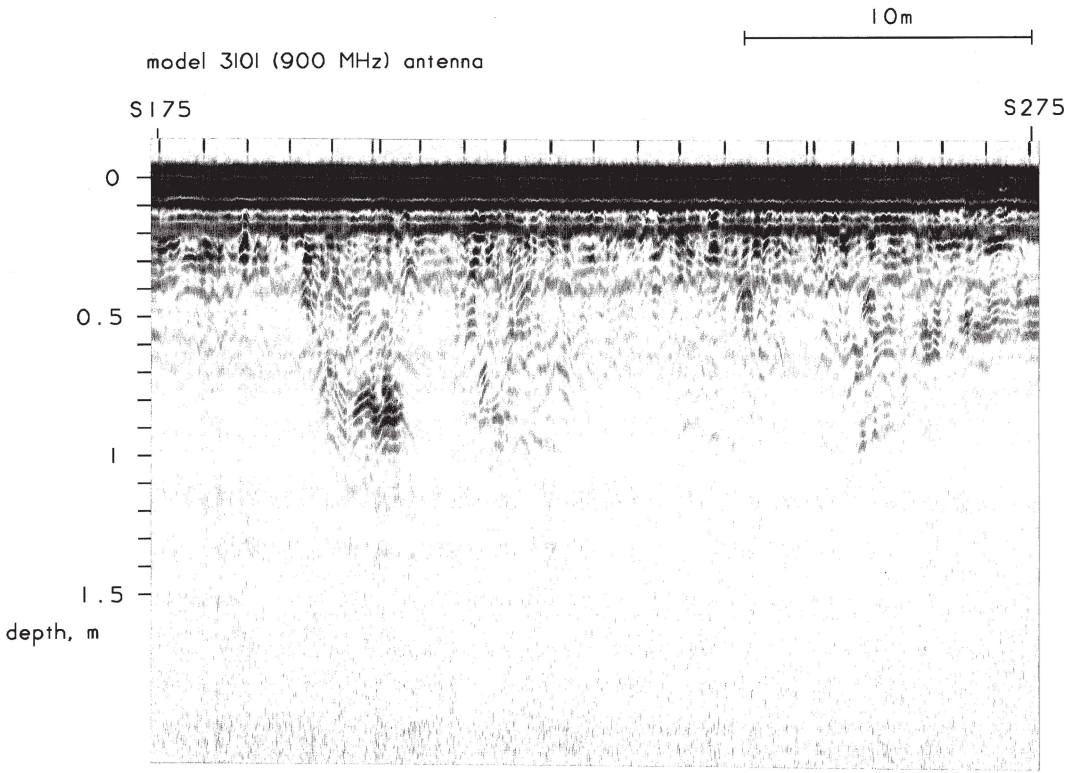

Fig. B108: A very high resolution profile. While small features are located, the deeper trenches are faint or undetected.

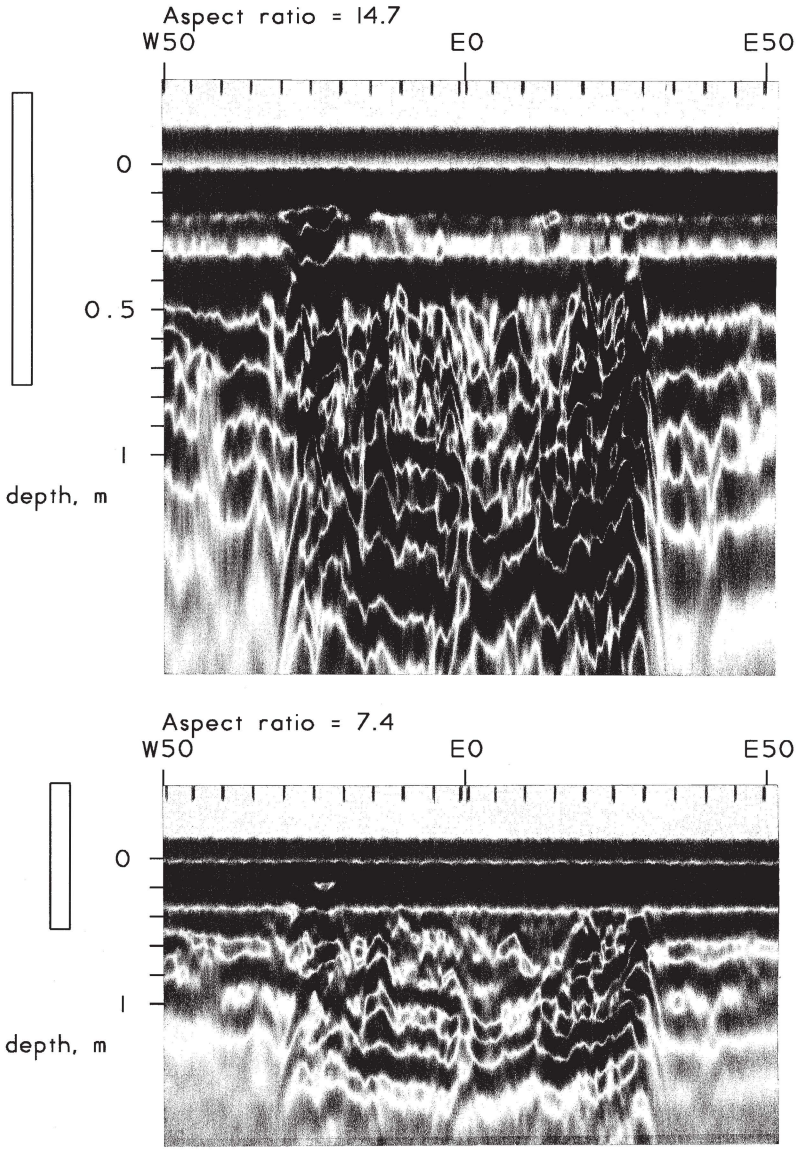

Fig. B109: Radar profiles with different scale compression.

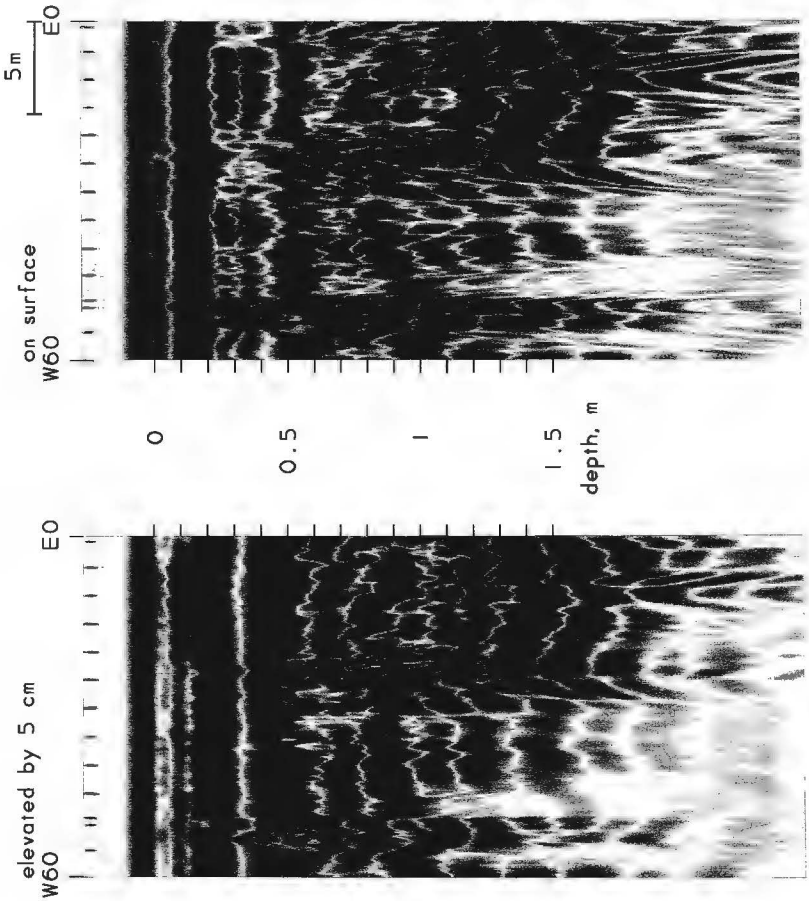

Fig. B110: The effect of antenna height. It is generally best that the radar antenna be lifted slightly from the surface.

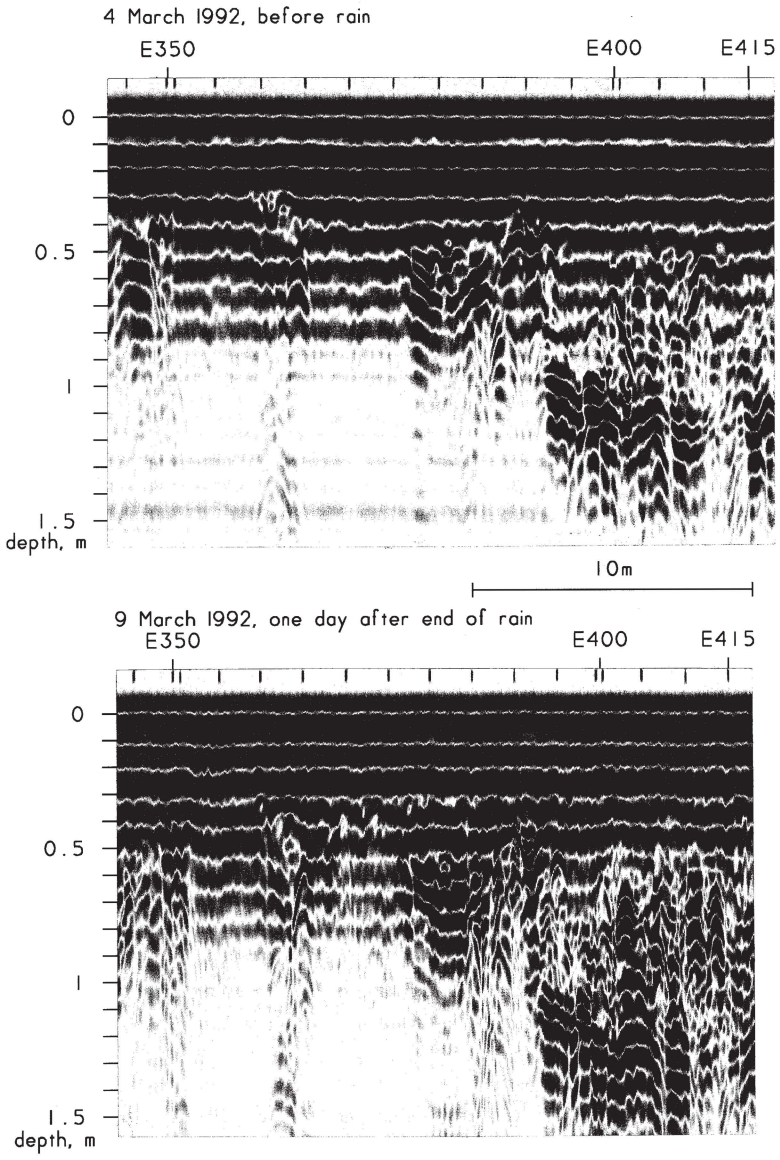

Fig. B111: The effect of rainfall on the radar profiles.

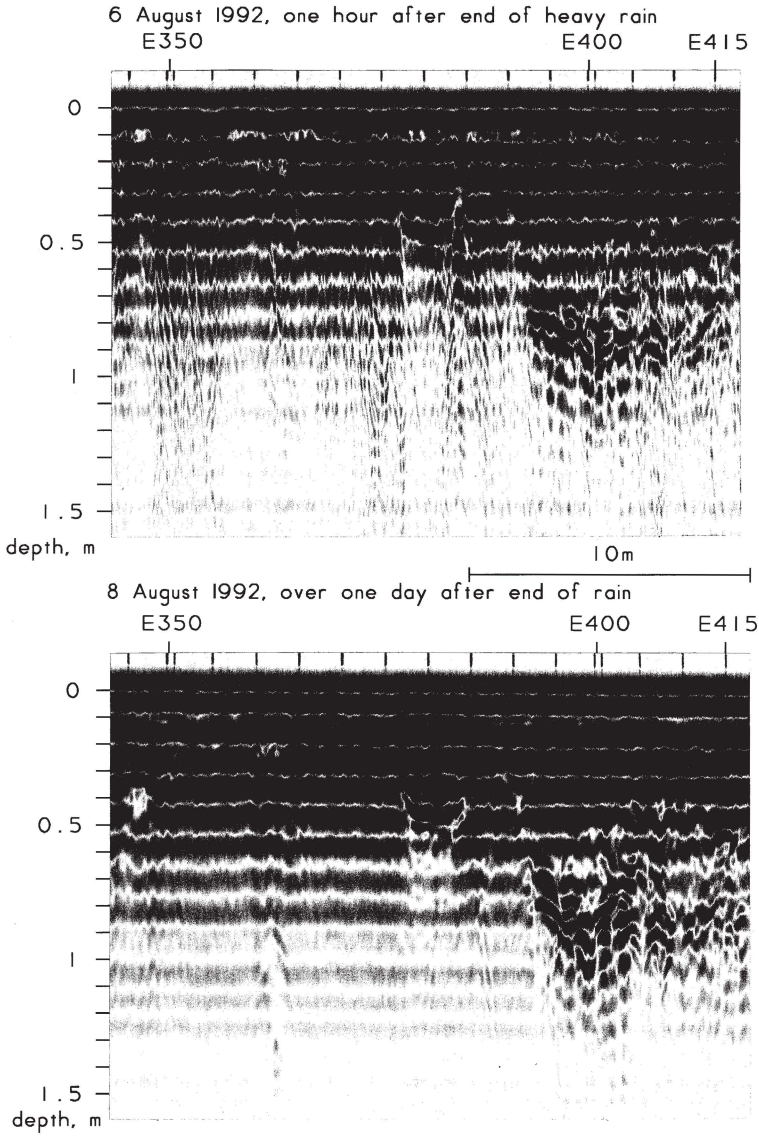

Fig. B112: Further rainfall effects. Shortly after a heavy rain, the radar profiles have a very poor image quality.

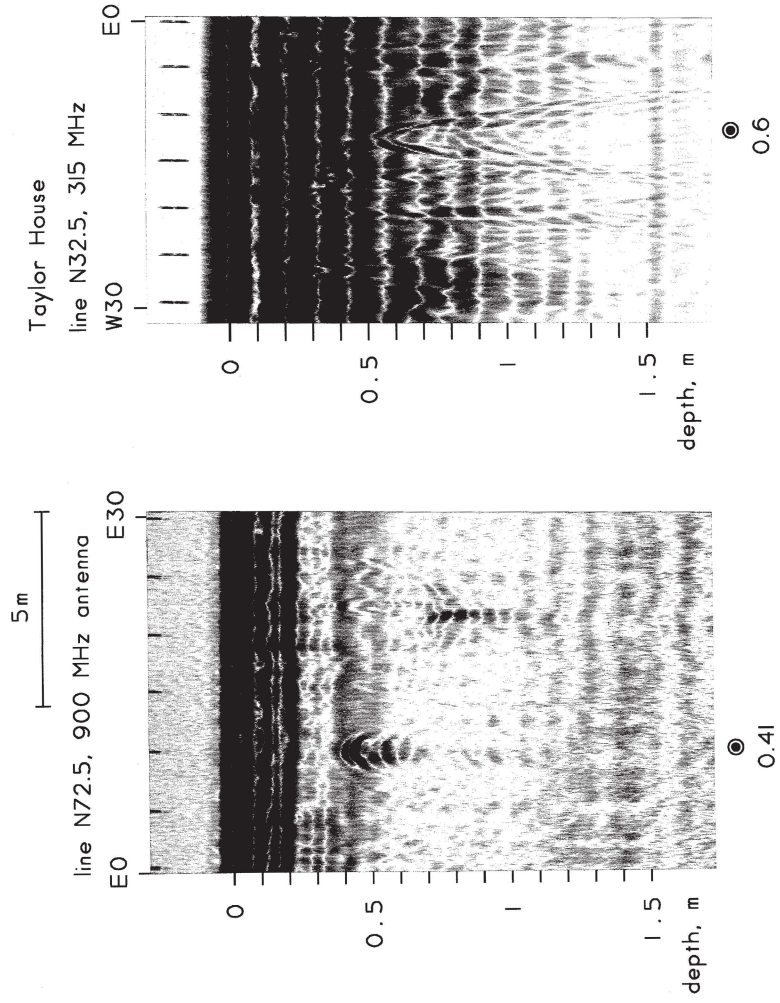

Fig. B113: Echoes for radar pulse velocity calibration. Distinct and smooth echo arcs like these allow the velocity to be determined.

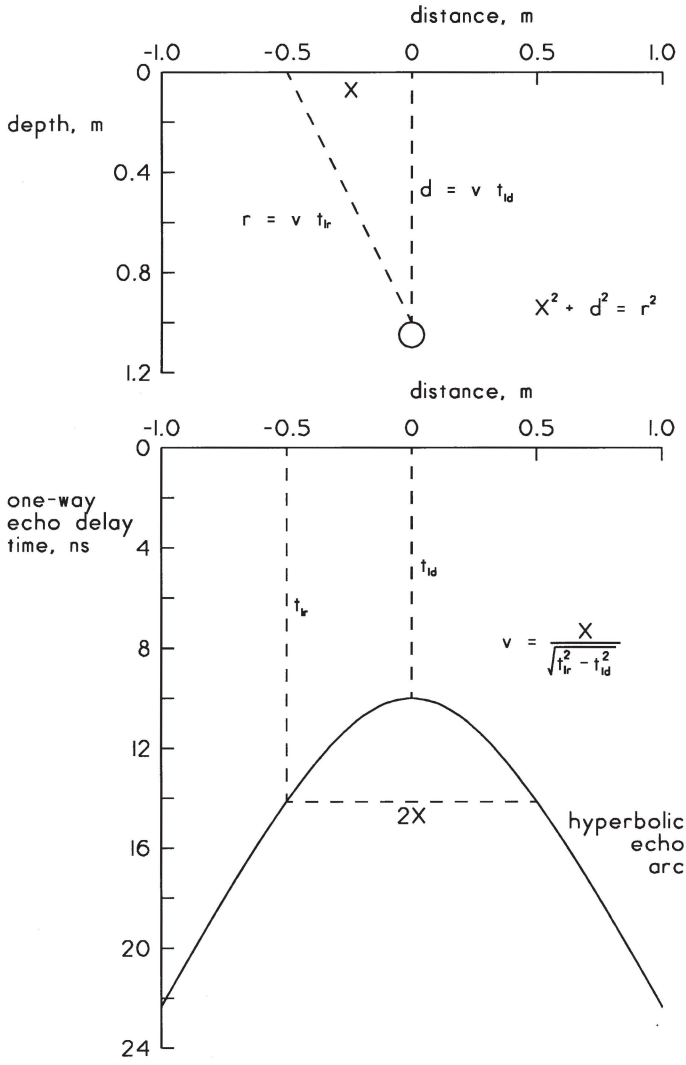

Fig. B114: The calculation of pulse velocity. It is based on the roundness of the hyperbolic echo arcs.

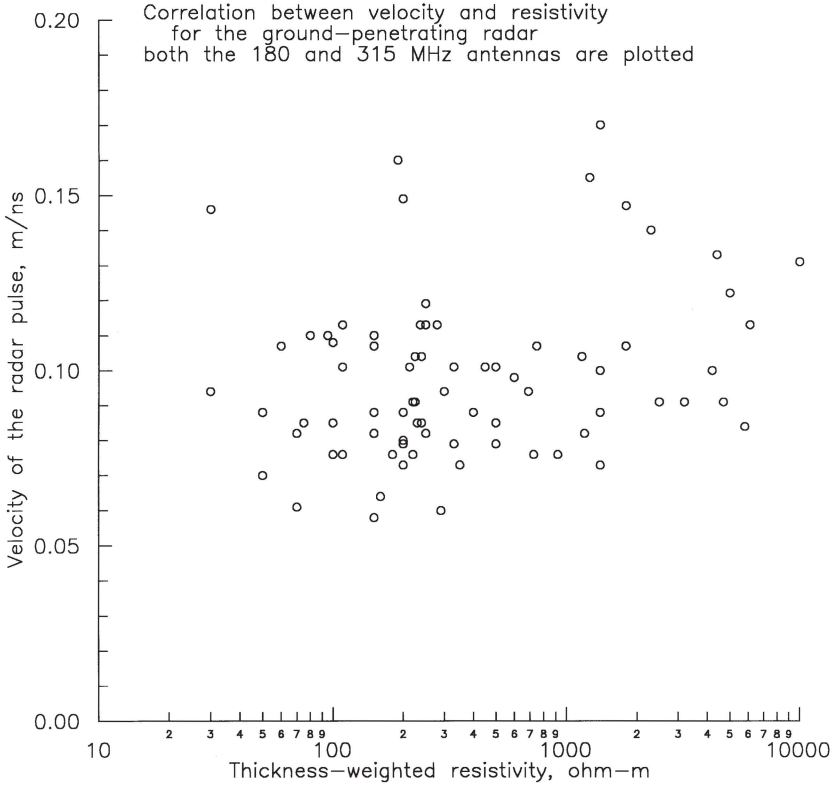

Fig. B115: Correlation between soil resistivity and pulse velocity. The velocity of the radar pulse increases somewhat as the soil resistivity increases.

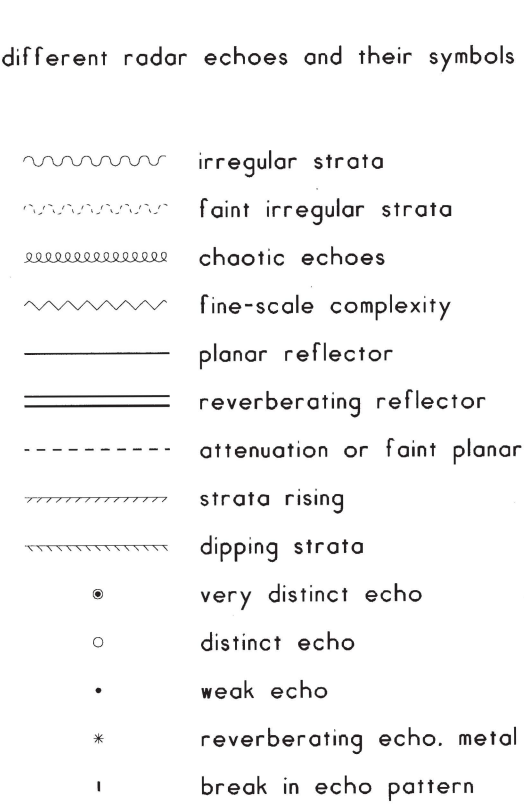

Fig. B116: A key to the classes of radar echoes. Different symbols may suggest the character of the echoes on a radar map.

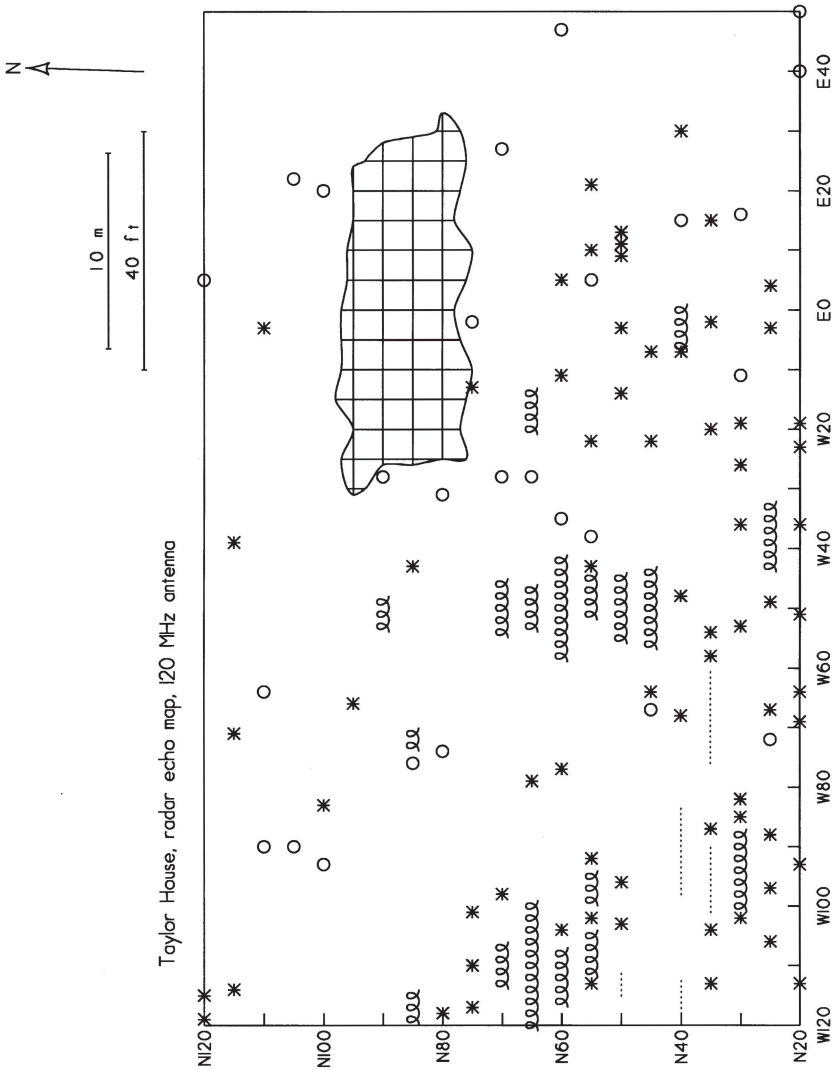

Fig. B117: The 1979 radar echo map of the Taylor House area.

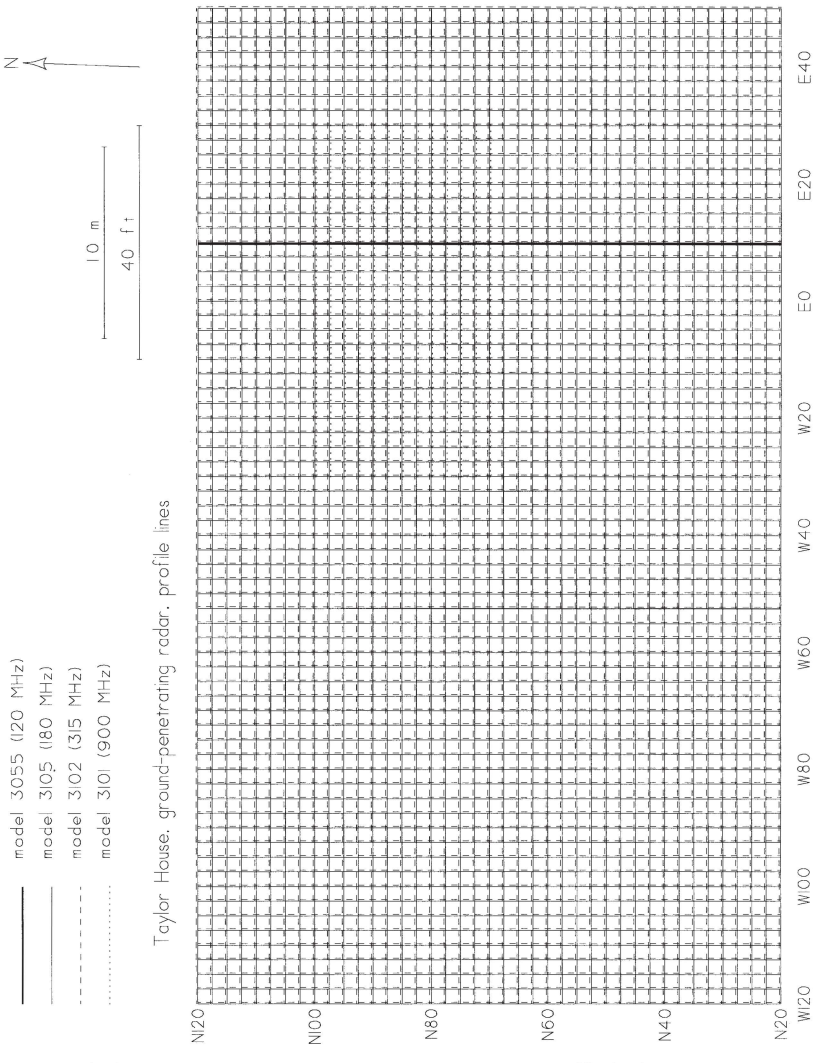

Fig. B118: Profile lines with the four different radar antennas at the Taylor House.

Fig. B119: The radar echoes from the medium resolution antenna.

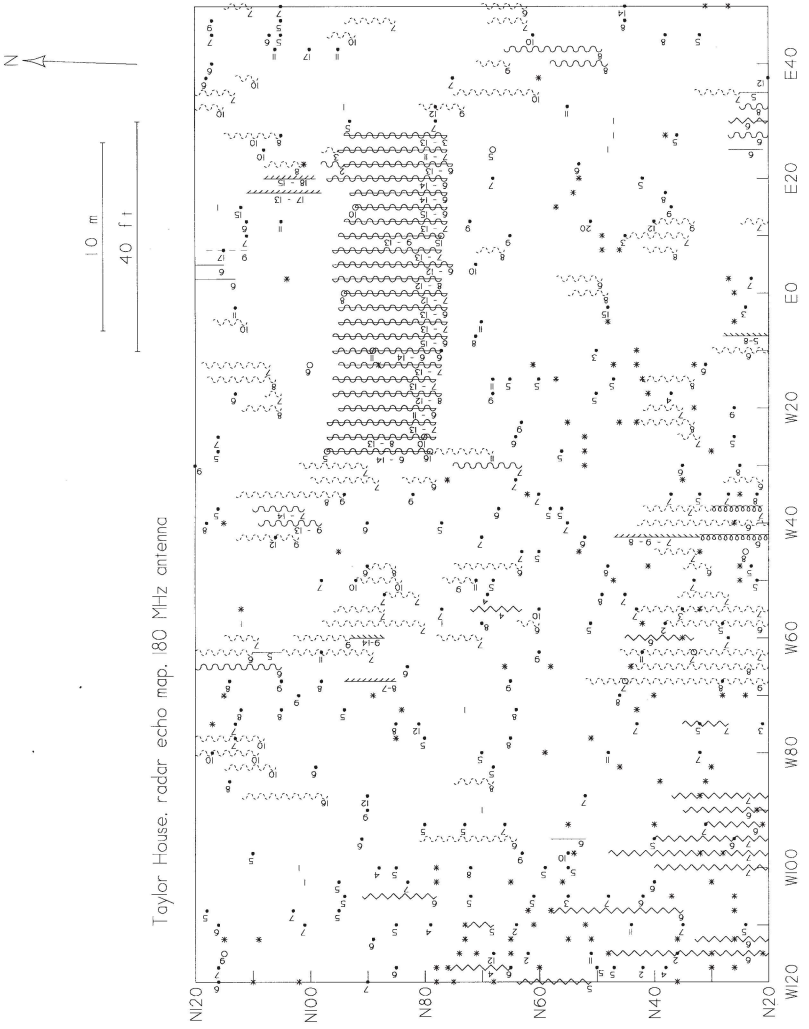

Fig. B120: Echoes from north-south, medium resolution profiles.

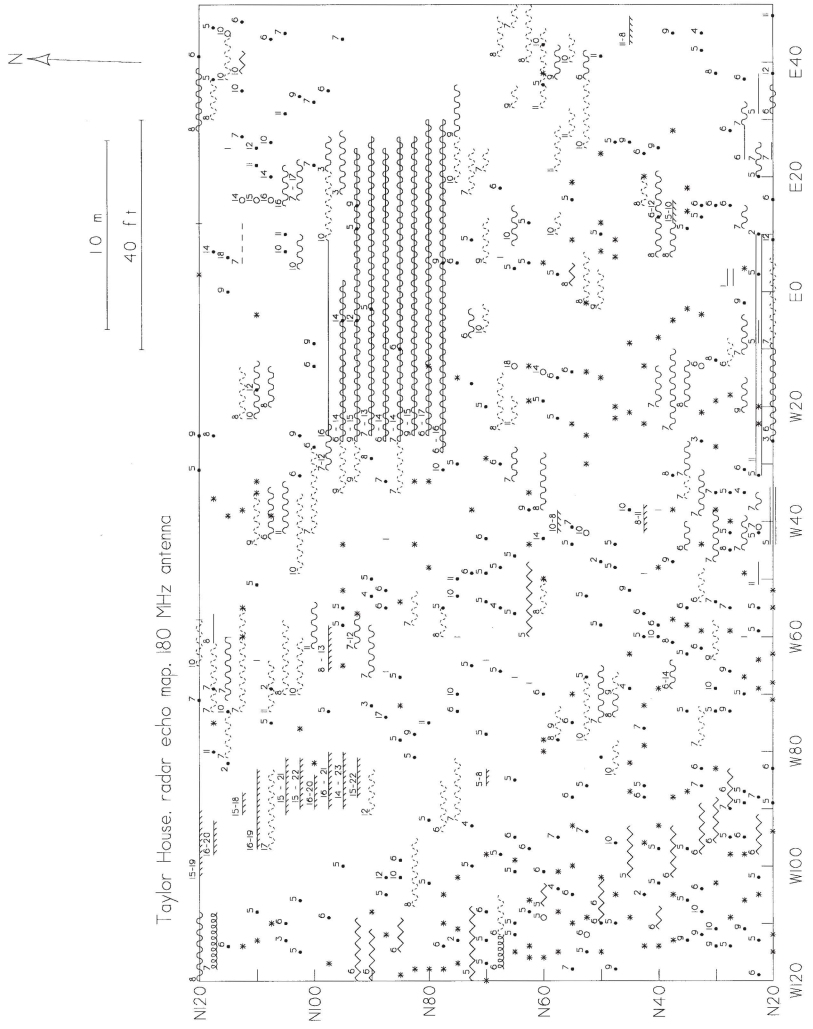

Fig. B121: Echoes from east-west, medium resolution profiles.

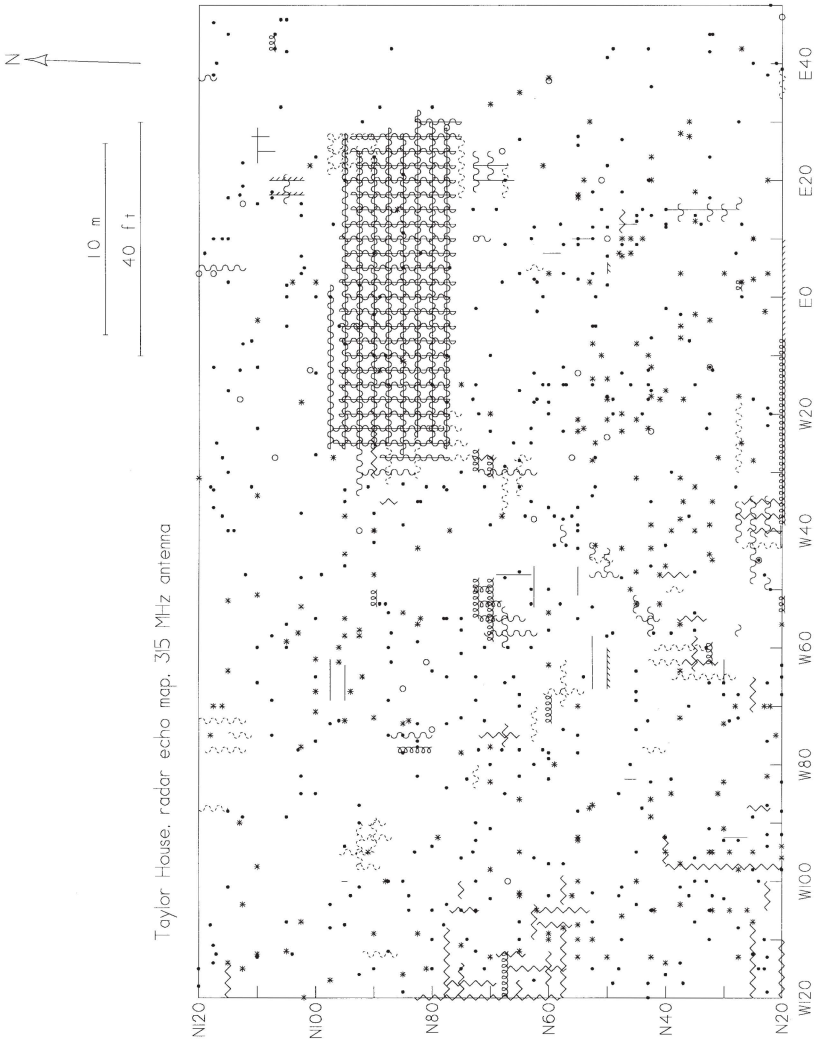

Fig. B122: All radar echoes from the high resolution antenna.

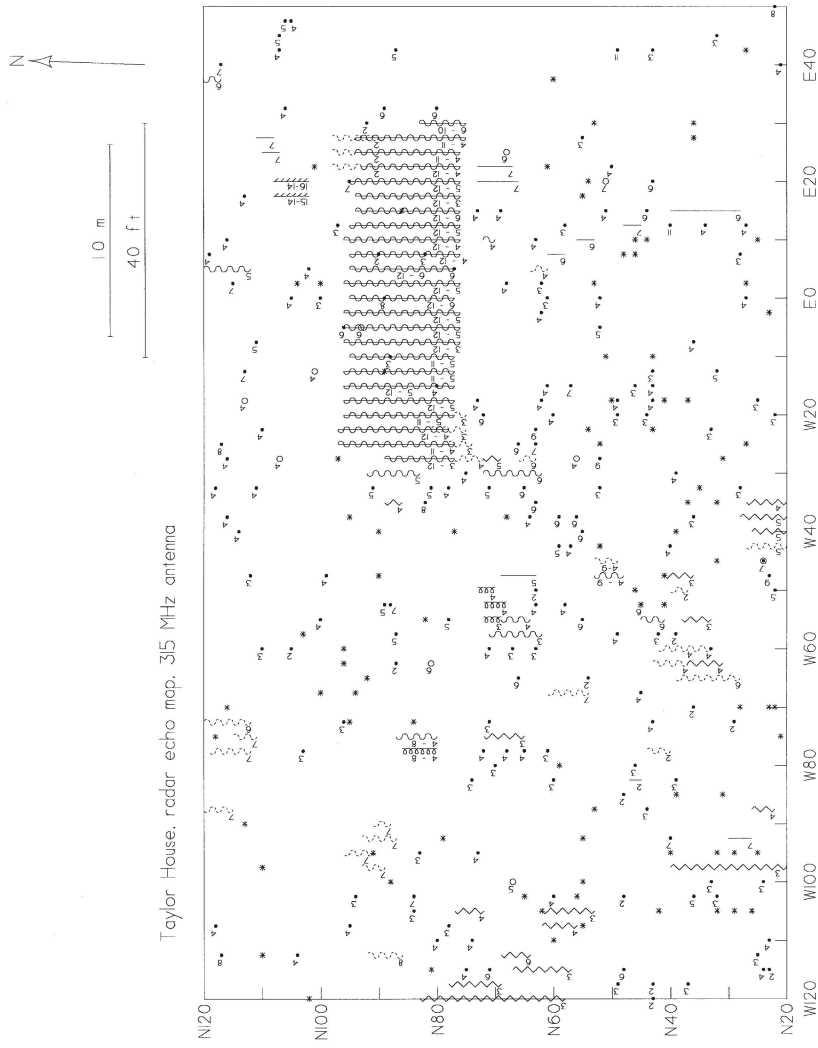

Fig. B123: Echoes from north-south, high resolution profiles.

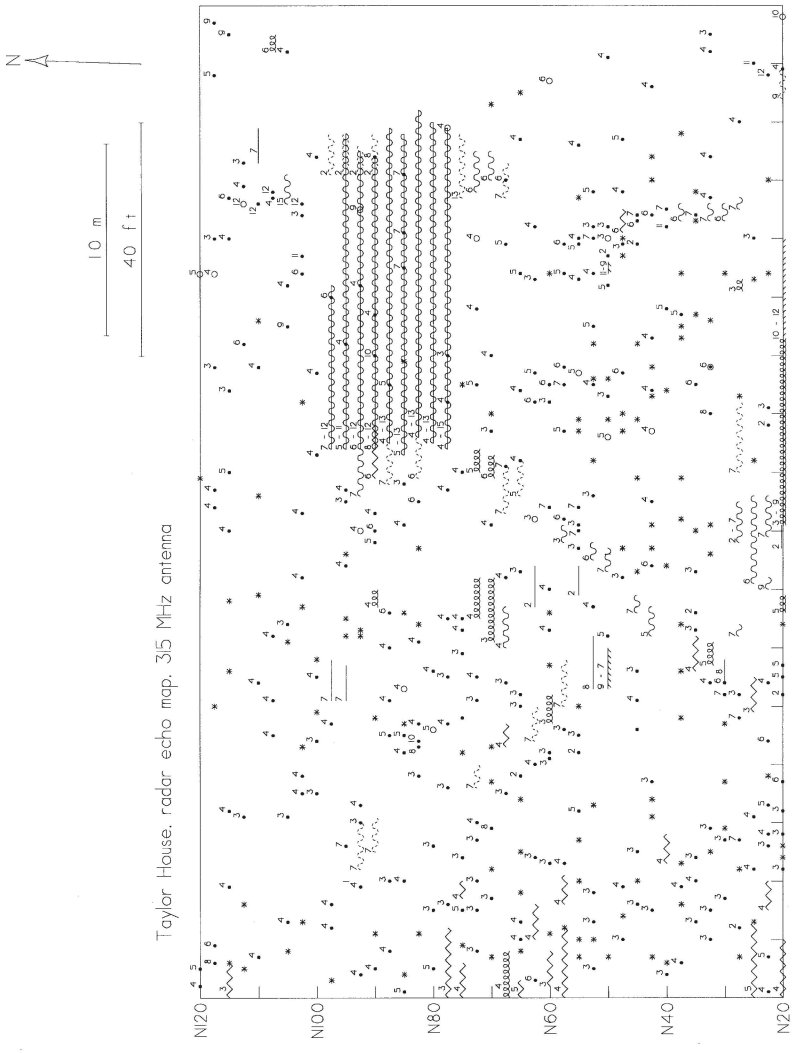

Fig. B124: Echoes from east-west, high resolution profiles.

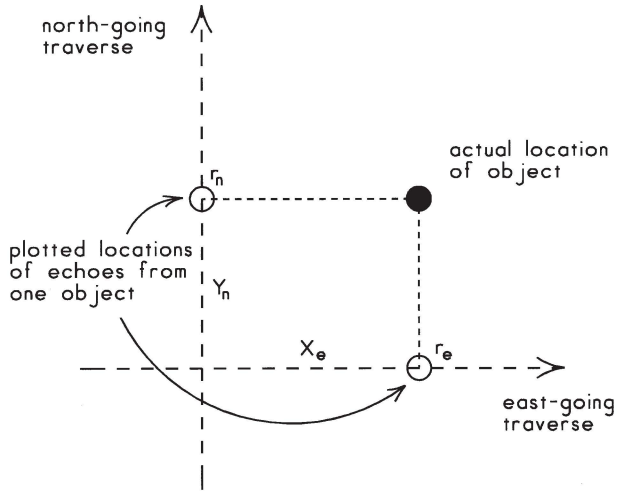

d = actual depth of object

r = range to object on radar profile

X, Y = distance to echo from line crossing

d_n = estimated depth from north-going traverse

$= \sqrt{r_n^2 - X_e^2}$

d_e = estimated depth from east-going traverse

$= \sqrt{r_e^2 - Y_n^2}$

Fig. B125: Plotting radar echoes. Perpendicular radar profiles allow the actual location of small objects to be determined.

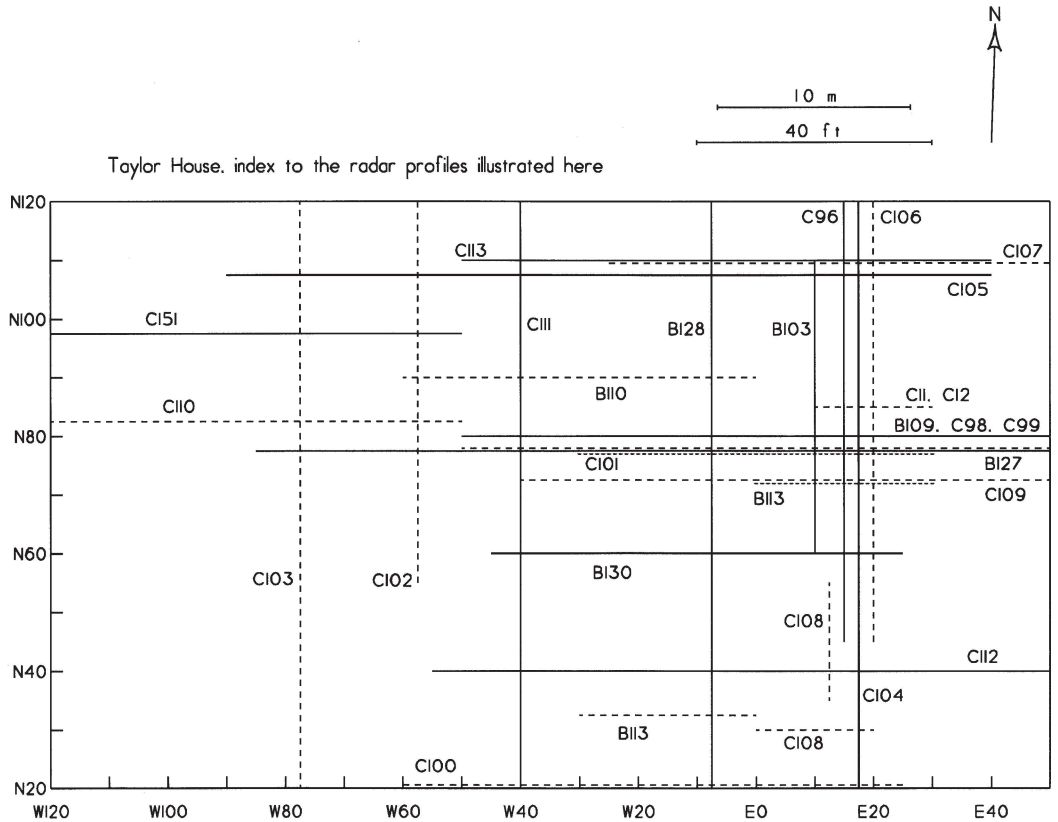

Fig. B126: An index of the radar profiles in this report.

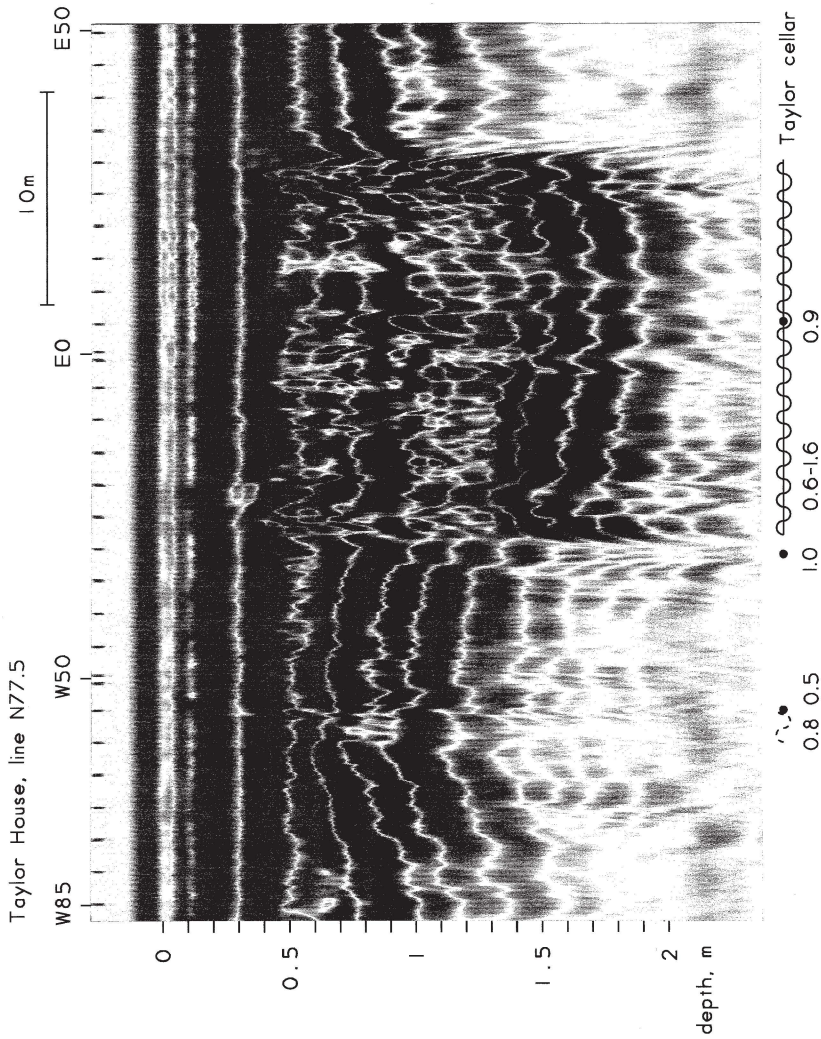

Fig. B127: A radar profile of the length of the Taylor House cellar. The was made with a medium resolution, 180 MHz antenna.

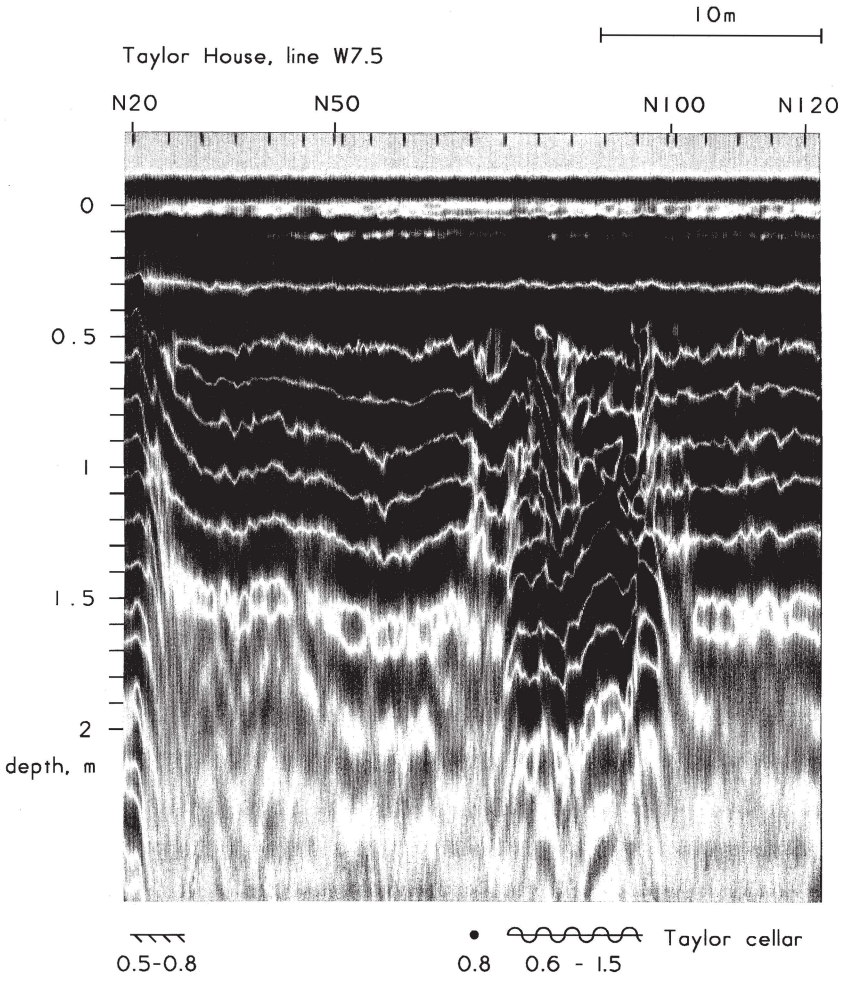

Fig. B128: A radar profile across the width of the cellar.

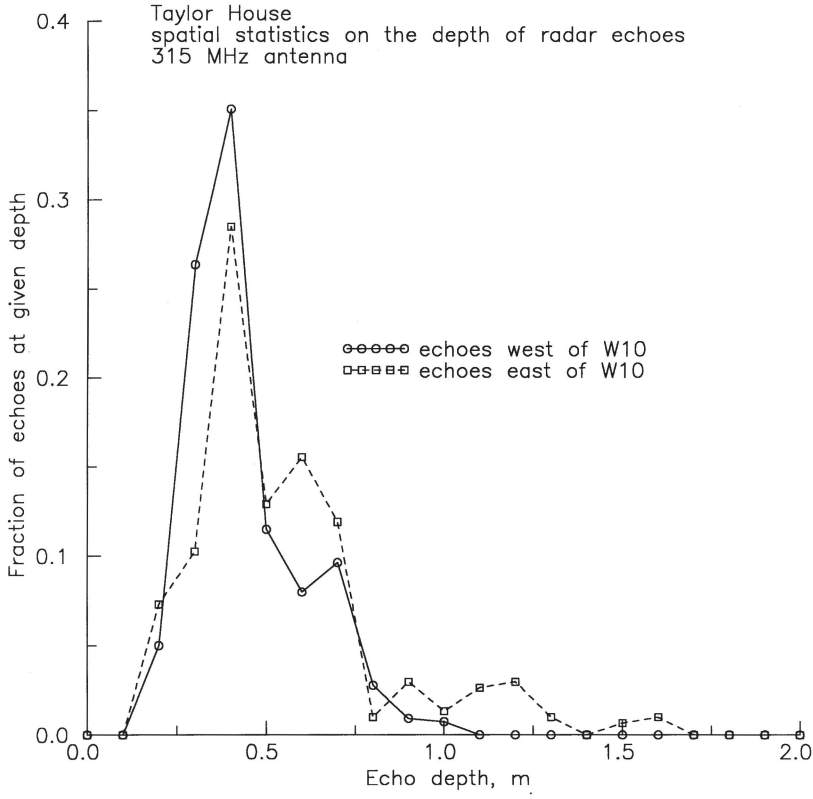

Fig. B129: The distribution of echo depths. These indicate the possibility of fill soil on the east side of the Taylor House grid. The echoes detected from the objects to the east of line W10 are slightly deeper than the echoes from objects to the west.

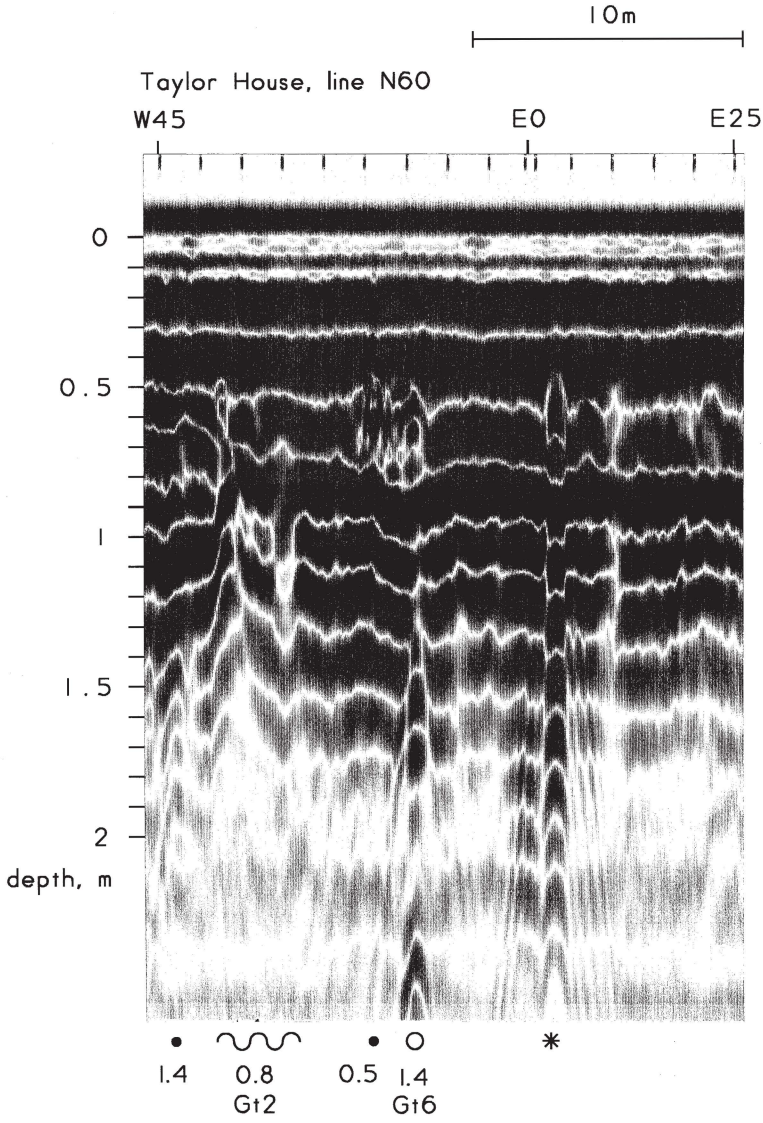

Fig. B130: A pulse reverberation at Gt6.

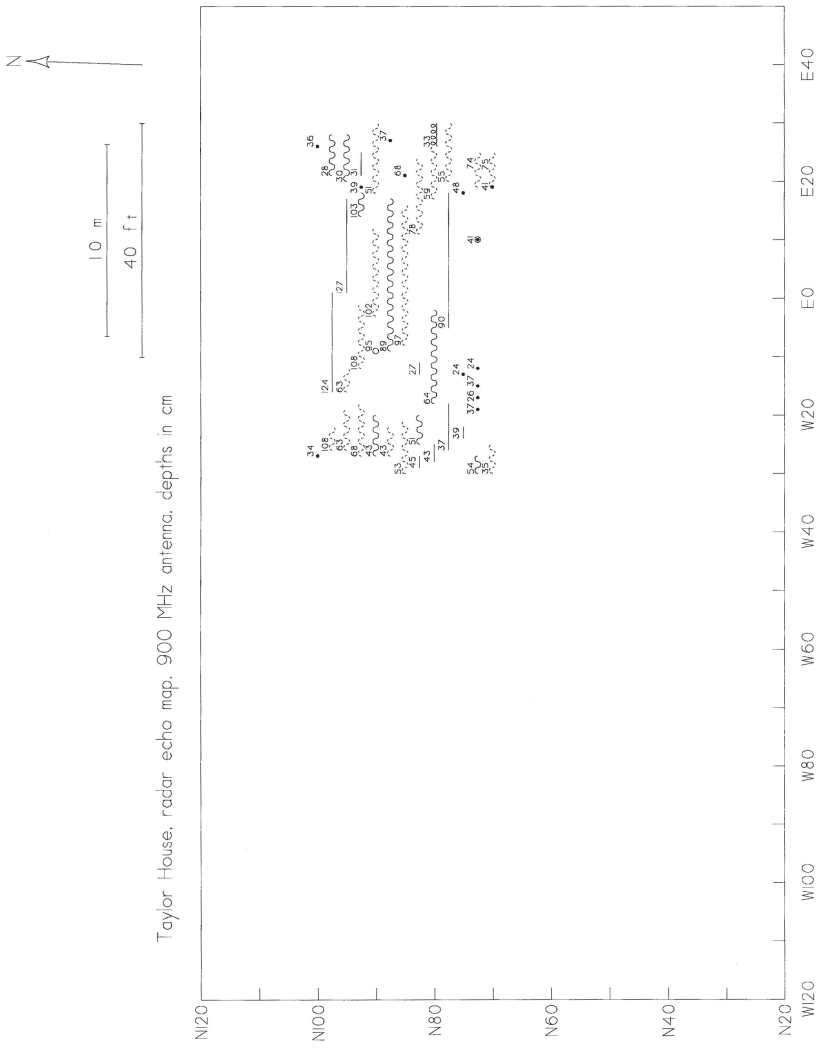

Fig. B131: Echoes from the very high resolution radar antenna. Some soil contrasts are located within the cellar.

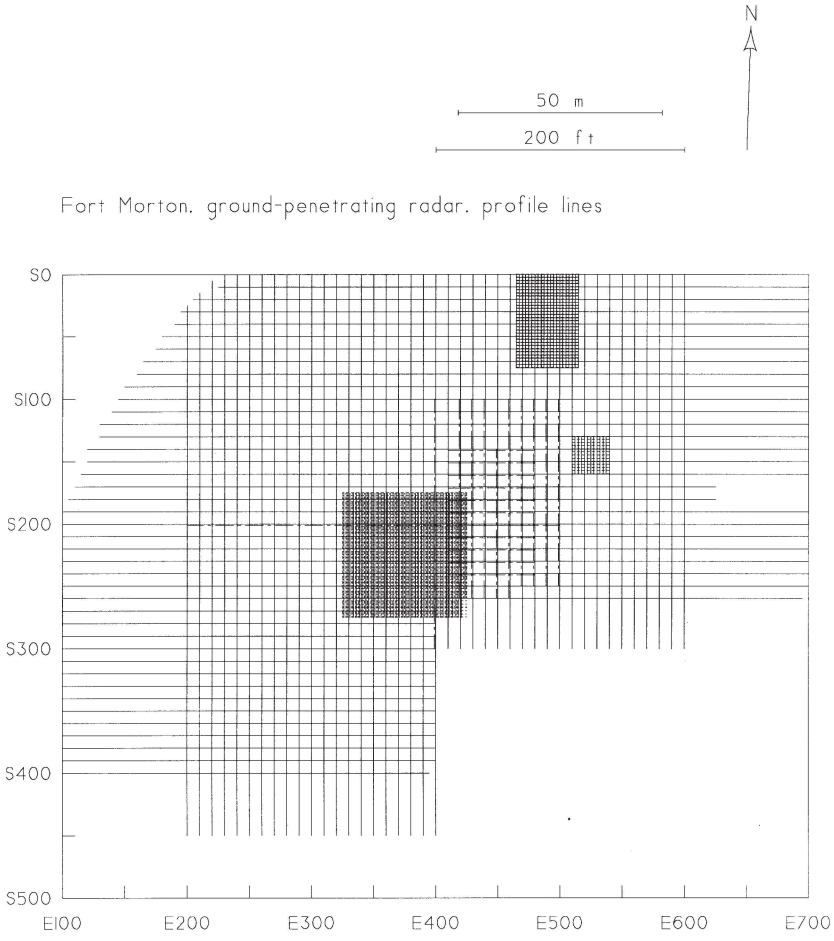

Fig. B132: The lines of the radar profiles at Fort Morton.

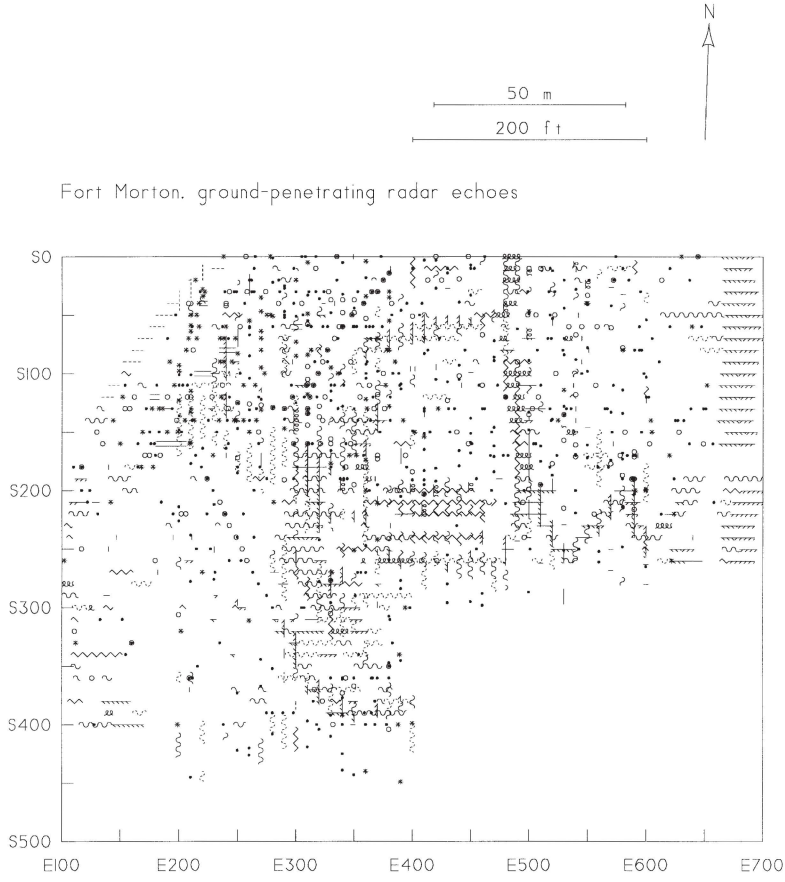

Fig. B133: The radar echoes from the main survey of Fort Morton. Groups of similar echoes outline the refilled trenches of the fortifications. The former park road in on the right side. Traces of 20th century farm buildings create a complex pattern in the northwest.

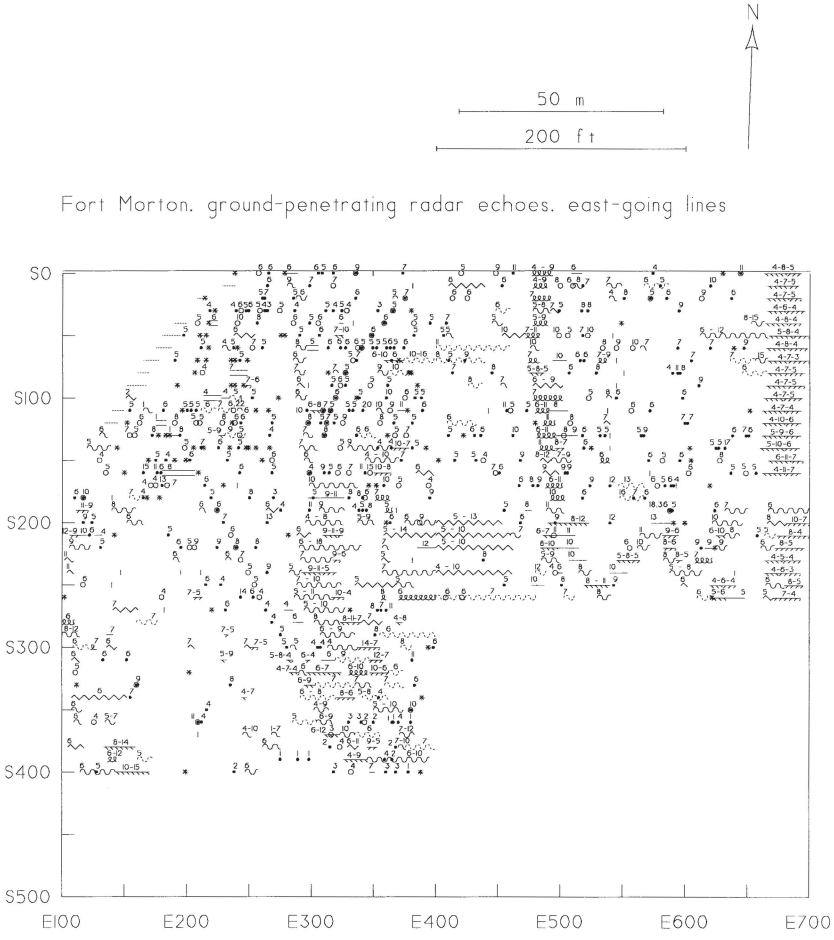

Fig. B134: Fort Morton radar echoes on east-west lines. The numbers next to the symbols show depths in decimeters.

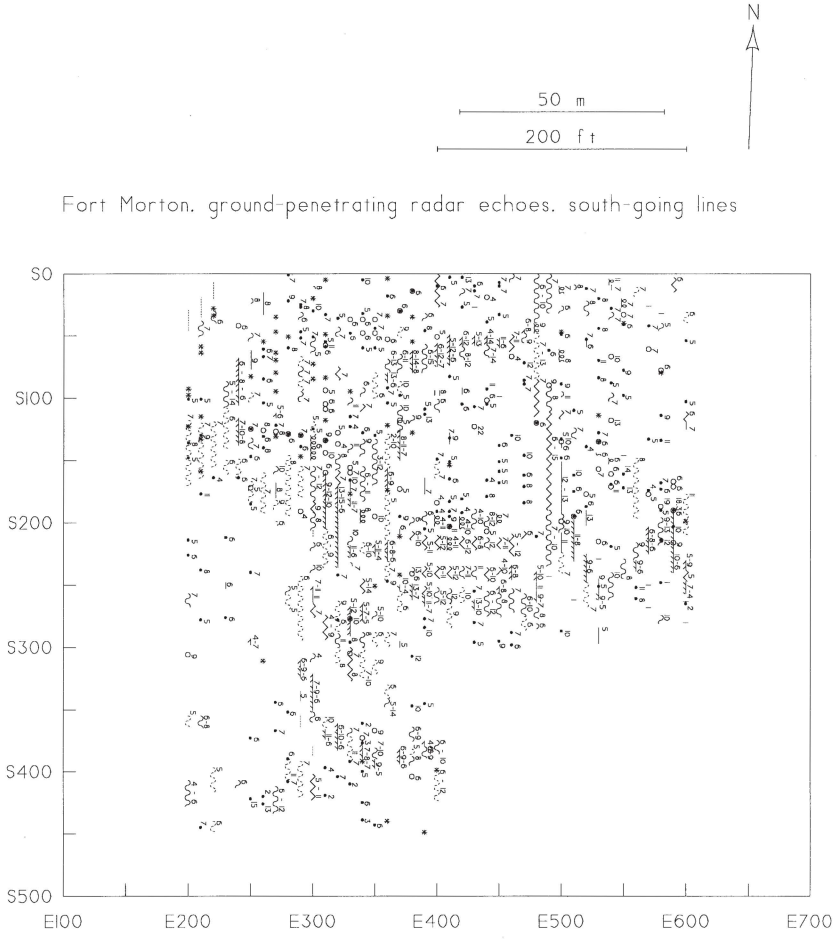

Fig. B135: Fort Morton radar echoes on north-south lines.

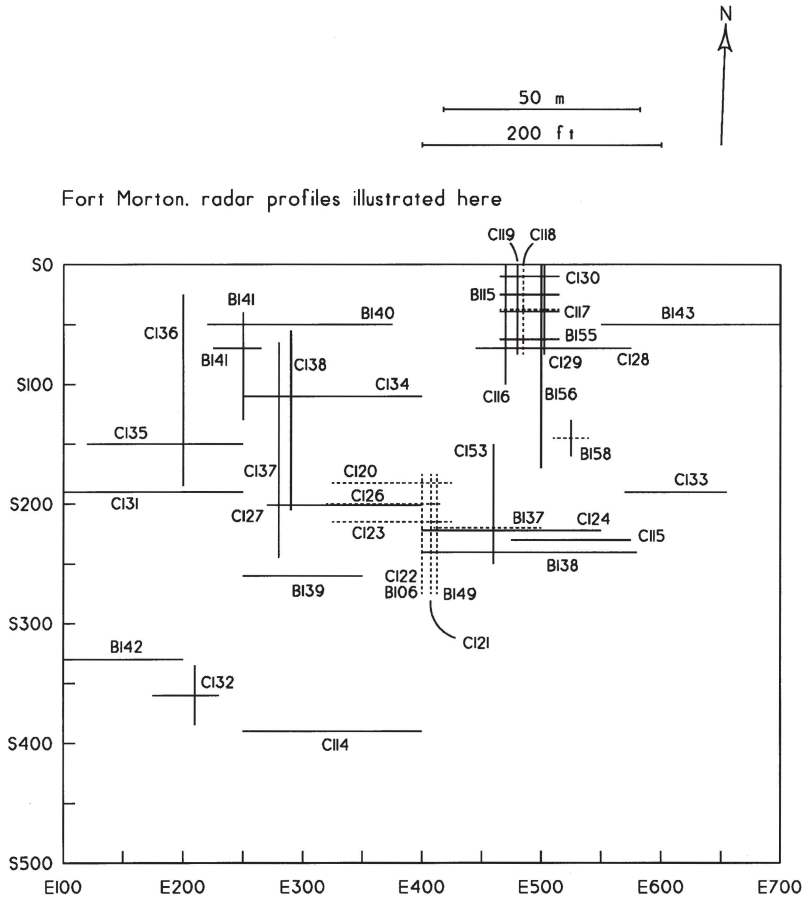

Fig. B136: An index to the radar profiles of Fort Morton. These lines are illustrated in this report.

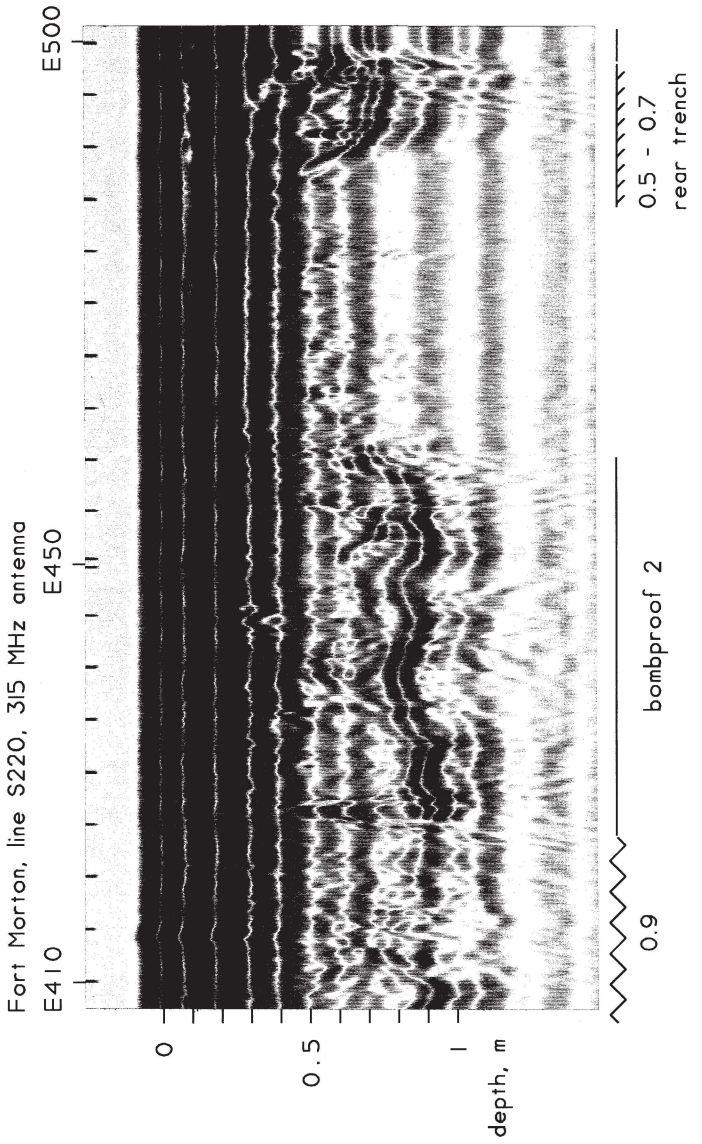

Fig. B137: Radar echoes from the lower surfaces of two trenches.

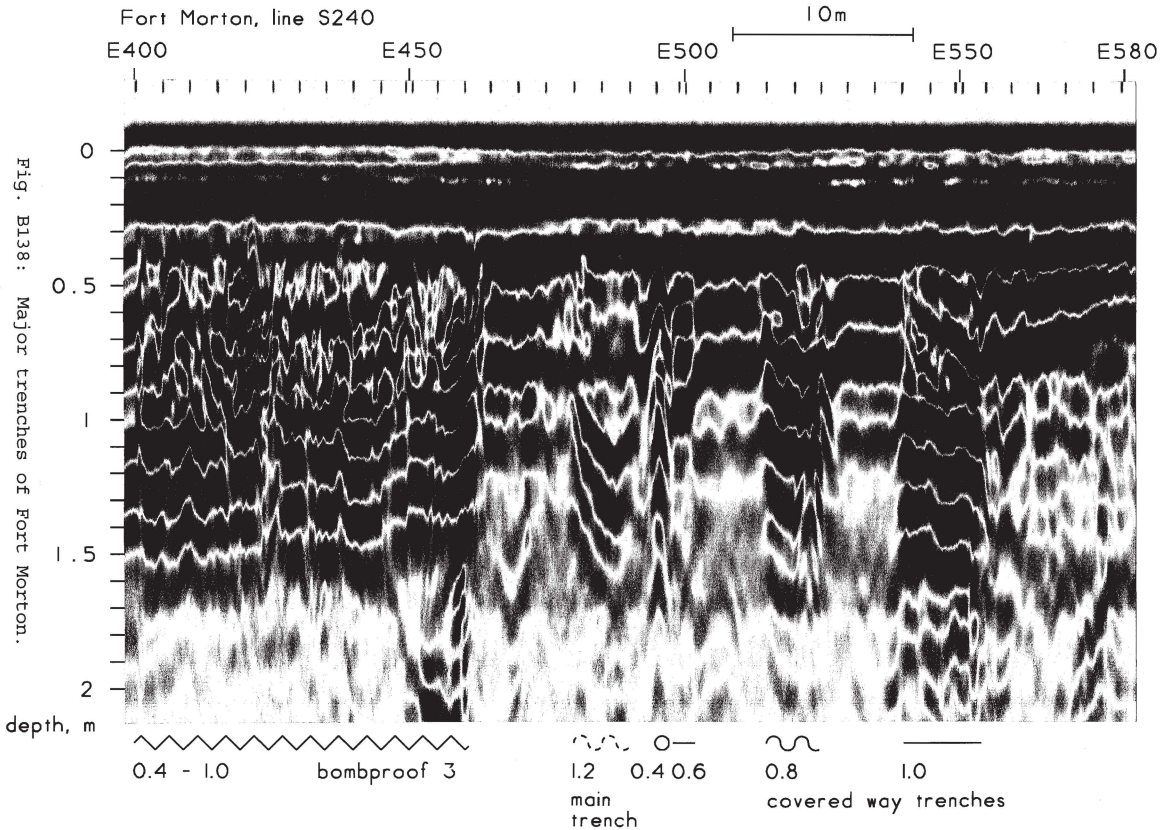

Fig. B138: Major trenches of Fort Morton.

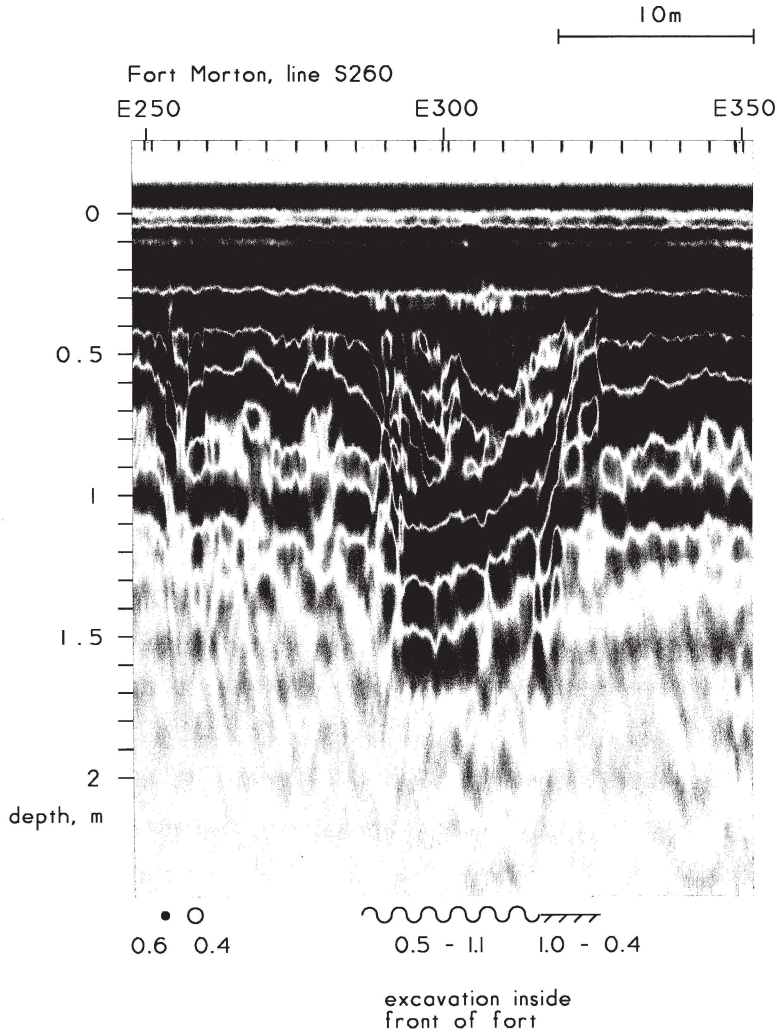

Fig. B139: The excavation which was just behind the parapet of the fort. The earthen parapet to the west of this was not detected.

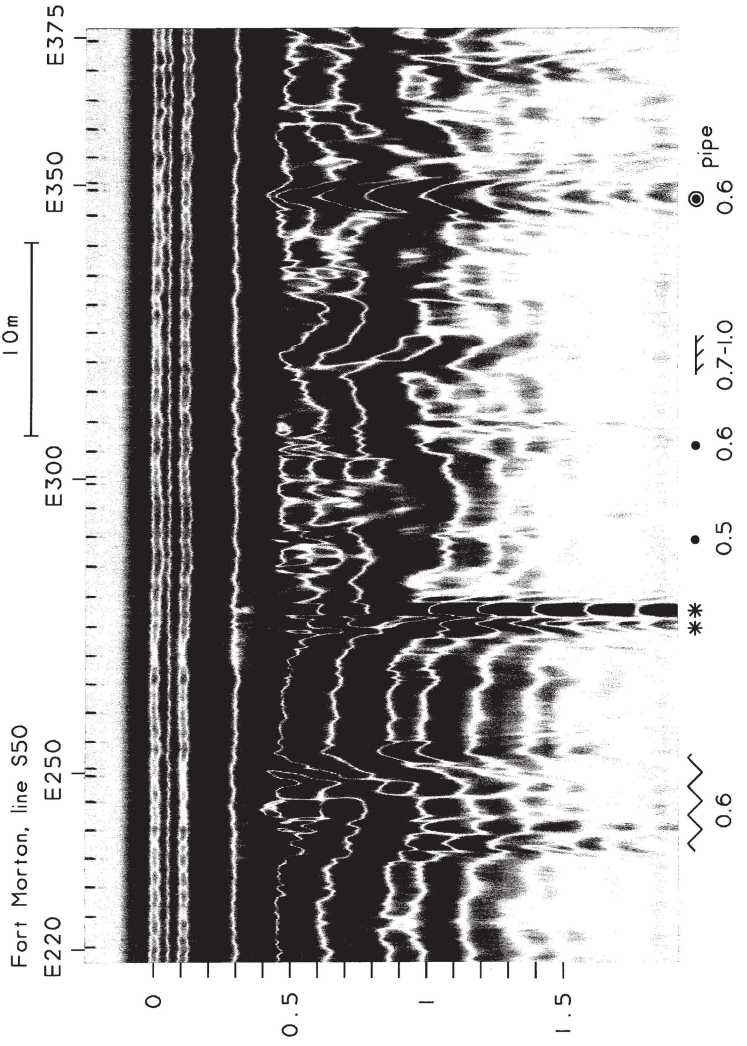

Fig. B140: Many complex radar echoes. The 20th century farm is the source of most of these.

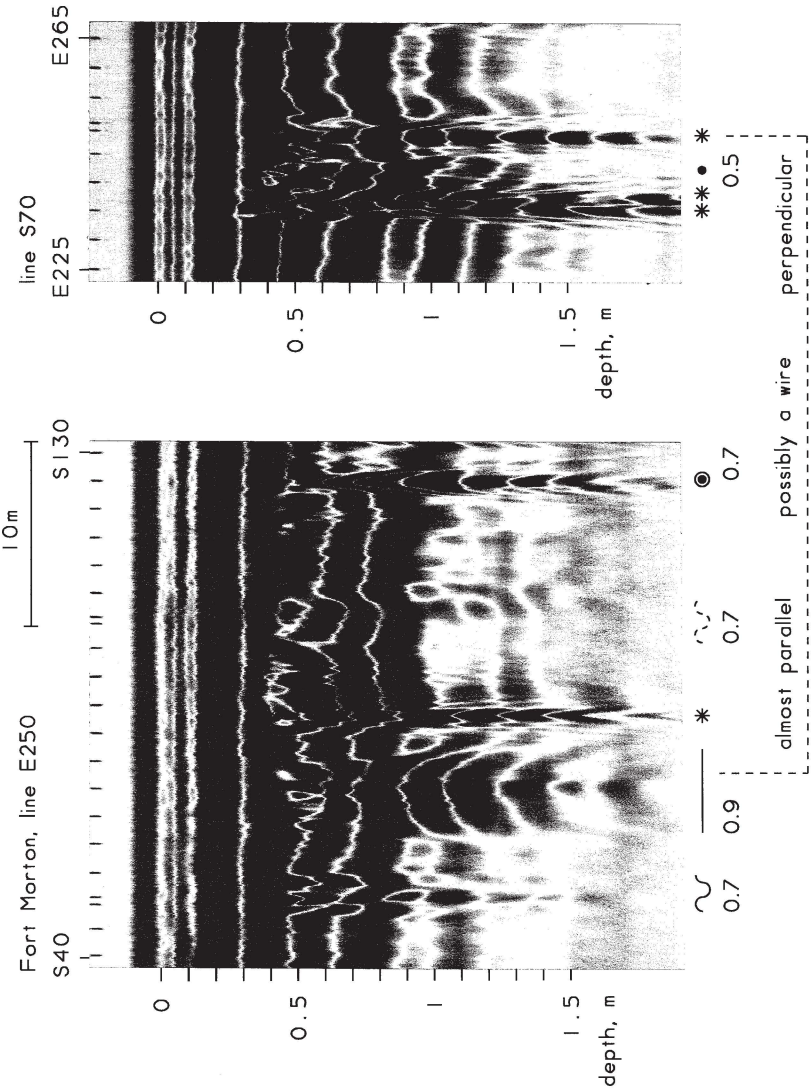

Fig. B141: Two perpendicular radar profiles. They may locate an underground wire.

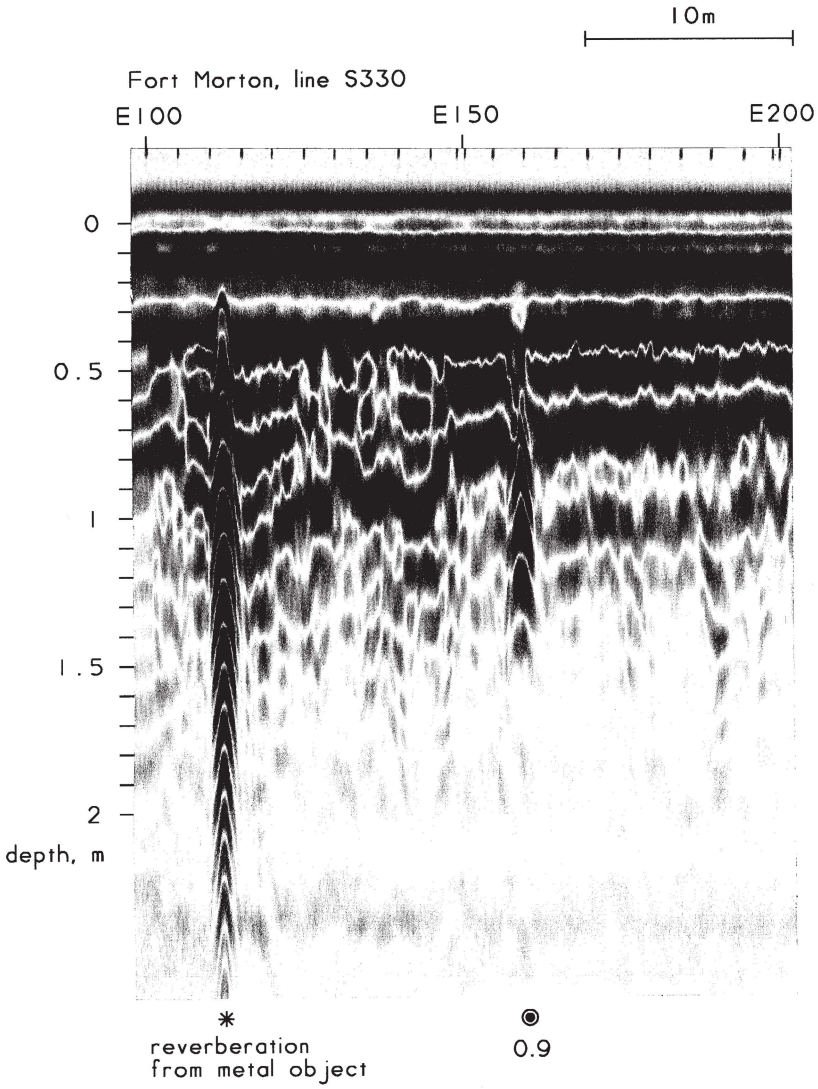

Fig. B142: An excellent example of the reverberation of the radar pulse. The metal object is less than 0.3 m underground.

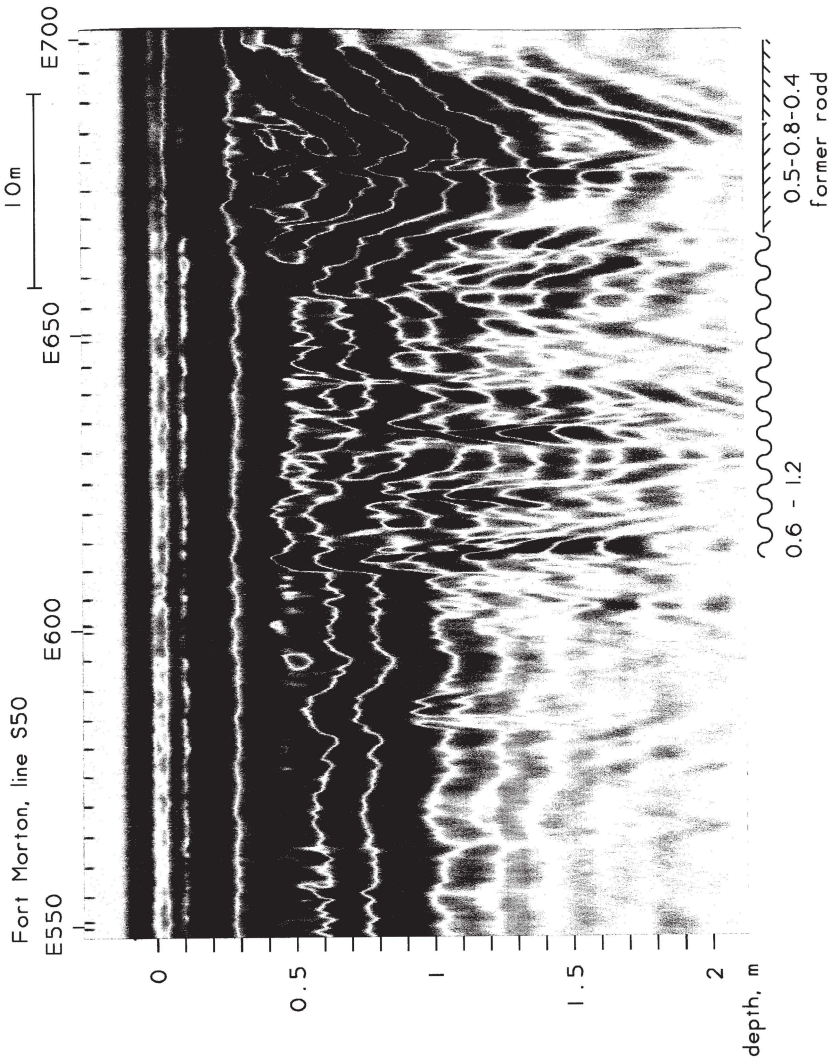

Fig. B143: Irregular soil strata. The unusual pattern from E610 to E660 is from an area outside of Fort Morton.

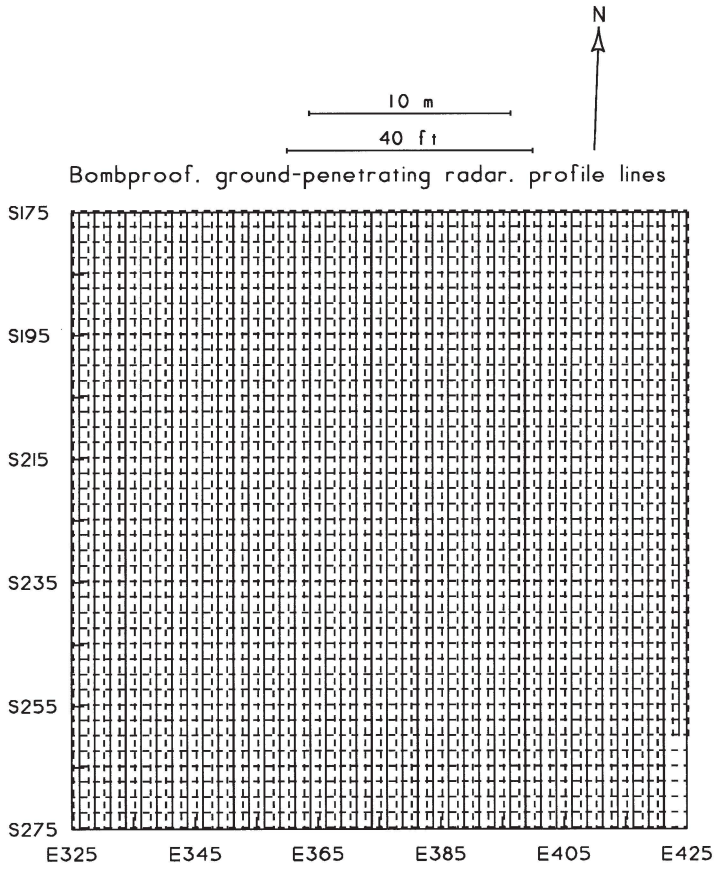

Fig. B144: Lines of profile in the Bombproof detail. Their close spacing allowed a high resolution on the location of trenches.

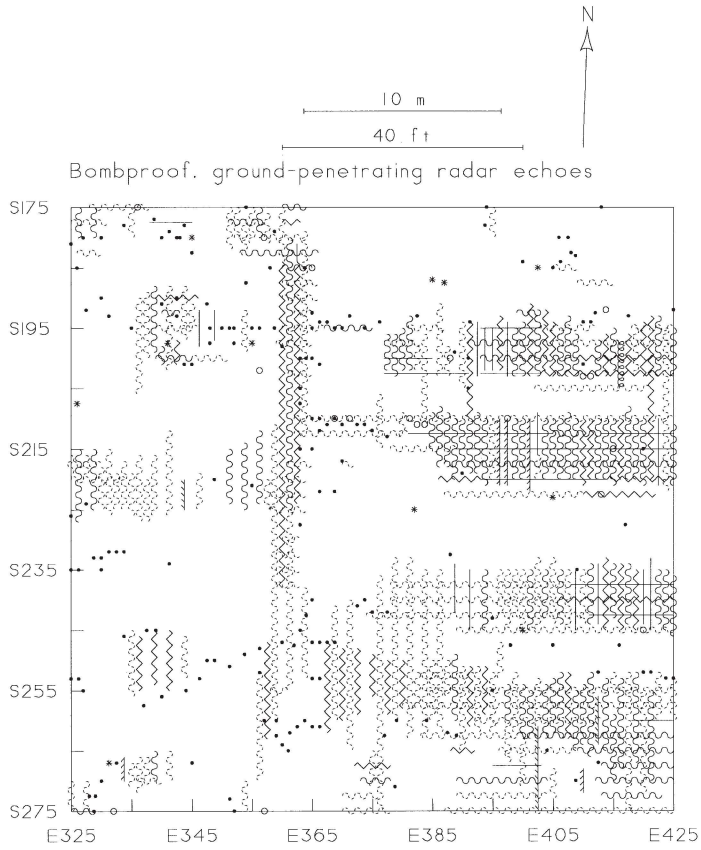

Fig. B145: The radar echo map of the Bombproof detail. Most of the refilled ditches are distinct here.

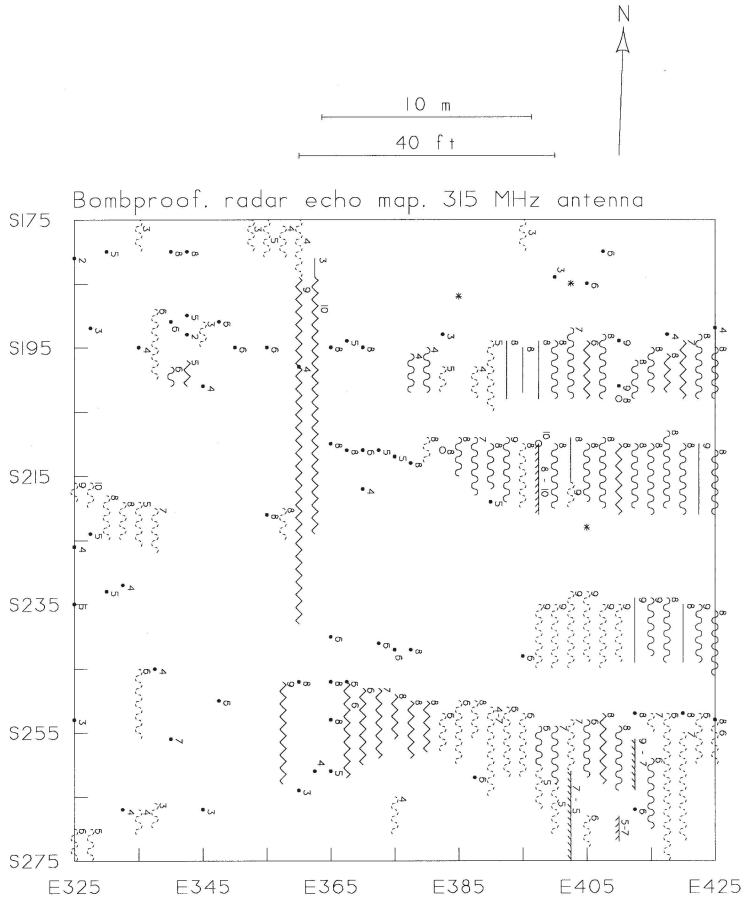

Fig. B146: Bombproof detail. This is an echo map from the south-going traverses with the high resolution radar antenna.

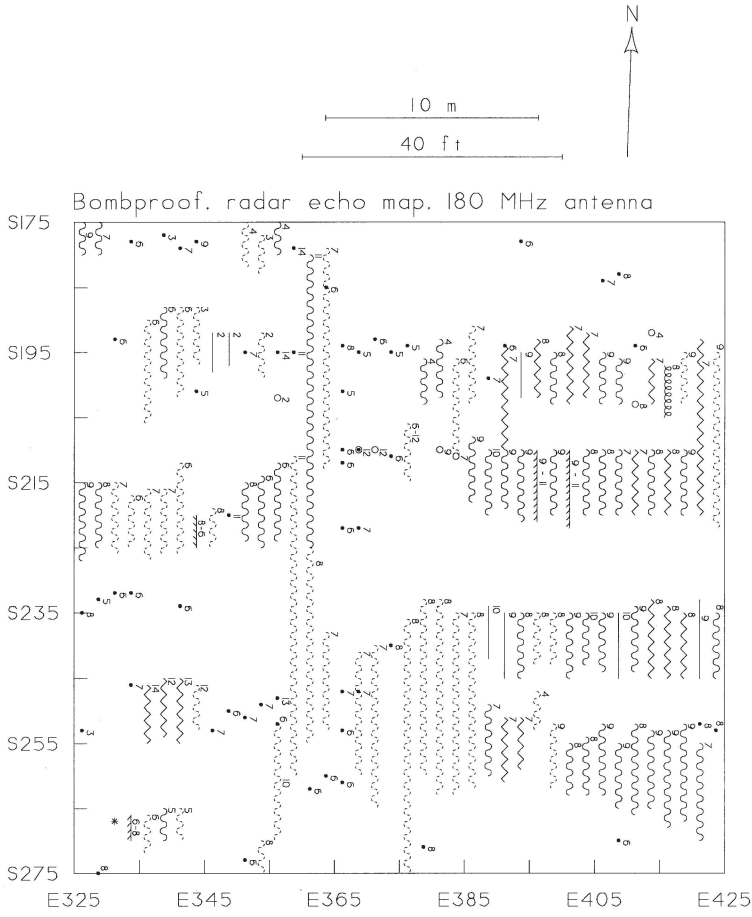

Fig. B147: Bombproof detail. This is an echo map from the south-going traverses with the medium resolution antenna.

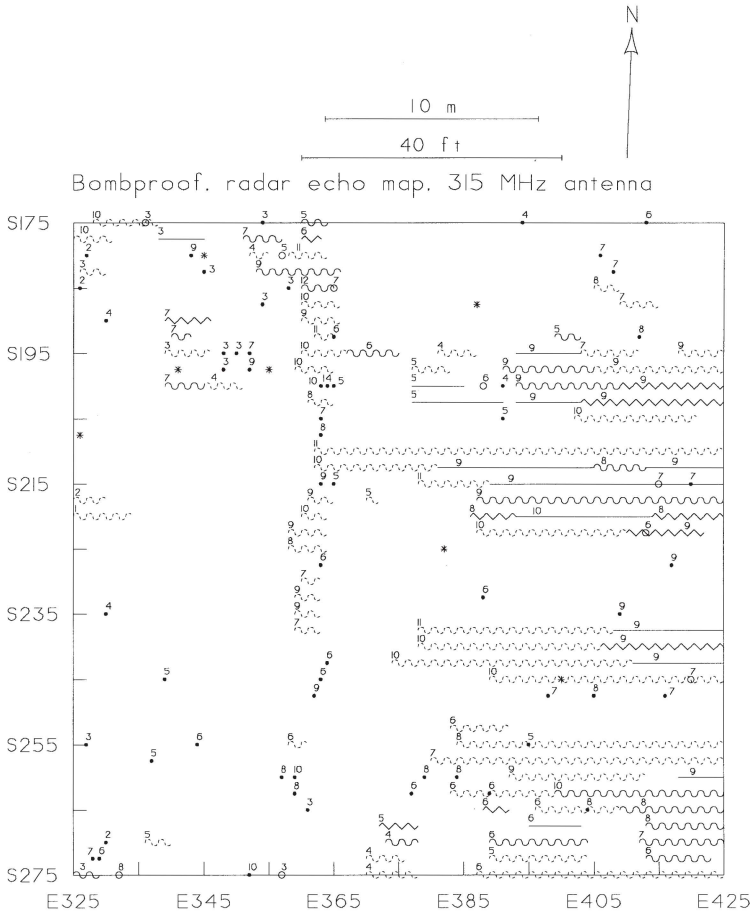

Fig. B148: Bombproof detail. This is an echo map from the east-going traverses with the high resolution antenna.

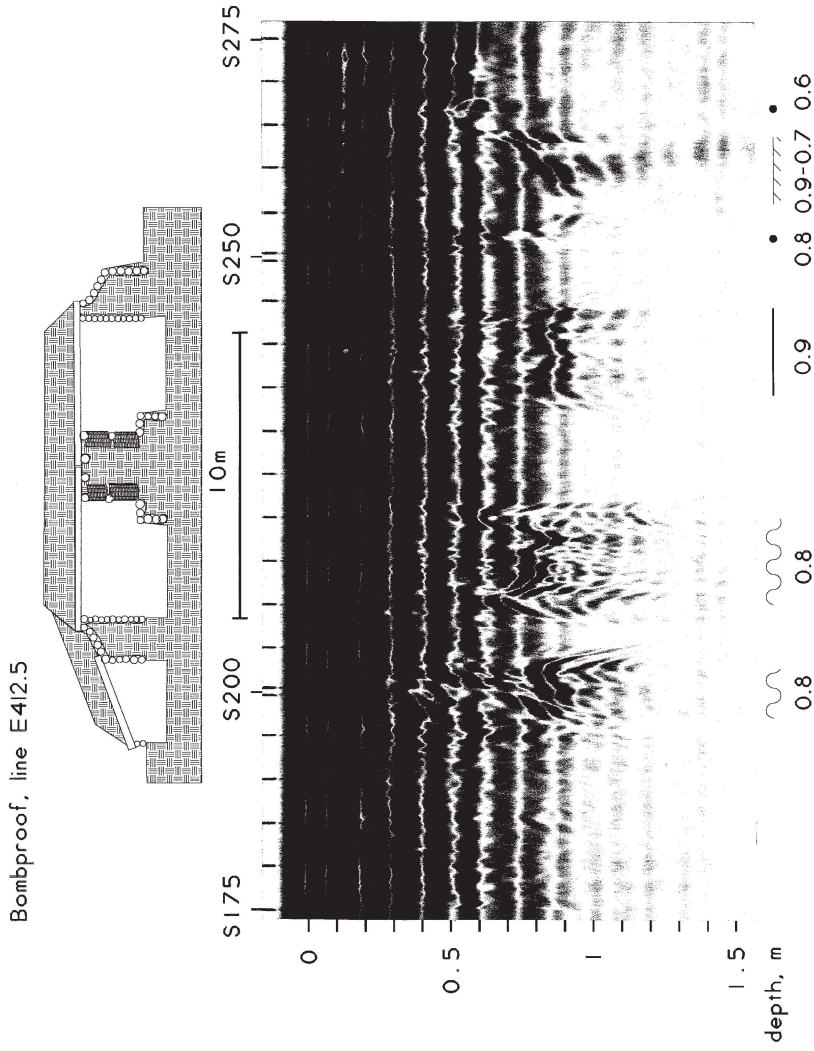

Fig. B149: Radar echoes of the bombproof. The drawing is a tracing of a diagram prepared during the Civil War.

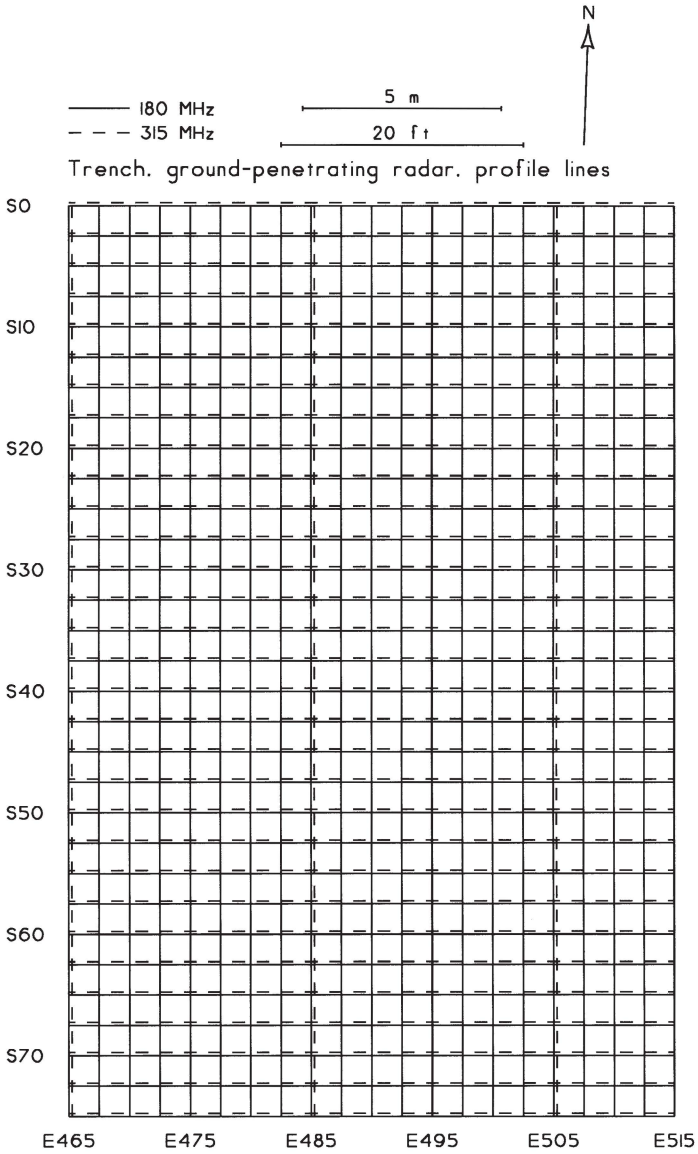

Fig. B150: The radar profile lines in the trench detail.

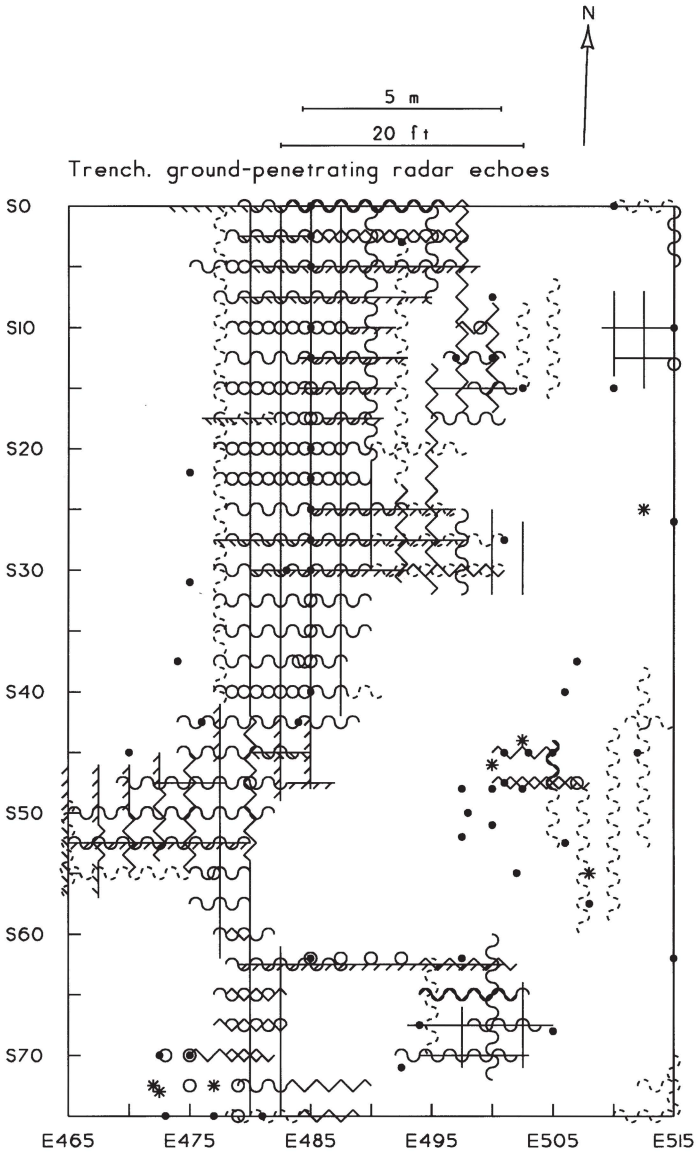

Fig. B151: A radar echo map of the main fortification trench.

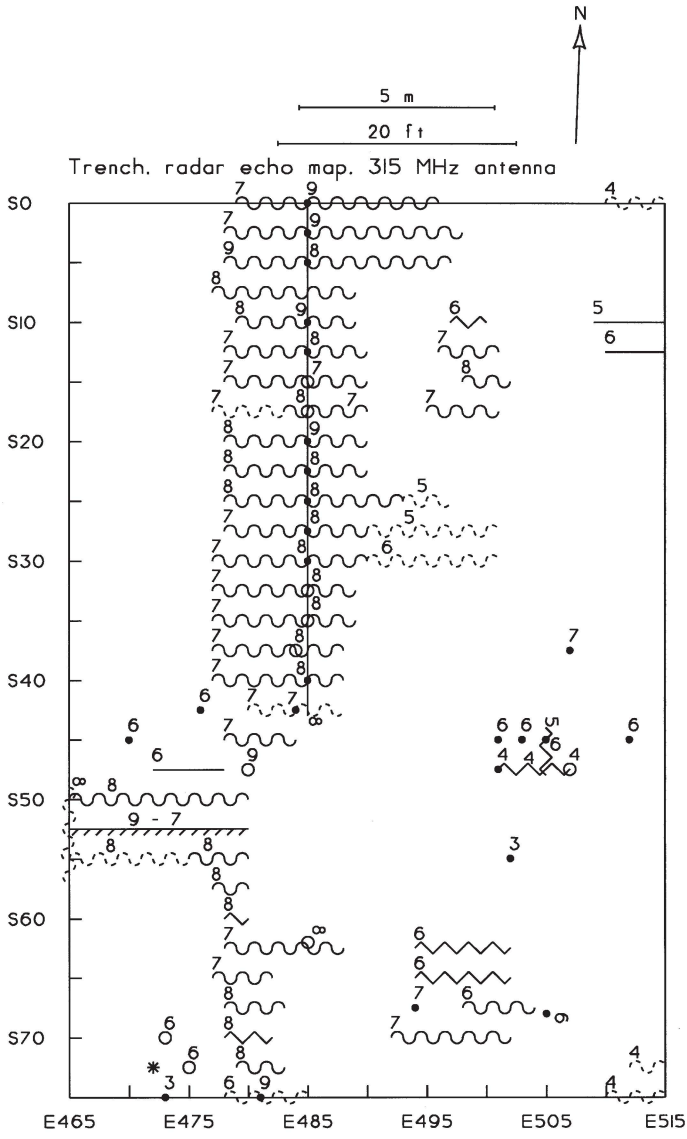

Fig. B152: Trench detail. Echoes of the high resolution antenna.

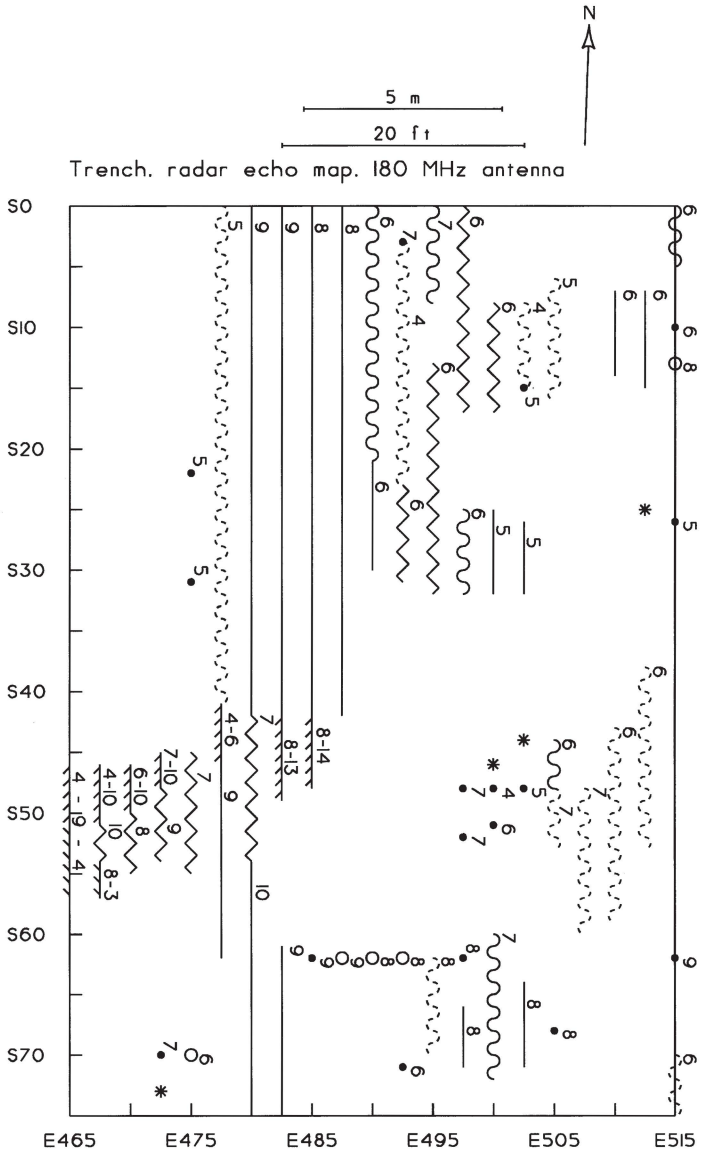

Fig. B153: Trench detail. Medium resolution echo map.

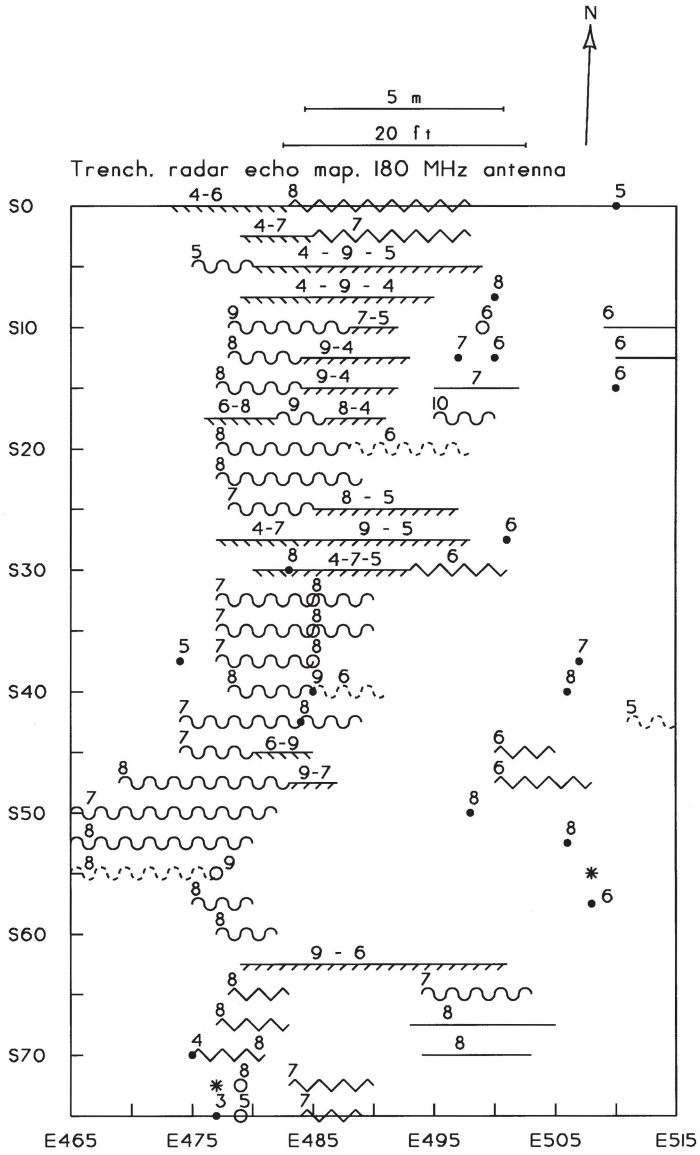

Fig. B154: Trench detail. Medium resolution echo map.

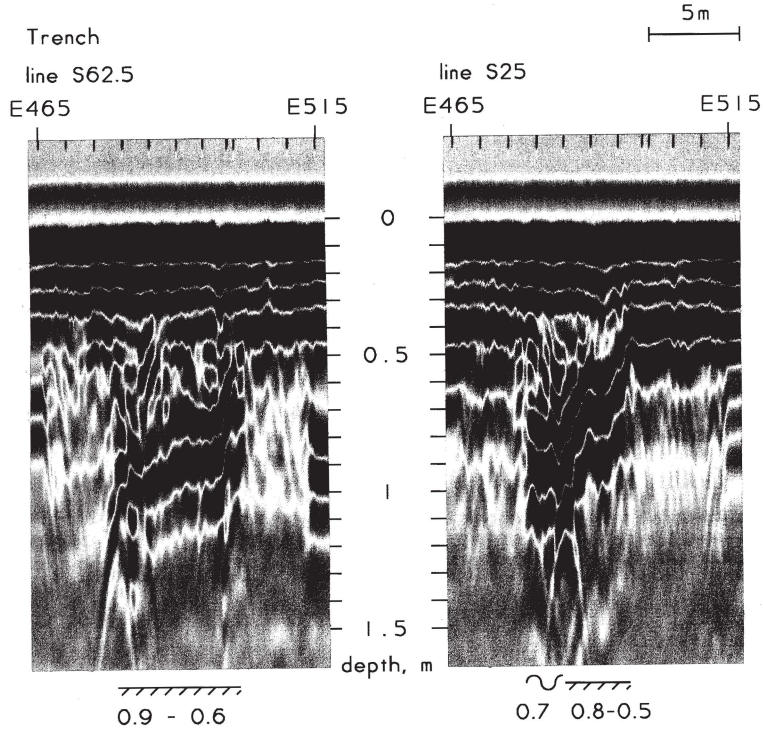

Fig. B155: Radar profiles of the main trench. The trench itself is on the left side of the echo; on these two lines, an extension of the trench to the east broadens the echo.

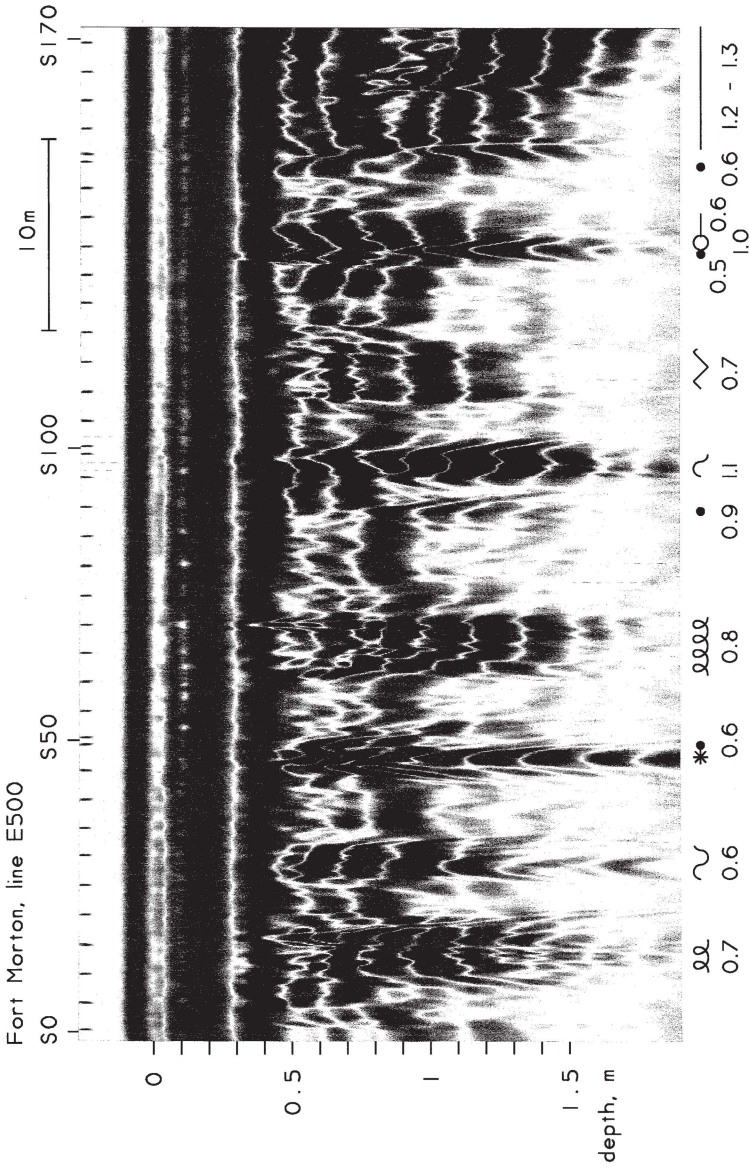

Fig. B156: Just behind the main line of fortification.

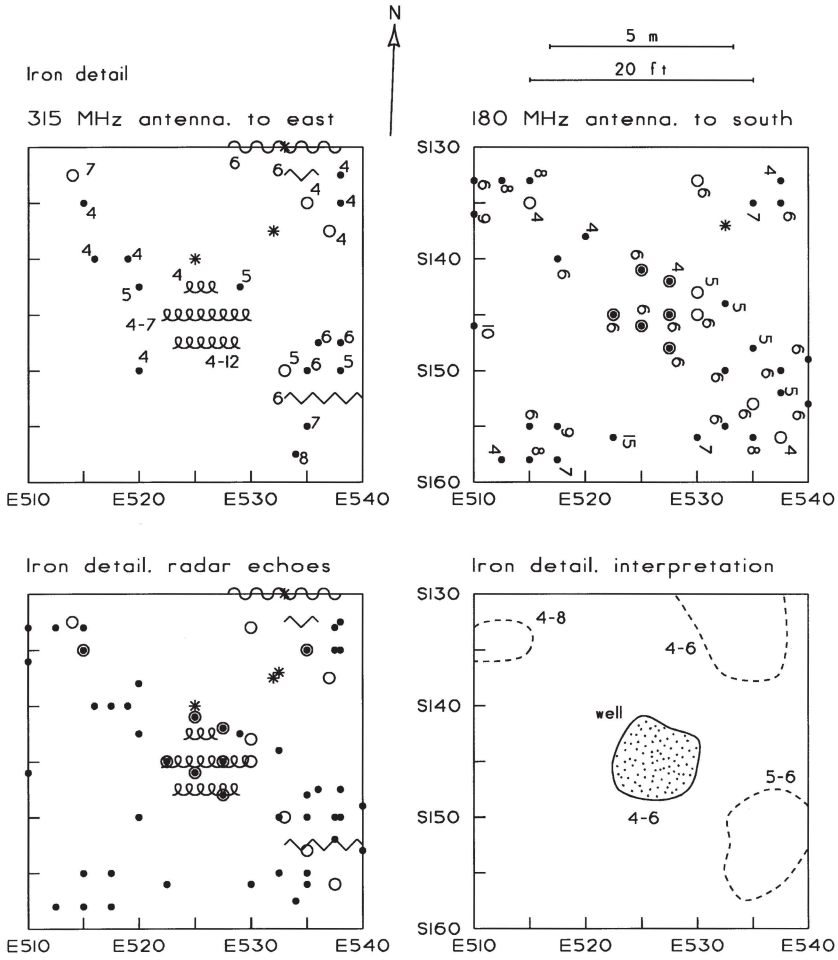

Fig. B157: Radar echo maps of the Iron detail. There is a group of complex echoes detected at the location of the well.

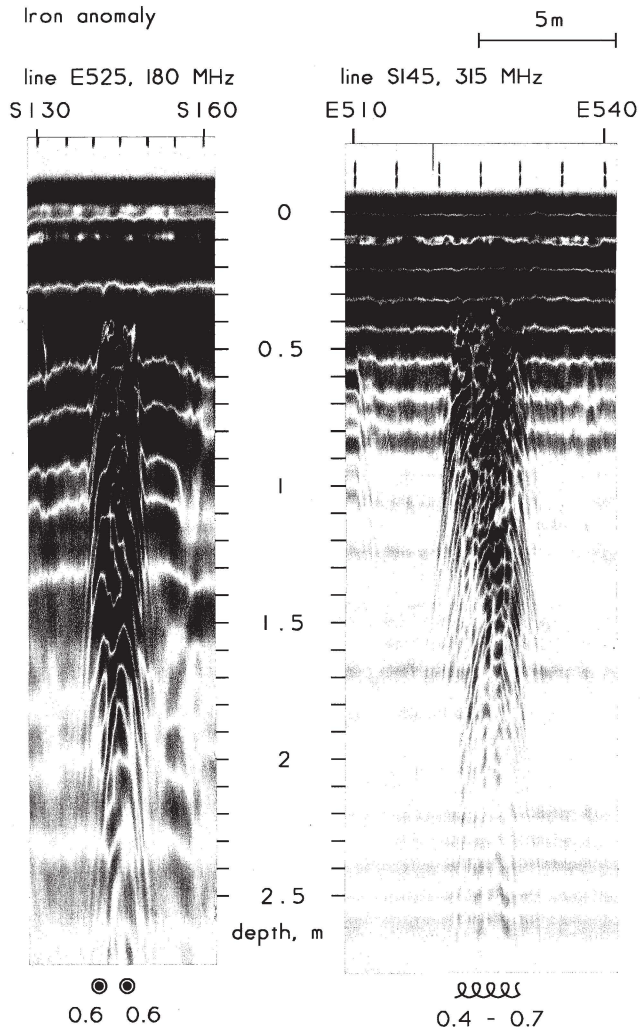

Fig. B158: The Iron detail. This complex reverberation could be caused by a cluster of metal objects.

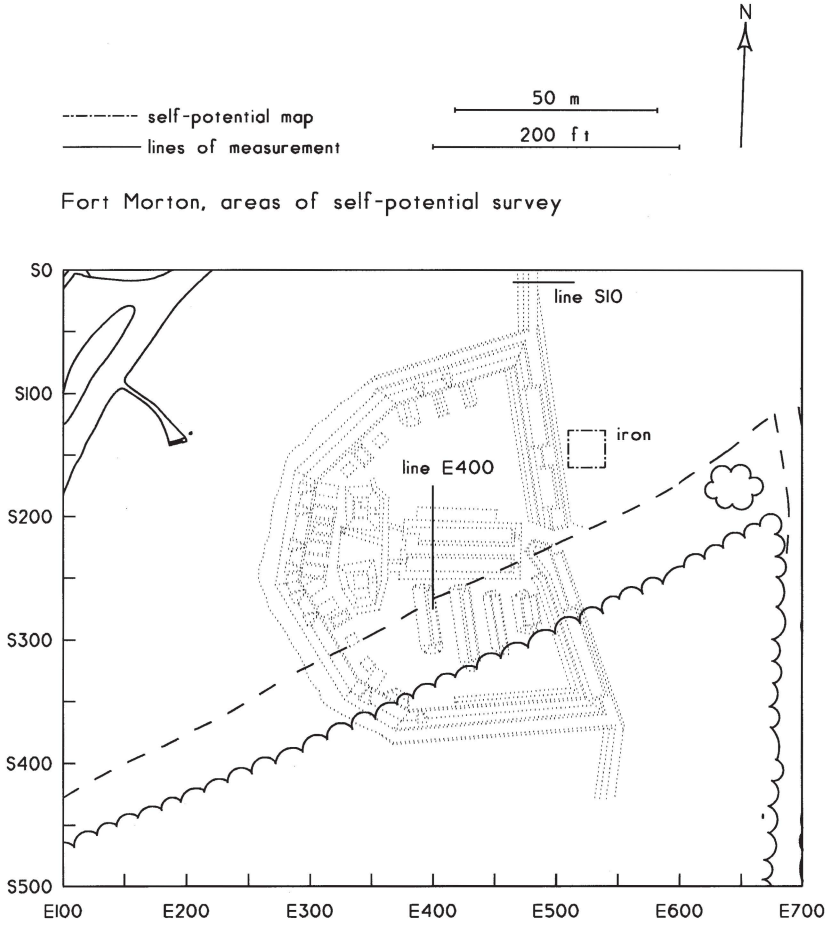

Fig. B159: Areas of the SP tests near Fort Morton.

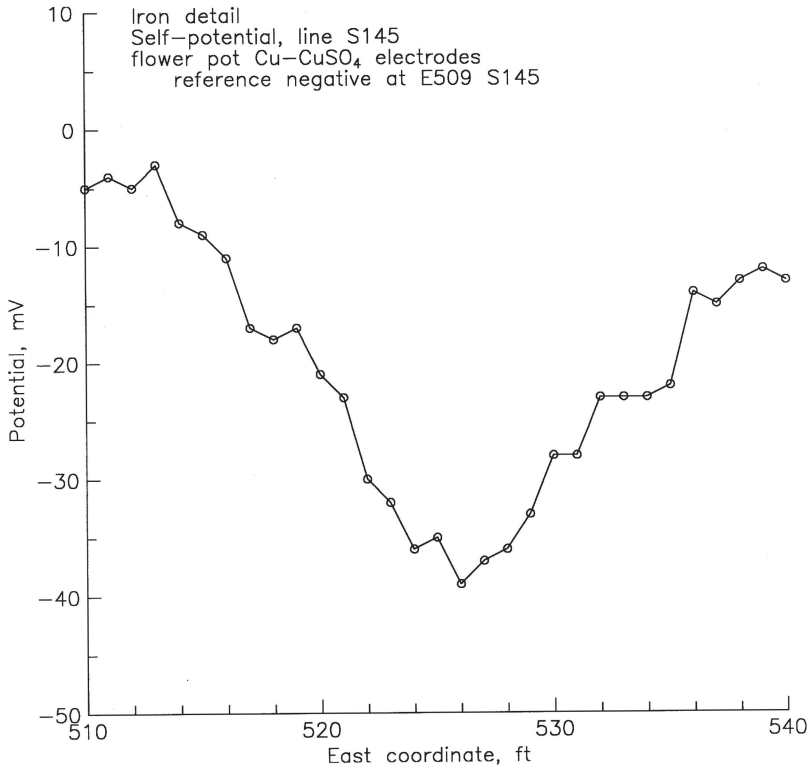

Fig. B160: Soil voltages at the Iron detail. The voltage is low at the location of the massive iron object. These measurements were made with self-potential electrodes made from ceramic flower pots.

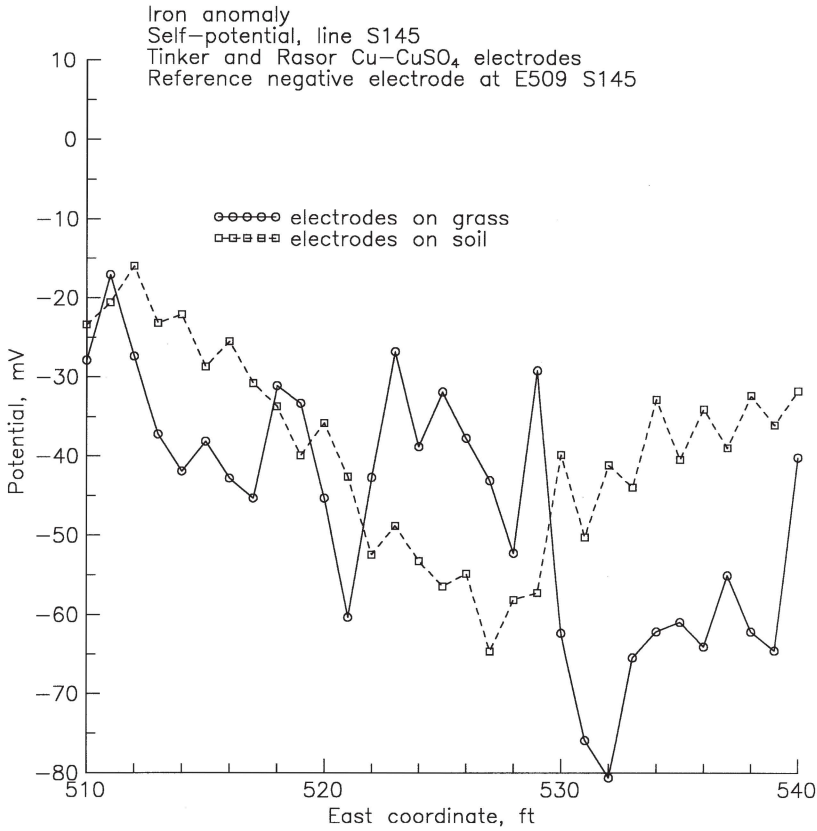

Fig. B161: Voltage tests over the iron anomaly. The grass must be removed from the surface, and the electrodes must be set on the bare soil in order to get good measurements.

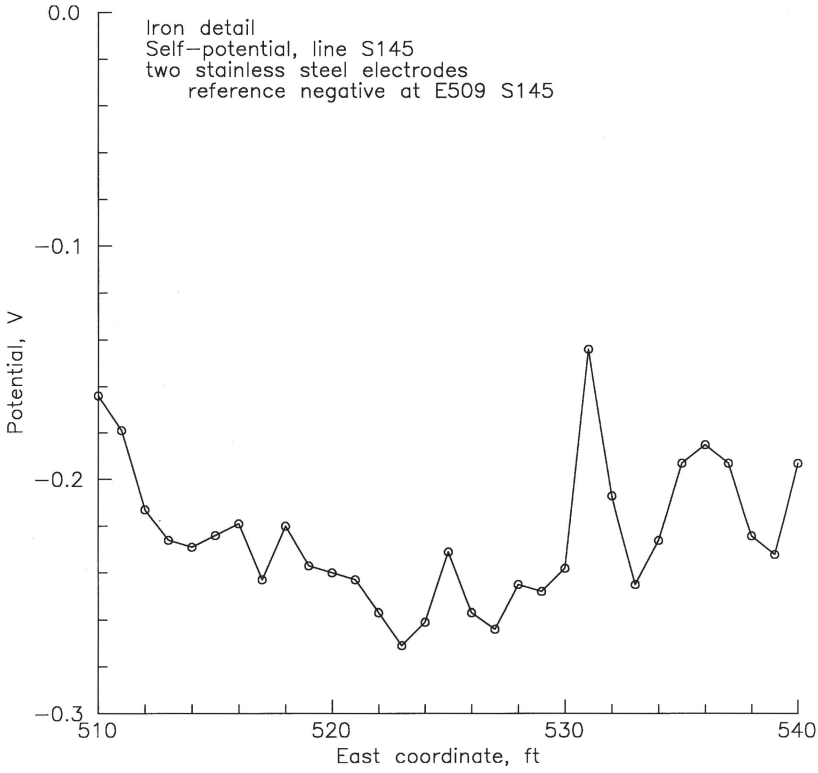

Fig. B162: Metal electrodes. They are poor SP electrodes. It is necessary to construct special non-polarizing electrodes.

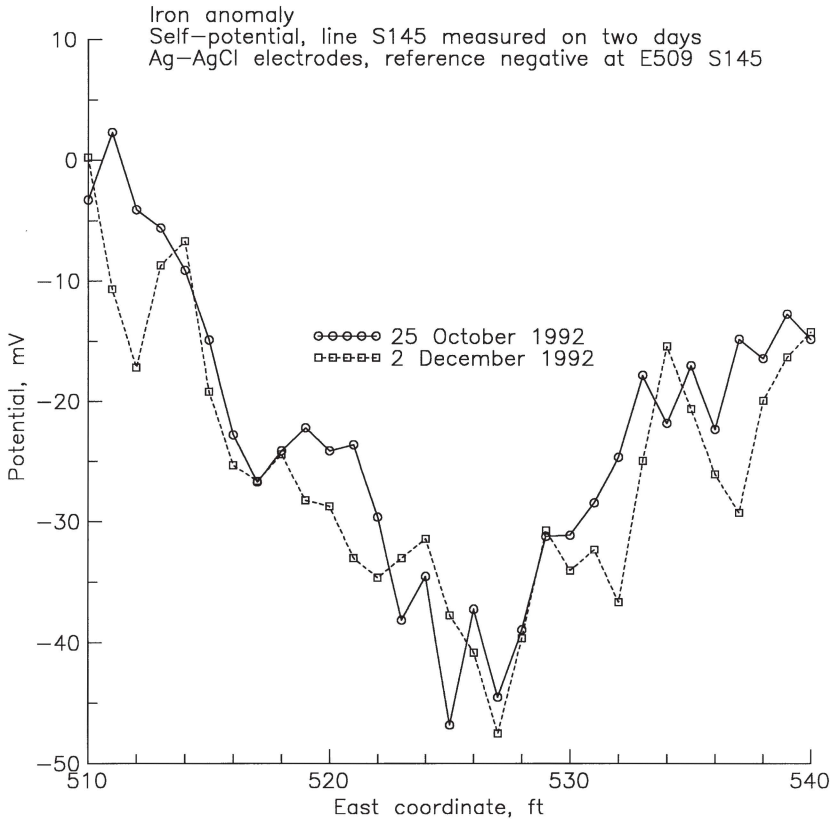

Fig. B163: Repeatability of SP measurements.

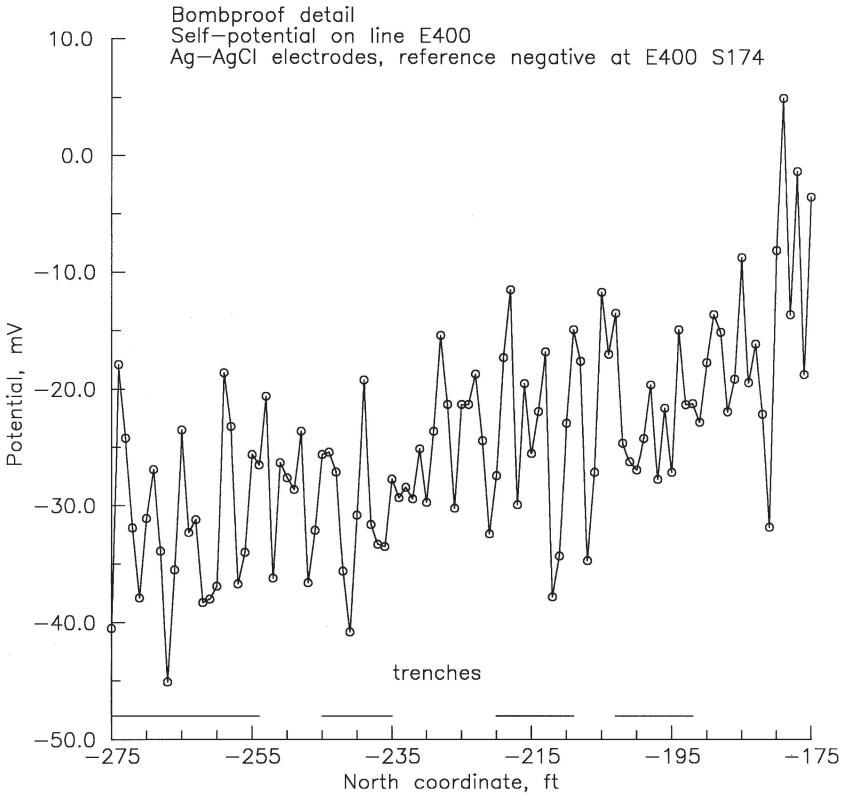

Fig. B164: Erratic voltage measurements. No evidence of the bombproof trenches was detected by the self-potential profile.

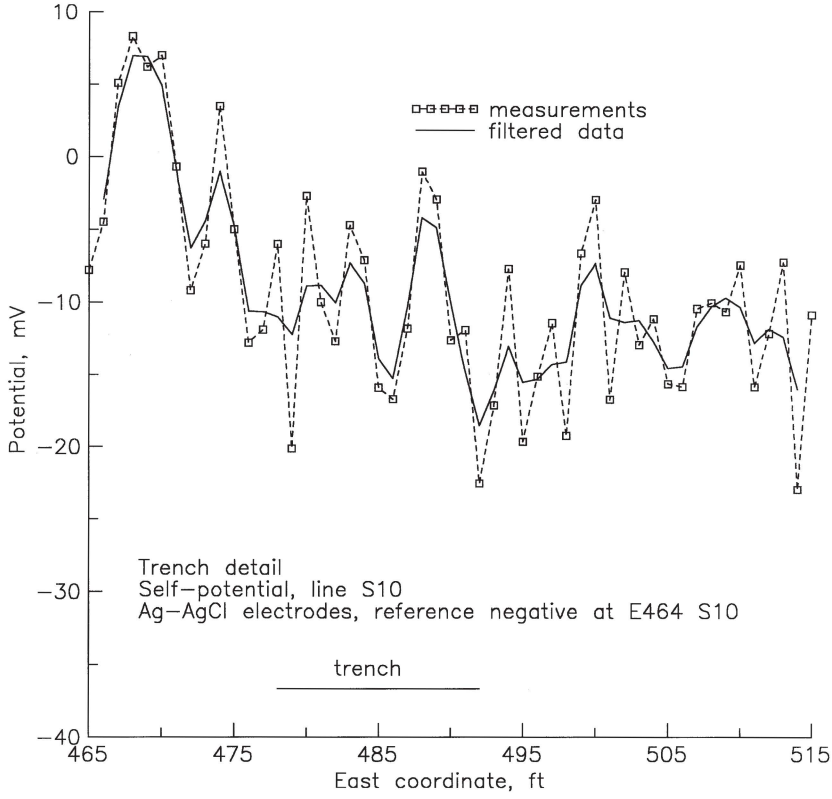

Fig. B165: A SP profile across the main fortification trench. Filtering did not help to reveal any valuable patterns.

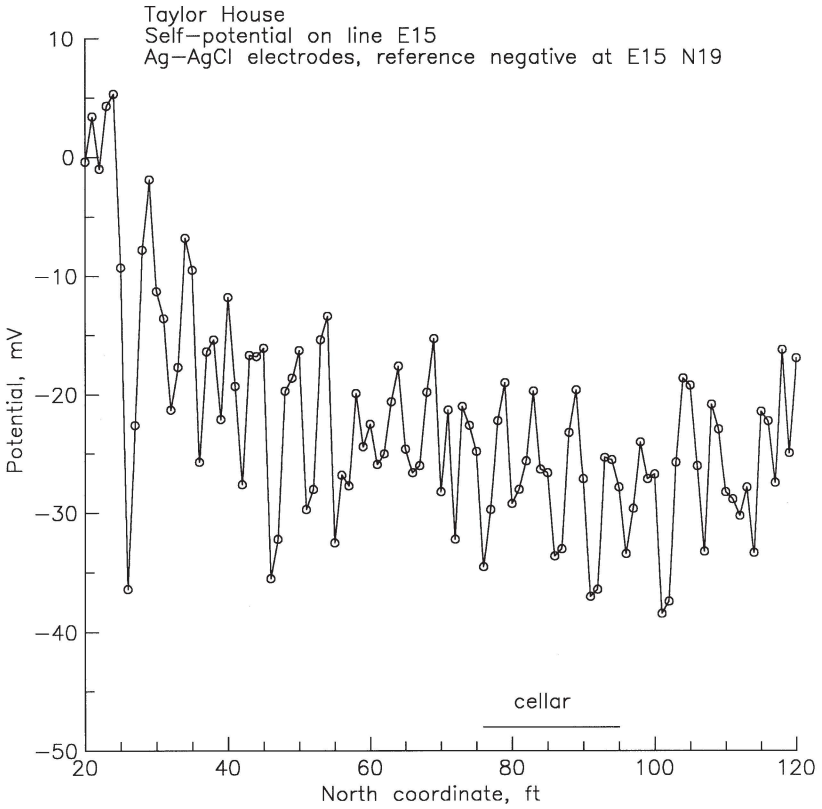

Fig. B166: An SP survey across the cellar of the Taylor House. There is no significant anomaly at the cellar.

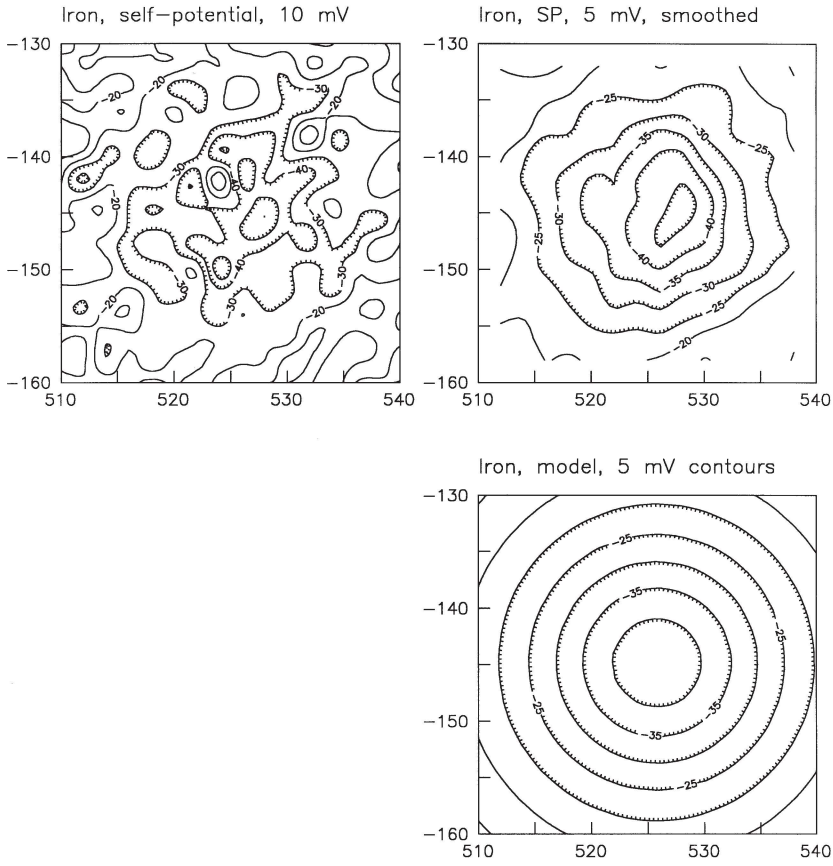

Fig. B167: A self-potential map, made over the Iron detail area.

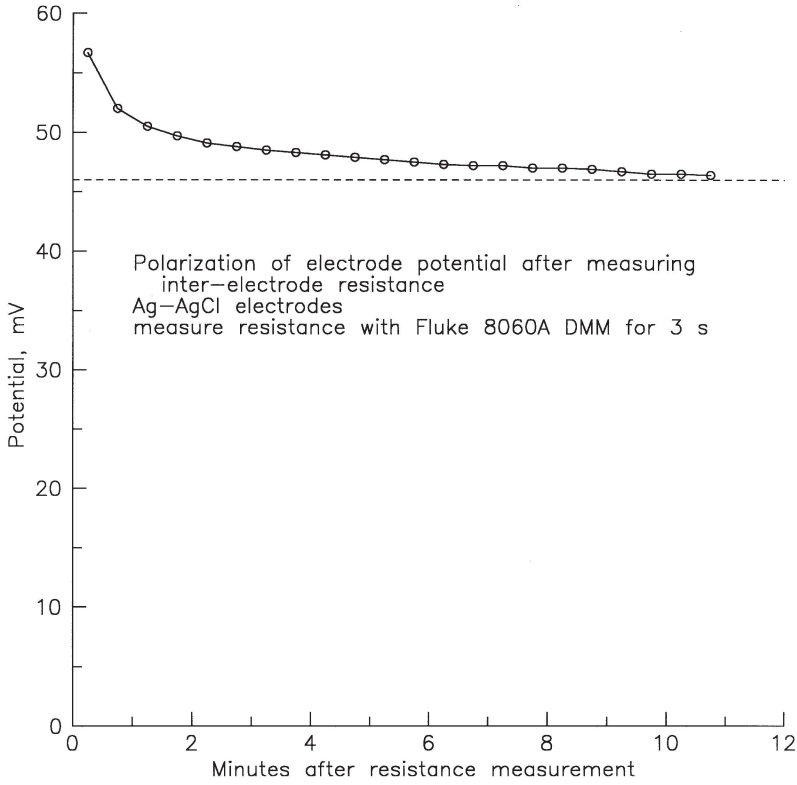

Fig. B168: The effect of a resistance measurement on SP electrodes. It will take several minutes before their voltage returns to normal.

Drift in the inter-electrode voltages of Ag-AgCl electrodes in 1992
Electrode #1 is the negative voltage reference

		electrode number				
date	time	2	3	4	5	0
13 October	7:00 pm	9.5	-8.8	-30.7	-15.1	
	10:00 pm	7.2	-9.3	-34.9	-15.5	
14 October	10:00 am	5.0	-8.5	-37.8	-14.5	
	12 noon	5.7	-8.6	-41.3	-12.4	
	3:00 pm	5.9	-8.0	-40.3	-12.1	-32.1
	5:30 pm	2.5	-9.6	-42.8	-12.7	-38.7
	8:30 pm	3.4	-9.3	-42.1	-11.4	-38.0
	10:30 pm	3.4	-9.3	-42.2	-12.6	-38.1
16 October	10:00 pm	3.8	-8.3	-40.7	-13.8	-38.0
17 October	10:00 am	3.9	-8.1	-40.8	-14.2	-37.7
	5:30 pm	6.5	-6.0	-38.7	-10.8	-35.7
25 October	10:08 am	6.8	-5.7	-40.8	-15.2	-40.0
	11:30 am	10.6	-0.8	-34.0	-9.5	-33.5
	11:56 am	10.2	-2.2	-35.2	-11.0	-34.9
	2:34 pm	8.6	-2.9	-35.8	-10.4	-36.3
	3:54 pm	10.2	0.1	-32.7	-10.0	-33.1
	4:12 pm	11.2	-0.9	-33.6	-9.6	-33.6
26 October	8:59 am	7.4	-4.8	-36.1	-14.2	-34.9
	9:17 am	9.5	-4.2	-34.2	-11.8	-32.9
	2:23 pm	8.6	-2.1	-32.9	-10.6	-36.1
2 December	9:52 am	8.9	3.9	-24.6	-5.4	-25.2
	10:55 am	6.1	-0.5	-29.2	-11.3	-26.4
	11:19 am	7.9	-2.2	-30.7	-10.8	-28.7
	12:27 pm	6.0	-2.8	-31.4	-14.9	-29.5
	1:28 pm	4.9	-5.2	-34.5	-12.9	-33.2
	2:48 pm	3.9	-4.4	-34.4	-15.8	-30.8

Fig. B169: The temporal change in voltages of Ag-AgCl electrodes.

Drift in the inter-electrode voltages of Cu-CuSO4 electrodes in 1992
Geoex electrode #3 is the negative voltage reference

		electrode number			
		Tinker and Rasor		Geoex	
date	time	1	2	1	2
17 October	7:45 pm	-1.6	-5.1	-2.5	-0.9
	9:00 pm	-0.5	-5.4	-3.6	-1.0
	11:00 pm	0.8	-4.8	-2.8	-0.5
25 October	12:03 pm	13.0	9.3		
	12:12 pm	9.8	6.5		
	12:17 pm	8.3	5.3		
	12:58 pm	4.3	1.3		
	1:08 pm	3.1	-0.1		
	1:15 pm	3.3	-0.9		
	1:58 pm	1.6	-2.6		

Fig. B170: The temporal change of Cu-CuSO4 electrodes.

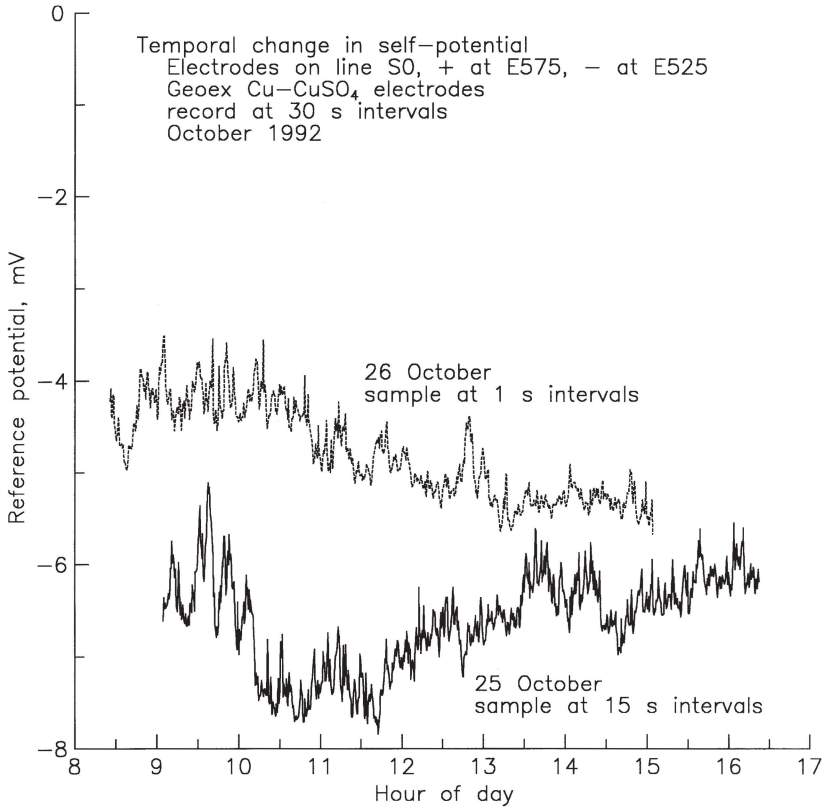

Fig. B171: The temporal SP noise at the site. It is small enough that it did not cause any difficulty for these surveys.

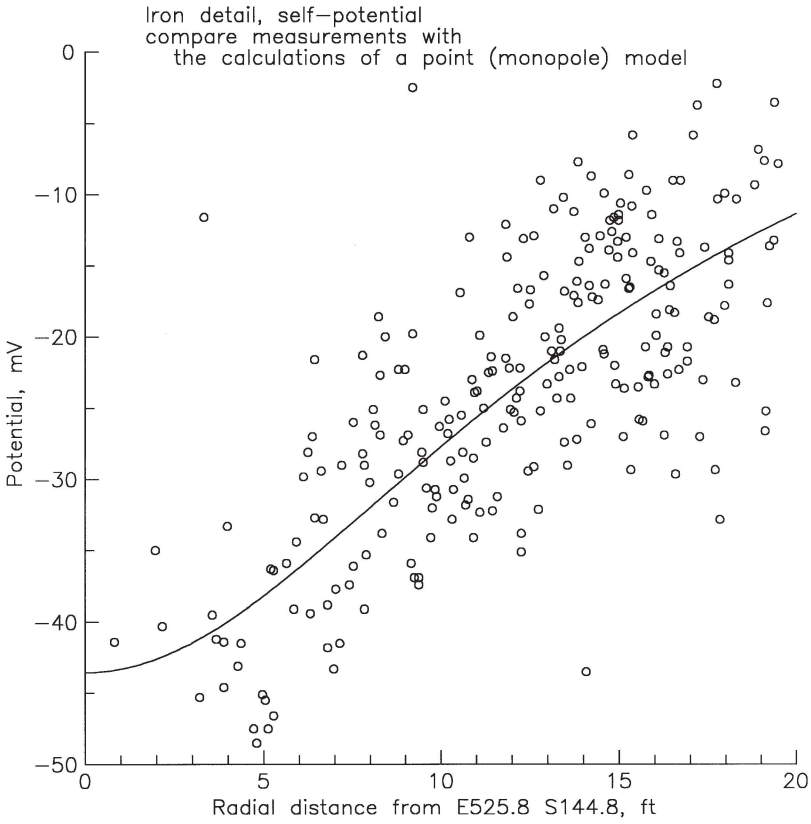

Fig. B172: A model for the SP measurements over the Iron detail. There was a large scatter in the measurements, but the general trend was modeled with a point source of current.

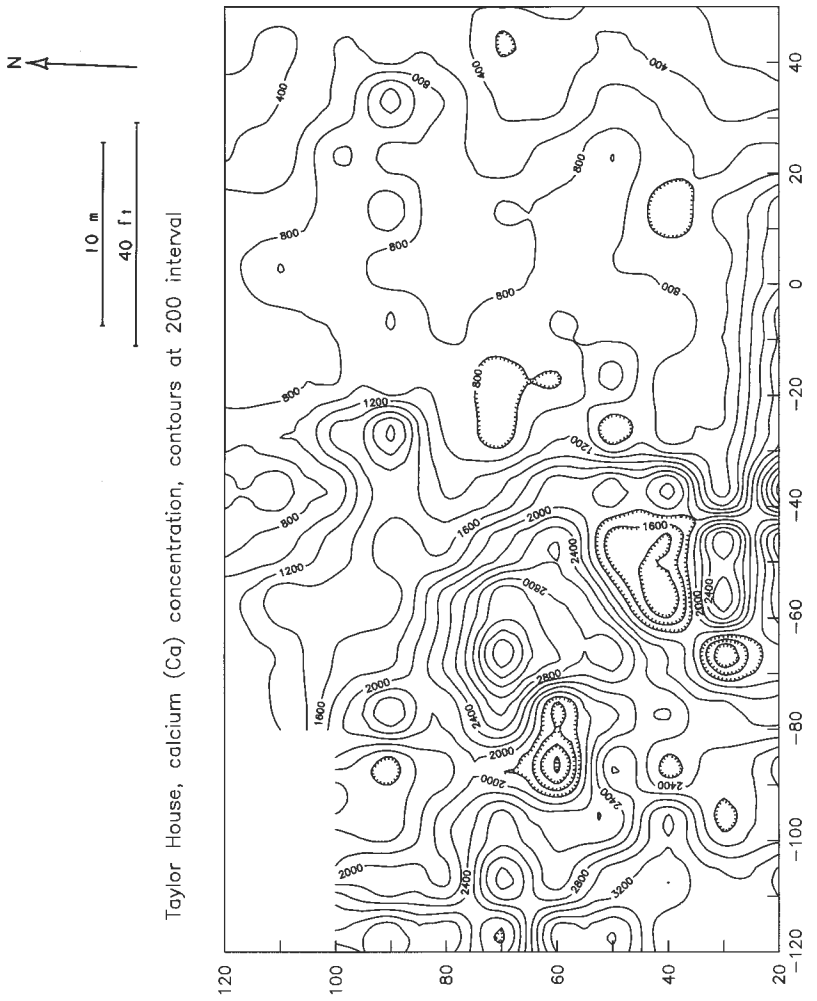

Fig. B173: The geochemical concentration of calcium at the Taylor House. It was high on the western side of the area.

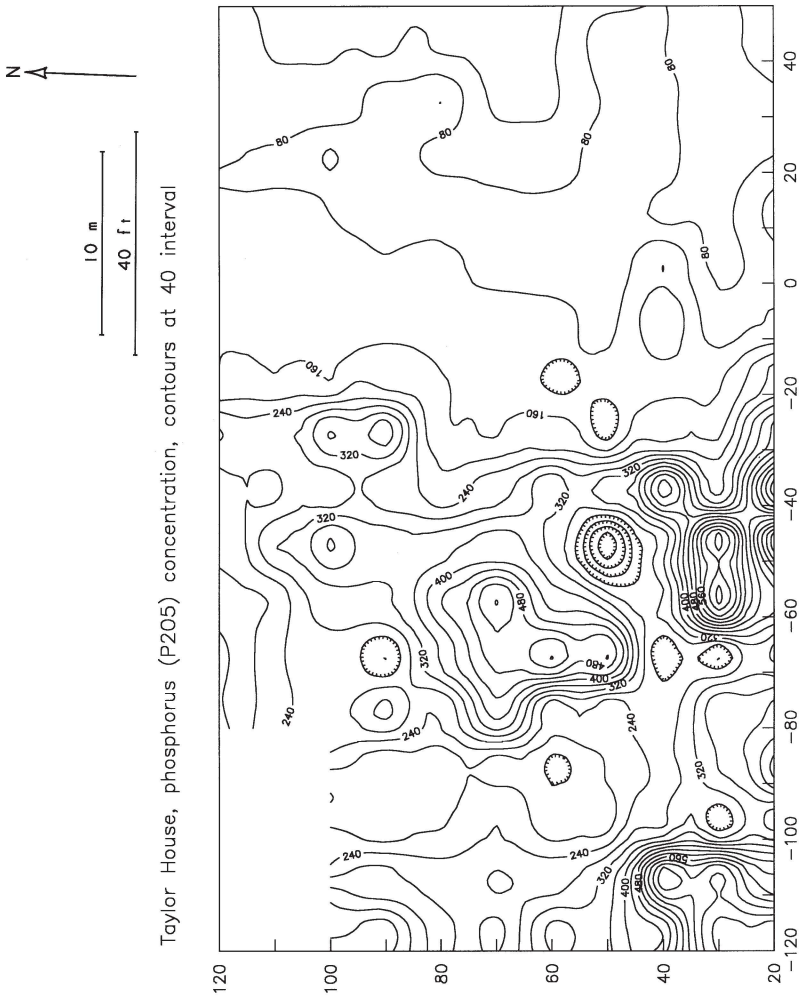

Fig. B174: Phosphate concentration. It was also high in the western half of the area.

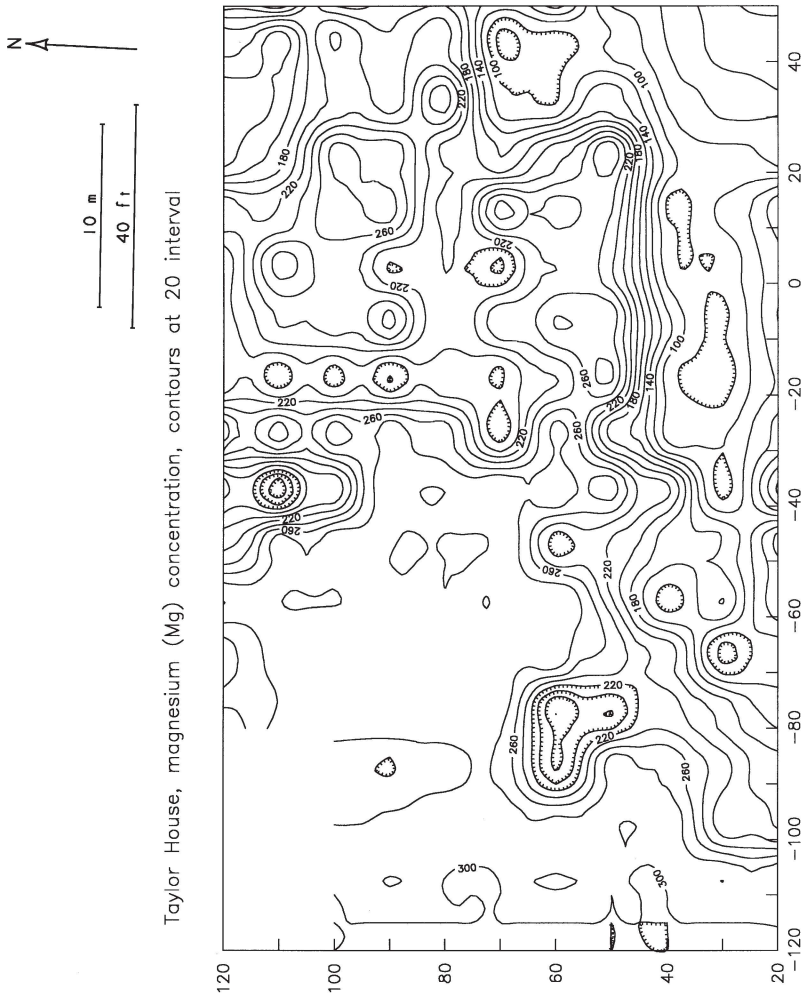

Fig. B175: Magnesium concentration. These chemical measurements were made as part of a project done by Brooke Blades.

Fig. B176: Potassium concentration.

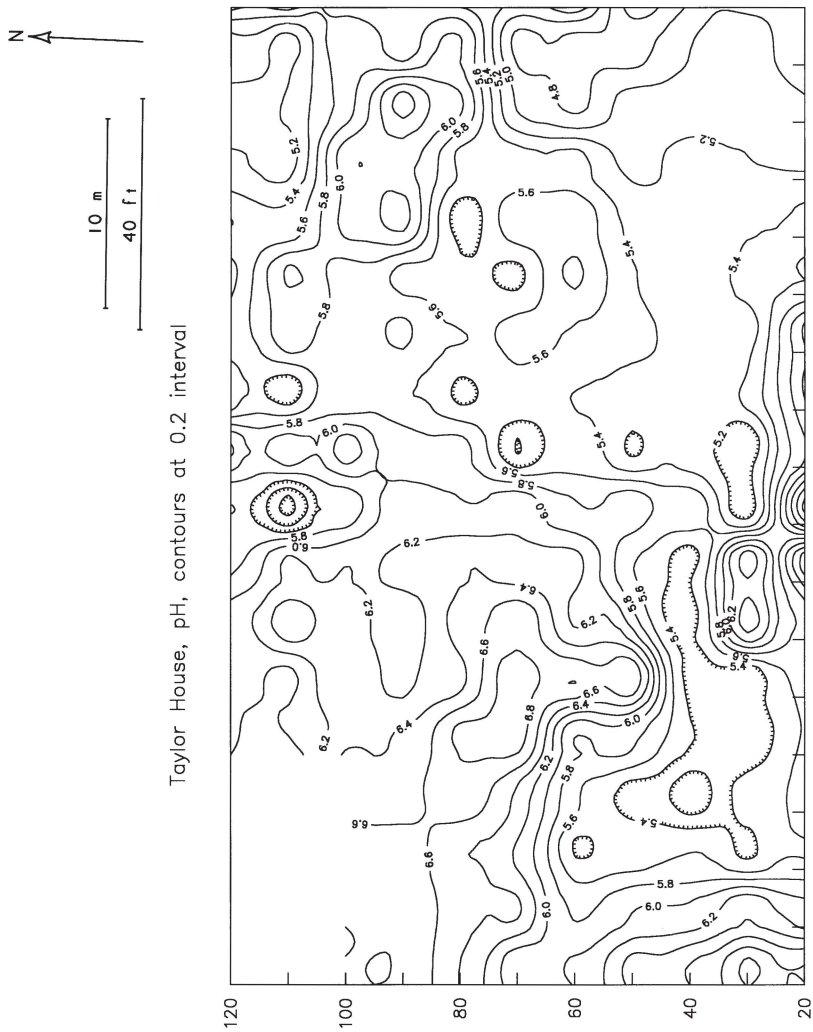

Fig. B177: Measurements of pH at the Taylor House.